

Renormalization in supersymmetric models

Renato Miguel Sousa da Fonseca

Supervisor: Doctor Jorge Manuel Rodrigues Crispim Romão

Co-Supervisor: Doctor Ana Margarida Domingues Teixeira

Thesis approved in public session to obtain the PhD Degree in
Physics

Jury final classification: Pass With Merit

Jury

Chairperson: Chairman of the IST Scientific Board

Members of the Committee:

Doctor Jean Orloff

Doctor José Wagner Furtado Valle

Doctor Jorge Manuel Rodrigues Crispim Romão

Doctor Filipe Rafael Joaquim

Doctor David Emmanuel da Costa

Doctor Ana Margarida Domingues Teixeira

Renormalization in supersymmetric models

Renato Miguel Sousa da Fonseca

Supervisor: Doctor Jorge Manuel Rodrigues Crispim Romão
Co-Supervisor: Doctor Ana Margarida Domingues Teixeira

Thesis approved in public session to obtain the PhD Degree in
Physics

Jury final classification: Pass With Merit

Jury

Chairperson: Chairman of the IST Scientific Board

Members of the Committee:

Doctor Jean Orloff, Full Professor, Laboratoire de Physique
Corpusculaire Clermont-Ferrand, Université Blaise Pascal, France

Doctor José Wagner Furtado Valle, Full Professor, CSIC, Instituto de
Física Corpuscular, Universitat de València, Spain

Doctor Jorge Manuel Rodrigues Crispim Romão, Full Professor,
Instituto Superior Técnico, Universidade de Lisboa, Portugal

Doctor Filipe Rafael Joaquim, Assistant Professor, Instituto Superior
Técnico, Universidade de Lisboa, Portugal

Doctor David Emmanuel da Costa, Assistant Researcher, Instituto
Superior Técnico, Universidade de Lisboa, Portugal

Doctor Ana Margarida Domingues Teixeira, Chargé de Recherche,
Laboratoire de Physique Corpusculaire Clermont-Ferrand, Université
Blaise Pascal, France

Funding Institutions

Fundação para a Ciência e a Tecnologia

ACKNOWLEDGMENTS

I would like to thank the following people:

- My supervisors, Jorge Romão and Ana Teixeira, for the trouble I have given them these last years.
- Those whom I have worked with in different research projects: Carolina Arbeláez, Martin Hirsch, Michal Malinský, Werner Porod, Florian Staub, and my supervisors as well.
- Members of CFTP, where this doctoral program was carried out.
- Members of the LPT in Orsay, the AHEP group in Valencia, and the LPC in Clermont-Ferrand, where I have spent some time. In particular, I thank Asmaa Abada, Martin Hirsch, and Ana Teixeira for having invited me there.
- Friends and colleagues which, knowingly or unknowingly, have been very supportive. In order not to fill the whole page and still risk forgetting someone, I will just mention here by name colleagues with whom I have shared office with: Marco Cardoso, Nuno Cardoso, João Esteves, António Figueiredo, David Forero, Mao Jing, Bruno Mera, Siavash Neshatpour, Tharnier Oliveira, Laslo Reichert, Hugo Serôdio and Catarina Simões. My gratitude goes also to Leonardo Pedro, for the interesting discussions and for reading part of this thesis.
- My family, to whom I dedicate this thesis.

Finally, I would like to acknowledge the support of the Portuguese State, provided through the grant SFRH/BD/47795/2008 from the *Fundação para a Ciência e a Tecnologia*.

RESUMO

Há motivos para acreditar que o Modelo Padrão é apenas uma teoria efetiva, havendo nova Física para além deste. Extensões supersimétricas são uma possibilidade: elas atenuam algumas das deficiências do Modelo Padrão, como por exemplo a instabilidade da massa do bóson de Higgs sob correções radiativas. Nesta tese são analisados alguns temas relacionados com a renormalização de modelos supersimétricos. Um deles é a automatização do cálculo do Lagrangiano e das equações do grupo de renormalização destes modelos — feito à mão, este é um processo complicado e onde podem ser introduzidos erros. As próprias equações genéricas do grupo de renormalização são estendidas de forma a abranger modelos que possuem um grupo de gauge com mais de um fator abeliano. Casos deste tipo surgem, por exemplo, em teorias de grande unificação. Para um vasto número de modelos inspirados no grupo $SO(10)$, é igualmente mostrado que o grupo de renormalização imprime na massa das spartículas alguma da informação sobre o comportamento destes a altas energias. Finalmente, em alguns casos estas teorias introduzem interações violadoras do sabor de leptões carregados, que podem levar a alterações no rácio $\Gamma(K \rightarrow e\nu)/\Gamma(K \rightarrow \mu\nu)$. Tendo em conta os limites experimentais noutras observáveis, a nossa análise mostra que qualquer alteração à previsão do Modelo Padrão será menor que a sensibilidade atual a esta observável.

PALAVRAS-CHAVE: Supersimetria, Grande unificação, Equações do grupo de renormalização, Mistura de $U(1)$ s, Teoria de grupos, Susyno, Modelos inspirados em $SO(10)$, Violação de sabor leptónico, Universalidade de sabor leptónico, Física de kaões

ABSTRACT

There are reasons to believe that the Standard Model is only an effective theory, with new Physics lying beyond it. Supersymmetric extensions are one possibility: they address some of the Standard Model's shortcomings, such as the instability of the Higgs boson mass under radiative corrections. In this thesis, some topics related to the renormalization of supersymmetric models are analyzed. One of them is the automatic computation of the Lagrangian and the renormalization group equations of these models, which is a hard and error-prone process if carried out by hand. The generic renormalization group equations themselves are extended so as to include those models which have more than a single abelian gauge factor group. Such situations can occur in grand unified theories, for example. For a wide range of $SO(10)$ -inspired supersymmetric models, we also show that the renormalization group imprints on sparticle masses some information on the higher energies behavior of the models. Finally, in some cases these theories introduce charged lepton flavor violating interactions, which can change the ratio $\Gamma(K \rightarrow e\nu)/\Gamma(K \rightarrow \mu\nu)$. In light of experimental bounds on other observables, our analysis shows that any change over the Standard Model prediction must be smaller than the current experimental sensitivity on this observable.

KEYWORDS: Supersymmetry, Grand unification, Renormalization group equations, $U(1)$ mixing, Group theory, Susyno, $SO(10)$ -inspired models, Lepton flavor violation, Lepton flavor universality, Kaon physics

CONTENTS

Acknowledgements	v
Resumo	vii
Abstract	ix
List of Tables	xix
List of Figures	xxiii
Abbreviations	1
I THE STANDARD MODEL AND BEYOND	1
1 INTRODUCTION	3
2 THE STANDARD MODEL AND SUPERSYMMETRY	5
2.1 Shortcomings of the Standard Model	7
2.1.1 The hierarchy problem	7
2.1.2 Unexplained structure and parameter values	8
2.1.3 Massive neutrinos	10
2.1.4 Dark matter, dark energy and gravity	10
2.1.5 Baryogenesis and leptogenesis	13
2.2 Supersymmetry and the MSSM	15
3 LEPTON FLAVOR VIOLATION	25
3.1 Massive neutrinos	25
3.1.1 A brief history of neutrino experiments	25
3.1.2 Neutrino oscillation parameters	26
3.1.3 Matter effects and solar neutrinos	28
3.1.4 Neutrinoless double beta decay experiments	29
3.1.5 Beta decay experiments	30
3.1.6 Cosmological bounds on neutrino masses	31
3.1.7 The origin and smallness of neutrino masses	31
3.2 Charged lepton flavor violation	36
3.2.1 Charged lepton flavor violation and SUSY	39
3.2.2 cLFV observables and limits on effective couplings	40
4 GROUP THEORY IN PARTICLE PHYSICS	45
4.1 The role of symmetry	45
4.2 Lie groups and their connection to Lie algebras	46
4.3 Lie Algebras	49
4.3.1 Basic concepts	49
4.3.2 Roots of simple Lie algebras	50
4.3.3 The Killing form	53
4.3.4 The Cartan matrix and the classification of all complex simple Lie algebras	54
4.3.5 Representations, weights and the Casimir operator	55
4.3.6 Subalgebras and branching rules	58
4.3.7 The Lie algebra of gauge symmetries	59
4.4 Space-time symmetries	61

4.4.1	The Lorentz and Poincaré groups	61
4.4.2	Lie algebras and representations of the Poincaré and Lorentz groups	63
4.5	Supersymmetry as a super-Poincaré group	66
II TOPICS ON THE RENORMALIZATION OF SUSY MODELS		71
5	CALCULATING THE RENORMALIZATION GROUP EQUATIONS OF A SUSY MODEL WITH SUSYNO	73
5.1	Introduction	73
5.2	Installation and quick start	74
5.3	The input of Susyno : defining a model	75
5.3.1	Gauge group	75
5.3.2	Representations/fields: the content of the model	76
5.3.3	Number of flavors and abelian discrete symmetries	78
5.3.4	Calling the function GenerateModel	78
5.4	The output of Susyno	79
5.4.1	Naming of parameters	79
5.4.2	Normalization of the parameters	80
5.4.3	Changing the default notation	81
5.5	Tests/validation of Susyno	83
5.6	List of available functions	83
5.7	Summary	85
6	RUNNING SOFT PARAMETERS IN SUSY MODELS WITH MULTIPLE $U(1)$ GAUGE FACTORS	87
6.1	Introduction	87
6.2	$U(1)$ mixing	87
6.3	Two loop RGEs	90
6.3.1	Notation and conventions	90
6.3.2	Strategy for the constructing the general substitution rules	91
6.3.3	Substitution rules	93
6.4	Obtaining the substitution rules	95
6.4.1	The role of the \mathbf{V}_i vectors and the \mathbf{M} matrix	95
6.4.2	RGEs with no $U(1)$ indices	95
6.4.3	RGEs with $U(1)$ indices	97
6.5	Comparison with other methods of including $U(1)$ -mixing effects	98
6.5.1	General discussion	98
6.5.2	Quantifying $U(1)$ -mixing effects with simple examples	99
6.6	Conclusions and outlook	102
7	SUPERSYMMETRIC $SO(10)$ -INSPIRED GUTS WITH SLIDING SCALES	105
7.1	Introduction	105
7.2	Models	107

7.2.1	Supersymmetric $SO(10)$ models: General considerations	107
7.2.2	Model class-I: One intermediate (left-right) scale	109
7.2.3	Model class-II: Additional intermediate Pati-Salam scale	114
7.2.4	Models with an $U(1)_R \times U(1)_{B-L}$ intermediate scale	118
7.3	Invariants	121
7.3.1	Leading-Log RGE Invariants	121
7.3.2	Classification of invariants	123
7.3.3	Invariants in class-I model	126
7.3.4	Model class-II	127
7.3.5	Model class-III	127
7.3.6	Comparison of classes of models	127
7.4	Summary	131
8	THE $\Gamma(K \rightarrow e\nu)/\Gamma(K \rightarrow \mu\nu)$ RATIO IN SUPERSYMMETRIC UNIFIED MODELS	135
8.1	The R_K ratio, lepton flavor universality, and lepton flavor violation	135
8.2	R_K in supersymmetric models	137
8.2.1	The LFV in the slepton mass matrices as the source of an enhanced Δr	140
8.3	Prospects for R_K : unified vs unconstrained SUSY models	142
8.3.1	mSUGRA inspired scenarios: cMSSM and the SUSY seesaw	143
8.3.2	mSUGRA inspired scenarios: inverse seesaw and LR models	145
8.3.3	mSUGRA inspired scenarios: NUHM	146
8.3.4	Unconstrained MSSM	148
8.4	Summary	150
9	CONCLUSIONS	153
III	APPENDIX	155
A	STRUCTURE OF THE STANDARD MODEL	157
A.1	The gauge theory	157
A.2	Electroweak symmetry breaking	159
B	IMPLEMENTATION OF SOME FUNCTIONS IN THE <code>SUSYNO</code> PROGRAM	161
B.1	Building the matrices of an arbitrary representation of a simple group	162
B.2	Invariant combinations of fields transforming under some representation of a simple group and generalized Clebsch-Gordan coefficients	167
B.3	Einstein convention applied to flavor indices	171
B.4	A Lagrangian-free computation of the RGEs	172
B.5	Running time	177

C	TWO-LOOP RGES FOR MODELS WITH GAUGE GROUPS CONTAINING AT MOST ONE $U(1)$	179
C.1	Simple gauge group	179
C.2	Product groups with at most one $U(1)$	182
D	MATCHING CONDITIONS FOR GAUGE COUPLINGS AND GAUGINO MASSES IN MODELS WITH $U(1)$ -MIXING	185
D.1	Gauge couplings	185
D.2	Gaugino masses	187
E	LISTS OF SUPERFIELDS IN LEFT-RIGHT MODELS	189
F	RENORMALIZATION OF THE $\nu\ell H^+$ VERTEX	193
	Bibliography	197

LIST OF TABLES

Table 1	Representations of the SM gauge group. All listed fermions are left-handed. 5
Table 2	Chiral superfields in the MSSM 18
Table 3	Vector superfields in the MSSM 18
Table 4	Best fit and 1σ ranges for the neutrino parameters obtained from a global three neutrino oscillation analysis [189]. The value of $\sin^2 \theta_{23}$ in parenthesis is also compatible with experimental data. See also [190–192] for comparable values. 27
Table 5	Upper limits on m_{ee} from different $0\nu\beta\beta$ experiments, obtained using the isotopes ^{76}Ge , ^{82}Se , ^{100}Mo , ^{130}Te , ^{136}Xe . 30
Table 6	Values of $a_i \equiv (g_i - 2)/2$, $i = e, \mu, \tau$ taken from [31 , 369 , 370] and [371–373] (1σ uncertainties are in parentheses). Note that a_e^{SM} differs from a_e^{exp} because α is not being extracted from the anomalous magnetic moment of the electron—see [31]. 42
Table 7	Experimental bounds on leptonic electric dipole moments. 42
Table 8	Experimental bounds on the branching ratio of decays $\ell_i \rightarrow \ell_j \gamma$ (90% CL) as well as expected future sensitivities. 43
Table 9	Currents bounds (90% CL) or values of some important observables which depend on the 4ℓ and $2\ell 2q$ cLFV effective operators in equations in (3.54)–(3.60). Future sensitivities are also shown. The Standard Model predicts $\text{BR}(B_s \rightarrow \mu\mu) = (3.23 \pm 0.27) \times 10^{-9}$ [394] and $\text{BR}(B \rightarrow \tau\nu) = (1.11 \pm 0.27) \times 10^{-4}$ (using $f_B = 190.6 \pm 4.7$ MeV [395–398], $V_{ub} = (4.15 \pm 0.49) \times 10^{-3}$ [105]). 43
Table 10	Simple gauge factor groups 75
Table 11	List of some frequently used representations of $SU(2)$, $SU(3)$, $SU(5)$ and $SO(10)$ 77
Table 12	Parameters of the MSSM assuming a field ordering $\{\mathbf{u}, \mathbf{d}, \mathbf{Q}, \mathbf{e}, \mathbf{L}, \mathbf{H}_u, \mathbf{H}_d\}$ and the gauge factor group ordering $\{\mathbf{U1}, \mathbf{SU2}, \mathbf{SU3}\}$. 82

Table 13	Low energy values of the entries of the gauge coupling and gaugino mass matrices (g_{ab} and M_{ab} with $a, b = Y, BL$) and the correctly fitted MSSM parameters (g_Y, M_Y)—see equations (D.12) and (D.17). All gaugino mass parameters are in GeV. We have set the GUT scale at 2×10^{16} with $g_G = 0.72$ and imposed an mSUGRA boundary condition taking $M_{1/2} = 1 \times 500$ GeV. At the one-loop level, we compare the case with no kinetic mixing effects included, the <i>rotated basis</i> and the full-fledged calculation. At the two-loop level, we include the case where g_Y and g_{BL} are split at the GUT scale due to threshold corrections. 103
Table 14	List of the 53 variants with a single LR scale. In each case, the fields shown are the extra ones, which are not part of the MSSM (the 2 Higgs doublets are assumed to come from one bi-doublet $\Phi_{1,2,2,0}$). The $\Delta b_3, \Delta b_2, \Delta b_R, \Delta b_{B-L}$ values can be obtained from the first column through equations (7.9) and (7.10). 111
Table 15	Values of the c_i^{f,R_j} coefficients entering equation (7.28), for $R_j = \text{MSSM, LR, PS}$ and $f = \tilde{E}, \tilde{L}, \tilde{D}, \tilde{U}, \tilde{Q}$. Values for the $U(1)_R \times U(1)_{B-L}$ regime are not shown, since equation (7.29) should be used instead. 121
Table 16	The 16 different combinations of signs for 4 invariants. We assign a “+” if the corresponding invariant, when the lowest intermediate scale is set to m_{SUSY} , is larger than its value when this scale is maximized, and “−” otherwise. As discussed in the text, only 9 of the 16 different sign combinations can be realized in the class-I and class-II models (sets 1, 2, 3, 6, 7, 8, 10, 14 and 16). In fact, class-I models always fall on sets 1, 2, 10 and 14, and this can be proven with simple arguments (see text). On the other hand, there are class-II models will all 9 invariant sign combinations. Class-III models can conceivably achieve three more sign combinations (sets 9, 11, 15), but we did not find any such case in a non-exhaustive search (also, no models in set 16 were found). 123
Table 17	Range of NUHM parameters leading to the scan of figure (31). 147
Table 18	Range of variation of the unconstrained MSSM parameters (dimensionful parameters in GeVs). A_0 denotes the common value of the low-energy sfermion trilinear couplings. 148

Table 19	Running time of the command <code>GenerateModel</code> without (“Time 1”) and with (“Time 2”) the option <code>CalculateEverything->True</code> (output was suppressed in both cases). Five models are presented: MSSM [430], R-parity violating MSSM (RPV MSSM) [439], NMSSM [431], and two $SO(10)$ models. Model “ $SO(10)$ #1” contains three 16 multiplets together with the representations 210 , 126 , $\overline{\mathbf{126}}$, 10 (one copy each). In model “ $SO(10)$ #2”, the representation 210 is replaced by the 45 plus the 54 . Note that <code>GenerateModel</code> will always compute the RGEs, regardless of the optional parameters; using <code>CalculateEverything->True</code> forces the program to calculate the Lagrangian explicitly (superpotential and soft SUSY breaking Lagrangian). In this last case, Clebsch-Gordan coefficients must be computed, and that is why “Time 2” can be significantly larger than “Time 1”. Note as well that the RPV MSSM, with or without optional parameters, takes a substantial amount of time to be computed essentially because the model contains equal representations, L and H_d , which are to be treated differently (in other words, the running time would be smaller if H_d was erased and instead we considered 4 flavors of L). 178
Table 20	Running time of the command <code>Invariants</code> which calculates generalized Clebsch-Gordan coefficients of arbitrary representations of an arbitrary gauge group. Note that there are fifty seven $SU(3)$ invariants in $\mathbf{3} \otimes \mathbf{6} \otimes \mathbf{10} \otimes \mathbf{15} \otimes \mathbf{15}' \otimes \mathbf{42}$, 1 $SO(10)$ invariant in $\mathbf{16} \otimes \mathbf{16} \otimes \overline{\mathbf{126}}$, and 3 E_6 invariants in $\mathbf{27} \otimes \mathbf{27} \otimes \mathbf{27} \otimes \mathbf{650}$. 178
Table 21	Running time of the command <code>RepMatrices</code> which calculates explicitly the matrices of arbitrary representations of an arbitrary simple gauge group. 178
Table 22	Naming conventions and transformation properties of fields in the left-right symmetric regime (excluding conjugates). The last row exhibits the Pati-Salam regime fields from which they may originate. The charges under the $U(1)_{B-L}$ group shown here were multiplied by a factor $\sqrt{\frac{8}{3}}$. 190
Table 23	Naming conventions and transformation properties of fields in the Pati-Salam regime (excluding conjugates). The last row exhibits the $SO(10)$ representations from which they may originate. 190
Table 24	Naming conventions and transformation properties of fields in the $U(1)$ mixing regime (excluding conjugates). The last row exhibits the left-right regime fields from which they may originate. The charges under the $U(1)_{B-L}$ group shown here were multiplied by a factor $\sqrt{\frac{8}{3}}$. 191

LIST OF FIGURES

- Figure 1 ATLAS and CMS preliminary data on the measured signal strength in five different channels, where the horizontal bars represent the 68% confidence level intervals. The vertical lines show the result of combining all channels, together with the 68% confidence level bands (picture edited from [32] and [33]). Notably, the new 8 TeV data pulls CMS's $H \rightarrow \gamma\gamma$ cross section below the one predicted by the SM. [6](#)
- Figure 2 ATLAS and CMS preliminary data on the Higgs mass, in the two channels with the best energy resolution ($H \rightarrow \gamma\gamma$, $H \rightarrow ZZ$), and also the combined results. Image edited from [34] and [33]. [6](#)
- Figure 3 Comparison of the 1-loop evolution of the gauge coupling constants ($\alpha_i = g_i^2/4\pi$) with the energy scale E , for the Standard Model and the Minimal Supersymmetric Standard Model. By changing the slope of the lines in this plot, the extra fields in the MSSM allow the gauge coupling constants to unify. [9](#)
- Figure 4 ATLAS 95% confidence level lower bounds for some SUSY masses and scales, obtained through the analysis of different signals. Edited from [148] (see this reference for details). The CMS collaboration has produced comparable results [149]. [21](#)
- Figure 5 Diagrams which generate the different seesaw mechanisms. The mediator field might be a fermionic singlet (type-I seesaw), a scalar triplet (type-II seesaw), or a fermionic triplet (type-III seesaw). [33](#)
- Figure 6 List of all the complex simple Lie algebras. In the Dynkin diagrams, we have added a label to each dot indicating the simple root it represents. A permutation of these labels leads to a Cartan matrix with a different arrangement of rows and columns, but the underlying Lie algebra is the same. [56](#)
- Figure 7 The vertex $\psi^{i\dagger}\psi^i A_\mu^a$ is proportional to V_i^a . [95](#)
- Figure 8 The $U(1)$ gaugino mass matrix \mathbf{M} mixes gaugino fields. M_{ab} is the a, b component of \mathbf{M} . [95](#)
- Figure 9 Diagram contributing to the one-loop RGE of the bilinear scalar soft terms b^{ij} . Notice the contraction of the a and b indices between the \mathbf{V} 's and \mathbf{M} . [96](#)
- Figure 10 Sub-diagrams which give rise to $S(R)$ and $\text{Tr}[S(r)m^2]$ factors in the RGEs. [96](#)
- Figure 11 The three contribution from $U(1)$ groups to the term $24g^4 MM^* C(r) S(R)$. [97](#)

- Figure 12 Diagrams from which the β functions of $U(1)$ gaugino masses and gauge couplings are calculated. Notice the isolated \mathbf{G} which appears in the RGEs of \mathbf{G} itself. 97
- Figure 13 Diagrams contributing to the term $16g^4 S(R) C(R) M$ in the RGEs. 98
- Figure 14 One-loop gauge-coupling evolution in the MRV model [271]. The position of the GUT scale, the unified gauge coupling and the intermediate symmetry-breaking scale m_R were chosen in such a way as to fit the electroweak data with $\alpha_Y^{-1}(m_Z) = 59.73$. The close-to-zero brown line in the $[m_{B-L}, m_R]$ energy range depicts the evolution of the off-diagonal entries of the $\mathbf{A}^{-1} = 4\pi (\mathbf{G}\mathbf{G}^T)^{-1}$ matrix which, at the one-loop level, scales linearly with $\log E$. Likewise, in this energy range the red and yellow lines are the (1, 1) and (2, 2) diagonal entries of this matrix. The apparent discontinuity in α_Y^{-1} at the m_{B-L} scale is due to the generalized matching condition (see appendix D for details). 101
- Figure 15 The same as in figure (14) but without the kinetic mixing effects taken into account. With the same GUT-scale boundary condition and m_R , the low-energy value of α_Y^{-1} is 62.51 (orange solid line) and it differs from the one obtained in the full calculation by as much as 4%. Alternatively, if one attempts to obtain the right value of $\alpha_Y^{-1}(m_Z)$ by adjusting the $SU(2)_R$ breaking scale, the new m'_R scale must be shifted with respect to the correct m_R by as much as 4 orders of magnitude (vertical solid and dashed lines). 102
- Figure 16 Maximum value of Δb allowed by perturbativity as function of the scale m_R (in GeV). The three different lines have been calculated for three different values for the unified coupling α_G^{-1} , namely $\alpha_G^{-1} = 0, 3, 10$. A LR scale below 10 TeV (1 TeV) requires $\Delta b_3 \lesssim 5.7$ (5.2) if the extreme value of $\alpha_G^{-1} = 0$ is chosen, and $\Delta b_3 \lesssim 5.1$ (4.7) for $\alpha_G^{-1} = 3$. 110
- Figure 17 Gauge coupling unification in LR models with $m_R = 10^4$ GeV. The left panel is for $(\Delta b_3^{LR}, \Delta b_2^{LR}, \Delta b_R^{LR}, \Delta b_{B-L}^{LR}) = (0, 0, 1, 15/2)$ while the right one is for $(4, 4, 10, 4)$. 111
- Figure 18 Maximum value of $\Delta b_4^{PS} - \Delta b_3^{LR}$ allowed by perturbativity as function of the scale m_{PS} in GeV. The different lines have been calculated for six different values of Δb_3^{LR} . For this plot we assumed that $m_R = 1$ TeV. 115
- Figure 19 The number of possible variants of class-II models as a function of m_{PS} , assuming $m_R \approx 1$ TeV and 10^{16} GeV $\lesssim m_G \lesssim 2 \times 10^{18}$ GeV. 116

- Figure 20 Gauge coupling unification for PS models with $m_R = 1$ TeV. In the plot to the left $(\Delta b_3^{LR}, \Delta b_L^{LR}, \Delta b_R^{LR}, \Delta b_{B-L}^{LR}, \Delta b_4^{PS}, \Delta b_L^{PS}, \Delta b_R^{PS}) = (3, 5, 10, 3/2, 8, 5, 17)$, while the plot to the right corresponds to $\Delta b's = (3, 4, 12, 6, 8, 4, 12)$. Note that in the left plot m_{PS} is lower than 40 TeV therefore, in order to respect leptoquark mass bounds, the m_R scale must be raised. 118
- Figure 21 Gauge coupling unification in models with an $U(1)_R \times U(1)_{B-L}$ intermediate scale, for $m_R = 10^3$ GeV. Left: $(\Delta b_3^{LR}, \Delta b_L^{LR}, \Delta b_R^{LR}, \Delta b_{B-L}^{LR}, \Delta b_3^{B-L}, \Delta b_L^{B-L}, \Delta \gamma_{RR}, \Delta \gamma_{XR}, \Delta \gamma_{XX}) = (0, 1, 3, 3, 0, 0, 1/2, -\sqrt{3/8}, 3/4)$; Right: $(2, 2, 4, 8, 2, 2, 1/2, -\sqrt{3/8}, 11/4)$. The brown line, which appears close to zero in the $U(1)_R \times U(1)_{B-L}$ regime, is the running of the off-diagonal element of the matrix A^{-1} , measuring the size of the $U(1)$ -mixing in the model. The running of the diagonal components (1, 1) and (2, 2) of this matrix in the $U(1)_R \times U(1)_{B-L}$ regime are given by the red and yellow lines, respectively. 120
- Figure 22 The m_R dependence of the invariants in class-I models. The values $\Delta b_i^{LR} = (\Delta b_3^{LR}, b_L^{LR}, \Delta b_R^{LR}, \Delta b_{BL}^{LR})$ are as follows: $(2, 2, 9, 1/2)$ in the set 1 plot, $(1, 1, 7, 1)$ in the set 2 plot, $(4, 4, 3, 29/2)$ in the set 10 plot, and $(0, 0, 2, 6)$ in the set 14 plot. For a discussion, see the main text. 126
- Figure 23 The m_R dependence of the invariants in class-II model. The examples shown correspond to the following $\Delta b = (\Delta b_3^{LR}, \Delta b_L^{LR}, \Delta b_R^{LR}, \Delta b_{BL}^{LR}, \Delta b_4^{PS}, \Delta b_L^{PS}, \Delta b_R^{PS})$: $(0, 1, 10, 3/2, 14, 9, 13)$ in the set 3 plot, $(0, 0, 1, 9/2, 63, 60, 114)$ in the set 6 plot, $(0, 3, 12, 3/2, 6, 3, 15)$ in the set 7 plot, $(0, 0, 9, 3/2, 11, 8, 12)$ in the set 8 plot, and $(0, 0, 7, 3/2, 11, 8, 10)$ in the set 16 plot. 128
- Figure 24 The m_{B-L} dependence of the invariants in two class-III models. The examples shown correspond to the following $(\Delta b_3^{LR}, \Delta b_L^{LR}, \Delta b_R^{LR}, \Delta b_{BL}^{LR}, \Delta b_3^{B-L}, \Delta b_L^{B-L}, \Delta \gamma_{RR}, \Delta \gamma_{XR}, \Delta \gamma_{XX})$: $(0, 1, 3, 3, 0, 0, 1/2, -\sqrt{3/8}, 3/4)$ in the left plot, and $(2, 2, 4, 8, 2, 2, 1/2, -\sqrt{3/8}, 11/4)$ in the one on the right. By comparing the endpoints of the QU and LE lines we can measure the relative effects of the MSSM and $U(1)$ -mixing in breaking the relation $QU = LE$; with m_{B-L} at its highest, the models are identical to the MSSM almost up to the unification scale, so the splitting of the lines QU and LE on the right of each plot measures the MSSM effect at its maximum. Analogously, the splitting of the lines QU and LE on the left of each plot measures the $U(1)$ -mixing breaking of the relation $QU = LE$ at its maximum, without the MSSM's contribution. Clearly, in these two examples the MSSM effect is bigger. 129

- Figure 25 Parametric (LE, QE) plot for the different variants (see text). The thicker lines labeled with I, II, III and IV indicate the result for the four prototype models presented in [467]. 130
- Figure 26 Parametric (LE, QE) plots for different PS-variants showing the effect of the PS scale. 131
- Figure 27 Tree level contributions to R_K —through the W boson, and through a charged Higgs. 136
- Figure 28 Corrections to the $\nu\ell H^+$ vertex, as discussed in the text. 138
- Figure 29 $m_0 - M_{1/2}$ plane for $\tan\beta = 40$ and $A_0 = -500$ GeV, with $\delta_{\tau e}^{RR} = 0.1$. On the left (right) panel, a type-I (II) SUSY seesaw, considering degenerate heavy mediators. Contour lines denote values of Δr (decreasing values: positive—in association with an orange-yellow-white color gradient; negative—blue gradients); solid (gray) regions are excluded due to the requirement of having the correct EWSB. A green dot-dashed line corresponds to the present LHC bounds on the cMSSM [554]. A full green line delimits the $\text{BR}(\tau \rightarrow e\gamma)$ exclusion region, while full (dot-dashed) red lines correspond to the bounds on $\text{BR}(B_s \rightarrow \mu\mu)$ [$\text{BR}(B_u \rightarrow \tau\nu)$]. Finally, the region delimited by blue lines corresponds to having $\text{BR}(\mu \rightarrow e\gamma)$ within MEG reach (current bound—solid line, future sensitivity—dashed line). 144
- Figure 30 mSUGRA (type-I seesaw) $m_0 - M_{1/2}$ plane for $\tan\beta = 40$ and $A_0 = 0$ GeV, with $\delta_{\tau e}^{RR} = 0.1$ (left panel) and $\delta_{\tau e}^{RR} = 0.7$ (right panel). Contour lines denote values of Δr (decreasing values: positive—in association with an orange-yellow-white color gradient; negative—blue gradients). A full green line delimits the $\text{BR}(\tau \rightarrow e\gamma)$ exclusion region, while full (dot-dashed) red lines correspond to the bounds on $\text{BR}(B_s \rightarrow \mu\mu)$ ($\text{BR}(B_u \rightarrow \tau\nu)$). Superimposed are the regions for the Higgs boson mass: the dark band is for $125 \leq m_{h^0} \leq 126$ (GeV) and the lighter one marks the region where $124 \leq m_{h^0} \leq 127$ (GeV). 146
- Figure 31 Left panel: Δr as a function of the charged Higgs mass, m_{H^+} (in GeV). Yellow points have been subject to no cuts, blue points comply with the bounds on the masses (LEP+LHC), red points satisfy all bounds except $\text{BR}(B_u \rightarrow \tau\nu)$ and green points satisfy all bounds. Right panel: $\text{BR}(B_u \rightarrow \tau\nu)$ versus m_{H^+} . Red points satisfy only the bounds on the masses (LEP+LHC) while green points comply with all bounds. 147

- Figure 32 Left panel: Δr as a function of the lightest Higgs boson mass m_h (in GeV) for the range of parameters shown in table (18). Red points satisfy the bounds on the spectrum (LEP+LHC), blue points satisfy all bounds except $\text{BR}(B_u \rightarrow \tau\nu)$ and green points satisfy all bounds. Right panel: m_{H^+} versus A_0 , with the same color code. Both plots were produced by varying the different input parameters as in table (18). 149
- Figure 33 Ranges of variation of Δr in the unconstrained MSSM as a function of m_{H^+} (left panel), and as a function of $\text{BR}(\tau \rightarrow e\gamma)$ (right panel). The different input parameters were varied as in table (18) (notice that $\delta_{\tau e}^{RR} = 0.5$). On the left panel red points satisfy the bounds on the masses (LEP+LHC), blue points satisfy all bounds except $\text{BR}(B_u \rightarrow \tau\nu)$ and green points comply with all bounds. Similar color code on the right panel, except that blue points now comply with all bounds except $\text{BR}(B_u \rightarrow \tau\nu)$ and $\text{BR}(\tau \rightarrow e\gamma)$ while yellow denotes points only failing the bound on $\text{BR}(\tau \rightarrow e\gamma)$. 150
- Figure 34 Specific fields which are needed to break a group (rows) into a given subgroup (columns). 189

NOMENCLATURE

ATLAS	A toroidal LHC apparatus
BAO	Baryon acoustic oscillations
BBN	Big Bang nucleosynthesis
BSM	Beyond the Standard Model
CKM	Cabibbo–Kobayashi–Maskawa
CL	Confidence Level
cLFV	Charged lepton flavor violation
CLIC	Compact linear collider
CMB	Cosmic microwave background
CMS	Compact muon solenoid
cMSSM	Constrained Minimal Supersymmetric Standard Model
COMET	Coherent muon to electron transition
CP	Charge-parity
CPT	Charge-parity-time
DM	Darkmatter
EDM	Electric dipole moment
EW	Electroweak
EWSB	Electroweak symmetry breaking
FV	Flavor violation
GCU	Gauge couplings unification
GIM	Glashow–Iliopoulos–Maiani
GUT	Grand unified theory
HRS	Hall-Rattazzi-Sarid
IH	Inverted hierarchy
ILC	International linear collider
KATRIN	Karlsruhe tritium neutrino

LEP	Large electron–positron collider
LFC	Lepton flavor conservation
LFV	Lepton flavor violation
LHC	Large hadron collider
LSP	Lightest supersymmetric particle
MEG	Muon to electron and gamma
MFV	Minimal flavour violation
MIA	Mass insertion approximation
MRV	Malinský-Romão-Valle
MSSM	Minimal Supersymmetry Standard Model
mSUGRA	Minimal supergravity
NH	Normal hierarchy
NMSSM	Next-to-Minimal Supersymmetric Standard Model
NP	New physics
NUHM	Non-universal Higgs mass
PMNS	Pontecorvo-Maki-Nakagawa-Sakata
PS	Pati-Salam
QCD	Quantum chromodynamics
RG	Renormalization group
RGE	Renormalization group equation
RPV	R-parity violation
RPV	R-parity violation
SM	Standard Model
SUSY	Supersymmetry, Supersymmetric
VEV	Vacuum expectation value
WMAP	Wilkinson microwave anisotropy probe

Part I

THE STANDARD MODEL AND BEYOND

INTRODUCTION

Our understanding of the fundamental laws of Physics at the microscopic level is encoded in a relativistic quantum field theory—the Standard Model of Particle Physics (SM). It is a gauge theory based on the group $U(1)_Y \times SU(2)_L \times SU(3)_c$ whose last missing piece, the Higgs particle, appears to have been finally discovered at CERN. However, despite its many successes at explaining observations made by different experiments, the SM has several shortcomings.

One of them is the so called hierarchy problem. In principle, the mass of a fundamental scalar, such as the Higgs doublet in the SM, is subject to large radiative corrections, making it very sensitive to physics at high energies. Therefore, it seems unnatural that there is a scalar with a mass of the order of the electroweak scale, much lower than the Planck scale at which standard quantum field theory is expected to break down.

On the other hand, there is no explanation for the structure and parameter values of the SM. Is there any justification for the measured values of the electron mass and charge, for instance? It might just be that the Universe turns out to be this way, without an underlying reason. However, the idea that the fundamental laws or Physics are simpler and more predictive than they appear, as in Grand Unified Theories (GUTs), should not be dismissed.

The Standard Model also fails to explain some important experimental and observational data. Massive neutrinos are one example. Another one is the presence of non-luminous, weakly interacting matter in the Universe, which is known to exist due to its gravitational effects at galactic and cosmological scales. Through gravity, it is also known that there is something—a dark energy—which permeates the Universe and accelerates its expansion. Its density does not change significantly with time and appears to be fairly homogeneous in space, behaving as a vacuum energy. Yet, the observed dark energy density is much lower than naive predictions made from the SM's energy scale. Another important cosmological puzzle is the fact that, even though the Standard Model predicts similar amounts of matter and anti-matter, astronomical observations reveal very little anti-matter in the Universe.

It is worth mentioning that the force of gravity, from which the presence of dark matter and dark energy is inferred, is not described by the SM. This is due to the fact that the theories of General Relativity and Quantum Mechanics are conceptually very different from one another, so much so that almost a century of theoretical research has failed to merge the two.

Supersymmetric (SUSY) Grand Unified Theories described in this thesis try to address some of these issues. Two distinct research lines are examined. The first one is the computation of the renormalization group equations (RGEs) which are needed for the study of the phenomenology of these models at the energy scales

accessible to experiments. A second topic concerns the phenomenology of SUSY GUTs, in particular relations between particle masses and the enhancement of the $\Gamma(K \rightarrow e\nu)/\Gamma(K \rightarrow \mu\nu)$ ratio through charged lepton flavor violation (cLFV) interactions. Both of these research lines involve radiative corrections and renormalization in SUSY models, hence the title of the thesis.

This work is organized as follows. The next chapter contains a review of the shortcomings of the Standard Model, explaining also how supersymmetry (SUSY) can overcome some of them. As such, chapter 2 also presents a description of supersymmetric (SUSY) models in general, and the Minimal Supersymmetric Standard Model (MSSM) in particular.

The experimental evidence for massive neutrinos, as well as possible ways of accommodating them by extending the SM, is presented separately in chapter 3. In it, the possibility of having charged lepton flavor violation in supersymmetric models (in addition to neutral lepton flavor violation in neutrino oscillations) is also reviewed. These processes are interesting because any observation of cLFV clearly signals the presence of new Physics.

Chapter 4 is dedicated to the use of symmetry in Particle Physics, and its aim is twofold. On the one hand, it complements chapter 2 by motivating the introduction of supersymmetry from a theoretical perspective: it is the only possible non-trivial extension of the space-time symmetry group. On the other hand, it reviews the main concepts needed for a systematic analysis of Lie algebras used in gauge theories.

This generic treatment of Lie algebras is essential to the Mathematica program *Susyno*, which is described in the chapter that follows (chapter 5) and which is based on [1]. With the defining elements of a SUSY model, the program computes its Lagrangian and provides the 2-loop RGEs.

Chapter 6, adapted from [2], presents the 2-loop RGEs of softly broken SUSY models with more than one $U(1)$ gauge factor group. In these models, the $F_{\mu\nu}$ tensor associated to a $U(1)$ factor mixes with the other ones, and this is a feature requiring special care.

Models with $U(1)$ -mixing are not rare: the intermediate stages in GUTs such as some of the ones analyzed in chapter 7 do have this feature. Details of the high energy structure of SUSY GUTs are imprinted in the soft scalar masses at lower energies, and in this chapter we consider $SO(10)$ -inspired models in this context [3].

Chapter 8 revisits the ratio $\Gamma(K \rightarrow e\nu)/\Gamma(K \rightarrow \mu\nu)$ in constrained and unconstrained supersymmetric models. In principle, in such models this ratio can be significantly different from the SM prediction, due to cLFV interactions. However, one should look carefully at this observable, taking into consideration also the bounds on $\text{BR}(B_u \rightarrow \tau\nu)$, $\text{BR}(\tau \rightarrow e\gamma)$ and $\text{BR}(B_s \rightarrow \mu\mu)$ [4].

Finally, chapter 9 presents some concluding remarks.

The Standard Model was developed in the 1960s and 1970s, incorporating the electroweak (EW) theory [5–7] and the theory of strong interactions [8–17]. The discovery of neutral currents [18] and the W/Z bosons [19], the evidence that hadrons are composite [20–22], and more recently the discovery of a Higgs particle¹ [27, 28] (see figures (1) and (2)), were important milestones in the confirmation of the Standard Model.

Being a Yang–Mills theory [29], the model is defined by its group, $U(1)_Y \times SU(2)_L \times SU(3)_C$, and its particle content, presented in table (1). The gauge symmetry, together with the space-time one, severely constrains the possible Lagrangian terms (see appendix A). The strength of these terms is controlled by free parameters, which have been measured over decades with ever increasing precision. Electroweak precision tests at LEP indicate a remarkable agreement between theory and experiment [30]. One noteworthy example is the excellent agreement (better than 1 part in 10^9) between the measured anomalous magnetic moment of the electron, and its predicted value [31]. In the strong sector however, due to difficulties in making precise non-perturbative computations, presently the agreement between theory and experiment can only be checked to the percent level.

Representation	$U(1)_Y \times SU(2)_L \times SU(3)_C$	Spin	Flavors
$Q = (u_L, d_L)^T$	$(+\frac{1}{6}, \mathbf{2}, \mathbf{3})$	$\frac{1}{2}$	3
u_R	$(+\frac{2}{3}, \mathbf{1}, \mathbf{3})$	$\frac{1}{2}$	3
d_R	$(-\frac{1}{3}, \mathbf{1}, \mathbf{3})$	$\frac{1}{2}$	3
$L = (\nu_L, e_L)^T$	$(-\frac{1}{2}, \mathbf{2}, \mathbf{1})$	$\frac{1}{2}$	3
e_R	$(-1, \mathbf{1}, \mathbf{1})$	$\frac{1}{2}$	3
$H = (H^+, H^0)^T$	$(+\frac{1}{2}, \mathbf{2}, \mathbf{1})$	0	1

Table 1: Representations of the SM gauge group. All listed fermions are left-handed.

Despite these successes, the SM is widely regarded as just an effective theory of a more fundamental one. In the next section, we review some of the reasons why it is thought that there must be some new physics beyond the Standard Model.

¹ The mechanism responsible for the breakdown of the EW symmetry was suggested by Englert, Brout, Higgs, Guralnik, Hagen, and Kibble [23–26]. For simplicity, we refer to the associated scalar particle(s) as *Higgs boson(s)*.

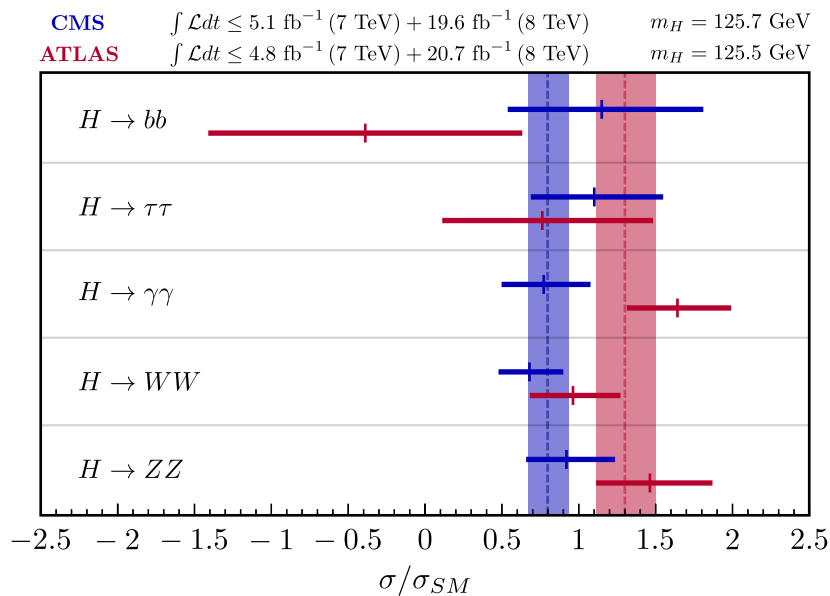


Figure 1: ATLAS and CMS preliminary data on the measured signal strength in five different channels, where the horizontal bars represent the 68% confidence level intervals. The vertical lines show the result of combining all channels, together with the 68% confidence level bands (picture edited from [32] and [33]). Notably, the new 8 TeV data pulls CMS's $H \rightarrow \gamma\gamma$ cross section below the one predicted by the SM.

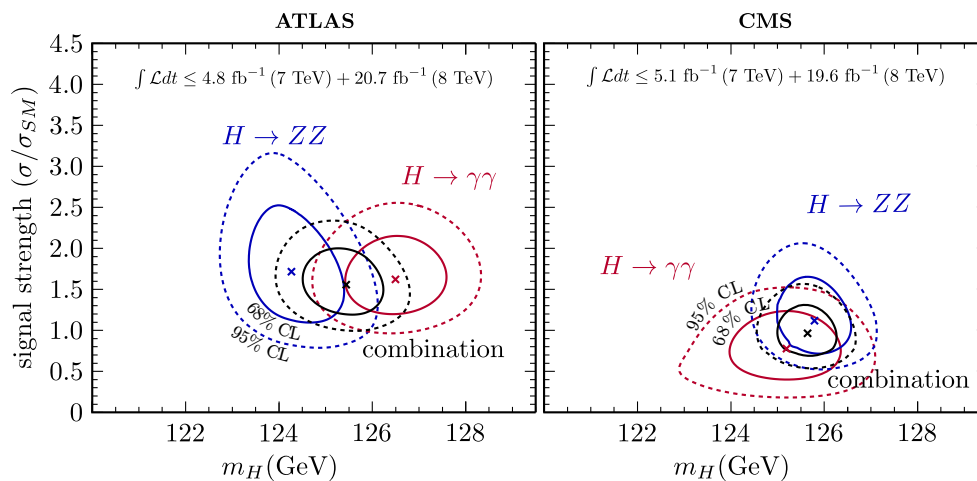


Figure 2: ATLAS and CMS preliminary data on the Higgs mass, in the two channels with the best energy resolution ($H \rightarrow \gamma\gamma$, $H \rightarrow ZZ$), and also the combined results. Image edited from [34] and [33].

2.1 SHORTCOMINGS OF THE STANDARD MODEL

2.1.1 *The hierarchy problem*

There has been a constant quest to explore ever smaller distances, or equivalently, ever higher energy regimes, in order to find a more fundamental understanding of the laws of Nature. It is therefore curious that the current Standard Model of Particle Physics is very sensitive to the cut-off scale Λ at which it ceases to be a valid effective theory [35–37]. This is because radiative corrections make the Higgs boson mass μ quadratically sensitive to this energy scale. Then, the measured value of μ , which is of the order of (Higgs vacuum expectation value)², must be the sum of a bare squared mass and a self energy of the order of Λ^2 . As such, unless we are willing to accept that there is a fine-tuned cancellation of these last two terms, the SM cut-off scale Λ must not be substantially larger than the electroweak scale. This is why it is widely believed that some new Physics must be present at the TeV energy range.

Following [38, 39], we recall that there is a precedent for this. In order to assemble a uniform, electrically charged sphere of radius R , it is necessary to spend some energy $E_{\text{self}} \sim \frac{1}{4\pi\epsilon_0} Q^2/R$ to overcome the repulsion between its charged components. Therefore, in the case of an electron with charge e , its total energy $m_e c^2$ is given by the sum of some bare mass term and this self energy E_{self} . Assuming that there is no accidental cancellation between these two terms, and since $\frac{1}{4\pi\epsilon_0} e^2/m_e c^2$ is of the order of femtometers, there are two possibilities: either the electron size is bigger than this, or classical electrodynamics ceases to be valid at distances smaller than $\sim 10^{-15}$ m. In either case, something previously unaccounted for becomes relevant at this scale. It turns out that the latter possibility is correct: quantum effects become significant, and classical electrodynamics is no longer a reliable theory at small distances.

In fact, with relativistic quantum electrodynamics, the divergence of the electron mass, which was linear in the cut-off scale $\Lambda \propto R^{-1}$, is reduced to a logarithmic one. The electron mass is said to be protected by the chiral symmetry, which relates the electron with its antiparticle (the newly introduced positron). Even though it is broken, this symmetry ensures that radiative corrections to m_e are proportional to m_e itself, implying that they can only depend on Λ through logarithms.

Similarly, in Yang–Mills theories such as the Standard Model, gauge bosons are massless due to the gauge symmetry. If this symmetry is spontaneously broken, the mass of gauge bosons becomes proportional to the Higgs mass, but the Higgs mass itself is not protected by any fundamental principle in the Standard Model. However, noting that bosons and fermions contribute radiatively to it with different signs, it is possible to build a symmetry that relates these two types of fields in such a way that the quadratic dependence of the Higgs mass on the cut off scale is canceled. Since it would mix different irreducible representations of the space-time symmetry group (bosons and fermions), this would therefore be a supersymmetry (see chapter 4 for a detailed discussion).

2.1.2 *Unexplained structure and parameter values*

The origin of the structure of the Standard Model, if there is one, remains a mystery. It is a Yang–Mills theory, but we do not know why there are three forces, with three distinct coupling strengths. The matter fields are scattered through small irreducible representations of the gauge group (there are only singlets, doublets of $SU(2)_L$ and triplets of $SU(3)_c$), but surprisingly the representations are such that the SM is an anomaly free theory, even though separately each matter field would generate anomalies (suggesting a connection between quarks and leptons). Left- and right-handed fermions are treated differently by the gauge symmetry, leading to a chiral theory with both charge-conjugation and parity symmetry violation. There is also the flavor puzzle, which relates to the existence of three copies of all fermionic representations even though, from a theoretical point of view, there seems to be no good reason for this.

In any case, once the symmetries and content of the SM have been established, building the most general Lagrangian consistent with them reveals a total of 19 physical parameters which must be measured:

- 3 gauge coupling constants;
- 9 fermion masses, 3 mixing angles and 1 phase;
- 2 parameters in the Higgs potential (μ and λ);
- 1 parameter related to topological effects and the strong CP problem (θ).

In the Standard Model, these are all free parameters. Yet, their values, obtained by different experiments, suggest that they are not completely arbitrary. For example, θ is very close to zero and also, in relation to the flavor structure of the SM, mixing angles are small in the quark sector and large in lepton sector.² On the other hand, fermion masses are spread over more than twelve orders of magnitude, exhibiting a strong hierarchy in flavor space (with the possible exception of neutrinos).

It is conceivable that our Universe is just the way it is, with no underlying reason. However, it is widely believed that this not the case, and that the Standard Model is just an effective model of a more fundamental and predictive one. A particular hypothesis that has received much attention over time [40–48] is the unification of all three forces of the SM in a grand unified theory, at high energies. In these theories, the fundamental gauge group is a simple one³ which spontaneously breaks into the smaller $U(1)_Y \times SU(2)_L \times SU(3)_c$ at low energies. Since the gauge group of a GUT is larger than the SM one, such a fundamental theory is more predictive than the effective one at lower energies. This implies that SM parameters, such as gauge and Yukawa couplings, are related amongst themselves in these theories. Also, the SM fields are assembled into larger representation of the fundamental

² Here we are assuming implicitly that the SM is extended in order to accommodate neutrinos with mass. Depending on whether or not neutrinos are Majorana particles, at least 9(7) new parameters are introduced in the theory.

³ It might also be a direct product of equal simple factor groups, together with some discrete symmetry relating them.

symmetry group, explaining (partially at least) why the matter fields are in the observed representations of the SM gauge group. It is indeed suggestive that all SM fermion representations fit in just two representations of the $SU(5)$ group (the $\bar{\mathbf{5}}$ and $\mathbf{10}$). In turn, together with a singlet representation (the right-handed neutrinos), these form an $SO(10)$ spinor representation ($\mathbf{16}$). We also note that, since non- $SU(n)$ simple Lie groups are known to be anomaly free [49, 50], this bundling of the SM fermions into a complete representation of $SO(10)$ ensures that the Standard Model is anomaly free.

Unification of the three forces can only occur if their strengths converge to a common value, as energy is increased and the full gauge symmetry is restored. The analysis of the renormalization group (RG) of the Standard Model does show that the differences between the three gauge coupling constants shrink as energy is increased. However, they never unify completely (figure (3)), but surprisingly, if the SM is supersymmetrized in a minimal way, the additional fields change the running of the gauge coupling constants in such a way that unification is indeed achieved.⁴ Even though the sensitivity to the SUSY scale is only logarithmic, we note that unification is consistent with $m_{SUSY} \sim 1$ TeV.

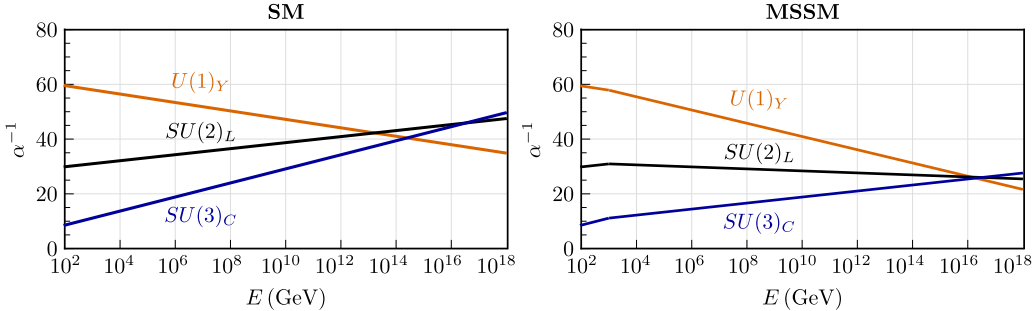


Figure 3: Comparison of the 1-loop evolution of the gauge coupling constants ($\alpha_i = g_i^2/4\pi$) with the energy scale E , for the Standard Model and the Minimal Supersymmetric Standard Model. By changing the slope of the lines in this plot, the extra fields in the MSSM allow the gauge coupling constants to unify.

Generally, GUTs lead to an unstable proton. The enlarged gauge symmetry transforms quarks into leptons and vice versa, which means that gauge interactions violate both baryon and lepton number. Indeed, through the exchange of heavy vector bosons (leptoquarks) with mass M_X , a dimension 6 effective operator allows the proton to decay into $e^+\pi^0$, with a partial lifetime $\tau(p \rightarrow e^+\pi^0) \sim M_X^4/\alpha_G^2 m_p^5$ where α_G is the unified coupling strength. In the non-supersymmetric SM, rough unification of the gauge coupling constants happens at $M_X \sim 10^{14-15}$ GeV, which implies that the proton lifetime is of the order of 10^{30-32} years [51, 52]. Yet experimental evidence shows that the proton's lifetime is much higher than this; Super-Kamiokande in particular has recently reported that $\tau(p \rightarrow e^+\pi^0)$ is larger than 1.29×10^{34} years at 90% confidence level [53]. In SUSY GUTs though, unification happens at higher energies, $M_X \sim 10^{16}$ GeV, and consequently $\tau(p \rightarrow e^+\pi^0)$ is predicted to be of the order of 10^{34-38} years (see [54, 55] and references

⁴ Note that SUSY is by no means the only way to achieve unification; adding other combinations of fields to the SM works equally well.

therein). On the other hand, exchanges of sparticles (the supersymmetric partners of known particles) can lead to dangerous dimension 5 operators [56–58] inducing the decay $p \rightarrow K^+\bar{\nu}$, which is experimentally constrained to be very rare as well ($\tau(p \rightarrow K^+\bar{\nu}) > 3.3 \times 10^{33}$ years at 90% confidence level [59]). Viable SUSY GUTs must therefore suppress or forbid altogether these operators. Also, in SUSY theories there are often renormalizable operators violating both baryon and lepton number which are gauge invariant. They are usually forbidden by the introduction of a special discrete symmetry, known as an R-symmetry. The MSSM is one such case, as we shall see latter on.

2.1.3 *Massive neutrinos*

A few years after the existence of neutrinos was postulated to explain the continuous beta decay spectrum, it was realized that their interaction cross section with matter is extremely small [60]. With a mean free path of several light-years in water (for typical beta decay energies), detection of such an elusive particle seemed all but impossible at the time. Yet neutrino physics has evolved remarkably, and nowadays it is possible to not only detect them but also measure some of their properties.

One of the most significant recent developments was the discovery that neutrinos have mass. In 1998 the Super-Kamiokande provided evidence that neutrinos oscillate [61], explaining the lower than expected solar neutrino flux, which had been both predicted and measured three decades earlier [62–64]. Since then, other solar, atmospheric, reactor and accelerator experiments have confirmed this phenomenon. Oscillations imply that neutrinos are massive and that leptons mix, but the Standard Model cannot accommodate this experimental evidence: neutrinos cannot have a Dirac mass (there are no right-handed neutrinos) nor a Majorana mass ($B - L$ is preserved even in non-perturbative processes [65–68]), so they are strictly massless in the Standard Model and therefore no leptonic mixing occurs.

This is an important and far reaching topic, which will be discussed in some detail latter on, in chapter 3. There, we review the known neutrino properties, as well as some of the theoretical frameworks that may account for them.

2.1.4 *Dark matter, dark energy and gravity*

For many decades, it has been known from the observation of the rotation speed of galaxies [69] that either something is wrong with the laws of gravity, or with the assumed sources of gravity. Over time, strong evidence has appeared in support of the latter hypothesis: it seems that there is more mass producing gravity beyond the ordinary one in stars and gas clouds. For example, in the Bullet Cluster [70], two colliding galaxy clusters leave behind interstellar gas (containing most of the ordinary baryonic matter), while most of the mass in the clusters goes right through one another, as measured via the weak gravitational lensing effect. This indicates that gravitational anomalies are localized and unrelated to normal matter.

At bigger, cosmological scales there is also strong evidence for the existence of non-luminous and non-baryonic cold dark matter (DM). From the precise measurement of the small anisotropies in the Cosmic Microwave Background (CMB), of the order of 1 part in 100000, it is estimated that the energy density of dark matter ρ_{cdm} in the Universe is [71]

$$\Omega_{cdm} = \frac{\rho_{cdm}}{\rho_c} = 0.263 \pm 0.013. \quad (2.1)$$

Here, $\rho_c = \frac{3H^2}{8\pi G}$ is the critical density of the Universe, H is the Hubble parameter valued today at $H_0 = 67.4 \pm 1.4$ km/s/Mpc by the Planck space observatory, and G is the gravitational constant. This value of ρ_{cdm} is much bigger than the energy density of baryons ρ_B , but lower than the one of the mysterious dark energy ρ_Λ , both of which are also obtainable from the CMB [71]:

$$\Omega_b = \frac{\rho_b}{\rho_c} = 0.049 \pm 0.002, \quad (2.2)$$

$$\Omega_\Lambda = \frac{\rho_\Lambda}{\rho_c} = 0.686 \pm 0.020. \quad (2.3)$$

Most of the dark matter must be made of some particle or particles yet to be discovered, and in order for its relic density to match observations, it must be completely stable or very long lived. It is also non-luminous and weakly interacting, having no electric charge nor color. Also, observations of the large scale structure of the Universe suggest that this dark matter must be mostly cold; in other words, it must be made of non-relativistic massive particles. This last property rules out an early dark matter candidate—the neutrinos in the SM or the MSSM [72–74] (it is now known that $\Omega_\nu \lesssim 0.01$ [71]). However, right-handed or sterile neutrinos are still viable candidates.

Given the observational evidence, dark matter is most likely predominantly made of particles with no electric charge nor color, with low velocities, and which are stable or very long lived. This last requirement is necessary in order to explain the observed dark matter relic abundance. There are in fact many dark matter candidates; the following are some of the best motivated ones (see for example [75]):

- Axions introduced as part of a solution to the strong CP problem, and their superpartners axinos.
- Kaluza-Klein excitations of SM fields, introduced in extra dimensions theories.
- Gravitinos, the superpartners of gravitons in theories where supersymmetry is imposed locally.
- Superpartners of SM particles, in particular the lightest supersymmetric particle (LSP) which often is a neutralino.

Concerning the last candidate in the above list, we note that with the introduction of R-parity in the MSSM to prevent the fast decay of the proton, the model gains

automatically a convincing DM candidate. The reason is simple: the R-charge assignment is such that SM fields get a multiplicatively conserved quantum number $+1$, while their yet to be discovered superpartners get -1 charges under this symmetry. Every term in the Lagrangian is invariant under this charge assignment, therefore perturbative processes must involve an even number of sparticles, and so the LSP cannot decay.

There is currently an ongoing effort by many collaborations to detect dark matter through its non-gravitational interactions. Direct detection experiments are buried deep underground in order to reduce background events and discern the rare scattering of dark matter particles off atomic nuclei. Indirect detection experiments, on the other hand, aim at observing the annihilation or decay products of dark matter, such as photons, electrons, positrons and neutrinos.

Direct detection experiments have produced conflicting results so far. The DAMA/NaI experiment and its successor DAMA/LIBRA have measured a signal with an annual modulation [76, 77] consistent with the varying relative speed of dark matter particles (with a mass of ~ 10 or ~ 70 GeV) as Earth orbits around the Sun. Such a modulation was also seen by the CoGeNT collaboration [78], in this case pointing to a ~ 10 GeV dark matter particle. Also, the CRESST experiment reported [79] a statistical significant excess of events. However, this set of results appears to be in contradiction [80] with the non-observation of an excess of events and/or an annual modulation by the CDMS [81, 82] and XENON collaborations [83]. Seemingly complicating matters further, in 2008 the CDMS observed two DM candidate events with germanium detectors (with low statistical significance) and recently, the same collaborations claims to have seen three more such events with its silicon detectors, consistent with a $6 - 15$ GeV dark matter particle [84]. The CDMS signal appears to be compatible with CoGeNT data, but not with the DAMA and CRESST results [84].

Indirect detection experiments have also produced some positive results (for a review, see [85]). The PAMELA [86], FERMI [87] and AMS-02 [88] experiments have measured an excess of positrons over the expected astrophysical background. Also, ATIC-2 [89], PPB-BETS [90], FERMI [91] and HESS [92, 93] see an excess of electrons plus positrons with energies of hundreds of GeV. However, no such excess of anti-protons was seen by PAMELA [94, 95]. If these signals are due to the annihilation of dark matter particles, taken together, they imply that dark matter is leptophilic, heavy (with a mass of \sim TeV) and with an annihilation cross section two orders of magnitude bigger than the one needed to explain its relic abundance. Finally, we note that there has been some claims of dark matter signals also in photon data; a notable one is that there is a gamma-ray line at around 130 GeV in FERMI's data [96, 97].

From the measurements of the anisotropies of the CMB, baryonic and dark matter account for only 30% of the energy density of the Universe. The remaining 70% are due to some dark energy (see equation (2.3)), which does not change much with time and appears to be roughly constant throughout space. It behaves like a cosmological constant in Einstein's equations, explaining therefore the observed accelerated expansion of the Universe [98, 99]. The simplest, microscopical

explanation for the cosmological constant is that it is due to the vacuum energy of some field(s). Even though these calculations have not been carried out rigorously, barring some cancellations, one expects that this energy density is roughly

$$\rho_{DE}^{\text{th}} \sim \int_0^\Lambda k^2 \sqrt{k^2 + m^2} dk \sim \Lambda^4, \quad (2.4)$$

for some cut-off energy Λ . Taking this Λ to be equal to the Planck mass ($\sim 10^{18}$ GeV) or even the lower EW scale (~ 100 GeV) yields a dark energy density dozens of orders of magnitude above the observed one, $\rho_{DE}^{\text{obs}} \sim (10^{-3} \text{ eV})^4$, and this the so-called cosmological constant problem (see for example [100]). Related to this, it is also puzzling that the energy density of the vacuum turns out to be, at the present time, of the same order of magnitude as the matter energy density (the coincidence problem).

To conclude this brief review of gravity related shortcomings of the SM, we also point out that the gravitational force itself is not described by the model. This is not a deficiency of the Standard Model in particular though, as it is well known that Quantum Mechanics in general is incompatible with General Relativity. Quantum Mechanics is very successful at describing small scale physics, while General Relativity has been shown to accurately explain the large scale dynamics of very massive systems. A back of the envelope calculation shows that at energies of the order of the Planck scale one would expect that quantum as well as gravitational effects become relevant, therefore a fundamental understanding of the laws of Physics appears to require a quantum theory of gravity. Nevertheless, it has been difficult to combine the two theories because they are very different in nature: in quantum field theory the metric is a background entity where fields propagate, while in General Relativity it is a classical but dynamical entity. Highlighting the challenging nature of uniting these two theories, almost a century of research has yielded many competing and unproven theories of quantum gravity, such a string theory, quantum loop gravity, supergravity, noncommutative geometry and twistor theory, just to name a few (for a recent review of these research programs, see the introductory section of [101]). We note in this regard that the Planck scale is much higher than the energies we can currently probe, so without dramatic experimental progress, it seems unlikely that this state of affairs will change.

2.1.5 *Baryogenesis and leptogenesis*

From the discussion above, one concludes that 95% of the content of the Universe is currently unknown. The remaining 5% are known to be mostly baryons, but even here there is a mystery (for reviews on this topic, see [102–104]). For temperatures lower than the proton mass, but before freeze-out, the baryon and anti-baryon number densities, n_b and $n_{\bar{b}}$, divided by the photon number density n_γ was

$$\frac{n_b}{n_\gamma}, \frac{n_{\bar{b}}}{n_\gamma} \sim \left(\frac{m_p}{T}\right)^{\frac{3}{2}} \exp\left(-\frac{m_p}{T}\right). \quad (2.5)$$

Using the known annihilation cross section for baryons, $\langle\sigma v\rangle\sim m_\pi^{-2}\sim(100\text{MeV})^{-2}$, we conclude that freeze-out happens for a temperature of about 20 MeV. However, this number is too low; it is 50 times smaller than the proton mass, meaning that the exponential factor in equation (2.5) heavily suppresses the number of baryons and anti-baryons, leading to ratios $n_b/n_\gamma, n_{\bar{b}}/n_\gamma$ of the order of 10^{-18} which would persist to this day. The observed baryon abundance (making up 5% of the Universe) implies a much larger value of n_b/n_γ though.

Yet another puzzle is that there seems to be very little anti-matter, despite the well know CPT symmetry relating matter and anti-matter. One possibility is that the Universe is made of regions with matter/anti-matter only, and that we happen to live in the middle of one of them. Since protons and anti-protons annihilate into detectable photons, these regions would need to be separated from one another by big gaps, possibly of the order of megaparsecs. This leads us to a second possibility, which is that those domains do not really exist, and the average baryon density n_b of the Universe is indeed bigger than its anti-baryon density $n_{\bar{b}}$. From the anisotropies of the CMB we know that [71]

$$\eta\equiv\frac{n_b-n_{\bar{b}}}{n_\gamma}=(6.05\pm 0.09)\times 10^{-10}. \quad (2.6)$$

Big Bang nucleosynthesis (BBN) provides another, independent measurement of η , because the production rate of some light nuclei, in particular ^2H , ^3He , ^4He and ^7Li , depends on this parameter. The value obtained in this way [105],

$$\eta=(5.8\pm 0.7)\times 10^{-10}, \quad (2.7)$$

agrees with the CMB value, although the abundance of ^7Li (and ^6Li) seems to point to a smaller η .

It is conceivable, in principle, that the Universe started with a baryon asymmetry which explains η , but this is unlikely because the Universe's inflationary period would have washed out this small initial asymmetry. So it seems more likely that at the beginning $n_b=n_{\bar{b}}$, and over time a non-zero η was dynamically generated. It turns out that the SM contains all the necessary ingredients to generate a baryonic asymmetry, even though it is a small one. These necessary ingredients were written down long ago [106]: in an out-of-equilibrium setting, there must be violation of baryon number, as well as violation of the C and CP symmetries. The SM fulfills all these conditions:

1. Due to its gauge invariance, in the SM it is possible to assign a baryon and a lepton number (B and L) to the various fields, which are conserved quantities in perturbative processes. However, these symmetries of the classical action are not symmetries of the quantum field theory, with conserves only $B-L$. The source of $B+L$ violation is the following. Not all gauge field configurations can be smoothly transformed into one another, and in particular there are infinite inequivalent configurations that minimize the energy. Separated by a potential barrier with a height $4\pi v/g\sim 5\text{TeV}$, these vacua solutions correspond to different values of $B+L$ and so there are solutions

to the field equations (instantons [65–67] and sphalerons [68]) related to transitions between these vacua which violate $B + L$. At low temperatures, the corresponding tunneling rate is negligible, but at the high temperatures of the early Universe this suppression can be overcome and the production rate of sphalerons can be significant [107].

2. The V-A structure of weak interactions violates the charge conjugation symmetry C maximally, and through the Cabibbo–Kobayashi–Maskawa (CKM) matrix V [108] they also violate the CP symmetry: $\text{Im} \left(V_{ij} V_{kl} V_{il}^* V_{kj}^* \right) \equiv J \sum_{m,n} \varepsilon_{ikm} \varepsilon_{jln}$, where $J = 2.96_{-0.16}^{+0.20} \times 10^{-5}$ is the Jarlskog invariant [109, 110]. Nevertheless, this value appears to be too small to generate the observed baryon asymmetry of the Universe [111–113].⁵
3. The SM provides out-of-equilibrium dynamics near its electroweak phase transition. When the Universe’s temperature dropped below the electroweak energy scale, in the middle of a EW symmetric plasma, bubbles started to form where the Higgs field had a (non-null) vacuum expectation value (VEV). These bubbles would have grown until they filled all space. For this to have happened though, this phase transition must have precise properties, and in particular the Higgs mass would have to be smaller than 70 GeV [114, 115] (for a review of this topic, see [116]).

So, generating the observed amount of baryons through the electroweak phase transition is not possible in the SM, but nevertheless it is an interesting idea which may work, for example, within the MSSM [117–120] although recent LHC data seem to disfavor it [121–125].

Another possibility is that the baryon asymmetry of the Universe was created from a leptonic one [126]. As we shall review in chapter 3, the SM needs to be extended in order to give mass to neutrinos, and if neutrinos are Majorana particles their mass term violates lepton number by two units. In the most conventional case, there are 3 heavy right-handed neutrinos N_i , with masses M_i and couplings $Y_i^\nu N_i LH$ to left-handed leptons and the Higgs doublet, which give a small mass $m_i^\nu = (Y_i^\nu v)^2 / M_i$ to the observed left-handed neutrinos through the seesaw mechanism. Produced in the early Universe, these heavy states would have generated an asymmetry of L ’s through CP violating decays, which in turn would have been transformed in a baryonic asymmetry by $B - L$ preserving sphalerons. This amounts to baryogenesis through leptogenesis.

2.2 SUPERSYMMETRY AND THE MSSM

Supersymmetry [127–129] addresses some of the SM shortcomings discussed previously. It consists of a symmetry which extends in a non-trivial way the one of Special Relativity and, for this reason, its irreducible representations—the supermultiplets—contain different irreducible representations of the Poincaré

⁵ The quantum chromodynamics (QCD) θ parameter is also a source of CP violation, but it too is very small (maybe even null).

group (each labeled with a helicity/spin, and a mass). In the following we review the main features of the Minimal Supersymmetric Standard Model (MSSM) which are mentioned latter on, throughout this thesis. Nevertheless, a more abstract discussion of SUSY can be read in chapter 4, which is dedicated exclusively to the use of symmetry in Particle Physics.

Some models are more supersymmetric than others. Yet, even a minimal amount of supersymmetry, sometimes called simple or $N = 1$ supersymmetry, is enough to severely restrict the couplings of a gauge theory. In order to write down the renormalizable Lagrangian of such a theory, a superpotential W is built,

$$W = \frac{1}{6} Y^{ijk} \Phi_i \Phi_j \Phi_k + \frac{1}{2} \mu^{ij} \Phi_i \Phi_j + L^i \Phi_i, \quad (2.8)$$

which is a cubic function of the chiral supermultiplets Φ_i , each containing a Weyl fermion ψ_i and a scalar ϕ_i . Alternatively, the Φ_i can be viewed as the scalar component ϕ_i of the chiral supermultiplets, in which case the Lagrangian density of a gauge theory associated to W can be written as

$$\begin{aligned} \mathcal{L}_{\text{SUSY}} = & -D^\mu \phi^{i*} D_\mu \phi_i + i \psi^{i\dagger} \bar{\sigma}^\mu D_\mu \psi_i - \frac{1}{2} \left(\frac{\delta^2 W}{\delta \phi_i \delta \phi_j} \psi_i \psi_j + \text{h.c.} \right) - \frac{\delta W}{\delta \phi_i} \left(\frac{\delta W}{\delta \phi_i} \right)^* \\ & - \frac{1}{4} F_{\mu\nu}^a F^{a\mu\nu} + i \lambda^{a\dagger} \bar{\sigma}^\mu D_\mu \lambda_a - \frac{1}{2} g^2 \left[(T^a)_{ij} \phi^{i*} \phi_j \right]^2 - g \kappa^a (T^a)_{ij} \phi^{i*} \phi_j \\ & - \left[\sqrt{2} g (T^a)_{ij} \phi^{i*} \psi_j \lambda^a + \text{h.c.} \right], \end{aligned} \quad (2.9)$$

with the field strength tensor and covariant derivatives as follows:

$$F_{\mu\nu}^a = \partial_\mu A_\nu^a - \partial_\nu A_\mu^a + g f^{abc} A_\mu^b A_\nu^c, \quad (2.10)$$

$$D_\mu \lambda^a = \partial_\mu \lambda^a + g f^{abc} A_\mu^b \lambda^c, \quad (2.11)$$

$$D_\mu \phi_i = \partial_\mu \phi_i - i g A_\mu^a (T^a)_{ij} \phi_j, \quad (2.12)$$

$$D_\mu \psi_i = \partial_\mu \psi_i - i g A_\mu^a (T^a)_{ij} \psi_j. \quad (2.13)$$

Here, g is the gauge coupling constant (the gauge group is assumed to be simple), f^{abc} are the group structure constants, and T^a are the representation matrices for each chiral supermultiplet. Note that the Fayet-Iliopoulos term with the κ parameter is only allowed for $U(1)$ gauge factors.

Supersymmetry pairs each fermion with a boson of equal mass. Since this is not seen experimentally, if SUSY is a symmetry of Nature, it must be a broken one at low energies. However, breaking it carelessly leads to a generic, non-supersymmetric theory with the scalar mass stability problem discussed previously. Therefore, in order to keep SUSY's good properties, namely the cancellation of quadratic divergences, the breaking terms must be of dimension lower than 4. In other words, SUSY breaking parameters must be dimensionful. If this is the case, supersymmetry is said to be only softly broken [130]. The most generic form usu-

ally considered for such terms is given by the following Lagrangian density,⁶ $\mathcal{L}_{\text{soft}}$, which should be added to $\mathcal{L}_{\text{SUSY}}$ in equation (2.9):

$$-\mathcal{L}_{\text{soft}} = \left(\frac{1}{2} M_a \lambda^a \lambda^a + \frac{1}{6} h^{ijk} \phi_i \phi_j \phi_k + \frac{1}{2} b^{ij} \phi_i \phi_j + s^i \phi_i + \text{h.c.} \right) + \left(m^2 \right)_j^i \phi_i \phi^{j*}. \quad (2.14)$$

Even though quadratic dependencies on the cutoff scale are gone, scalar masses in general, and the Higgs one in particular, still depend quadratically on other particle masses. As such, there is a clear motivation for an electroweak scale supersymmetry, where the soft masses are perhaps an order of magnitude, at most, above the Higgs vacuum expectation value.

If the SM is supersymmetrized, adding as little new fields as possible, we end up with the MSSM—the Minimal Supersymmetric Standard Model. Two of its features stand out. First, one Higgs doublet is no longer enough⁷ so the MSSM contains two, H_u and H_d , with different hypercharges. One of them (H_d) is in the same representation of the gauge group as left-handed leptons therefore, unless some differentiation is introduced, H_d is a fourth generation of left-handed leptons. Also, as discussed already in relation to the proton decay in GUTs, it is necessary to suppress or restrict altogether some baryon number violating couplings which are allowed by the gauge symmetry. To this end, in the MSSM there is a Z_2 -symmetry called R-parity, under which the down Higgs doublet and left-handed leptons are assigned different charges. The full chiral content of the MSSM is given in table (2), while gauge bosons and gauginos are presented in table (3).

The MSSM is completely specified by the chiral supermultiplet representations under the gauge group, and the $Z_2(R)$ charge assignments. All that remains is to write down the superpotential and soft SUSY breaking Lagrangian, using some notation for the model parameters:

$$\begin{aligned} W &= Y_{ij}^u \hat{U}_i^c \hat{Q}_j \cdot \hat{H}_u + Y_{ij}^d \hat{D}_i^c \hat{Q}_j \cdot \hat{H}_d + Y_{ij}^\ell \hat{E}_i^c \hat{L}_j \cdot \hat{H}_d + \mu \hat{H}_u \cdot \hat{H}_d, \quad (2.15) \\ -\mathcal{L}_{\text{soft}} &= \left[\frac{1}{2} M_1 \tilde{B} \tilde{B} + \frac{1}{2} M_2 \tilde{W}^a \tilde{W}^a + \frac{1}{2} M_3 \tilde{g}^a \tilde{g}^a + h_{ij}^u \tilde{u}_{Ri}^* \tilde{Q}_j \cdot H_u \right. \\ &\quad \left. + h_{ij}^d \tilde{d}_{Ri}^* \tilde{Q}_j \cdot H_d + h_{ij}^\ell \tilde{e}_{Ri}^* \tilde{L}_j \cdot H_d + b H_u \cdot H_d + \text{h.c.} \right] \\ &\quad + \left(m_Q^2 \right)_{ij} \tilde{Q}_i^* \tilde{Q}_j + \left(m_u^2 \right)_{ji} \tilde{u}_{Ri}^* \tilde{u}_{Rj} + \left(m_d^2 \right)_{ji} \tilde{d}_{Ri}^* \tilde{d}_{Rj} \\ &\quad + \left(m_L^2 \right)_{ij} \tilde{L}_i^* \tilde{L}_j + \left(m_e^2 \right)_{ji} \tilde{e}_{Ri}^* \tilde{e}_{Rj} + m_{H_u}^2 H_u^* H_u + m_{H_d}^2 H_d^* H_d. \quad (2.16) \end{aligned}$$

The R-charges of the superfields are in tables (2) and (3), but frequently it is more helpful to view things in terms of the bosons and fermions forming a superfield. In this respect, we note that R-symmetries are special since they express a symmetry

⁶ In some conditions [131], it is also possible to add Dirac masses to gauginos, $\psi_i \lambda_a$, and trilinear couplings $\phi^{i*} \phi_j \phi_k$.

⁷ There are two reasons for this. The first one is that the superpotential must be a holomorphic function of the superfields, which means that the SM trick of using the doublets H and H^* to give mass to down and up quarks/leptons cannot be used in supersymmetric theories. The second one is that simply doubling the number of SM fields would give rise to an anomalous theory, because of the introduction of a fermionic partner of the Higgs doublet.

Super-multiplet	Boson	Fermion	$U(1)_Y \times SU(2)_L \times SU(3)_C$	$Z_2(R)$	Flavors
\widehat{Q}	$\widetilde{Q} = (\widetilde{u}_L, \widetilde{d}_L)^T$	$Q = (u_L, d_L)^T$	$(+\frac{1}{6}, \mathbf{2}, \mathbf{3})$	-1	3
\widehat{U}^c	\widetilde{u}_R^*	u_R^\dagger	$(-\frac{2}{3}, \mathbf{1}, \overline{\mathbf{3}})$	-1	3
\widehat{D}^c	\widetilde{d}_R^*	d_R^\dagger	$(+\frac{1}{3}, \mathbf{1}, \overline{\mathbf{3}})$	-1	3
\widehat{L}	$\widetilde{L} = (\widetilde{\nu}_L, \widetilde{e}_L)^T$	$L = (\nu_L, e_L)^T$	$(-\frac{1}{2}, \mathbf{2}, \mathbf{1})$	-1	3
\widehat{E}^c	\widetilde{e}_R^*	e_R^\dagger	$(+1, \mathbf{1}, \mathbf{1})$	-1	3
\widehat{H}_u	$H_u = (H_u^+, H_u^0)^T$	$\widetilde{H}_u = (\widetilde{H}_u^+, \widetilde{H}_u^0)^T$	$(+\frac{1}{2}, \mathbf{2}, \mathbf{1})$	+1	1
\widehat{H}_d	$H_d = (H_d^0, H_d^-)^T$	$\widetilde{H}_d = (\widetilde{H}_d^0, \widetilde{H}_d^-)^T$	$(-\frac{1}{2}, \mathbf{2}, \mathbf{1})$	+1	1

Table 2: Chiral superfields in the MSSM

Fermion	Boson	$U(1)_Y \times SU(2)_L \times SU(3)_C$	$Z_2(R)$
\widetilde{B}	B	$(0, \mathbf{1}, \mathbf{1})$	+1
\widetilde{W}^a	W^a	$(0, \mathbf{3}, \mathbf{1})$	+1
\widetilde{g}^a	g^a	$(0, \mathbf{1}, \mathbf{8})$	+1

Table 3: Vector superfields in the MSSM

of the SUSY algebra, which may or may not be respected in a given model (see chapter 4). It is however important to note that they do not commute with supersymmetries and so, it turns out that in the particular case of the MSSM or any other $N = 1$ supersymmetric model, the fermion and the boson in a superfield are oppositely charged under R-parity. We can write this charge as a function of the spin s and the familiar baryon and lepton numbers [56]:

$$R = (-1)^{-2s+3B+L} . \quad (2.17)$$

It is tacitly assumed that the superfields \widehat{Q} ($B = 1/3$) and $\widehat{U}^c, \widehat{D}^c$ ($B = -1/3$) are the only ones with a non-null baryon number, while \widehat{L} ($L = 1$) and \widehat{E}^c ($L = -1$) are the only ones with a non-null lepton number. Without R-parity, lepton number violating terms $\widehat{L}\widehat{L}\widehat{E}^c, \widehat{L}\widehat{D}^c\widehat{Q}, \widehat{L}\widehat{H}_u$ as well as the baryon number violation term $\widehat{U}^c\widehat{D}^c\widehat{D}^c$ would be allowed in the superpotential. Yet the stability of the proton requires that the coupling of one of these two sets of terms must be very small or null [132–137].

The EW symmetry breaking and the mass eigenstates of this supersymmetrized version of the SM are the following. From the two Higgs VEVs, $\langle H_u^0 \rangle$ and $\langle H_d^0 \rangle$,

we may compute a SM-like one, $v = \sqrt{\langle H_u^0 \rangle^2 + \langle H_d^0 \rangle^2}$, and parametrize the ratio $\langle H_u^0 \rangle / \langle H_d^0 \rangle$ with an angle β :

$$\langle H_u^0 \rangle \equiv v_u = v \sin \beta, \quad \langle H_d^0 \rangle \equiv v_d = v \cos \beta. \quad (2.18)$$

At tree level, in addition to the $U(1)_Y$ and $SU(2)_L$ coupling constants, the neutral Higgs potential depends only on the μ , b , $m_{H_u}^2$ and $m_{H_d}^2$ parameters. As such, there must to be a connection between these parameters and $\{\beta, v\}$, or alternatively $\{\beta, m_Z\}$. This connection is provided by the minimization conditions of the scalar potential:

$$\sin 2\beta = \frac{2b}{2|\mu|^2 + m_{H_u}^2 + m_{H_d}^2}, \quad (2.19)$$

$$m_Z^2 = \frac{|m_{H_d}^2 - m_{H_u}^2|}{\sqrt{1 - \sin^2 2\beta}} - m_{H_u}^2 - m_{H_d}^2 - 2|\mu|^2. \quad (2.20)$$

Using these relations, the variables $\{|\mu|, b\}$ can then be swapped by $\{m_Z, \tan \beta\}$, which is common practice. Note however that by opting to use the latter ones, the sign of μ must still be provided.

Doubling the number of Higgs fields in the MSSM yields a total of 5 massive Higgs bosons after EW symmetry breaking. Three are neutral (the CP-even h^0 and H^0 , and the CP-odd A^0) and two are charged (H^\pm):

$$\begin{aligned} \begin{pmatrix} H_u^0 \\ H_d^0 \end{pmatrix} &= \begin{pmatrix} v_u \\ v_d \end{pmatrix} + \frac{1}{\sqrt{2}} \begin{pmatrix} \cos \alpha & \sin \alpha \\ -\sin \alpha & \cos \alpha \end{pmatrix} \begin{pmatrix} h^0 \\ H^0 \end{pmatrix} \\ &\quad + \frac{i}{\sqrt{2}} \begin{pmatrix} \sin \beta & \cos \beta \\ -\cos \beta & \sin \beta \end{pmatrix} \begin{pmatrix} G^0 \\ A^0 \end{pmatrix}, \end{aligned} \quad (2.21)$$

$$\begin{pmatrix} H_u^+ \\ H_d^{-*} \end{pmatrix} = \begin{pmatrix} \sin \beta & \cos \beta \\ -\cos \beta & \sin \beta \end{pmatrix} \begin{pmatrix} G^+ \\ H^+ \end{pmatrix}. \quad (2.22)$$

The three G fields in these expressions are the pseudo-Nambu-Goldstone bosons [138, 139], which become the longitudinal components of the massive EW bosons. The mixing angle α is given by

$$\frac{\tan 2\alpha}{\tan 2\beta} = \frac{2|\mu|^2 + m_{H_u}^2 + m_{H_d}^2 + m_Z^2}{2|\mu|^2 + m_{H_u}^2 + m_{H_d}^2 - m_Z^2}. \quad (2.23)$$

At tree level, the mass of the Higgs particles are the following:

$$m_{A^0}^2 = 2|\mu|^2 + m_{H_u}^2 + m_{H_d}^2, \quad (2.24)$$

$$m_{h^0, H^0}^2 = \frac{1}{2} \left(m_{A^0}^2 + m_Z^2 \mp \sqrt{(m_{A^0}^2 - m_Z^2)^2 + 4m_Z^2 m_{A^0}^2 \sin^2 2\beta} \right), \quad (2.25)$$

$$m_{H^\pm}^2 = m_{A^0}^2 + m_W^2. \quad (2.26)$$

In this approximation, the mass of h^0 (the lightest Higgs) increases with $m_{A^0}^2$, so there is an upper bound for it which is reached in the limit $m_{A^0} \gg m_Z$ [140, 141]:

$$m_{h^0} < m_Z |\cos 2\beta| < m_Z. \quad (2.27)$$

This stringent, electroweak related bound on the lightest Higgs mass follows from the fact that h^0 's quartic coupling λ is fixed and proportional to $g^2 + g'^2$, unlike in the SM where it is a free parameter. The mass value in equation (2.27) was nevertheless excluded by LEP2, which set a 114.4 GeV lower limit on the Higgs mass, at 95% confidence level (CL) [142]. This result seemingly precludes SUSY at the EW scale, or at least a very big set of SUSY models, such as the MSSM. However, the Higgs mass is known to be very sensitive to radiative corrections; the quadratic dependence on the cutoff scale has been eliminated, but there are still quadratic dependencies on the splitting between particle and sparticle masses introduced by $\mathcal{L}_{\text{soft}}$. Therefore, in theory, the lightest Higgs in the MSSM can have an arbitrarily large mass, but in order not to reintroduce a fine tuning problem in the theory, these radiative corrections should not be too large. There is no unique and objective criterion to evaluate this, but there is a general belief that the sparticles masses should not be much heavier than 1 TeV. Yet, to this date, LHC searches for gluino and squarks have found nothing (see figure (4)). However, the recent discovery of a 125 GeV Higgs particle is compatible with a 1 TeV scale supersymmetry, because the limit on m_{h^0} is raised to 135 GeV by radiative corrections (see [131] and references therein). The main contribution usually comes from an incomplete cancellation between top and stop loops [143–145], which can be written in an approximate way as follows (see also [146, 147]):

$$m_{h^0}^2 < m_Z^2 + \frac{3g^2 m_t^4}{8\pi^2 m_W^2} \left[\log \left(\frac{m_S^2}{m_t^2} \right) + \frac{X_t^2}{m_S^2} \left(1 - \frac{X_t^2}{12m_S^2} \right) \right], \quad (2.28)$$

where $X_t \equiv A_t - \mu \cot \beta$ ($h^x \equiv A_x Y^x$) is the stop mixing parameter and $m_S \equiv \sqrt{m_{\tilde{t}_1} m_{\tilde{t}_2}}$ is their geometric mean mass. The stops \tilde{t}_1 and \tilde{t}_2 are mainly a mixture of the superpartners of the right and left handed stops. In fact, while the effect is

ATLAS 95% confidence level lower bounds for SUSY masses

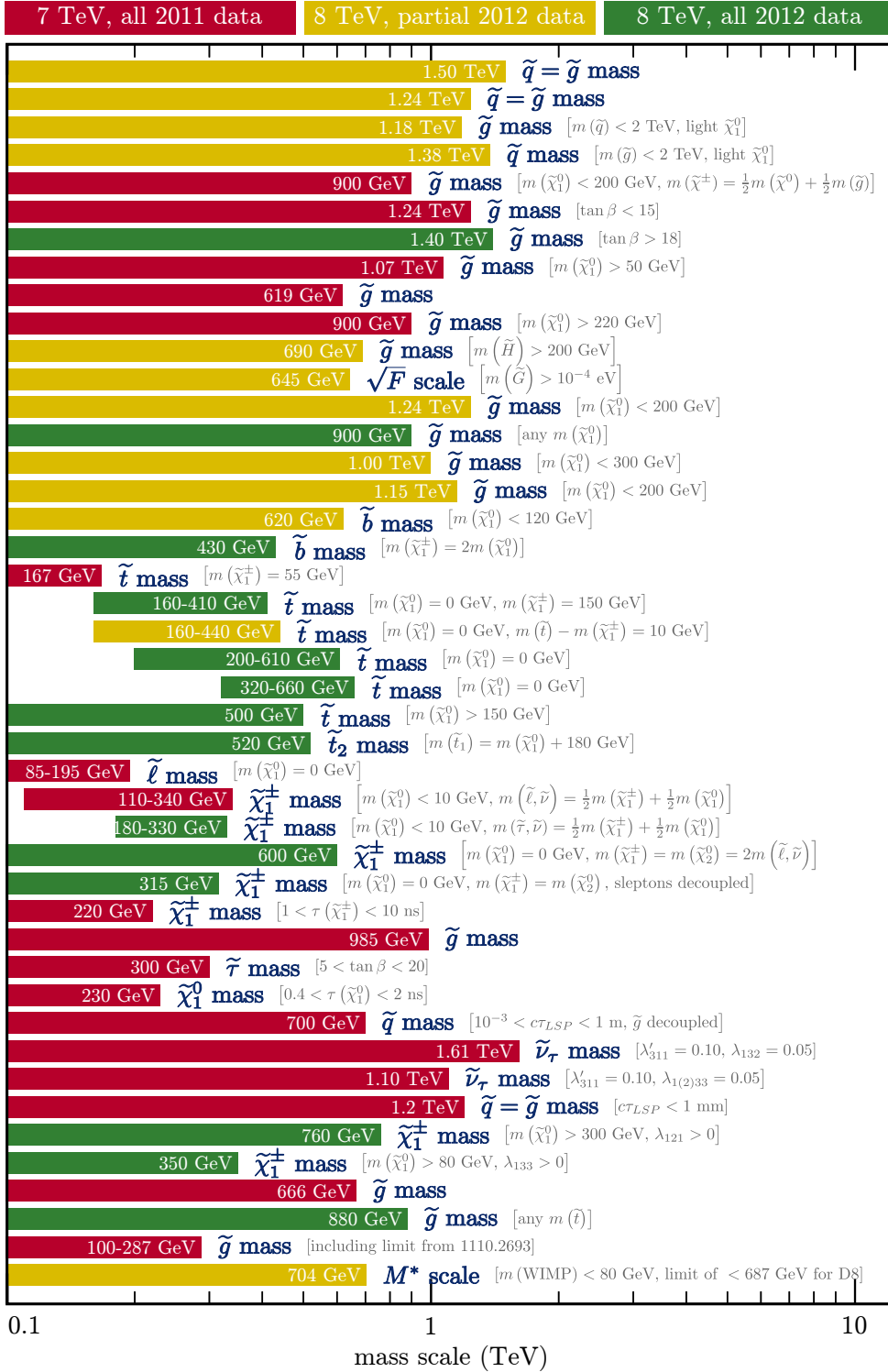


Figure 4: ATLAS 95% confidence level lower bounds for some SUSY masses and scales, obtained through the analysis of different signals. Edited from [148] (see this reference for details). The CMS collaboration has produced comparable results [149].

more pronounced in the third generation, all squarks and all sleptons mix amongst themselves. Consider the following squark and slepton mass terms,

$$\begin{aligned}
-\mathcal{L} = \dots + & \left(\tilde{u}_L^* \tilde{u}_R^* \right) M_u^2 \begin{pmatrix} \tilde{u}_L \\ \tilde{u}_R \end{pmatrix} + \left(\tilde{d}_L^* \tilde{d}_R^* \right) M_d^2 \begin{pmatrix} \tilde{d}_L \\ \tilde{d}_R \end{pmatrix} \\
& + \left(\tilde{e}_L^* \tilde{e}_R^* \right) M_\ell^2 \begin{pmatrix} \tilde{e}_L \\ \tilde{e}_R \end{pmatrix} + \tilde{\nu}_L^* M_\nu^2 \tilde{\nu}_L + \dots \quad (2.29)
\end{aligned}$$

Since there are three generations of chiral superfields, M_u^2 , M_d^2 , M_ℓ^2 are 6×6 matrices and M_ν^2 is a 3×3 mass matrix. They have the following block form:

$$M_u^2 = \begin{pmatrix} m_Q^2 + Y^{u\dagger} Y^u |v_u|^2 + \Delta_{\tilde{u}_L} \mathbb{1} & \text{(h.c.)} \\ h^u v_u - \mu^* Y^u v_d^* & m_u^2 + Y^u Y^{u\dagger} |v_u|^2 + \Delta_{\tilde{u}_R} \mathbb{1} \end{pmatrix}, \quad (2.30)$$

$$M_d^2 = \begin{pmatrix} m_Q^2 + Y^{d\dagger} Y^d |v_d|^2 + \Delta_{\tilde{d}_L} \mathbb{1} & \text{(h.c.)} \\ h^d v_d - \mu^* Y^d v_u^* & m_d^2 + Y^d Y^{d\dagger} |v_d|^2 + \Delta_{\tilde{d}_R} \mathbb{1} \end{pmatrix}, \quad (2.31)$$

$$M_\ell^2 = \begin{pmatrix} m_L^2 + Y^{\ell\dagger} Y^\ell |v_d|^2 + \Delta_{\tilde{e}_L} \mathbb{1} & \text{(h.c.)} \\ h^\ell v_d - \mu^* Y^\ell v_u^* & m_e^2 + Y^\ell Y^{\ell\dagger} |v_d|^2 + \Delta_{\tilde{e}_R} \mathbb{1} \end{pmatrix}, \quad (2.32)$$

$$M_\nu^2 = \left(m_L^2 + \Delta_{\tilde{\nu}_L} \mathbb{1} \right), \quad (2.33)$$

where the Δ 's depend on the electric charge Q and the $SU(2)_L$ isospin T_3 of each field,

$$\Delta_\phi \equiv \left[(T_{3\phi} - Q_\phi) m_Z^2 + Q_\phi m_W^2 \right] \cos 2\beta. \quad (2.34)$$

The off-diagonal blocks in these mass matrices mix left and right sparticles, but in some situations they can be ignored for the first two generations. On the other hand, mixing between stops, sbottoms and staus is significant, therefore $\tilde{t}_{L/R}$, $\tilde{b}_{L/R}$ and $\tilde{\tau}_{L/R}$ give rise to mass eigenstates $\tilde{t}_{1/2}$, $\tilde{b}_{1/2}$ and $\tilde{\tau}_{1/2}$. For stops in particular, this mixing is enhanced with a big X_t factor, and so a 125 GeV Higgs boson seems to imply a large top trilinear coupling A_t and/or a large $\tan \beta$.⁸ However, these two parameters also have implications for low-energy Physics; in particular many processes violating charged lepton number depend on the sixth power of $\tan \beta$, while $\text{BR}(B_s \rightarrow \mu\mu)$ is sensitive to A_t . We shall mention this again in chapter 3.

The fermionic superpartners of the Higgs and electroweak vector bosons—the Higgsinos and electroweak gauginos—also mix, forming mass eigenstates known as neutralinos $\chi_{1,2,3,4}^0$ (neutral) and charginos $\chi_{1,2}^\pm$ (charged):

$$-\mathcal{L} = \frac{1}{2} \tilde{N}^T M_{\tilde{N}} \tilde{N} + \frac{1}{2} \tilde{C}^T M_{\tilde{C}} \tilde{C} + \text{h.c.} + \dots, \quad (2.35)$$

⁸ The radiative corrections to $m_{h^0}^2$ given by equation (2.28) are maximal for $X_t = \sqrt{6} M_S$ and minimal when $X_t = 0$.

with $\tilde{N} = (\tilde{B}, \tilde{W}^0, \tilde{H}_d^0, \tilde{H}_u^0)^T$, $\tilde{C} = (\tilde{W}^+, \tilde{H}_u^+, \tilde{W}^-, \tilde{H}_d^-)^T$ and the matrices $M_{\tilde{N}}$, $M_{\tilde{C}}$ are given by

$$M_{\tilde{N}} = \begin{pmatrix} M_1 & \cdot & \cdot & (\text{sym.}) \\ 0 & M_2 & \cdot & \cdot \\ -\frac{g'v_d}{\sqrt{2}} & \frac{gv_d}{\sqrt{2}} & 0 & \cdot \\ \frac{g'v_u}{\sqrt{2}} & -\frac{gv_u}{\sqrt{2}} & -\mu & 0 \end{pmatrix}, \quad (2.36)$$

$$M_{\tilde{C}} = \begin{pmatrix} 0 & \cdot & \cdot & (\text{sym.}) \\ 0 & 0 & \cdot & \cdot \\ M_2 & gv_u & 0 & \cdot \\ gv_d & \mu & 0 & 0 \end{pmatrix}. \quad (2.37)$$

The MSSM as described above contains 124 physical real degrees of freedom [150, 151], which hardly makes it a minimal model in terms of number of parameters. The SM, with just 19 degrees of freedom, is able to describe successfully most of the experimental data, so it is not surprising that a large portion of the MSSM's bigger parameter space is already excluded. Unsuppressed couplings and mass terms can lead to large charged lepton flavor violation, flavor changing neutral currents and/or new sources of CP violation which lead to big electric dipole moments, all of which are experimentally ruled out (see chapter 3). For this reason, analyzing the phenomenology of the MSSM is complicated unless its parameter space is reduced by taking into account low energy experimental data. The phenomenological MSSM (pMSSM) [152] is one commonly used constrained model, where there are only 19 input parameters (although this model is often generalized): it assumes that there are no new complex phases in $\mathcal{L}_{\text{soft}}$, that the soft SUSY breaking scalar masses are diagonal and the same for the first/second generations, and also that trilinear scalar couplings are null for the first/second generations.

From a theoretical point of view, the large parameter space of the MSSM is also a problem because this model is more fundamental than the SM, and yet it is less predictive. The source of this problem is our lack of knowledge of the SUSY breaking mechanism, which forces the introduction of the most general soft SUSY breaking Lagrangian. Knowing this, several *ansätze* for $\mathcal{L}_{\text{soft}}$ were proposed over the years by different authors, inspired on different SUSY breaking mechanisms. We shall mention here only the minimal supergravity inspired MSSM (mSUGRA) [153–155], also known as the constrained MSSM (cMSSM) [156], which hypothesizes that SUSY is broken in some hidden sector which only communicates with the visible one through the gravitational interaction. The assumptions on the parameters at the GUT scale m_G (which is the scale at which the gauge couplings unify) are the following:

1. Gaugino mass unification: $M_1(m_G) = M_2(m_G) = M_3(m_G) = M_{1/2}$.
2. Universal scalar SUSY breaking masses: $m_{\tilde{Q}}^2 = m_{\tilde{L}}^2 = m_u^2 = m_d^2 = m_e^2 \equiv m_0^2$ and $m_{H_u}^2 = m_{H_d}^2 = m_0^2$.

3. Universal trilinear SUSY breaking terms: $h^x \equiv A_0 Y^x$, $x = u, d, \ell$.

As for the parameters μ and b , through the equations (2.19) and (2.20) they can be replaced by $\tan \beta$ and $\text{sign}\mu$. Therefore, mSUGRA requires only 5 input parameters: $M_{1/2}$ (the common gaugino mass), m_0 (the common scalar mass), A_0 (the common trilinear coupling factor), $\tan \beta$ (the ratio of neutral Higgs VEVs at the electroweak scale), and $\text{sign}\mu$. The limited parameter space, as well as the smallness of the induced CP and flavor violations, makes the mSUGRA interesting. However, the discovery at CERN of a heavy Higgs implies that SUSY masses must be heavier than originally thought, and this is particularly true for the mSUGRA since there are less ways to raise m_{h^0} without raising the whole sparticle spectrum [157–169]. In chapter 8 we shall encounter a generalization of the mSUGRA, where the Higgs scalar masses $m_{H_u}^2$ and $m_{H_d}^2$ are free parameters. This Non-Universal Higgs Masses (NUHM) model [170, 171] is interesting because it decouples the Higgs masses from the other scalar masses, potentially enhancing the amplitude of some Higgs mediated processes.

3.1 MASSIVE NEUTRINOS

3.1.1 *A brief history of neutrino experiments*

Pontecorvo was the first to suggest that detection of neutrinos was feasible, using big amounts of liquid chlorine [172]. With this method, in 1956 Cowan and Reines detected reactor anti-neutrinos $\bar{\nu}_e$ [173] (their initial idea was to use nuclear explosions [174]) and years later, in 1962 and 2000, neutrinos associated with the muon and the tau were also directly observed [175, 176]. In the meantime, several experiments were built to detect neutrinos of extraterrestrial origin. Nuclear reactions in the Sun's core make it by far the biggest available source of such neutrinos in the detectable energy range (\sim MeV). When the flux of these neutrinos was first measured [64], it did not match the theoretical prediction which was derived with remarkable precision from nuclear cross sections and life-times [62]. It was realized [177–179] that neutrino oscillations/conversion could be the reason for the solar neutrino deficit [180–182]: most of the Sun's energy is produced by the proton-proton chain reaction, where protons combine to produce heavier nuclei (such as deuterium, ^2He , ^3He , ^4He , ^7Li , ^7Be , ^8Be and ^8B) as well as positrons and electron neutrinos ν_e . If these neutrinos change their nature between production and detection, the measured flux can be lower than the calculated value. After mounting evidence from the Homestake [64], Kamiokande [183], SAGE [184], and GALLEX [185] experiments, in 2002 the SNO collaboration confirmed that this is indeed the explanation for the solar neutrino problem [186].

A few years earlier though, the heavy water Cherenkov detector Super-Kamiokande, built to detect proton decay, had already found evidence of the oscillation of neutrinos with higher energies (\sim GeV) produced by the collisions of cosmic rays with nuclei in the upper atmosphere [61]. These collisions produce pions which then decay into electron and muon neutrinos, and data showed a deficit of the latter which could however be explained by the oscillation of ν_μ into another neutrino type, possibly ν_τ . The fact that this deficit depended on the neutrino flight distance (or equivalently the zenith angle) made this evidence even more compelling.

Other solar, atmospheric, reactor and beam neutrino experiments have since then provided increasingly accurate values of the neutrino oscillation parameters (see for example [187] for an up-to-date review of the experimental and theoretical progress).

3.1.2 Neutrino oscillation parameters

Assuming that neutrinos are massive and that leptons mix, the mass eigenstates ν_i of non-degenerate neutrinos are a linear combination of the neutrino states ν_α produced in weak interactions. These two bases are related by the leptonic mixing matrix U —the so called Pontecorvo-Maki-Nakagawa-Sakata (PMNS) matrix:

$$\nu_\alpha = \sum_i U_{\alpha i} \nu_i. \quad (3.1)$$

In the plane wave formalism, ultrarelativistic neutrinos ν_α with an energy E have a probability of oscillating to a different flavor ν_β , after traveling a distance L in vacuum, which is given by [188]

$$P(\nu_\alpha \rightarrow \nu_\beta) = \delta_{\alpha\beta} - 4 \sum_{i < j} \operatorname{Re} \left(J_{\alpha\beta}^{ij} \right) \sin^2 \varphi_{ij} + 2 \sum_{i < j} \operatorname{Im} \left(J_{\alpha\beta}^{ij} \right) \sin 2\varphi_{ij}, \quad (3.2)$$

where

$$J_{\alpha\beta}^{ij} \equiv U_{\alpha i}^* U_{\beta i} U_{\alpha j} U_{\beta j}^*, \quad \varphi_{ij} \equiv \frac{\Delta m_{ij}^2 L}{4E}, \quad \Delta m_{ij}^2 = m_i^2 - m_j^2. \quad (3.3)$$

This expression implies that oscillation experiments are only sensitive to squared mass differences. In other words, shifting all squared masses by a constant term, $m_i^2 \rightarrow m_i^2 + M^2$, does not change the oscillation probabilities.

It is instructive to consider just two neutrino flavors. In such case, there is only one mass squared difference Δm^2 and the mixing matrix is described by a single angle θ : $U_{11} = U_{22} = \cos \theta$ and $U_{12} = -U_{21} = \sin \theta$. In this simplified scenario, equation (3.2) is given by

$$P(\nu_\alpha \rightarrow \nu_\beta) = \sin^2 2\theta \sin^2 \frac{\Delta m^2 L}{4E}, \quad \alpha \neq \beta. \quad (3.4)$$

There are two important quantities here: the oscillation depth $\sin^2 2\theta$ which corresponds to the maximum oscillation probability ($\theta = \pm\pi/4$ maximizes it), and the oscillation length l_ν given by

$$l_\nu \equiv \frac{4\pi E}{\Delta m^2} \approx 2.48 \frac{E}{1 \text{ GeV}} \frac{1 \text{ eV}^2}{\Delta m^2} \text{ km}. \quad (3.5)$$

The picture that emerges from various experiments is that the three neutrinos weakly interacting with charged leptons mix into three mass eigenstates. The two mass squared differences and the mixing angles obtained from a global analysis are given in table (4). From matter effects in the Sun (see below), it is known that the mass eigenstate denoted by ν_1 is lighter than ν_2 , and since $|\Delta m_{31}^2| \gg \Delta m_{21}^2$, there are two possible orderings of the three neutrino masses, depending on the sign of Δm_{31}^2 : the normal hierarchy (NH) $m_1 < m_2 < m_3$ and the inverted hierarchy (IH) $m_3 < m_1 < m_2$.

Parameter	Best fit $\pm 1\sigma$ errors
$\Delta m_{21}^2 (10^{-5} \text{ eV}^2)$	$7.62^{+0.19}_{-0.19}$
$ \Delta m_{31}^2 (10^{-3} \text{ eV}^2)$	$\begin{cases} 2.55^{+0.06}_{-0.09} & \text{NH} \\ 2.43^{+0.07}_{-0.06} & \text{IH} \end{cases}$
$\sin^2 \theta_{12}$	$0.320^{+0.016}_{-0.017}$
$\sin^2 \theta_{23}$	$\begin{cases} 0.613^{+0.022}_{-0.04} \left(0.427^{+0.034}_{-0.027} \right) & \text{NH} \\ 0.600^{+0.026}_{-0.031} & \text{IH} \end{cases}$
$\sin^2 \theta_{13}$	$\begin{cases} 0.0246^{+0.0029}_{-0.0028} & \text{NH} \\ 0.0250^{+0.0026}_{-0.0027} & \text{IH} \end{cases}$

Table 4: Best fit and 1σ ranges for the neutrino parameters obtained from a global three neutrino oscillation analysis [189]. The value of $\sin^2 \theta_{23}$ in parenthesis is also compatible with experimental data. See also [190–192] for comparable values.

The three angles in table (4) are a reference to the usual parametrization of the lepton mixing matrix,

$$U = \begin{pmatrix} 1 & 0 & 0 \\ 0 & c_{23} & s_{23} \\ 0 & -s_{23} & c_{23} \end{pmatrix} \begin{pmatrix} c_{13} & 0 & s_{13}e^{-i\delta} \\ 0 & 1 & 0 \\ -s_{13}e^{i\delta} & 0 & c_{13} \end{pmatrix} \begin{pmatrix} c_{12} & s_{12} & 0 \\ -s_{12} & c_{12} & 0 \\ 0 & 0 & 1 \end{pmatrix}, \quad (3.6)$$

where $s_{ij}, c_{ij} \equiv \sin \theta_{ij}, \cos \theta_{ij}$, in analogy to the quark sector (see equation (A.29)). This assumes that neutrinos are Dirac particles, with a mass term $\bar{\nu}_L m_\nu \nu_R + \text{h.c.}$, where ν_L are the active neutrinos and ν_R are singlets under the gauge group (right-handed neutrinos). However, neutrinos can be Majorana particles, in which case the effective light neutrino mass term is of the form $\nu_L^T m_\nu C \nu_L + \text{h.c.}$. If so, neutrinos can be created and annihilated in pairs, violating lepton number. In this latter instance, in general it is not possible to remove from the mixing matrix as many complex phases as in the Dirac case, so a diagonal phase matrix $\text{diag}(1, \exp i\alpha_{21}/2, \exp i\alpha_{31}/2)$ must be added to U in equation (3.6). These Majorana phases (α_{21} and α_{31}) have not yet been measured, and in fact it is still an open question whether or not neutrinos are Majorana particles. Neutrinoless double beta decay experiments, described latter on, are and will be attempting to answer this question, although the determination of the Majorana phases is hampered by uncertainties in nuclear matrix elements [193–198].

Another unanswered question is whether or not CP is violated in the leptonic sector (see [199] for a review of this topic). CP invariance implies that $P(\bar{\nu}_\alpha \rightarrow \bar{\nu}_\beta) = P(\nu_\alpha \rightarrow \nu_\beta)$, and since $P(\bar{\nu}_\alpha \rightarrow \bar{\nu}_\beta) = P(\nu_\alpha \rightarrow \nu_\beta)^*$, this relation can be rewritten as $\sum_{i < j} \text{Im} \left(J_{\alpha\beta}^{ij} \right) \sin 2\varphi_{ij} = 0$. From this expression, similarly to the quark sector, one concludes that CP violation requires three neutrinos (or

more), all mass differences and mixing angles must be non-null, and in addition δ must be different from $0, \pi$, otherwise the mixing matrix U is real. Currently, this Dirac phase δ is poorly constrained from data, so much so that at $1\sigma, 2\sigma$ CL it can take any value [189, 190]. As such, it is not yet known if leptons conserve CP , but given that θ_{13} was recently measured to be quite large, this might be determined in the near future through a combination of reactor and superbeam data [199].

It should be noted that there are some anomalies in data which cannot be explained within the 3 active neutrino oscillations paradigm. There is a well known claim concerning the observation of neutrinoless double beta decay [200] (see below) and also some signals that could be pointing towards the existence of sterile neutrinos: the appearance of electron neutrinos and anti-neutrinos in the LSND and MiniBoone experiments ($\nu_\mu \rightarrow \nu_e, \bar{\nu}_\mu \rightarrow \bar{\nu}_e$) [201–205], as well as the disappearance of ν_e 's in gallium experiments, and of $\bar{\nu}_e$'s in reactor experiments [206–210].

3.1.3 Matter effects and solar neutrinos

When neutrinos travel through large bodies, such as the Earth or the Sun, there are important matter effects that must be taken into account [180–182]. Matter contains electrons but no muon nor taus, so there is a coherent scattering of ν_e 's with electrons only. The effective neutrino Hamiltonian is changed by this charged current interaction,

$$H = \frac{1}{2E} U^\dagger m^2 U \rightarrow H' = H + \sqrt{2} G_F n_e \text{diag}(1, 0, 0), \quad (3.7)$$

where m^2 may be taken to be $\text{diag}(0, \Delta m_{21}^2, \Delta m_{31}^2)$, G_F is the Fermi constant, and n_e is the electron density in the medium. Importantly, the eigenstates $\nu_i^{(m)}$ of H' are not the same as the vacuum ones ν_i (the eigenstates of H). In addition, the three energy eigenvalues also change from $m_i^2/2E$ (the eigenvalues of H) to some H'_i (the eigenvalues of H'), so the phases φ_{ij} in equation (3.3) must be replaced by $(H'_i - H'_j) L$. This is best seen with only two neutrino flavors: ν_e (electron neutrinos) and ν_a (muon and tau neutrinos taken together), with a squared mass splitting Δm^2 and one mixing angle θ . There are now two distinct and competing scales (see [211] and references contained therein): the oscillation length l_ν previously introduced in equation (3.5), and the neutrino refraction length

$$l_m \equiv \frac{\sqrt{2}\pi}{G_F n_e}. \quad (3.8)$$

When the two are roughly similar ($l_\nu = l_m \cos 2\theta$ to be precise) there is a resonance and the mixing angle in matter $\theta^{(m)}$ is maximal ($\sin^2 2\theta^{(m)} = 1$). As such, for neutrinos with energy E there is a layer in the Sun where the matter density is close to the one satisfying this resonance condition: $n_e^R = \Delta m^2 \cos 2\theta / 2\sqrt{2}EG_F$. Depending on whether or not the neutrino originates from a region with n_e larger than n_e^R , the neutrino state that emerges from the Sun can be very different. In this brief discussion, we mention only the extreme but important case when at the neutrino production point one has $n_e \gg n_e^R$. In this case, mixing is small at production

($\theta^{(m)} \approx \pi/2$), so the electron neutrino ν_e is essentially an energy eigenstate $\nu_2^{(m)}$. As the neutrino travels through different Solar layers, there is an electron density gradient which in principle allows transitions between energy eigenstates $\nu_2^{(m)}$ and $\nu_1^{(m)}$; in practice this density variation is small, so this transition can be neglected (adiabatic approximation). On the other hand, the flavor decomposition of these two mass eigenstates changes with density, so a $\nu_e = \nu_2^{(m)}$ neutrino produced in the Sun's core emerges from its surface as a $\nu_2^{(m)} = \nu_2 \neq \nu_e$ neutrino. The probability that the electron neutrino survives this journey is given by $|\langle \nu_2 | \nu_e \rangle|^2 = \sin^2 \theta$. We note however that for lower energy neutrinos the conversion probability is different.

Solar neutrinos then travel in the vacuum until they reach the Earth. Even though the velocity difference between the ultra relativistic neutrinos produced in the Sun is small, $\Delta v \approx \Delta m^2/2E$, the Earth-Sun distance is big enough to destroy any coherence that existed at the source. As such, high energy solar neutrinos ($E \sim 10$ MeV) reach the Earth as an incoherent flux of ν_2 's, which still suffer minor matter effects as they transverse the Earth, giving rise to a small day/night variation in the detection rate of electron neutrinos, of the order of a few percent. In summary then, the measured flux of solar neutrinos is significantly smaller than originally expected essentially because electron neutrinos are adiabatically converted in the Sun into other neutrino species.

3.1.4 Neutrinoless double beta decay experiments

Despite the major contribution of oscillation experiments to our understanding of neutrinos, they are unable to measure all neutrino properties. In particular, the nature and absolute value of neutrino masses are not yet known, and one promising way to probe and determine them is through neutrinoless double beta decay experiments. If neutrinos are Majorana particles it should be possible for a nuclide (A, Z) to decay into $(A, Z + 2) + 2e$ without the emission of neutrinos, thus violating lepton number: a neutrinoless double beta decay ($0\nu\beta\beta$). In fact, if neutrinoless double beta decays are detected, the 6-point $\bar{u}udd\bar{e}\bar{e}$ effective vertex responsible for it gives rise to a small neutrino Majorana mass via a four loop diagram, therefore the two concepts are inseparably linked [212–215].

To observe such rare decays, normal beta decays must be suppressed. Some nuclides with an even atomic number Z and an even mass number A (^{48}Ca , ^{76}Ge , ^{82}Se , ^{100}Mo , ^{116}Cd , ^{130}Te , ^{136}Xe , ^{150}Nd) are well suited for these experiments, as their energy is higher than the one of $(A, Z + 2)$ but lower than the one of $(A, Z \pm 1)$, so decays into these last states are kinematically forbidden. Even so, the second order lepton flavor conserving decay $(A, Z) \rightarrow (A, Z + 2) + 2e + 2\bar{\nu}_e$ ($2\nu\beta\beta$) must be taken into account, and because both $0\nu\beta\beta$ and $2\nu\beta\beta$ are rare processes, measuring them is challenging. Several collaborations have either already attempted to do it or will try to do so in the future (for a recent review, see [216]).

Neutrinoless double beta decay can arise due to various mechanisms, for example in SUSY theories [217–219]. Assuming however that this process is driven by the

Experiment	Isotope	m_{ee} upper limit (eV; 90% CL)
Heidelberg-Moscow [229]	^{76}Ge	0.35
IGEX [230]	^{76}Ge	0.33 – 1.35
CUORICINO [231]	^{130}Te	0.30 – 0.70
KamLAND-Zen [232]	^{136}Xe	0.3 – 0.6
EXO-200 [233]	^{136}Xe	0.14 – 0.38
NEMO-3 [234]	^{100}Mo	0.31 – 0.96
NEMO-3 [234]	^{82}Se	0.94 – 2.6

Table 5: Upper limits on m_{ee} from different $0\nu\beta\beta$ experiments, obtained using the isotopes ^{76}Ge , ^{82}Se , ^{100}Mo , ^{130}Te , ^{136}Xe .

exchange of light Majorana neutrinos, the half life $T_{1/2}^{0\nu}$ can be written in a model independent way as

$$\frac{1}{T_{1/2}^{0\nu}} = G^{0\nu} |ME|^2 m_{ee}^2, \quad (3.9)$$

where $G^{0\nu}$ is a phase-space factor [220], ME is the nuclear matrix element and

$$m_{ee} \equiv \sum_i |U_{ei}^2 m_i|. \quad (3.10)$$

Even though there are sizable theoretical uncertainties in the calculation of nuclear matrix elements [221–227], by measuring the $0\nu\beta\beta$ decay rate it is possible to shed light on the absolute neutrino mass scale and, at least in theory, on the Majorana phases (see however [193–198, 228]). Table (5) summarizes current upper bounds on m_{ee} from these experiments. It should be mentioned here that there is also a well known claim by two members of the Heidelberg-Moscow group that $0\nu\beta\beta$ decays have already been recorded, yielding $m_{ee} = 0.11 – 0.56$ at 95% CL [200].

3.1.5 Beta decay experiments

A more obvious way to measure the neutrino absolute mass scale, suggested by Pauli upon postulating its existence, is by measuring the end-point of the electron spectrum in normal beta decay reactions, which depends on

$$m_\beta \equiv \sqrt{\sum_i |U_{ei}^2| m_i^2}. \quad (3.11)$$

Unlike m_{ee} measured by $0\nu\beta\beta$ experiments which can be zero even for non-null neutrino masses, in m_β no cancellations can occur between the different terms involving the neutrino masses m_i . By measuring tritium beta decays, the Mainz [235] and Troitzk [236, 237] experiments have established that $m_\beta < 2.3$ eV, 2.2 eV (95% CL), respectively, and in the future the KATRIN collaboration is expected to

have a 5σ discovery potential for $m_\beta = 0.35$ eV. Tritium is an isotope particularly well suited for these experiments because it possesses a low electron spectrum end-point (18.6 keV), and at the same time its short half-life makes it very active. This is important because it increases the number of events, which is crucial for the measurement of the electron's spectrum near the endpoint, as it is expected that only 1 in 5×10^{12} beta decays will produce an electron in the last eV of the spectrum [238].

3.1.6 *Cosmological bounds on neutrino masses*

Neutrino masses influence several astrophysical observables, therefore it is possible make inferences about them by looking at the Cosmos (for a pre-Planck review, see [239]). In particular, by combining CMB data from Planck [71], WMAP [240] and high resolution experiments [241–244] the Planck collaboration obtained the 95% confidence level limit

$$\sum_{\nu} m_{\nu} < 0.66 \text{ eV} \quad [\text{Planck+WMAP+high res.}] \quad (3.12)$$

on the sum of neutrino masses. Even though baryon acoustic oscillation (BAO) [245–248] are not sensitive to neutrino masses, they break the degeneracy between some of the other parameters in the standard cosmological model. As such, using this additional input, the limit on neutrinos masses is significantly reduced:

$$\sum_{\nu} m_{\nu} < 0.23 \text{ eV} \quad [\text{Planck+WMAP+high res.+BAO}]. \quad (3.13)$$

Matter power spectrum data, on the other hand, is sensitive to $\sum_{\nu} m_{\nu}$. As such, using data from the WiggleZ Dark Energy Survey [249], the authors of [250] go even further and set the limit

$$\sum_{\nu} m_{\nu} < 0.15 \text{ eV} \quad [\text{Planck+BAO+WiggleZ}]. \quad (3.14)$$

Noting that for normal (inverted) hierarchy neutrinos one has $0.05(0.1) \leq \sum_{\nu} m_{\nu}$, it is conceivable that in the near future the two hierarchies might be discernible through cosmological observations.

3.1.7 *The origin and smallness of neutrino masses*

In analogy to quarks and charged leptons, the simplest way to give mass to neutrinos in the SM is to introduce right-handed neutrinos ν_R :¹

$$-\mathcal{L}^I = \dots + Y_{ij}^{\nu} \bar{\nu}_{Ri} L_j \cdot H + \text{h.c.} \quad (3.15)$$

One problem with such a lepton number conserving Dirac mass term is that neutrinos have masses smaller than the electronvolt, implying that the entries of the

¹ In the remainder of this section, repeated indices are to be summed over.

Yukawa matrix Y^ν must be of the order of 10^{-12} . This is a very small number and it should be compared to the top's Yukawa coupling, which is close to 1 (such strong fermion mass hierarchy is connected to the flavor problem which was mentioned in chapter 2). In addition, if we introduce right-handed neutrinos in the theory, we are bound to include all terms allowed by the symmetries and not just the Yukawa coupling in equation (3.15). Since the ν_R 's are fermions and singlets under the SM gauge group, there is only one extra renormalizable term allowed:

$$-\mathcal{L}^I = \dots + \frac{1}{2} \nu_R^T m_R^* C \nu_R + \text{h.c.}, \quad C \equiv i\gamma^2 \gamma^0. \quad (3.16)$$

Together with the Dirac mass term shown in equation (3.15), this Majorana mass term for the right-handed neutrinos generates a Majorana mass for the light, mostly left-handed neutrinos, at tree level:

$$-\mathcal{L}^I = \dots + \frac{1}{2} \nu_L^T m_\nu^I C \nu_L + \text{h.c.}, \quad m_\nu^I = -Y^{\nu T} m_R^{-1} Y^\nu \langle H^0 \rangle^2. \quad (3.17)$$

To derive this expression, one assumes that right-handed Majorana neutrino masses are much heavier than Dirac masses, in such a way that for practical purposes the states ν_R become non-dynamical and can be integrated out. As such, equation (3.17) is to be seen as the ν_L mass generated at tree level by the exchange of heavy ν_R states, after electroweak symmetry breaking (EWSB). This scenario, where the heavy mediators are fermions which are singlets under the Standard Model gauge group, is known as seesaw type-I. In the basis where both m_R and the light neutrino mass matrix m_ν^I are diagonal, the Yukawa matrix Y^ν has the form [251]

$$Y^\nu = \frac{i}{\langle H^0 \rangle} \sqrt{m_R} \mathcal{O} \sqrt{m_\nu^I} U^\dagger, \quad (3.18)$$

where \mathcal{O} is some orthogonal matrix which accounts for the mixing involving the heavy neutrino states.

We note however that this is just one of many possibilities of generating a Majorana mass. Gauge invariance does not forbid neutrino masses; it is rather the accidental global $U(1)_L$ symmetry of the renormalizable SM Lagrangian which does, so once lepton number violating interactions are introduced, the dimension 5 Weinberg effective operator [252]

$$\frac{c_{ij}}{2} \left(\varepsilon_{\alpha\gamma} \varepsilon_{\beta\delta} L_{\alpha i}^T C L_{\beta j} H_\gamma H_\delta \right) + \text{h.c.} \quad (3.19)$$

is generated (Greek and Roman indices denote $SU(2)_L$ and flavor components, respectively). Consequently, after EWSB neutrinos get a mass term $\frac{c_{ij}}{2} \langle H^0 \rangle^2 \nu_{L i}^T C \nu_{L j} + \text{h.c.}$ with coefficients c_{ij} of the order M^{-1} , where M is the mass scale of the mechanism which generates the effective Weinberg operator. Unlike Dirac neutrino masses which require exceedingly small Yukawa interactions, Majorana neutrino masses are automatically small even if the Yukawa interactions are large, provided that $M \gg \langle H^0 \rangle$.

There are in fact other ways to generate the above operator at tree level (it can also be generated radiatively [253–256]). There ought to be two vertices with

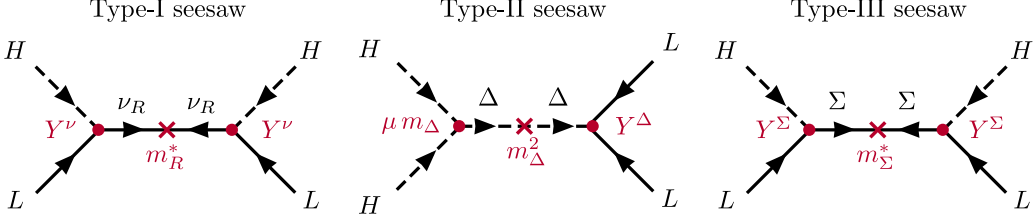


Figure 5: Diagrams which generate the different seesaw mechanisms. The mediator field might be a fermionic singlet (type-I seesaw), a scalar triplet (type-II seesaw), or a fermionic triplet (type-III seesaw).

L 's, H 's and some mediator field. If the two H 's are in the same vertex, HH must be in a triplet representation of $SU(2)_L$ (because the singlet combination is antisymmetric), so the mediator must be a scalar triplet $\Delta = (\Delta^{++}, \Delta^+, \Delta^0)$ (type-II seesaw [257–263]). If, on the other hand, each vertex contains both an L and an H , then the LH combination can be either in an invariant or in a triplet representation of $SU(2)_L$, so the mediator field must be a fermion singlet ν_R (type-I seesaw [264–268]) or a fermion triplet $\Sigma = (\Sigma^+, \Sigma^0, \Sigma^-)$ (type-III seesaw [269]).

The type-I seesaw mechanism has been described above, in equations (3.15)–(3.17). In type-II seesaw, the scalar triplet Δ has the following mass and interaction terms with leptons and the SM Higgs doublet H :

$$\begin{aligned}
-\mathcal{L}^{II} = & Y_{ij}^\Delta \left[\Delta^{++} e_{Li}^T C e_{Lj} - 1/\sqrt{2} \Delta^+ (e_{Li}^T C \nu_{Lj} + i \leftrightarrow j) + \Delta^0 \nu_{Li}^T C \nu_{Lj} \right] \\
& - \mu^* m_\Delta^* \left[\Delta^{++} (H^{+*})^2 + \sqrt{2} \Delta^+ H^{+*} H^{0*} + \Delta^0 (H^{0*})^2 \right] \\
& + \frac{m_\Delta^2}{2} \left[|\Delta^{++}|^2 + |\Delta^+|^2 + |\Delta^0|^2 \right] + \text{h.c.}, \quad (3.20)
\end{aligned}$$

leading to an effective neutrino mass matrix of the form

$$m_\nu^{II} = \frac{\mu \langle H^0 \rangle^2}{m_\Delta} Y^\Delta. \quad (3.21)$$

In type-III seesaw, two or more fermionic triplets $\Sigma_i = (\Sigma_i^+, \Sigma_i^0, \Sigma_i^-)$ are necessary to reproduce neutrino oscillation data:

$$\begin{aligned}
-\mathcal{L}^{III} = & Y_{ij}^\Sigma \left(\sqrt{2} H^+ \bar{\Sigma}_i^+ \nu_{Lj} + H^+ \bar{\Sigma}_i^0 e_{Lj} + H^0 \bar{\Sigma}_i^0 \nu_{Lj} - \sqrt{2} H^0 \bar{\Sigma}_i^- e_{Lj} \right) \\
& + \frac{1}{2} (m_\Sigma^*)_{ij} \left(\Sigma_i^{+T} C \Sigma_j^- + \Sigma_i^{-T} C \Sigma_j^+ + \Sigma_i^{0T} C \Sigma_j^0 \right) + \text{h.c.} \quad (3.22)
\end{aligned}$$

Here, we used $\bar{\Sigma}_i^\pm \equiv \overline{(\Sigma_i^\pm)}$. The neutral component of triplets plays an analogous role to the one of ν_R in a type-I seesaw. As such, the effective neutrino mass matrix is given by

$$m_\nu^{III} = -Y^{\Sigma T} m_\Sigma^{-1} Y^\Sigma \langle H^0 \rangle^2. \quad (3.23)$$

There are also other, more complex tree level seesaw realizations. We shall mention here the inverse [270] and linear [271] seesaws, both of which can be seen as particular cases of type-I seesaw since there is the introduction of fermion singlets ν_R, S in the theory. However, in these models the couplings of S with ν_R, ν_L is constrained: in general, one can write a neutrino mass matrix

$$m_\nu = \begin{pmatrix} 0 & m_D & m_{LS} \\ m_D^T & m_R & m_{RS} \\ m_{LS}^T & m_{RS}^T & m_S \end{pmatrix} \quad (3.24)$$

in the basis (ν_L, ν_R^c, S) . If $m_{LS} = m_R = 0$ and $m_{RS} \gg m_S$ there is a double or inverse seesaw, yielding an effective light neutrino effective mass

$$m_\nu^{ISS} = m_D \left(m_{RS}^T \right)^{-1} m_S m_{RS}^{-1} m_D^T, \quad (3.25)$$

which is the same as $m_D M^{-1} m_D^T$ with $M \equiv m_{RS} m_S^{-1} m_{RS}^T$. Note that lepton number is conserved when $m_S \rightarrow 0$, so the assumption $m_{RS} \gg m_S$ is natural [36]. As such, the smallness of neutrino masses can be achieved in this framework by a small m_S instead of a big m_{RS} . Alternatively, setting $m_S = 0$ and having a small lepton number violating m_{LS} yields the linear seesaw mechanism:

$$m_\nu^{LSS} = m_{LS} m_{RS}^{-1} m_D^T + (\text{transpose}). \quad (3.26)$$

It is possible as well to incorporate the different seesaw mechanisms in extended frameworks, as in the case of SUSY models. Consider the MSSM, with a superpotential given by equation (2.15). A type-I seesaw is obtained by introducing invariant superfields \widehat{N}_i^c (usually three), each containing a right-handed neutrino ν_{Ri} and its scalar superpartner $\tilde{\nu}_{Ri}$, and by adding to the superpotential the following terms:

$$W^I = Y_{ij}^\nu \widehat{N}_i^c \widehat{L}_j \cdot \widehat{H}_u + \frac{1}{2} (m_R)_{ij} \widehat{N}_i^c \widehat{N}_j^c. \quad (3.27)$$

There are also additional soft SUSY breaking terms: $h_{ij}^\nu \tilde{\nu}_{Ri}^* \tilde{L}_j \cdot H_u$, $(m_\nu^2)_{ij} \tilde{\nu}_{Ri} \tilde{\nu}_{Rj}^*$, $b^\nu \tilde{\nu}_R^* \tilde{\nu}_R^*$, and $s^\nu \tilde{\nu}_R^*$. Should this model be embedded in a cMSSM framework, the parameters m_ν^2 and h^ν will obey universality conditions ($m_\nu^2 = m_0^2 \mathbb{1}$ and $h^\nu = A_0 Y^\nu$). The light neutrino mass matrix is the same as in equation (3.17).

The implementation of a type II SUSY seesaw model requires the addition of at least two $SU(2)_L$ triplet superfields [272]. However, if gauge coupling unification is to be preserved, complete $SU(5)$ multiplets must be added to the MSSM content: the $\mathbf{15}$ and $\overline{\mathbf{15}}$. Under the SM gauge group, the $\mathbf{15}$ decomposes as $\widehat{S} \oplus \widehat{T} \oplus \widehat{Z}$, with $\widehat{S} = (\mathbf{6}, \mathbf{1}, -2/3)$, $\widehat{T} = (\mathbf{1}, \mathbf{3}, 1)$ and $\widehat{Z} = (\mathbf{3}, \mathbf{2}, 1/6)$. On the other hand, $\overline{\mathbf{15}} = \widehat{S} \oplus \widehat{T} \oplus \widehat{Z}$, with $\widehat{S} = (\overline{\mathbf{6}}, \mathbf{1}, 2/3)$, $\widehat{T} = (\mathbf{1}, \mathbf{3}, -1)$ and $\widehat{Z} = (\overline{\mathbf{3}}, \mathbf{2}, -1/6)$. In the $SU(5)$

broken phase, below the GUT scale, the superpotential contains the following terms:

$$W^{II} = \frac{1}{\sqrt{2}} \left(Y^T \widehat{L} \widehat{T} \widehat{L} + Y^S \widehat{D}^c \widehat{S} \widehat{D}^c \right) + Y^Z \widehat{D}^c \widehat{Z} \widehat{L} + \frac{1}{\sqrt{2}} \left(\lambda_1 \widehat{H}_d \widehat{T} \widehat{H}_d + \lambda_2 \widehat{H}_u \widehat{T} \widehat{H}_u \right) + m_T \widehat{T} \widehat{T} + m_Z \widehat{Z} \widehat{Z} + m_S \widehat{S} \widehat{S}, \quad (3.28)$$

where gauge and flavor indices we omitted for simplicity (the soft breaking Lagrangian can be found in [272]). After having integrated out the heavy fields, the effective neutrino mass matrix reads

$$m_\nu^{II} = \frac{\lambda_2 \langle H_u^0 \rangle^2}{m_T} Y^T. \quad (3.29)$$

In order to embed a type III seesaw in SUSY models, the **24** representation of $SU(5)$ is used [273]. It contains the fermionic triplet Σ mentioned above: $\mathbf{24} = \widehat{B} + \widehat{G} + \widehat{W} + \widehat{X} + \widehat{\bar{X}}$, with $\widehat{B} = (\mathbf{1}, \mathbf{1}, 0)$, $\widehat{G} = (\mathbf{8}, \mathbf{1}, 0)$, $\widehat{W} = (\mathbf{0}, \mathbf{3}, 0)$, $\widehat{X} = (\mathbf{3}, \mathbf{2}, -5/6)$ and $\widehat{\bar{X}} = (\bar{\mathbf{3}}, \mathbf{2}, 5/6)$. The extra superpotential terms are the following:

$$W^{III} = Y^W \widehat{H}_u \widehat{L} \widehat{W} - \sqrt{\frac{3}{10}} Y^B \widehat{H}_u \widehat{L} \widehat{B} + Y^X \widehat{H}_u \widehat{\bar{X}} \widehat{D}^c + \frac{1}{2} m_B \widehat{B} \widehat{B} + \frac{1}{2} m_G \widehat{G} \widehat{G} + \frac{1}{2} m_W \widehat{W} \widehat{W} + \frac{1}{2} m_X \widehat{X} \widehat{\bar{X}}. \quad (3.30)$$

The fermionic component of \widehat{W} is the Σ , but there is also a gauge invariant \widehat{B} superfield, whose fermionic component behaves like a right-handed neutrino ν_R^c . As such, after integration of the heavy fields there is a mixture of type-I and type-III seesaw contributions to the effective light neutrino mass:

$$m_\nu^{III} = - \langle H_u^0 \rangle^2 \left[\frac{3}{10} Y^B m_B^{-1} (Y^B)^T + \frac{1}{2} Y^W m_W (Y^W)^T \right]. \quad (3.31)$$

Alternatively, neutrino masses can be generated without changing the MSSM field content, violating R-parity instead [274–281]—for a review, see [282–284]. We have mentioned in the previous chapter that if R-parity is not imposed as a symmetry of the Lagrangian, the following baryon and lepton number terms are allowed in the superpotential:

$$W^{\mathcal{R}_p} = \frac{1}{2} \lambda^{ijk} \widehat{L}_i \cdot \widehat{L}_j \widehat{E}_k^c + \lambda'^{ijk} \widehat{L}_i \cdot \widehat{Q}_j \widehat{D}_k^c + \frac{1}{2} \lambda''^{ijk} \widehat{U}_i^c \widehat{D}_j^c \widehat{D}_k^c + \epsilon^i \widehat{L}_i \cdot \widehat{H}_u. \quad (3.32)$$

Some neutrinos get a tree level mass due to mixing with the neutral electroweak gauginos and Higgsinos, while other neutrino masses are generated radiatively. Crucially, unlike in the seesaw mechanism where neutrino masses are generated at high-energy scales, in SUSY models with broken R-parity only electroweak scale physics is at play. These models are particularly interesting because neutrino parameters (masses, mixing angles, phases) can be related with accelerator observables, such as the decay properties of the LSP [285].

Nevertheless, generic R-parity breaking models have an obvious down-side: they introduce a large number of extra parameters (λ^{ijk} , λ'^{ijk} , λ''^{ijk} , ϵ^i , plus the ones associated with soft SUSY breaking couplings). The bilinear R-parity violating model avoids this problem by introducing only the 6 bilinear R-parity breaking terms: $\epsilon^i \widehat{L}_i \cdot \widehat{H}_u$ in the superpotential and $-b^i \epsilon^i \widetilde{L}_i \cdot \widetilde{H}_u$ in $-\mathcal{L}_{\text{soft}}$ [286]. This minimal extension of the MSSM shares some of the features of more general models [136, 285, 287–296]. The neutrino mass matrix is given by

$$m_\nu = \frac{M_1 g^2 + M_2 g'^2}{\mu v_u v_d (M_1 g^2 + M_2 g'^2) - 2\mu^2 M_1 M_2} \Lambda \Lambda^T, \quad (3.33)$$

where Λ is a vector with components

$$\Lambda_i = \mu \langle \widetilde{\nu}_i \rangle + v_d \epsilon^i, \quad i = e, \mu, \tau. \quad (3.34)$$

The sneutrino VEVs appearing in this last equation are non-zero once $\epsilon^i \neq 0$; they obey the following equations:

$$0 = -b v_u + (m_{H_d}^2 + \mu^2) v_d + v_d D - \mu \langle \widetilde{\nu}_i \rangle \epsilon^i, \quad (3.35)$$

$$0 = -b v_d + (m_{H_u}^2 + \mu^2) v_u - v_u D + \langle \widetilde{\nu}_i \rangle b^i \epsilon^i + v_u \epsilon^i \epsilon^i, \quad (3.36)$$

$$0 = \langle \widetilde{\nu}_j \rangle D + \epsilon^j \left(-\mu v_d + b^j v_u + \langle \widetilde{\nu}_i \rangle \epsilon^i \right) + \langle \widetilde{\nu}_i \rangle \text{Re} \left(m_{L}^2 \right)_{ij}, \quad (3.37)$$

where

$$D \equiv \frac{1}{8} (g^2 + g'^2) (v_d^2 - v_u^2 + \langle \widetilde{\nu}_i \rangle^2). \quad (3.38)$$

In these expressions the index i is to be summed over, while j is not. The neutrino mass matrix m_ν in equation (3.33) has a single eigenvalue different from zero (given by the trace of m_ν), which is associated with the atmospheric mass scale. On the other hand, the smaller solar mass scale is generated radiatively by bottom-sbottom, tau-stau and neutrino-sneutrino pairs in loops. At tree level, since two masses are degenerate, one mixing angle can be rotated away (it reappears nevertheless once radiative corrections are taken into account). The two remaining ones are given by

$$\tan \theta_{13} = -\frac{\Lambda_e}{\sqrt{\Lambda_\mu^2 + \Lambda_\tau^2}}, \quad (3.39)$$

$$\tan \theta_{23} = -\frac{\Lambda_\mu}{\Lambda_\tau}. \quad (3.40)$$

3.2 CHARGED LEPTON FLAVOR VIOLATION

Neutrino oscillations do not conserve the flavor of neutral leptons. As such, one is lead to consider the possibility that in the charged sector there are analogue processes which also violate lepton flavor. In the following, we discuss this possibility.

In the Standard Model one can assign a lepton quantum number L to all fields such that all terms in the Lagrangian preserve the associated $U(1)_L$ symmetry. In fact, for massless neutrinos, it is possible to do so for each lepton flavor: three separate quantum numbers $L_{e,\mu,\tau}$ are consequently preserved in perturbative processes. However, once the Standard Model is minimally extended to accommodate massive neutrinos, the $U(1)_{L_{e,\mu,\tau}}$ flavor symmetries are broken, even though L is still preserved if neutrinos are Dirac particles. The observed neutrino oscillations imply that this lepton flavor violation (LFV) is sizable in the neutral sector, yet the resulting effect in charged leptons is small. For definiteness, consider the branching ratio of $\mu \rightarrow e\gamma$ which is GIM suppressed; it is kept small by the unitarity of the leptonic mixing matrix and by the smallness of the (Dirac) neutrino squared mass differences [297–301]:

$$\text{Br}(\mu \rightarrow e\gamma) = \frac{3\alpha}{32\pi m_W^4} \left| \sum_i U_{ei} U_{\mu i}^* m_{\nu_i}^2 \right|^2 \sim \frac{3\alpha}{32\pi} c_{13}^2 s_{13}^2 s_{23}^2 \left(\frac{\Delta m_{31}^2}{m_W^2} \right)^2 \sim 10^{-55}. \quad (3.41)$$

Charged lepton flavor violation (cLFV) processes with such small branching ratios are not measurable. This turns out to be an interesting feature of these processes: since the Standard Model and its trivial extensions predict no charged lepton flavor violation, its observation would be a clear signal of new Physics (for example, low scale seesaw models, extra dimensions, little Higgs models, etc.).

In some softly broken SUSY models the situation changes dramatically; generic soft SUSY breaking terms introduce large sources of cLFV, to the extent that such terms must be constrained to avoid conflict with current experimental bounds. For example, in the constrained MSSM the trilinear terms are proportional to the Yukawa couplings and the soft SUSY breaking masses are assumed to be diagonal in flavor space at the GUT scale (chapter 2). As such, the Yukawa couplings alone control the flavor structure of the model and for this reason there is no LFV, even accounting for the effect of the renormalization group evolution of the parameters down to low scales.

This principle of having only SM sources of flavor violation in an extended theory is the main idea behind the concept of minimal flavor violation (MFV) [302]. With the exception of Yukawa interactions, all terms in the SM's Lagrangian are invariant under a global $SU(3)_Q \times SU(3)_u \times SU(3)_d \times SU(3)_L \times SU(3)_e$ symmetry. As such, to control its breaking, the Yukawa couplings are usually promoted to constant spurion fields which transform under this symmetry in the necessary way to preserve it. In the quark sector, this means that the Yukawa matrices transform as $(Y_u)_{ij} \sim (\mathbf{3}, \bar{\mathbf{3}}, \mathbf{1}, \mathbf{1}, \mathbf{1})$ and $(Y_d)_{ij} \sim (\mathbf{3}, \mathbf{1}, \bar{\mathbf{3}}, \mathbf{1}, \mathbf{1})$. Therefore, in a MFV MSSM

the squark masses and trilinear couplings in the soft SUSY breaking sector of the MSSM must have the following form (see [303]):

$$m_Q^2 = \tilde{m}^2 \left(a_1 \mathbb{1} + a_2 Y^{u\dagger} Y^u + a_3 Y^{d\dagger} Y^d + \dots \right), \quad (3.42)$$

$$m_x^2 = \tilde{m}^2 \left(b_1^x \mathbb{1} + b_2^x Y^{x*} Y^{xT} + \dots \right), \quad x = u, d, \quad (3.43)$$

$$h^x = A_0 Y^x \left(c_1^x \mathbb{1} + c_2^x Y^{u\dagger} Y^u + c_3^x Y^{d\dagger} Y^d + \dots \right), \quad x = u, d, \quad (3.44)$$

where the a_i , $b_i^{u,d}$ and $c_i^{u,d}$ are *a priori* free dimensionless parameters. They are not constrained in any way unless the MSSM is embedded in some more fundamental, higher energy theory. The cMSSM, as mentioned above, is such an example: at the energy scale where the three gauge couplings unify, all coefficients are zero except for $a_1 = b_1^{u,d} = c_1^{u,d} = 1$. Even so, we must keep in mind that the renormalization group flow will generate non-zero contributions to the coefficients shown explicitly above of the order of $1/(4\pi)^2 \log m_{GUT}/m_{SUSY}$.

Unlike the quark sector, in the lepton sector the situation is not as straightforward. To establish a MFV framework, a flavor symmetry as well as a ‘minimal’ set of parameters that are allowed to violate it must be defined. Crucially, in the lepton sector this depends on the unknown nature of neutrinos. We shall not consider all possibilities here, but it is instructive to see what happens in the case where no new fields are added to the MSSM (R-parity must be a broken symmetry). In this case, the sources of LFV are the charged lepton Yukawa matrix, $Y^\ell \sim (\mathbf{1}, \mathbf{1}, \mathbf{1}, \mathbf{3}, \bar{\mathbf{3}})$, and the neutrino mass matrix $m_\nu \sim (\mathbf{1}, \mathbf{1}, \mathbf{1}, \bar{\mathbf{6}}, \mathbf{1})$ generated from the Weinberg operator in equation (3.19). In analogy to the quark sector in the MSSM, the slepton masses and the leptonic trilinear couplings are restricted to the following form:

$$m_L^2 = \tilde{m}^2 \left(a_1 \mathbb{1} + a_2 Y^{\ell\dagger} Y^\ell + a_3 m_\nu^* m_\nu + \dots \right), \quad (3.45)$$

$$m_e^2 = \tilde{m}^2 \left(b_1 \mathbb{1} + b_2 Y^{\ell*} Y^{\ell T} + b_3 Y^{\ell*} Y^{\ell T} Y^{\ell*} Y^{\ell T} + b_4 Y^{\ell*} m_\nu m_\nu^* Y^{\ell T} + \dots \right), \quad (3.46)$$

$$h^\ell = A_0 Y^\ell \left(c_1 \mathbb{1} + c_2 Y^{\ell\dagger} Y^\ell + c_3 m_\nu^* m_\nu + \dots \right). \quad (3.47)$$

Once again a_i , b_i and c_i should be seen as free parameters in an effective theory framework. Note that, unlike m_L^2 and h^ℓ , the right handed slepton mass matrix m_e^2 only depends on m_ν through a term $m_\nu^2 (Y^\ell)^2$, whose leading coefficient is suppressed by a two loop factor $1/(4\pi)^4$ (see next subsection). The predictive power of the MFV hypothesis can be seen in these equations, as they connect the amplitudes of charged lepton flavor violating processes with neutrino oscillations parameters. Even though the coefficients of each term in the equations above are not predicted, their order of magnitude can be estimated. Furthermore, a systematic suppression of otherwise dangerous cLFV interactions is achieved.

3.2.1 Charged lepton flavor violation and SUSY

Stringent upper bounds on cLFV observables (see next subsection) imply that the misalignment between the soft SUSY breaking mass matrices m_e^2 , m_L^2 and the lepton Yukawa matrix Y^ℓ is small. For various applications, it is useful to make an expansion on these misalignment. Indeed, in the basis where the Yukawa couplings are diagonal,² rather than trying to fully diagonalize the 6×6 sleptons mass matrix

$$M_\ell^2 \equiv \begin{pmatrix} \tilde{m}_{LL}^2 & \tilde{m}_{LR}^2 \\ \tilde{m}_{LR}^{2\dagger} & \tilde{m}_{RR}^2 \end{pmatrix}, \quad (3.48)$$

it is often more convenient not to do so and instead separate each block \tilde{m}_{XY}^2 into a diagonal and an off-diagonal part. This last part is usually written with a δ :

$$\left(\tilde{m}_{XY}^2\right)_{ij} \equiv \delta_{ij}^{XY} \sqrt{(\tilde{m}_{XX}^2)_{ii} (\tilde{m}_{YY}^2)_{jj}} \text{ for } (i, X) \neq (j, Y). \quad (3.49)$$

The diagonal masses $(\tilde{m}_{LL}^2)_{ii}$ and $(\tilde{m}_{RR}^2)_{ii}$ are Gaussian integrated in the path integrals together with the kinetic terms, appearing therefore in the slepton propagators. On the other hand, the off-diagonal δ_{ij}^{XY} terms are treated as interactions (two-point vertices). This approach is known as the mass insertion approximation (MIA) [304–307]. The effect of actually performing the rotation to the slepton mass basis is achieved in this scheme in the limit where all diagrams with an arbitrarily large number of mass insertions is considered. As such, it is to be expected that this approximation is good as long as the δ 's are small (see for instance [308] for a quantitative analysis). The advantage of the MIA is that it provides simpler analytical expressions for the amplitude of lepton flavor violating processes, making their dependence on the Lagrangian parameters more transparent, as there are no rotation matrices other than the CKM one (for hadronic processes) and possibly the PMNS one.

Alternatively, one can compute the amplitude of the desired processes in the mass eigenbasis, and then make a polynomial expansion of the loop functions which depend on the masses of virtual particles. Doing so makes it possible to eliminate the rotation matrices appearing in the expressions and convert them into the Lagrangian parameters that contribute to the sparticles mass matrices. In this approach, the validity of the MIA is directly tied to the smallness of the splitting between the physical masses of sparticles with the same quantum numbers, which in turn can be related to the smallness of the off-diagonal entries of the mass matrices in the gauge basis.

We have mentioned above that the introduction of neutrino masses in the Standard Model generates negligible charged lepton flavor violation. However, in SUSY models this is no longer true. For definiteness, we shall consider the cMSSM which, at the GUT scale m_G contains universal and diagonal soft mass terms. Since the flavor structure is controlled uniquely by the Yukawa matrix Y^ℓ , there is no cLFV.

² The same rotation is performed on leptons and sleptons, in such a way that the lepton-slepton-gaugino and lepton-slepton-Higgsino interactions are kept diagonal in flavor space.

Once a seesaw mechanism is introduced, the situation changes as there are then two or more flavored matrices in the lepton sector. Equation (3.41) would suggest that the resulting cLFV is small yet, due to the effect of the renormalization group in the charged left-slepton mass matrix and trilinear soft couplings, this turns out not to be the case [309]. In type I seesaw

$$\left(m_L^2\right)_{ij} \approx -\frac{1}{8\pi^2} \left(3m_0^2 + A_0^2\right) \left(Y^{\nu\dagger}LY^\nu\right)_{ij}, i \neq j, \quad (3.50)$$

$$h_{ij}^\ell \approx -\frac{3}{16\pi^2} A_0 \left(Y^\ell Y^{\nu\dagger}LY^\nu\right)_{ij}, i \neq j, \quad (3.51)$$

with $L_{ij} = \log m_G/m_{R_i} \delta_{ij}$. Since right handed charged leptons do not couple directly with Y^ν , at one loop order

$$\left(m_e^2\right)_{ij} \approx 0, i \neq j. \quad (3.52)$$

With type II seesaw, the expressions for the renormalization group induced LFV are similar [272]. In particular, the off-diagonalities in m_L^2 and h^ℓ are proportional to the combination $Y^{T\dagger}LY^T$, where Y^T was introduced in equation (3.28).

Processes violating the flavor of charged leptons are sensitive to these off-diagonalities. For example, the decays $\ell_i \rightarrow \ell_j \gamma$ are induced by neutralino-slepton and chargino-sneutrino loops, yielding a branching ratio (using $\delta_{ij}^{RR} \approx 0$) [305, 310–312]

$$\text{BR}(\ell_i \rightarrow \ell_j \gamma) \propto \frac{\alpha^3}{G_F^2 m_{SUSY}^4} \left(\delta_{ij}^{LL}\right)^2 \tan^2 \beta, \quad (3.53)$$

where m_{SUSY} is the mass scale of the virtual sparticles in the loops. As such, in SUSY GUTs the problem of neutrino mass generation is directly related to potentially large cLFV effects, which may be measurable in low [251, 310, 311, 313–337] and high energy experiments [338–366].

3.2.2 cLFV observables and limits on effective couplings

Charged lepton flavor violation can be analyzed in a model independent, effective field theory framework, where heavy fields are integrated out (see [367, 368]). With the SM field content, it is not possible to build renormalizable lepton flavor violating operators, therefore these operators must be of dimension $n = 5$ or higher. Observables can then be expressed as a function of the coefficients of such operators, which can be calculated for specific models. From a dimensional analysis alone, these LFV operators are expected to be suppressed by a factor $1/m_{NP}^{n-4}$ where m_{NP} is the new Physics mass scale (\gtrsim TeV), so usually it is enough to consider operators up to dimension 6.

The only dimension 5 LFV operator is the one mentioned previously in equation (3.19), which gives mass to neutrinos after EWSB (it is common to all seesaw mechanisms). On the other hand, there are various dimension 6 operators, which

depend on the high energy model: they may contain two leptons and a gauge boson, four leptons, or two leptons and two quarks.

$$\mathcal{O}_{ij}^{\ell B(W)} = \bar{L}_i [\gamma^\mu, \gamma^\nu] e_{Rj} H B_{\mu\nu} (W_{\mu\nu}) , \quad (3.54)$$

$$\mathcal{O}_{ijkl}^{LL} = (\bar{L}_i \gamma^\mu L_j) (\bar{L}_k \gamma_\mu L_l) , \quad (3.55)$$

$$\mathcal{O}_{ijkl}^{ee} = (\bar{e}_{Ri} \gamma^\mu e_{Rj}) (\bar{e}_{Rk} \gamma_\mu e_{Rl}) , \quad (3.56)$$

$$\mathcal{O}_{ijkl}^{\ell\ell} = (\bar{L}_i e_{Rj}) (\bar{e}_{Rk} L_l) , \quad (3.57)$$

$$\mathcal{O}_{ijkl}^{LQ} = (\bar{L}_i \gamma^\mu L_j) (\bar{Q}_k \gamma_\mu Q_l) , \quad (3.58)$$

$$\mathcal{O}_{ijkl}^{Lu(d)} = (\bar{e}_{Ri} \gamma^\mu e_{Rj}) (\bar{u}(d)_{Rk} \gamma_\mu u(d)_{Rl}) , \quad (3.59)$$

$$\mathcal{O}_{ijkl}^{\ell q} = (\bar{L}_i e_{Rj}) (\bar{d}_{Rk} Q_l) , \quad (3.60)$$

For simplicity, $SU(2)$ indices were omitted in these expressions. After EWSB, the operators $\mathcal{O}_{ij}^{\ell B(W)}$ give rise to electric and magnetic dipole moments, as well as $\ell_i \rightarrow \ell_j \gamma$ transitions. The four lepton operators \mathcal{O}_{ijkl}^{LL} , \mathcal{O}_{ijkl}^{ee} and $\mathcal{O}_{ijkl}^{\ell\ell}$ contribute to the processes $\ell_i \rightarrow \ell_j \ell_k \ell_l$, $\ell_i \ell_j \rightarrow \ell_k \ell_l$, and they can also be probed in Z decays into a pair of leptons. Finally, \mathcal{O}_{ijkl}^{LQ} , $\mathcal{O}_{ijkl}^{Lu(d)}$ and $\mathcal{O}_{ijkl}^{\ell q}$ contribute to leptonic and semileptonic decays of mesons.

Bounds can be placed on the coefficients that multiply these operators. For example, consider the charged part of $\mathcal{O}_{ij}^{\ell\gamma}$ —a mixture of $\mathcal{O}_{ij}^{\ell B}$ and $\mathcal{O}_{ij}^{\ell W}$ —after EWSB:

$$\mathcal{L} = \frac{em_{\ell_i}}{8} A_{ij} \bar{e}_{Ri} [\gamma^\mu, \gamma^\nu] e_{Lj} F_{\mu\nu}^{\text{em}} + \text{h.c.} , \quad (3.61)$$

where A_{ij} are some coefficients. When $i \neq j$, this operator contributes to the dipole transitions $\ell_i \rightarrow \ell_j \gamma$, while diagonal entries $i = j$ generate leptonic anomalous magnetic moments, $a_i \equiv g_i/2 - 1$, and electric dipole moments d_i (see for example [31]):

$$\frac{\text{BR}(\ell_i \rightarrow \ell_j \gamma)}{\text{BR}(\ell_i \rightarrow \ell_j \nu_i \bar{\nu}_j)} = \frac{48\pi^3 \alpha}{G_F^2} (|A_{ij}|^2 + |A_{ji}|^2) , \quad (3.62)$$

$$\Delta a_i = 2m_{\ell_i}^2 \text{Re}(A_{ii}) \quad (\text{no sum in } i) , \quad (3.63)$$

$$d_i = em_{\ell_i} \text{Im}(A_{ii}) \quad (\text{no sum in } i) . \quad (3.64)$$

The anomalous magnetic moments of the two lightest charged leptons have been measured to a good accuracy, so much so that a_e is used to determine the fine structure constant α , and Δa_μ provides a precision test for the EW theory at the quantum level. Interestingly, the present experimental value of Δa_μ differs from the SM prediction by more than 3σ (see table (6)). It is also possible to compute a discrepancy between a_e^{exp} and a_e^{SM} as long as α is obtained from another observable; this was done in [31], where the fine structure constant was extracted from the measurement of the atomic recoil frequency shift of photons absorbed or emitted

i	a_i^{exp}	a_i^{SM}	Δa_i
$e (\times 10^{14})$	11 596 521 8076 (27)	11 596 521 8178 (76)	-102 (81)
$\mu (\times 10^{11})$	116 592 089 (63)	116 591 828 (49)	261 (80)
$\tau (\times 10^3)$	-18 (17)	1.177 21 (5)	-19 (17)

Table 6: Values of $a_i \equiv (g_i - 2)/2$, $i = e, \mu, \tau$ taken from [31, 369, 370] and [371–373] (1σ uncertainties are in parentheses). Note that a_e^{SM} differs from a_e^{exp} because α is not being extracted from the anomalous magnetic moment of the electron—see [31].

ℓ	$d_\ell^{exp} (e \cdot \text{cm})$
e	$(-2.4 \pm 5.9) \times 10^{-28}$ [375]
μ	$(-1 \pm 9) \times 10^{-20}$ [376]
τ	$(1.15 \pm 1.70) \times 10^{-17}$ (Re) [377] $(-0.83 \pm 0.86) \times 10^{-17}$ (Im)

Table 7: Experimental bounds on leptonic electric dipole moments.

by ^{133}Cs atoms using atom interferometry. On the other hand, due to its short lifetime, the anomalous magnetic moment of the τ is poorly measured.

To the magnetic moment μ measuring the strength of the coupling between a particle’s spin \vec{S} and an external magnetic field \vec{B} , there is an associated electric dipole moment (EDM) d which measures the coupling strength between \vec{S} and an external electric field \vec{E} . A P , T and CP (by the CPT theorem) preserving theory yields $d = 0$ for the various particles, because a term $\vec{S} \cdot \vec{E}$ changes sign under these symmetries. The Standard Model does violate these symmetries through the complex phase in the CKM matrix, but even so the predicted electric dipole moments are minute, assuming that the QCD θ parameter is zero. Experimentally, it has been confirmed that electric dipole moments are small (see table (7) for the leptonic limits); current measurements are in fact compatible with null electric dipole moments, but future improvements in the experimental sensibilities can change this [374].

On the other hand, the off-diagonal entries of the A matrix in equation (3.61) are also constrained by strict bounds on the branching ratios of $\ell_i \rightarrow \ell_j \gamma$ decays, as well as $\mu - e$ coherent conversion in the vicinity of an atomic nucleus (table (8)). Some collaborations plan to decrease significantly these limits in the future; in particular, the $\mu - e$ coherent conversion bound is expected to be improved by 4 orders of magnitude in the next decade by the Mu2e and COMET collaborations.

A thorough listing of limits of the other effective operators in equations (3.54)–(3.60) can be found in [368]. Table (9) contains some of the most important observables which constraint the dimension 6 operators with four leptons and two leptons plus two quarks.

	Current bound	Future sensitivity
BR ($\mu \rightarrow e\gamma$)	5.7×10^{-13} [378]	6×10^{-14} [379]
BR ($\tau \rightarrow e\gamma$)	3.3×10^{-8} [380]	3×10^{-9} [381]
BR ($\tau \rightarrow \mu\gamma$)	4.4×10^{-8} [380]	$(5 - 10) \times 10^{-9}$ [382], 2.4×10^{-9} [381]
$\frac{\sigma(\mu N \rightarrow eN)}{\sigma(\mu N \rightarrow \text{capture})}$	7×10^{-13} (Au) [383]	10^{-16} (Al) [385], 2×10^{-17} (Al) [386]
	4.3×10^{-12} (Ti) [384]	10^{-18} (Ti) [387]

Table 8: Experimental bounds on the branching ratio of decays $\ell_i \rightarrow \ell_j \gamma$ (90% CL) as well as expected future sensitivities.

	Current bound/value	Future sensitivity
BR ($\mu \rightarrow eee$)	$< 1.0 \times 10^{-12}$ [388]	$\sim 10^{-16}$ [389]
BR ($\tau \rightarrow eee$)	$< 2.7 \times 10^{-8}$ [390]	$\sim 10^{-10}$ [381]
BR ($\tau \rightarrow \mu\mu\mu$)	$< 2.1 \times 10^{-8}$ [390]	$(1 - 3) \times 10^{-9}$ [382], $\sim 10^{-10}$ [381]
BR ($B_s \rightarrow \mu\mu$)	$3.2_{-1.2}^{+1.5} \times 10^{-9}$ [391]	0.15×10^{-9} [392]
BR ($B \rightarrow \tau\nu$)	$(1.65 \pm 0.34) \times 10^{-4}$ [105]	3% – 4% [393]

Table 9: Currents bounds (90% CL) or values of some important observables which depend on the 4ℓ and $2\ell 2q$ cLFV effective operators in equations in (3.54)–(3.60). Future sensitivities are also shown. The Standard Model predicts BR ($B_s \rightarrow \mu\mu$) = $(3.23 \pm 0.27) \times 10^{-9}$ [394] and BR ($B \rightarrow \tau\nu$) = $(1.11 \pm 0.27) \times 10^{-4}$ (using $f_B = 190.6 \pm 4.7$ MeV [395–398], $V_{ub} = (4.15 \pm 0.49) \times 10^{-3}$ [105]).

4.1 THE ROLE OF SYMMETRY

Symmetry seems to be an essential feature of the fundamental laws of Physics. It is not a question of aesthetics though: symmetry makes predictions by restricting the set of theories which can describe Nature. In this chapter we discuss two cases of relevance in High Energy Physics, namely space-time and gauge symmetries.

Consider the Theory of Relativity, where a system is described by a metric g and a manifold \mathcal{M} . Under a change of coordinates $x \rightarrow x'$ the metric transforms as $g_{ab} \rightarrow g'_{ab} = \frac{\partial x^c}{\partial x'^a} \frac{\partial x^d}{\partial x'^b} g_{cd}$, and we can ask what are the transformations that preserve the metric, $g = g'$. These are called *isometries*, and in the case of the Minkowski metric $\eta = \text{diag}(1, -1, -1, -1)$ of Special Relativity they form the Poincaré group. If translations are ignored, we are left with the group of homogeneous isometries—the Lorentz group. We shall look into these two groups latter on in this chapter, and also at how SUSY enlarges this space-time symmetry in a unique, non-trivial way. Knowing how symmetry is of such importance in fundamental Physics, the fact that the space-time symmetry group can be extended, is in itself a powerful theoretical motivation for considering supersymmetric theories, as alluded already in chapter 2.

On the other hand, modern Particle Physics models are Yang–Mills theories which possess some continuous gauge symmetry. This is a Lie group, just like the Poincaré and Lorentz groups, but there is a significant difference between them: unlike the gauge symmetry group, the Lorentz and Poincaré groups are not compact because of the metric’s signature, and as a consequence the irreducible representations of these latter groups cannot be simultaneously finite dimensional and unitary. We shall see this in some detail latter on.

The SM, as well as the MSSM, are based on the $U(1)_Y \times SU(2)_L \times SU(3)_c$ group which at energies below the EW scale breaks into $U(1)_{em} \times SU(3)_c$ due to the Higgs mechanism (see the appendix A). Early on, it was realized that the SM gauge group itself could be the remnant of a larger symmetry that is broken at low energies. The prospect of having theories with a single gauge coupling constant is particularly interesting; this happens only if the gauge group is simple or the direct product of equal simple factors, together with some discrete symmetry that permutes these factors [40–48]. Such models would unify all forces, thereby providing a simpler description of the laws of Physics. Ideally, something analogous would happen to the particle content of the theory: there would be only one representation of this fundamental gauge group containing all the known matter particles. This would dramatically reduce the number of parameters and thus yield a much more predictive model.

At this point however, it seems difficult to formulate a completely unified model. Nevertheless, the quest for a bigger gauge symmetry group is an interesting and

actively pursued one. In order to have a global view of the possible ways of extending the SM in this way, we shall be exploring some theoretical features of Lie algebras (see also [399–404]). Some of the aspects discussed here were used on the Mathematica program `Susyno`, described latter on in chapter 5. One important result is the Serre-Chevalley relations in equations (4.25)–(4.27). In words, they state that a simple Lie algebra which allows the simultaneous diagonalization of n of its generators can be seen as being made of n copies of the $SU(2)$ group. The way that the 3 generators of each $SU(2)$ interact/commute with the generators of the other $SU(2)$'s defines the structure of the algebra and, surprisingly, these commutation relations are very simple in a particular basis; they are completely determined by the so-called Cartan matrix of the algebra. Therefore, with equations (4.25)–(4.27) it is possible to generalize the procedure used to build the explicit representation matrices of $SU(2)$ to any simple group! In turn, with the explicit matrices of any representation of any simple group, it is possible to write the Lagrangian invariant under such group (see chapter 5 and also appendix B).

Finally, let us mention in passing the role of a few discrete symmetries in High Energy Physics. In connection with the relativistic nature of field theories, there are the charge, parity and time reversal operations (C , P and T) which are of great importance in our understanding of these theories. Then there are the abelian discrete symmetries associated with baryon (B) and lepton (L) number conservation, which are related to the R-parity in the MSSM. Also, as mentioned in chapter 2, our lack of understanding of the flavor structure of the SM has lead to the use of discrete non-abelian flavor symmetries as a means to predict, or at least constrain some of the mixing angles and fermion masses. It is worth noting however that, unlike continuous symmetries, the discrete symmetries that we know of appear to be violated by Nature: C , P and T are broken symmetries, even though the last two are part of the Lorentz group; baryon and lepton number are violated in non-perturbative processes [65–68] and their conservation at the perturbative level can be seen as a consequence of the Lagrangian gauge invariance (a continuous symmetry). Nevertheless, broken or not, discrete symmetries are of great relevance in fundamental Physics.

4.2 LIE GROUPS AND THEIR CONNECTION TO LIE ALGEBRAS

Particle Physics deals almost invariably with Lie algebras instead of Lie groups, to the point that sometimes both these expressions are used to denote the group's algebra. Therefore, before addressing Lie algebras, we begin by briefly reviewing the connection between these two concepts.

A set G forms a group if there is an operation \cdot (group multiplication) such that for any $a, b \in G$, $a \cdot b$ is also an element of G and, in addition, the following holds:

- The group multiplication is associative, meaning that $(a \cdot b) \cdot c = a \cdot (b \cdot c)$ for any $a, b, c \in G$.
- G contains an identity element e such that $a \cdot e = a$ for any $a \in G$.
- For all $a \in G$ there is an $a^{-1} \in G$ (the inverse of a) such that $a \cdot a^{-1} = e$.

The number of elements of G may be finite in number or not. This latter case is the one which interests us, in particular when the group elements can be labeled by continuous parameters (G is said to be a **continuous group**). In addition, the set G can be a manifold differentiable to all orders, with a group multiplication function $G \times G \rightarrow G$ also differentiable to all orders. This is the main feature of a Lie group, even though the exact definition of such a group varies across the literature. The requirement that G is a group and an infinitely differentiable manifold at the same time gives rise to an interesting object which combines these two mathematical structures in a non-trivial way.

At this point, it is worth mentioning that Yang–Mills theories deal with invertible linear transformations that act on some n complex fields.¹ These transformations forms a group, the **complex general linear group** $GL(n, \mathbb{C})$, which consists of all $n \times n$ complex matrices with a non-null determinant, together with the operation of matrix multiplication. Any subgroup of $GL(n, \mathbb{C})$ is called a **linear group** and we may therefore restrict our analysis to these ones.

We shall now move on to consider algebras. An **algebra** \mathfrak{g} over a field K is a vector space \mathfrak{g} over a field K together with a bilinear operation \times , such that $a \times b \in \mathfrak{g}$ for any $a, b \in \mathfrak{g}$. This means that for any $a, b, c \in \mathfrak{g}$ and $k \in K$ the following holds:

- $(a + b) \times c = a \times c + b \times c$ and $a \times (b + c) = a \times b + a \times c$;
- $(ka) \times b = a \times (kb) = k(a \times b)$.

This definition is very general and as such the resulting object does not possess much structure. A Lie algebra is one that satisfies two additional conditions:

- $a \times a = 0$;
- $(a \times b) \times c + (c \times a) \times b + (b \times c) \times a = 0$.

In most cases, we consider Lie algebras of linear transformations, so a particular notation is used for this bilinear operation \times , which is a commutator $[\cdot, \cdot]$. The reason for this is simple: consider two linear transformations represented in a given basis by two matrices A and B . Then the matrix commutator $[A, B] = AB - BA$ defines a bilinear relation with the properties of the \times just described. Therefore the set of linear transformations on a given vector space forms a Lie algebra. This is the case we are interested in, so we shall use this notation henceforth.

We have so far described the concepts of Lie group and Lie algebra separately without connecting the two. Intuitively, there is a Lie algebra associated to a Lie group that describes its local structure. It turns out that this Lie algebra contains almost everything there is to know about the underlying Lie group and for this reason, in many situations we only consider the Lie algebras, or equivalently, elements of the Lie group infinitesimally close to the identity element e .

Recall that for a point g of a differentiable manifold G , the tangent space at g ($\equiv T_g G$) is the vector space consisting of all $\gamma'(0)$ where $\gamma(t)$ is any path in G such that $\gamma(0) = g$. This vector space has the same dimension as the manifold G

¹ The fact that some fields are strictly real is of no consequence to the present discussion.

and it forms a Lie algebra under the so-called Lie bracket. Elaborating a little on this point, note that a vector X in $T_e G$ (the tangent space at the group's identity element e) can be used to create a vector field in all of G by using the group's multiplication to transport it everywhere. The resulting vector field is said to be left or right invariant depending on how this translation is done. Suppose then that there are two such vector fields X and Y —their Lie bracket is defined to be the vector field

$$[X, Y] = \left(X^b \partial_b Y^a - Y^b \partial_b X^a \right) \partial_a, \quad (4.1)$$

which is also left/right invariant. Under this operation, invariant vector fields (or equivalently $T_e G$ since we can move vectors on G) forms a Lie algebra. The right side of equation (4.1) can be understood as the commutator of the vectors X and Y if we use as a coordinate basis the vectors $\partial/\partial x^a = \partial_a$ such that $X = X^a \partial_a$ and $Y = Y^a \partial_a$.

One useful tool in making the connection between the Lie group G and its Lie algebra $T_e G$ is the so-called **exponential map**. As we will see, a Lie algebra admits a pseudo-metric (the Killing form) so we may define geodesics in G [400]. It turns out that these geodesic curves correspond to one-parameter subgroups of G . If γ is one such geodesic with $\gamma(0) = e$ then the exponential map is defined by the relation

$$\text{Exp} [\gamma'(0)] \equiv \gamma(1) . \quad (4.2)$$

Following [400], we used a capital “E” here because this rather abstract definition generalizes the usual one of the exponential function, as applied to matrices and complex numbers. Nevertheless, henceforth we will safely consider $\text{Exp} = \text{exp}$. The exponential map in equation (4.2) relates a member of the group, $\gamma(1)$, with a member of its algebra, $\gamma'(0)$, and it turns out that for finite dimensional Lie groups, any element of G close enough to the identity can be written in this way. In fact, this is valid for all elements connected to the identity e of a compact group. On the other hand, since the exponential map is a continuous function, elements of G disconnected from e cannot be given in this form. Also, if G is not compact, the exponential map may not be surjective. As an example, consider \mathbb{R} which is a Lie group under addition; its Lie algebra is also \mathbb{R} but $\text{exp}(\mathbb{R}) = \mathbb{R}^+ \neq \mathbb{R}$.

From this discussion, it follows that different groups can have the same algebra. We shall see this with two examples. The first pair of groups we shall consider is $G = \mathbb{R}$, the real numbers with the sum operation, and $G = U(1)$, the group of complex numbers of unit modulus, with the multiplication operation. In both cases the Lie algebra is isomorphic to \mathbb{R} , even though the groups are different.

Consider next $SU(2)$, the group of 2×2 unitary complex matrices with determinant 1, and $SO(3)$, the group of 3×3 real symmetry matrices with unit determinant, or alternatively the group of linear transformations that preserves

the scalar product $\mathbf{x} \cdot \mathbf{y} = x^i y_i$ of two \mathbb{R}^3 vectors, \mathbf{x} and \mathbf{y} . Defining $\Sigma(\mathbf{x}) \equiv x^i \sigma_i$ where σ_i are the three Pauli matrices, it is easy to check that

$$\text{Tr}[\Sigma(\mathbf{x})\Sigma(\mathbf{y})] = 2\mathbf{x} \cdot \mathbf{y}. \quad (4.3)$$

On the other hand, notice that if U is a unitary matrix, then $U\Sigma(\mathbf{x})U^{-1}$ can also be written as $\Sigma(\mathbf{x}')$ for some vector \mathbf{x}' . This vector is a rotation of the original one, $\mathbf{x}' = R_U\mathbf{x}$ since $\mathbf{x}' \cdot \mathbf{y}' = \mathbf{x} \cdot \mathbf{y}$ by relation (4.3). This map $U \rightarrow R_U$ from $SU(2)$ to $SO(3)$ preserves the group structure of $SO(3)$ (meaning that $UV \rightarrow R_U R_V$) and in fact we can get all \mathbb{R}^3 rotations in this way. However, $R_U = R_{-U}$ for any $U \in SU(2)$ which means that different elements of $SU(2)$, U and $-U$, give the same rotation so these two groups are not the same ($SU(2)$ covers twice the $SO(3)$ group). Nonetheless, these two groups share the same algebra and this helps to explain why the $SU(2)$ group can play the role of the rotation group in quantum mechanics. Latter on, in connection to the relativistic Lorentz group, we shall encounter a similar situation.

4.3 LIE ALGEBRAS

4.3.1 Basic concepts

Since it is a vector space, we can choose a basis for a Lie algebra \mathfrak{g} . We call the elements of such basis the **generators of the algebra**, t_a , with $a = 1, \dots, n$, where n is the **dimension of the algebra**. As such, any $x \in \mathfrak{g}$ can be written as a linear combination $c^a t_a$. In a **real algebra** these coefficients c_a are real, while in a **complex algebra** they are complex. In subsection 4.3.7, we shall see that despite the proliferation of complex quantities in Yang–Mills theories, the gauge symmetry must have a real Lie algebra. Nevertheless, unless otherwise stated, in the following we consider the algebras to be complex.

The concepts of abelian, simple, semi-simple and reductive Lie algebra are equally important. An **abelian Lie algebra** \mathfrak{g} is one for which the Lie bracket is always zero, $[\mathfrak{g}, \mathfrak{g}] = 0$.² Note that every abelian Lie algebra can be broken down into several $\mathfrak{u}(1)$'s.

To proceed we need the concept of an ideal of an algebra: a set $\mathfrak{s} \subset \mathfrak{g}$ is a **subalgebra** of \mathfrak{g} if \mathfrak{s} closes under the Lie bracket operation: $[\mathfrak{s}, \mathfrak{s}] \subset \mathfrak{s}$. If $\mathfrak{s} \subset \mathfrak{g}$ meets the more demanding condition that $[\mathfrak{g}, \mathfrak{s}] \subset \mathfrak{s}$ then \mathfrak{s} is an **ideal** of L (and clearly a subalgebra too). In a way, subalgebras and ideals stand for Lie algebras in the same way as subgroups and invariant subgroups stand for groups, respectively. Note that for every Lie algebra \mathfrak{g} there are two trivial ideals, the 0 algebra of null dimension, and \mathfrak{g} itself; the other non-trivial ones are called **proper ideals** of \mathfrak{g} .

A Lie algebra is **simple** if it is non-abelian and has no proper ideals. On the other hand, a **semi-simple Lie algebra** is a non-null Lie algebra with no proper abelian ideals [399]. The connection between these two last concepts is made more clear with the notion of **direct sum** $\mathfrak{g} = \mathfrak{g}_1 \oplus \dots \oplus \mathfrak{g}_n$ of Lie algebras $\mathfrak{g}_1, \dots, \mathfrak{g}_n$.

² This notation means the following: the set generated by taking the commutator of all combinations of $x_1, x_2 \in \mathfrak{g}$ contains only one element—the zero vector.

Any element of this \mathfrak{g} can be written as a linear combination of elements of the \mathfrak{g}_i , and in addition each \mathfrak{g}_i must be an ideal of \mathfrak{g} . As a consequence of this last requirement, $[\mathfrak{g}_i, \mathfrak{g}_j] = 0$ for $i \neq j$. Then, the important result is that a semi-simple Lie algebra is a direct sum of simple Lie algebras. On the other hand, a direct sum of simple and abelian Lie algebras is called a **reductive Lie algebra** [400].

In subsection 4.3.7 we will argue that gauge symmetries must be given by a reductive Lie algebra. Since abelian Lie algebras are just direct sums of trivial $\mathfrak{u}(1)$ algebras, the complexity of reductive Lie algebras is completely encoded in the structure of simple groups. Therefore in the following we focus on simple Lie algebras.

Another important concept is that of a **representation** (of a Lie algebra): it is a linear map ρ which associates to every $x \in \mathfrak{g}$ a linear operator over some vector space, typically \mathbb{C}^n . In other words, $\rho(x)$ can be seen as a matrix and the linearity of ρ implies that $\rho(\alpha x + \beta y) = \alpha\rho(x) + \beta\rho(y)$ for some $x, y \in \mathfrak{g}$ and $\alpha, \beta \in \mathbb{R}$ or \mathbb{C} . In addition, to be a representation this linear map must preserve the structure of \mathfrak{g} , which means that $\rho([x, y]) = [\rho(x), \rho(y)]$. Note that we are only considering here the cases when the Lie algebra \mathfrak{g} itself is a set of matrices, so there is a blurring between \mathfrak{g} and its trivial representation $\rho = \text{Identity}$. As such, the set of matrices that defines \mathfrak{g} is sometimes called its **fundamental** or **defining representation**.

While usually $\rho(x)$ is a linear operator over \mathbb{C}^n , there is an important case where the vector space is \mathfrak{g} itself. Consider again $x, y \in \mathfrak{g}$; then for every x we can associate a linear transformation over \mathfrak{g} , $\text{ad } x$, such that $\text{ad } x(y) \equiv [x, y]$. Note that this map is linear and also $\text{ad}([x, y]) = [\text{ad}(x), \text{ad}(y)]$, so it is a representation. We call $\text{ad } x$ the **adjoint representation** of x . Furthermore, if t_1, \dots, t_n are some generators of the Lie algebra, we can use them as a basis and get the adjoint representation as a set of $n \times n$ matrices. To do so, we compute $\text{ad } t_i(t_j) = [t_i, t_j] \equiv c_{ij}^k t_k$ so $\text{ad } t_i$ can be seen as a matrix with entries $(\text{ad } t_i)_{kj} = c_{ij}^k$. These c_{ij}^k coefficients are known as the **structure constants** of \mathfrak{g} and are often viewed as carrying fundamental information of the underlying Lie algebra. However, note that they depend on the choice of generators, and are therefore basis dependent numbers.

4.3.2 Roots of simple Lie algebras

A useful tool in the study of simple Lie algebras is the so called root space decomposition, where a very particular basis for the algebra is used. The starting point consists of finding the largest set $\mathfrak{h} \in \mathfrak{g}$ such that $[\mathfrak{g}, \mathfrak{h}] = \mathfrak{h}$ (so that \mathfrak{h} is an ideal of \mathfrak{g}) and $[\mathfrak{h}, \mathfrak{h}] = 0$. Such \mathfrak{h} is called a **maximal abelian subalgebra**, **maximal toral subalgebra** or **Cartan subalgebra** of \mathfrak{g} . Note that there can be different Cartan subalgebras for a given \mathfrak{g} , but it can be shown that all choices are equivalent. The dimension of any of these Cartan subalgebras of \mathfrak{g} is known as the **rank** of the Lie algebra.

In Physics, this subalgebra can be directly related to the quantum number of fields since its elements are a maximal set of matrices that can be simultaneously diagonalizable. For example, in $SU(2)$ we have the 1-dimensional sub-

algebra generated by $\sigma_3 = \text{diag}(1, -1)$ and in $SU(3)$ we may consider the 2-dimensional space generated by the Gell-Mann matrices $\lambda_3 = \text{diag}(1, -1, 0)$ and $\lambda_8 = \frac{1}{\sqrt{3}}\text{diag}(1, 1, -2)$.

Once we have chosen a particular Cartan subalgebra \mathfrak{h} of \mathfrak{g} , there are bases of \mathfrak{g} , known as **Cartan-Weyl bases**, such that the adjoint representation of all $h \in \mathfrak{h}$ is diagonal. Thus, if we write these basis elements as e_α , $[h, e_\alpha]$ is proportional to e_α and we may denote the proportionality constant as $\alpha(h)$:

$$[h, e_\alpha] \equiv \alpha(h) e_\alpha. \quad (4.4)$$

The $\alpha(h)$ appearing in this equation is a number which depends linearly on h , so for each e_α it can be viewed as function α that converts elements of \mathfrak{h} into numbers (a functional). Therefore these α belong to the dual vector space of \mathfrak{h} , which is denoted as \mathfrak{h}^* , and they are known as **roots** (the eigenvalues of $\text{ad}(h)$) while the e_α are called **root vectors** (the eigenvectors of $\text{ad}(h)$). We stress again that even though α is an eigenvalue of $\text{ad}(h)$, it is not to be seen as a number because we want to consider an arbitrary $h \in \mathfrak{h}$ and not just a specific one, so α is a function of h . The root vector e_α on the other hand must be an eigenvector of $\text{ad}(h)$, for all h . In practice, since every h is a linear combination of some basis elements h_1, \dots, h_n of \mathfrak{h} , for every e_α the corresponding root α can be seen as the list of numbers $\alpha(h_1), \dots, \alpha(h_n)$. There is however a detail: if a given α is zero, or in other words $\alpha(h_1) = \dots = \alpha(h_n) = 0$, then it is not considered a root and this happens only when e_α itself is in the Cartan subalgebra \mathfrak{h} . The **root system** Δ is the name given to the set of all roots of a Lie algebra.

We have just achieved a **root space decomposition** of \mathfrak{g} :

$$\mathfrak{g} = \bigoplus_{\alpha} \mathfrak{g}_{\alpha} = \mathfrak{h} + \bigoplus_{\alpha \neq 0} \mathfrak{g}_{\alpha}, \quad (4.5)$$

where \mathfrak{g}_{α} is the subspace of the Lie algebra \mathfrak{g} consisting of all elements $x \in \mathfrak{g}$ such that $[h, x] = \alpha(h)x$ for an arbitrary $h \in \mathfrak{h}$ (\mathfrak{g}_{α} is called a **root space**). In other words, \mathfrak{g}_{α} is the eigenspace of $\text{ad}(h)$ with eigenvalue α and it can be shown that $\mathfrak{g}_{\alpha \neq 0}$ is always a 1-dimensional space: it is made up of e_α and multiples of it—confer with equation (4.4). Note that this is usually not true for \mathfrak{g}_0 , which coincides with the Cartan subalgebra \mathfrak{h} , and is therefore an n -dimensional space.

In order to make this discussion less abstract, consider $\mathfrak{su}_{\mathbb{C}}(2)$, which is the **complexified** algebra of $SU(2)$ (linear combinations of the generators can be complex). We do this complexification because we will be assuming that the algebras are complex, and with this understanding we will drop the \mathbb{C} subscript. The Pauli matrices are commonly chosen as generators,

$$\sigma_1 = \begin{pmatrix} 0 & 1 \\ 1 & 0 \end{pmatrix}, \quad \sigma_2 = \begin{pmatrix} 0 & -i \\ i & 0 \end{pmatrix}, \quad \sigma_3 = \begin{pmatrix} 1 & 0 \\ 0 & -1 \end{pmatrix}, \quad (4.6)$$

whose commutators are

$$[\sigma_i, \sigma_j] = 2i\varepsilon_{ijk}\sigma_k. \quad (4.7)$$

The third Pauli matrix can be taken as the generator of the Cartan subalgebra, but $[\sigma_3, \sigma_{1(2)}]$ is not proportional to $\sigma_{1(2)}$ (see equation (4.4)), so we change to a Cartan-Weyl basis:

$$e = \frac{1}{2}(\sigma_1 + i\sigma_2) = \begin{pmatrix} 0 & 1 \\ 0 & 0 \end{pmatrix}, \quad f = \frac{1}{2}(\sigma_1 - i\sigma_2) = \begin{pmatrix} 0 & 0 \\ 1 & 0 \end{pmatrix},$$

$$h = \sigma_3 = \begin{pmatrix} 1 & 0 \\ 0 & -1 \end{pmatrix}. \quad (4.8)$$

This e and f are known in Physics as raising and lowering operators. According to equation (4.4), e and f are root vectors with roots

$$\alpha_e(h) = 2, \quad \alpha_f(h) = -2, \quad (4.9)$$

so the root system of $\mathfrak{su}(2)$ is $\Delta = \{\alpha_e, \alpha_f\} = \{\pm\alpha_e\}$. Similarly, for $\mathfrak{su}(3)$ we may use

$$\{x_1, \dots, x_8\} = \frac{1}{2} \left\{ \lambda_1 + \lambda_2, \lambda_1 - \lambda_2, \lambda_4 + \lambda_5, \lambda_4 - \lambda_5, \lambda_6 + \lambda_7, \lambda_6 - \lambda_7, \lambda_3, \frac{2}{\sqrt{3}}\lambda_8 \right\}, \quad (4.10)$$

as a basis of the algebra (λ_i are the eight Gell-Mann matrices). The Cartan subalgebra is generated by x_7 and x_8 and

$$\alpha_{1(2)}(ax_7 + bx_8) = \pm a, \quad (4.11)$$

$$\alpha_{3(4)}(ax_7 + bx_8) = \pm \left(-\frac{1}{2}a + b \right), \quad (4.12)$$

$$\alpha_{5(6)}(ax_7 + bx_8) = \pm \left(\frac{1}{2}a + b \right), \quad (4.13)$$

$$\alpha_{7(8)}(ax_7 + bx_8) = 0, \quad (4.14)$$

so the root system is $\{\alpha_1, \dots, \alpha_6\} = \{\pm\alpha_1, \pm\alpha_3, \pm(\alpha_1 + \alpha_3)\}$. Two features emerge here which turn out to be true for any simple algebra: the first one is that for every root α there is an opposite one, $-\alpha$. The second is that some of the roots are linear combinations of other roots, which is to be expected, as roots are objects in \mathfrak{h}^* (the dual vector space of the Cartan subalgebra \mathfrak{h}), and therefore there can be at most n independent α 's, where n is the algebra rank. In fact, it turns out there are always exactly n linearly independent roots. For latter use, we would like now to define negative and positive roots and this can be done as follows. First we choose n linearly independent roots $\{\alpha_1, \dots, \alpha_n\}$, with some arbitrary but fixed ordering. Every root α can then be written as a linear combination $\alpha = c^i \alpha_i$ and α is said to be a **positive root** if the first non-zero c^i is a positive number. Any positive root that is not the sum of two positive roots is called a **simple root** and there are always n such roots. We shall denote by Δ_+ the set of all positive roots of a simple Lie algebra, and Π will represent the set of simple roots.

Simple roots are very important because, as we shall see, they carry all the information on the structure of the Lie algebra, and for this reason they are used

in the classification of complex simple Lie algebras. Before discussing this, we need to introduce a pseudo-inner product called the Killing form. As for the notation, for convenience we shall indicate summations explicitly when there is one, in the following three subsections.

4.3.3 The Killing form

The **Killing form** (\cdot, \cdot) provides something similar to a scalar product in a Lie algebra \mathfrak{g} :

$$(y, z) \equiv \text{Tr} [\text{ad}(y) \text{ad}(z)] \quad (4.15)$$

for $y, z \in \mathfrak{g}$. With a basis x_1, \dots, x_n of \mathfrak{g} , this is the same as $\sum_i [y, [z, x_i]]_{\text{coefficient in } x_i}$. Notice that while the Killing form is symmetric, $(y, z) = (z, y)$, in general it is degenerate, meaning that for some non-null y we have $(y, z) = 0$ for any z . However, there is a theorem due to Cartan which states that a Lie algebra is semi-simple if and only if the Killing form is non-degenerate. Even so, if the algebra is complex then $(iy, iy) = -(y, y)$, which means that (\cdot, \cdot) is neither positive nor negative definite. On the other hand, the particular real Lie algebras used in gauge theories (see subsection 4.3.7) are such that, as long as $y \neq 0$, (y, y) is always negative (this is a theorem due to Weyl).

It can be shown that if another representation is used in equation (4.15) instead of the adjoint one, the resulting bilinear function $(\cdot, \cdot)'$ differs from (\cdot, \cdot) by just a multiplicative factor. As such, we note that the Dynkin index $S(R)$ used in Physics must be related to the Killing form by some multiplicative factor (subsection 4.3.7).

The Killing form, being a bilinear non-degenerate form on the simple Lie algebra \mathfrak{g} and in particular on its Cartan subalgebra \mathfrak{h} , can be used to identify the dual space \mathfrak{h}^* (the space to which roots belong) with \mathfrak{h} itself. Indeed, for every root $\alpha \in \mathfrak{h}^*$ there is an $h_\alpha \in \mathfrak{h}$ such that

$$\alpha(k) = (h_\alpha, k) , \quad (4.16)$$

with $k \in \mathfrak{h}$. Consider then \mathfrak{h}_0^* , the space of real combinations of the roots such that (h_α, h_β) is positive or zero for any $\alpha, \beta \in \mathfrak{h}_0^*$. With the Killing form it is possible to define a genuine inner product

$$\langle \alpha, \beta \rangle \equiv (h_\alpha, h_\beta) \quad (4.17)$$

on this space, which means that we can talk about norms and angles between roots. We note in particular that equation (4.4) can be written as $[h_\beta, e_\alpha] = \alpha(h_\beta) e_\alpha = \langle \alpha, \beta \rangle e_\alpha$. Normalizing both root vectors e_α and Cartan subalgebra elements h_β will lead us in the next subsection to the Chevalley-Serre basis.

4.3.4 The Cartan matrix and the classification of all complex simple Lie algebras

If $\{\alpha_1, \dots, \alpha_n\}$ are the simple roots of a complex simple Lie algebra \mathfrak{g} then the **Cartan matrix** A of \mathfrak{g} , defined as

$$A_{ij} \equiv \frac{2 \langle \alpha_i, \alpha_j \rangle}{\langle \alpha_j, \alpha_j \rangle}, \quad (4.18)$$

can be shown to encode all the information about \mathfrak{g} , and therefore it provides a way to classify all such algebras. This is a $n \times n$ matrix with peculiar properties which are a consequence of restrictions in the angles and norms of simple roots. Without proof, some of the more important ones are the following:

1. $A_{ii} = 2$;
2. $A_{ij} = 0, -1, -2$ or -3 for $i \neq j$;
3. $A_{ij}A_{ji} = 0, 1, 2$ or 3 for $i \neq j$, and in the first case $A_{ij} = A_{ji} = 0$;
4. There is at most one entry in A with a value smaller than -1 ;
5. The sum of the negative entries of each column or row of A is never smaller than -3 ;
6. $\det A \neq 0$.

Notice that the Cartan matrix is not symmetric in general. The reason is that different α_i may have different squared norms $\langle \alpha_i, \alpha_i \rangle$. In any case, from properties 2, 3 and 4 of the Cartan matrix, we can infer that a simple Lie algebra \mathfrak{g} contains at most simple roots of two different squared norms, differing by a factor of 2 or 3. The absolute normalization of the α_i is irrelevant though.

Since A is such a special matrix, it is very often translated into a **Dynkin diagram**. This is done by representing each α_i by a dot and connecting the dots of α_i and $\alpha_j \neq \alpha_i$ by $A_{ij}A_{ji} = \max(|A_{ij}|, |A_{ji}|)$ lines. If all roots have the same norm, $A_{ij}A_{ji}$ will always be 0 or 1, so all connections are with a single line, and the algebra is called **simply laced**. If this is not the case, the simple roots with double or triple line connections must be distinguished in the Dynkin diagram, and a common convention is to use a white dot for the one with the bigger norm and a black dot for the simple root with the smaller norm.

As a consequence of the peculiarities of the Cartan matrix, it is easy to list all possibilities. There are four infinite families of Lie algebras, also known as the **classical Lie algebras**,

$$A_n = \mathfrak{su}(n+1) \quad n \geq 1, \quad B_n = \mathfrak{so}(2n+1) \quad n \geq 2, \quad (4.19)$$

$$C_n = \mathfrak{sp}(2n) \quad n \geq 3, \quad D_n = \mathfrak{so}(2n) \quad n \geq 4, \quad (4.20)$$

and five singular or **exceptional Lie algebras** designated as

$$G_2, F_4, E_6, E_7, E_8. \quad (4.21)$$

Their Cartan matrices and Dynkin diagrams are shown in figure (6). From the diagrams, it is clear that the constraints in equations (4.19) and (4.20) on n can be relaxed a little: for example there is a C_2 , but it is the same as B_2 . Also, $D_3 = A_3$ and $A_1 = B_1 = C_1 = D_1$. As for D_2 , its Dynkin diagram consists of two disconnected dots, meaning that this algebra consists of two A_1 's that are independent of each other ($D_2 = A_1 \oplus A_1$), so it is not a simple Lie algebra.

The Cartan matrix is related to the commutator of elements of the algebra. For a set of simple roots $\alpha_1, \dots, \alpha_n$ we define the following $3n$ elements of the Lie algebra (the **Chevalley-Serre basis**):

$$e_i \equiv e_{\alpha_i}, \quad (4.22)$$

$$f_i \equiv \frac{2}{(e_{\alpha_i}, e_{-\alpha_i}) \langle \alpha_i, \alpha_i \rangle} e_{-\alpha_i}, \quad (4.23)$$

$$h_i \equiv \frac{2}{\langle \alpha_i, \alpha_i \rangle} h_{\alpha_i}. \quad (4.24)$$

Recall that $e_{\alpha}(e_{-\alpha})$ are the root vectors associated to the root/eigenvalue $\alpha(-\alpha)$ and h_{α} is the member of the Cartan subalgebra \mathfrak{h} such that $\alpha(k) = (h_{\alpha}, k)$ for a $k \in \mathfrak{h}$ (equation (4.16)). Then, it can be shown that the commutator between these elements of the algebra is given by the **Chevalley-Serre relations**:

$$[e_i, f_j] = \delta_{ij} h_j, \quad (4.25)$$

$$[h_i, e_j] = A_{ji} e_j, \quad (4.26)$$

$$[h_i, f_j] = -A_{ji} f_j, \quad (4.27)$$

where A is the Cartan matrix. Except for $\mathfrak{su}(2)$, these $3n$ elements do not generate the algebra, which is larger. For example, $\mathfrak{su}(3)$ has rank 2 ($n = 2$) but its dimension is 8, which is bigger than 3×2 . However, the missing generators can be obtained by successive commutations of the lowering and raising operators e_i and f_i , until no new elements are created: $[e_i, e_j], [e_i, [e_j, e_k]], \dots, [f_i, f_j], [f_i, [f_j, f_k]], \dots$. It is also worth noting the similarity between e_i, f_i and h_i in equations (4.25)–(4.27) and the raising (e), lowering (f) and diagonal (h) operators of $\mathfrak{su}(2)$ in equation (4.8). In a transparent way, the Chevalley-Serre relations tell us that a Lie algebra of rank n can be viewed as being made up of n copies of $\mathfrak{su}(2)$, one for each dot on the Dynkin diagram, and that the interactions between these $\mathfrak{su}(2)$ copies are encoded by the Cartan matrix. Despite the apparent simplicity of these relations, they endow simple Lie algebras with intricate properties, all of which are calculable from the Cartan matrix.

4.3.5 Representations, weights and the Casimir operator

In $\mathfrak{su}(2)$ every irreducible representation is identifiable by a non-negative integer $2s$, where s is the half-integer spin in Particle Physics, and this representation contains $2s + 1$ different isospin components $2t_3 = 2s, 2s - 2, \dots, -2s + 2, -2s$. Noting that $A_1 = \mathfrak{su}(2)$ is the most basic of simple groups, we shall now see how this generalizes for other simple groups with a rank $n > 1$. The generalization of

Simple algebra	Dynkin diagram	Cartan matrix
A_n		$\begin{pmatrix} 2 & -1 & & 0 \\ -1 & \ddots & \ddots & \\ & \ddots & \ddots & -1 \\ 0 & & -1 & 2 \end{pmatrix}$
B_n		$\begin{pmatrix} 2 & -1 & & 0 \\ -1 & \ddots & \ddots & \\ & \ddots & \ddots & -1 \\ 0 & & -1 & 2 & -2 \\ & & & -1 & 2 \end{pmatrix}$
C_n		$\begin{pmatrix} 2 & -1 & & 0 \\ -1 & \ddots & \ddots & \\ & \ddots & \ddots & -1 \\ 0 & & -1 & 2 & -1 \\ & & & -2 & 2 \end{pmatrix}$
D_n		$\begin{pmatrix} 2 & -1 & & 0 \\ -1 & \ddots & \ddots & \\ & \ddots & \ddots & -1 & -1 \\ & & -1 & 2 & 0 \\ 0 & & -1 & 0 & 2 \end{pmatrix}$
E_6		$\begin{pmatrix} 2 & -1 & 0 & 0 & 0 & 0 \\ -1 & 2 & -1 & 0 & 0 & 0 \\ 0 & -1 & 2 & -1 & 0 & -1 \\ 0 & 0 & -1 & 2 & -1 & 0 \\ 0 & 0 & 0 & -1 & 2 & 0 \\ 0 & 0 & -1 & 0 & 0 & 2 \end{pmatrix}$
E_7		$\begin{pmatrix} 2 & -1 & 0 & 0 & 0 & 0 & 0 \\ -1 & 2 & -1 & 0 & 0 & 0 & 0 \\ 0 & -1 & 2 & -1 & 0 & 0 & -1 \\ 0 & 0 & -1 & 2 & -1 & 0 & 0 \\ 0 & 0 & 0 & -1 & 2 & -1 & 0 \\ 0 & 0 & 0 & 0 & -1 & 2 & 0 \\ 0 & 0 & -1 & 0 & 0 & 0 & 2 \end{pmatrix}$
E_8		$\begin{pmatrix} 2 & -1 & 0 & 0 & 0 & 0 & 0 & 0 \\ -1 & 2 & -1 & 0 & 0 & 0 & 0 & 0 \\ 0 & -1 & 2 & -1 & 0 & 0 & 0 & -1 \\ 0 & 0 & -1 & 2 & -1 & 0 & 0 & 0 \\ 0 & 0 & 0 & -1 & 2 & -1 & 0 & 0 \\ 0 & 0 & 0 & 0 & -1 & 2 & -1 & 0 \\ 0 & 0 & 0 & 0 & 0 & -1 & 2 & 0 \\ 0 & 0 & -1 & 0 & 0 & 0 & 0 & 2 \end{pmatrix}$
F_4		$\begin{pmatrix} 2 & -1 & 0 & 0 \\ -1 & 2 & -2 & 0 \\ 0 & -1 & 2 & -1 \\ 0 & 0 & -1 & 2 \end{pmatrix}$
G_2		$\begin{pmatrix} 2 & -3 \\ -1 & 2 \end{pmatrix}$

Figure 6: List of all the complex simple Lie algebras. In the Dynkin diagrams, we have added a label to each dot indicating the simple root it represents. A permutation of these labels leads to a Cartan matrix with a different arrangement of rows and columns, but the underlying Lie algebra is the same.

twice the isospin components t_3 are called the weights of a representation, and in practice they are a list of n integers each (for $\mathfrak{su}(2)$, $n = 1$ so each weight is a number). The weights of an irreducible representation can be sorted, and the representation itself is labeled by its highest weight, which in practice is a list of n non-negative integers—the so-called Dynkin coefficients of the representation.

To see this in some detail, consider a Φ which transforms under some representation of a Lie algebra \mathfrak{g} , in a basis where all the representation matrices \mathcal{H} of the Cartan subalgebra elements h are diagonal. Then for each component w of Φ^w

$$\mathcal{H}\Phi^w \equiv M^w(h)\Phi^w. \quad (4.28)$$

The M^w are called **weights**, and they are functions that transform elements of the Cartan subalgebra into plain numbers, just like roots. So, as with roots, we can view them as a list of n numbers by establishing a basis $\{h_i\}$ for the Cartan subalgebra. In particular, if we use the Chevalley-Serre basis such that \mathcal{H}_i is the representation matrix of h_i then, by equation (4.24), we have

$$\mathcal{H}_i\Phi^w = \frac{2\langle M^w, \alpha_i \rangle}{\langle \alpha_i, \alpha_i \rangle} \Phi^w \equiv M_i^w \Phi^w, \quad (4.29)$$

so the weight M^w is reduced to a list of plain numbers M_i^w , $i = 1, \dots, n$. It turns out that these numbers are always integers, just like $2t_3$ in $\mathfrak{su}(2)$. Once the weights M^w for the different w are sorted, the biggest one $\Lambda \equiv \max\{M^w\}$ can be used to label the representation, as mentioned above. The n numbers

$$\Lambda_i = \frac{2\langle \Lambda, \alpha_i \rangle}{\langle \alpha_i, \alpha_i \rangle} \quad (4.30)$$

are non-negative and are called the **Dynkin coefficients** of a representation. With (a) the Cartan matrix of the algebra and (b) the Λ_i Dynkin coefficients of a representation, all properties of the representation can be computed.

At this point, we should mention that, unlike in $\mathfrak{su}(2)$, two different components Φ^w and $\Phi^{w'}$ of the vector Φ may have the same weight ($M^w = M^{w'}$). In other words, the eigenspaces of the representation matrix \mathcal{H} of an arbitrary element of the Cartan subalgebra (the **weight spaces**) are in general degenerate/multi-dimensional.³ This weight multiplicity can be computed with **Freudenthal's formula**, and summing together the multiplicities of all weights yields the dimension of the representation, which is given by **Weyl's dimension formula** (see [399, 400, 403] for more details).

These weights have a number of interesting properties. For example, they come in α -strings: given a weight M and some root α of the algebra, in general there is a sequence of $M - m\alpha, M - (m - 1)\alpha, \dots, M, \dots, M + p\alpha$ where the limits m and p are easily calculable: it can be shown for example that $m - p = \frac{2\langle M, \alpha \rangle}{\langle \alpha, \alpha \rangle}$. Consider now the following. Each string has a virtual middle at $M_0 \equiv M + \frac{(p-m)}{2}\alpha = M - \frac{\langle M, \alpha \rangle}{\langle \alpha, \alpha \rangle}\alpha$,

³ The adjoint representation of an n -rank algebra is an excellent example: since the n generators of the Cartan subalgebra commute between themselves, the weight space associated to $M = 0$ is n -dimensional.

which may or may not be a real weight. So an inversion of an α -string will transform the generic weight M into $M_0 - (M - M_0) = M - 2\frac{\langle M, \alpha \rangle}{\langle \alpha, \alpha \rangle} \alpha$. This is a symmetry of the weight system:

$$S_\alpha : M \rightarrow M - 2\frac{\langle M, \alpha \rangle}{\langle \alpha, \alpha \rangle} \alpha. \quad (4.31)$$

All such symmetries, when taking into consideration different α 's, generate the **Weyl group**. Indeed, the set of reflections induced by the n simple roots is enough to generate the whole Weyl group. However, this does not mean that every element of the Weyl group is of the form S_α for some root α (the Weyl group is often much larger than the set $\{S_\alpha\}$). We shall not discuss it any further, but this symmetry of the weight system has many application, in particular it is often used to speed up computations.

As a final topic concerning representations, we note that it is possible to build an operator, quadratic in the generators, that commutes with the whole algebra. This is the well know **Casimir operator** C . It turns out that a Cartan-Weyl basis is more suitable to build such an operator: if for every root α of the algebra the root vectors are normalized such that $[e_\alpha, e_{-\alpha}] = h_\alpha$, then

$$C = \sum_{\alpha_i, \alpha_j \in \Pi} \frac{2(A^{-1})_{ij}}{\langle \alpha_i, \alpha_i \rangle} h_{\alpha_i} h_{\alpha_j} + 2 \sum_{\alpha \in \Delta^+} e_\alpha e_{-\alpha}, \quad (4.32)$$

where A is the Cartan matrix. We recall here that Π and Δ^+ are the sets of simple and positive roots, respectively (see subsection 4.3.2). Since it commutes with the algebra, C is proportional to the identity operator, and after some calculations it can be shown that when applied to an irreducible representation with highest weight Λ , the Casimir operator is given by

$$C = \left\langle \lambda, \lambda + \sum_{\alpha \in \Delta^+} \alpha \right\rangle \mathbb{1} = \sum_{i,j} \frac{1}{2} \Lambda_i (A^{-1})_{ij} \langle \alpha_j, \alpha_j \rangle (\Lambda_j + 2) \mathbb{1}, \quad (4.33)$$

which is rather easy to calculate from the Cartan matrix A and Dynkin coefficients Λ_i of the representation. If the smallest root is taken to be of norm 1, $\min(\langle \alpha_i, \alpha_i \rangle) = 1$, then it turns out that $C = (n^2 - 1)/2n \mathbb{1}$ for the **fundamental representation** of $\mathfrak{su}(n)$, whose Dynkin coefficients are $\Lambda_i = \delta_{i1}$. This matches the normalization used in Particle Physics.

4.3.6 Subalgebras and branching rules

We shall not deal at length with the issue of finding the subalgebras of a given Lie algebra, even though this is of great importance in Particle Physics and GUTs in particular. Sometimes the vacuum state in a quantum field theory breaks the gauge symmetry, and in such a case, one first tries to find which part of the original symmetry is still preserved. Once this is known, it is then necessary to study how the representations of the original Lie algebra behave under the new one, which is

preserved by the vacuum state (the **branching rules**). To address the first part of the problem in a systematic way, the concept of **maximal subalgebra** is needed: \mathfrak{g}' is said to be a maximal subalgebra of \mathfrak{g} if there is no other subalgebra \mathfrak{g}'' of \mathfrak{g} such that $\mathfrak{g} \subset \mathfrak{g}'' \subset \mathfrak{g}'$ (other than the trivial cases $\mathfrak{g}'' = \mathfrak{g}$ or \mathfrak{g}'). By studying maximal subalgebras only, there is no need to say, for instance, that $\mathfrak{su}(3)$ may break into $\mathfrak{u}(1)^3$ as this becomes obvious once it is known that $\mathfrak{su}(3)$ can break into its maximal subalgebra $\mathfrak{su}(2) \oplus \mathfrak{u}(1)$, and in turn $\mathfrak{su}(2)$ can break into its maximal subalgebra $\mathfrak{u}(1)^2$.

A subalgebra is classified as regular or special depending on how its Cartan subalgebra is related to the one of its parent algebra. A **regular subalgebra** \mathfrak{g}' of \mathfrak{g} is one whose Cartan subalgebra \mathfrak{h}' is contained in the Cartan subalgebra \mathfrak{h} of \mathfrak{g} and the set of roots Δ' of \mathfrak{g}' is contained in the set of roots Δ of \mathfrak{g} . If this is not the case, \mathfrak{g}' is said to be a **special subalgebra** of \mathfrak{g} . Grand Unified Theories deal almost invariably with regular subalgebras. This turns out to be very convenient, because the maximal regular subalgebras with an $\mathfrak{u}(1)$ ideal of a simple Lie algebra are easy to derive: deleting a dot in the Dynkin diagram of \mathfrak{g} yields a semi-simple algebra \mathfrak{m} , and $\mathfrak{u}(1) \oplus \mathfrak{m}$ is shown to be a maximal regular subalgebra of \mathfrak{g} . As an example, deleting the appropriate dots, we immediately conclude that $E_8 \rightarrow E_7 \oplus \mathfrak{u}(1)$, $E_7 \rightarrow E_6 \oplus \mathfrak{u}(1)$, $E_6 \rightarrow \mathfrak{so}(10) \oplus \mathfrak{u}(1)$, $\mathfrak{so}(10) \rightarrow \mathfrak{su}(5) \oplus \mathfrak{u}(1)$, $\mathfrak{su}(5) \rightarrow \mathfrak{su}(3) \oplus \mathfrak{su}(2) \oplus \mathfrak{u}(1)$, which is a symmetry breaking chain potentially applicable in High Energy Physics.

4.3.7 The Lie algebra of gauge symmetries

Consider now the use of Lie algebras in Yang–Mills theories. To preserve the kinetic term of the fields in the Lagrangian, these must be in a unitary representation of the Lie algebra. Resuming the use of Einstein’s summation convention for repeated indices, usually a gauge transformation is written as

$$U = \exp [i\varepsilon^a R(t_a)] , \quad (4.34)$$

with an explicit i . Therefore, the parameters ε^a of the transformation must be real and the representation matrices $R(t_a)$ of t_a must be hermitian, otherwise U is not unitary. This is an important observation: even though complex numbers appear often in these theories (for example in the Pauli matrices), the gauge symmetry must be given by a real Lie algebra. As such, note that strictly speaking the generators of the algebra are it_a instead of t_a . For example, consider the Pauli matrices which obey the relation $[\sigma_i, \sigma_j] = 2i\varepsilon_{ijk}\sigma_k$: these cannot be the generators of the real algebra $\mathfrak{su}_{\mathbb{R}}(2)$ because they do not close under the Lie bracket operation. Note also that the raising and lower operators in equation (4.8) do not generate the same real Lie algebra as $i\sigma_i$, because the two basis are related by complex coefficients.

At this point, it might seem odd that in this section, as well as in several textbooks [399, 401], it is assumed that the Lie algebras are complex. In particular, figure (6) contains the classification of all complex simple Lie algebras. There is a good reason for this though. In order to see it, we need to say a few words

about the connection between real and complex algebras. Suppose that \mathfrak{g} is a real Lie algebra: instead of taking just real linear combinations of its generators, if we take complex linear combinations as well, the resulting set will always close under commutations, so $\mathfrak{g}_{\mathbb{C}} \equiv \mathfrak{g} \oplus i\mathfrak{g}$ is a complex Lie algebra. This $\mathfrak{g}_{\mathbb{C}}$ is called the **complexification** of \mathfrak{g} , and \mathfrak{g} is said to be a **real form** of $\mathfrak{g}_{\mathbb{C}}$. There is a “many to one” relation then: the complexification of multiple real Lie algebras can be the same complex Lie algebra, or equivalently, a complex Lie algebra can have many real forms. For example, the real Lie algebras generated by $\{i\sigma_i\}$ and $\{e, g, h\}$ are two real forms of $\mathfrak{su}_{\mathbb{C}}(2)$: they are called the **compact real form** and the **normal** or **split real form**, respectively, and they exist for any complex simple Lie algebra.

It turns out that the Lie algebra of gauge theories must be the (unique) compact real form of some complex simple Lie algebra, if U in equation (4.34) is to be a unitary matrix. This is a consequence of the following considerations:

1. The generators $\{it_a\}$ of any real simple Lie algebra can be rotated and normalized such that $(it_a, it_b) = \text{sign}(a) \delta_{ab}$; in other words, the Killing form can be diagonalized, but its signature cannot be changed as the algebra is real. The compact real form is the unique real form with $(it_a, it_b) = -\delta_{ab}$, or in other words the signature of the Killing form is $(-, -, \dots, -)$. Recall that the Killing form (it_a, it_b) is proportional to $-\text{Tr}[R(t_a)R(t_b)]$ for any non-trivial representation R , with a positive proportionality factor.
2. The hermitian matrices $R(t_a)$ in equation (4.34) have real eigenvalues, so $\text{Tr}[R(t_a)R(t_b)]$ must always be non-negative for any representation R .

In other words, the hermiticity of the matrices $R(t_a)$ requires that $\text{Tr}[R(t_a)R(t_b)]$ is positive, and this is only true for the compact real form. In relation to this, note that in Particle Physics one has the trace condition:

$$\text{Tr}[R(t_a)R(t_b)] = S(R) \delta_{ab}, \quad (4.35)$$

where the positive number $S(R)$ is the **Dynkin index** of the representation R . Therefore, in summary, for every semi-simple Lie algebra (see figure (6)) there is a unique compact Lie algebra, with similar properties, whose generators can be chosen to satisfy this last equation. The expression for the Casimir operator,

$$C = R(t_a)R(t_a) = C(R) \mathbb{1}, \quad (4.36)$$

provides a simple way to convert a Cartan-Weyl basis into the one used in Physics, by comparing equations (4.32) and (4.36).

To conclude the analysis of the relation between the physical and mathematical canonical approach to Lie algebras, we must consider one final issue. It is often said that the gauge symmetry must be given by a direct sum of a semi-simple Lie algebra and $\mathfrak{u}(1)$'s (i.e., a reductive Lie algebra), but the reason for it is usually omitted. There are many other non-reductive Lie algebras, for example the one generated by x_1, x_2 such that $[x_1, x_2] = x_2$. We have previously seen why a gauge symmetry must be associated to a Lie algebra, but why should it be a reductive

one? To answer this question we start by noting that the gauge bosons are in the adjoint representation of the gauge group:

$$A_\mu \rightarrow \exp [i\varepsilon^a R_{\text{ad}}(t_a)] A_\mu \quad (4.37)$$

for a space-time independent transformation. The adjoint representation matrices are connected to the structure constants, $[R_{\text{ad}}(t^a)]_{bc} = ic_{ac}^b$, and their hermiticity implies that the structure constants c_{ac}^b must be antisymmetric in all three indices. If the Lie algebra \mathfrak{g} is a direct sum of two vector spaces, \mathfrak{m} and \mathfrak{m}^T , and if \mathfrak{m} is an ideal of L ($[\mathfrak{g}, \mathfrak{m}] \subset \mathfrak{m}$) then the hermiticity of the adjoint representation implies that the orthogonal vector space \mathfrak{m}^T is also an ideal of \mathfrak{g} : $[\mathfrak{g}, \mathfrak{m}^T] \subset \mathfrak{m}^T$. Therefore, \mathfrak{g} is the direct sum of the subalgebras \mathfrak{m} and \mathfrak{m}^T , and if we pick \mathfrak{m} to be the biggest abelian ideal of \mathfrak{g} , then \mathfrak{m}^T is semi-simple. In conclusion, the unitarity of the transformation (4.37) implies that $\mathfrak{g} = (\text{abelian algebra}) \oplus (\text{semi-simple algebra}) = \oplus (\mathfrak{u}(1) \text{ or simple algebras})$.

4.4 SPACE-TIME SYMMETRIES

4.4.1 The Lorentz and Poincaré groups

The way the laws of Physics are written in a given coordinate frame depends on the space-time metric. As mentioned at the beginning of this chapter, the Poincaré group is the group of space-time transformations which leaves the Minkowski metric η invariant, so it is the space-time symmetry group of the laws of Physics in flat space-time. It is easy to verify that such transformations must be of the form [404]

$$x^\mu \rightarrow x'^\mu = \Lambda^\mu_\nu x^\nu + b^\mu, \quad (4.38)$$

for some matrix Λ and a vector b . The inhomogeneous part of these transformations, given by the b vector, can take any value, and it corresponds to translations in the four space-time directions. Ignoring these, we are left with the homogeneous part of the Poincaré group—the Lorentz group. Each transformation of the x^μ under this group is given by a Λ matrix and, in order for equation (4.38) to be an isometry of the flat space-time metric, we must ensure that

$$\eta = \Lambda^T \eta \Lambda. \quad (4.39)$$

The group of Λ 's which satisfy this equation is sometimes denoted by $O(1, 3)$, as the above equation matches the definition of the 4-dimensional orthogonal group, except that the signature of η is $(+ - - -)$ instead of $(+ + + +)$. It is well known that this group, the Lorentz group, is made up of rotations between the last three coordinates (the spacial ones), and pseudo-rotations/boosts between the first coordinate (time) and the other ones. We shall come shortly to this, when we review

the algebra of the Lorentz group. But before going into the topic of infinitesimal transformations, it is worth mentioning that the matrices

$$\Lambda_T \equiv \text{diag}(-1, +1, +1, +1) , \quad (4.40)$$

$$\Lambda_P \equiv \text{diag}(+1, -1, -1, -1) \quad (4.41)$$

also satisfy equation (4.39), although they represent neither boosts nor rotations; they represent time (Λ_T) and space (Λ_P) reversal operations. Because of the existence of these transformations, topologically $O(1, 3)$ is not a connected set. But if we remove them (appropriately), the resulting group, which is named the restricted or proper Lorentz group and denoted by $SO(1, 3)^+$, is indeed connected. To summarize this relation, we can write⁴

$$O(1, 3) = SO(1, 3)^+ \rtimes \{\mathbb{1}, \Lambda_T, \Lambda_P, \Lambda_T \Lambda_P\} . \quad (4.42)$$

Note that by removing in this way the Λ_T and Λ_P transformations from $O(1, 3)$, all the remaining Λ have unit determinant, yet we cannot call the resulting group $SO(1, 3)$ because we also removed $\Lambda_T \Lambda_P = -\mathbb{1} \in SO(1, 3)$.

It turns out that, at the microscopic level, the laws of Physics are not invariant under Λ_T and Λ_P , at least at the energies probed so far,⁵ so at this point $SO(1, 3)^+$, the proper Lorentz group, would seem to be the true space-time symmetry group. If there were only scalar and vector quantities such as the Higgs fields (H^0, H^+), the electromagnetic field (A^μ), or coordinates (x^μ) this would be true. However, the study of the electron essentially reveals that a 360° rotation adds a minus sign to its wave function, instead of leaving it invariant. The implication of this experimental result is that the space-time symmetry group cannot be just $SO(1, 3)^+$; it must be the bigger $SL(2, \mathbb{C})$, which is the group of 2×2 matrices with complex entries and unit determinant (it is named the two dimensional special linear group over \mathbb{C}). Much like the case of $SO(3)$ and $SU(2)$ discussed previously, there is a 1:2 relation between $SO(1, 3)^+$ and $SL(2, \mathbb{C})$, and this accounts for the minus sign gained by the electron wavefunction under a 360° rotation. To see this *double covering* of $SO(1, 3)^+$ by the $SL(2, \mathbb{C})$ group⁶ we can use the $\sigma^\mu = (1, -\boldsymbol{\sigma})$ matrices. First note that any $\Lambda \in SO(1, 3)^+$ transforms a 4-vector x^μ while preserving the pseudo-norm $x^T \eta x$. Then we identify any of these 4-vectors x^μ with the 2×2 matrix $x^\mu \sigma_\mu$

⁴ The symbol \rtimes stands for a semi-direct product of two groups. If $G = N \rtimes H$, it means that each element $g \in G$ can be written as the product of an element $n \in N$ and $h \in H$. The product of $g_1 = (n_1, h_1)$ with $g_2 = (n_2, h_2)$ is given by $(n_3, h_1 h_2)$ with $n_3 = n_1 h_1 n_2 h_1^{-1}$, which is different from the relation $n_3 = n_1 n_2$ in a direct product. Clearly both N and H are automatically subgroups of G , but in addition it is necessary for N to be an invariant subgroup of G for this construction to make sense.

Another way to relate the two groups is the following: $SO(1, 3)^+$ is an invariant subgroup of $O(1, 3)$, so it divides $O(1, 3)$ in cosets (4 in this case). The cosets form a group (generically called the factor group) denoted by $O(1, 3)/SO(1, 3)^+$, which turns out to be $\{\mathbb{1}, \Lambda_T, \Lambda_P, \Lambda_T \Lambda_P\}$.

⁵ It may be that time-reversal T and parity P are fundamental symmetries of Nature which are broken at the energies we can probe experimentally.

⁶ The group $SL(2, \mathbb{C})$ is sometimes called $\text{Spin}(1, 3)^+$. In this nomenclature, $\text{Pin}(1, 3)$ and $\text{Spin}(1, 3)$ are the double covers of $O(1, 3)$ and $SO(1, 3)$, respectively. See for instance [405].

whose determinant is precisely $x^T \eta x$, so under a transformation $\Lambda \in SO(1, 3)^+$ of $x^\mu \rightarrow x'^\mu = \Lambda^\mu_\nu x^\nu$ we can associate the following change of $x^\mu \sigma_\mu$:

$$x^\mu \sigma_\mu \rightarrow \lambda (x^\mu \sigma_\mu) \lambda^\dagger = x'^\mu \sigma_\mu, \quad (4.43)$$

for some unknown λ matrix with determinant ± 1 . The equality in this expression follows from the fact that any hermitian 2×2 matrix is a linear combination of the four σ_μ matrices. Taking only the cases with $\det \lambda = 1$, we can therefore relate a $\Lambda \in SO(1, 3)^+$ with a $\lambda \in SL(2, \mathbb{C})$ but crucially we note that both $\lambda, -\lambda \in SL(2, \mathbb{C})$ are associated to the same Λ :

$$\Lambda^\mu_\nu x^\nu \sigma_\mu = x'^\mu \sigma_\mu = \lambda (x^\mu \sigma_\mu) \lambda^\dagger = (-\lambda) (x^\mu \sigma_\mu) (-\lambda)^\dagger. \quad (4.44)$$

We now briefly describe how this is related to relativistic fermions. We first note that the well-known γ matrices form a 2^4 -dimensional Clifford algebra generated by the matrices $\mathbb{1}, \gamma^\mu, \gamma^\mu \gamma^\nu, \gamma^\mu \gamma^\nu \gamma^\sigma, \gamma^\mu \gamma^\nu \gamma^\sigma \gamma^\rho$ ($0 \leq \mu < \nu < \sigma < \rho \leq 3$) with each γ obeying the relation

$$\gamma^\mu \gamma^\nu + \gamma^\nu \gamma^\mu = 2\eta^{\mu\nu}.$$

When $x \rightarrow x'$, the Dirac equation for a spin $1/2$ field Ψ is known to be invariant if $\Psi(x) \rightarrow \exp\left(\sum_{ij} c_{ij} [\gamma_i, \gamma_j]\right) \Psi(x)$ where the c_{ij} are some real numbers, and it can be shown that these transformations with an even number of γ matrices and unit determinant form the group $SL(2, \mathbb{C})$. More details on this connection between Clifford algebras and the Spin groups ($SL(2, \mathbb{C}) = \text{Spin}(1, 3)^+$; see footnote 6) for an arbitrary number of spatial and temporal dimensions can be found in [406] and references contained therein.

4.4.2 Lie algebras and representations of the Poincaré and Lorentz groups

The previous discussion concerned mainly the global properties of the space-time symmetry group. However, according to the discussion in section 4.2 many of important features of the a Lie group are encoded in its local structure. Therefore, without worrying too much about the details of the last subsection, we shall now briefly review the relevant aspects of infinitesimal Lorentz and Poincaré transformations, which lead directly to their algebras.

Consider first an infinitesimal translation given by δb^μ

$$x^\mu \rightarrow T(\delta b) x^\mu = x^\mu + \delta b^\mu. \quad (4.45)$$

The transformation $T(\delta b)$, valid not just for a vector such as coordinates x , can be obtained with the usual trick of considering ∂_μ to be the basis vectors in which we are taking the coordinates x^μ and δb^μ . In this way, we have $x \equiv x^\mu \partial_\mu$ and $\delta b \equiv \delta b^\mu \partial_\mu$ vectors and the transformation we seek is given by

$$T(\delta b) = \mathbb{1} + \delta b \equiv \mathbb{1} - i \delta b^\mu P_\mu, \quad (4.46)$$

or

$$T(b) = \exp(-ib^\mu P_\mu) \quad (4.47)$$

for finite translations. Here $P_\mu = i\partial_\mu$ is the conserved 4-momentum vector, the generator of translations. Similarly, $J_{\mu\nu} = i(x_\mu\partial_\nu - x_\nu\partial_\mu)$ generates boosts and rotations of the proper Lorentz group:

$$\Lambda(\omega) = \exp\left(-\frac{i}{2}\omega^{\mu\nu} J_{\mu\nu}\right), \quad (4.48)$$

where $\omega^{\mu\nu}$ are real parameters which are taken to be antisymmetric in $(\mu\nu)$ since $J_{\mu\nu} = -J_{\nu\mu}$, so there are 6 independent real parameters (3 boosts and 3 rotations).

The computation of the Lie algebra of the Poincaré group is straightforward, and it yields the following:

$$[P_\mu, P_\nu] = 0, \quad (4.49)$$

$$[P_\mu, J_{\nu\rho}] = i(\eta_{\mu\nu}P_\rho - \eta_{\mu\rho}P_\nu), \quad (4.50)$$

$$[J_{\mu\nu}, J_{\rho\sigma}] = i(\eta_{\mu\rho}J_{\sigma\nu} - \eta_{\nu\sigma}J_{\mu\rho} + \eta_{\nu\rho}J_{\mu\sigma} - \eta_{\mu\sigma}J_{\rho\nu}). \quad (4.51)$$

We shall now use the algebra of the Poincaré and Lorentz groups to derive their irreducible representations. Starting with the latter one, we shall see that Lorentz group algebra is similar to the one of $SU(2) \times SU(2)$. To reach such conclusion, first separate $J_{\mu\nu}$ into the 3 generators of rotations J_i and the 3 generators of boosts K_i :

$$J_i \equiv \frac{1}{2}\varepsilon_{ijk}J^{jk}; K_i \equiv J_{i0}, \quad i, j, k \in \{1, 2, 3\}. \quad (4.52)$$

We can then define

$$A_i^{R/L} \equiv \frac{1}{2}(J_i \pm iK_i), \quad i = 1, 2, 3, \quad (4.53)$$

and the interesting result is that the three A_i^R as well as the three A_i^L obey the $SU(2)$ algebra, and in addition the generators of one kind commute with those of the other:

$$[A_i^{R/L}, A_j^{R/L}] = i\varepsilon_{ijk}A_k^{R/L}, \quad (4.54)$$

$$[A_i^{R/L}, A_j^{L/R}] = 0. \quad (4.55)$$

However, there is an important detail here. The algebra of the proper Lorentz group algebra is not exactly the same as the one of $SU(2) \times SU(2)$ because we used a complex combination of J_i 's and K_i 's in equation (4.53), even though we are working with real algebras. In other words, the proper Lorentz group is given by the exponentiation of (real coefficients) $\times iJ_i, iK_i$, while $SU(2) \times SU(2)$ is given by the exponentiation of (real coefficients) $\times iA_i^L, iA_i^R$ and the two are not the same. This is directly related to the fact that $SU(2) \times SU(2)$ is a compact Lie group,

while $SL(2, \mathbb{C})$ is not. As a consequence, the (finite) representations of the proper Lorentz group are not unitary.

Just like $SU(2)_L \times SU(2)_R$ generated by $A_i^{R/L}$, each of the irreducible representations of the proper Lorentz group is given by two non-negative half-integers (j_L, j_R) . Since $A_i^{R*} = -A_i^L$, we have the relation $(j_L, j_R) = (j_R, j_L)^*$. Also, the basis vectors $|m_L, m_R\rangle$ of such a representation take the values $m_L = -j_L, -j_L + 1, \dots, j_L$ and $m_R = -j_R, -j_R + 1, \dots, j_R$ so (j_L, j_R) is a $(2j_L + 1)(2j_R + 1)$ -dimensional representation. Note also that since the J_3 generator of rotations is given by $A_3^R + A_3^L$, the angular quantum number m is equal to $m_R + m_L$, which means that a representation (j_L, j_R) of the proper Lorentz groups is composed of $j = j_L + j_R, j_L + j_R - 1, \dots, |j_L - j_R|$ irreducible representations of the rotation group. Consider the following examples:

- $(j_L, j_R) = (0, 0)$ is a 1-dimensional representation with $j = 0$. Such a field ϕ is called a scalar.
- $(j_L, j_R) = (1/2, 0)$ is a 2-dimensional representation with $j = 1/2$. Such a field ψ_L is a left-handed Weyl spinor.
- $(j_L, j_R) = (0, 1/2)$ is a 2-dimensional representation with $j = 1/2$. Such a field ψ_R is a right-handed Weyl spinor.
- $(j_L, j_R) = (1/2, 1/2)$ is a 4-dimensional representation with a $j = 0$ part and another one with $j = 1$. Such a field A_μ is called a 4-vector (its first component A_μ^0 is a scalar under rotations and the other three components form a vector).

On the other hand, a Dirac spinor $\Psi = (1/2, 0) \oplus (0, 1/2)$ does not form an irreducible representation of the proper Lorentz group, as it is made of right- and left-handed Weyl spinors.

We now consider the unitary representations of the Poincaré group, which are infinite dimensional. We note in passing that, while the true symmetry of space-time is given by the Poincaré group, the wave functions used to write Lagrangian densities are Lorentz representations (see [404, 407] for details on this connection). From equations (4.49)–(4.51) we see that the Poincaré group is not just the product of the translations group with the Lorentz group, and for that reason its representations are markedly different from the ones of the proper Lorentz group. We can start by diagonalizing the P_μ operator such that for an eigenstate state $|p\rangle$ we have

$$P_\mu |p\rangle \equiv p_\mu |p\rangle . \quad (4.56)$$

Without entering into details, if $p_\mu p^\mu > 0$ the irreducible representations of the Poincaré group are labeled with the continuous parameter m (interpreted physically as a mass) and a non-negative half-integer number s (the spin). In particular, these quantities are related to the two group Casimir operators

$$P_\mu P^\mu = m^2 , \quad (4.57)$$

$$W_\mu W^\mu = -m^2 s(s + 1) , \quad (4.58)$$

where $W^{\lambda\mu\nu\sigma} = -1/2\varepsilon^{\lambda\mu\nu\sigma} J_{\mu\nu} p_\sigma$ is the so-called Pauli-Lubański pseudo-vector [408], which is given by $W^0 = 0$ and $W^i = mJ^i$, $i = 1, 2, 3$ in the frame where $P_\mu = (m, \mathbf{0})$. The (infinite) set of states $\{|p_\mu, \lambda\rangle\}$ such that $p_\mu p^\mu = m^2$ and $\lambda = -s, -s + 1, \dots, s$ is the eigenvalue of the J_3 generator of rotations forms a basis for the vector space of the irreducible representation (m, s) .

If $p_\mu p^\mu = 0$, special care is needed. If $p_\mu = 0$ then this 4-vector is an invariant and the irreducible representations of the Poincaré group can be labeled as (j_L, j_R) , in analogy to the representations of the Lorentz group. Physically however, the interesting situation is when $p_\mu \neq 0$, corresponding to physical particles with no mass. The irreducible representations in this case can be labeled with a single half-integer λ (the helicity) which is the eigenvalue of the J_3 generator of rotations. Again, the infinite set of states $\{|p_\mu, \lambda\rangle\}$ such that $p_\mu p^\mu = 0$ constitutes a basis for the vector space of the λ -representation, but notice that λ is fixed here, unlike in the $p_\mu p^\mu > 0$ case. In other words, Poincaré transformations do not change the helicity of a particle. An implication of this is that the photon, with two polarizations, is actually a reducible representation of the Poincaré group, $-1 \oplus +1$ (CPT invariance requires the simultaneous presence of positive and negative helicities).

There is one final case, when $p_\mu p^\mu < 0$, which corresponds to tachyons. We shall not deal with it here and instead point to [404] for details.

4.5 SUPERSYMMETRY AS A SUPER-POINCARÉ GROUP

Can the symmetry of Nature be non-trivially larger than the Poincaré group? Under the assumptions of the 1967 Coleman-Mandula theorem [409], the answer is negative: the symmetry group G of the scattering matrix S must be a direct product of the Poincaré group and some other internal symmetries such as the gauged ones.⁷ This celebrated theorem assumes the following (ignoring some technical details):

1. G contains a subgroup locally isomorphic to the Poincaré group;
2. There is a finite number of one-particle states with finite mass, and their energy is always positive;
3. Elastic-scattering amplitudes are analytic functions of the s and t Mandelstam variables;
4. Any two plane waves scatter at almost all energies (i.e., the scattering matrix S is non-trivial);
5. G is a connected symmetry group which can be built from the generators of infinitesimal symmetry transformations.

The Coleman-Mandula theorem therefore does not allow symmetries to change simultaneously space-time coordinates and internal quantum numbers of fields. As

⁷ This also defines an internal symmetry: it consists of any symmetry commuting with the Poincaré group.

a consequence, particles with a given mass m and spin s (or just helicity λ), which are irreducible representations of the Poincaré group, cannot be related/grouped together in bigger representations of a bigger group.

The assumptions presented above are the list given in [409]. However, implicitly the Coleman-Mandula theorem also assumes that G transforms bosons into bosons and fermions into fermions and it turns out [127–129] that a super-Poincaré symmetry (supersymmetry) relating bosons to fermions is actually possible. The Coleman-Mandula theorem was eventually extended by Haag, Łopuszański and Sohnius [410] to include this possibility, and it became clear that the structure of such supersymmetries is very constrained, making these extensions of the Poincaré symmetry almost unique.

Let us then review some of the theoretical aspects of supersymmetry, following [131, 411–419]. As a first step, we shall try to motivate the existence of commutator and anti-commutator relations in a supersymmetric algebra. An infinitesimal supersymmetric transformation can be written as

$$S(\delta\alpha) = \mathbb{1} - i\delta\alpha^a G_a, \quad (4.59)$$

where the $\delta\alpha^a$ are the transformation parameters and the G_a the generator operators. Here the $\delta\alpha^a$ are assumed to be \mathbb{Z}_2 -graded parameters, meaning that they may commute or anticommute between themselves, depending on some numbers $\eta_A = \pm 1$ associated with them (the grading):

$$\delta\alpha^a \delta\alpha^b = (-1)^{\eta_a \eta_b} \delta\alpha^b \delta\alpha^a. \quad (4.60)$$

If we require that the transformation $S(\delta\alpha)$ commutes with these graded parameters, then the generators G_a themselves must behave like graded parameters:

$$G_a G_b = (-1)^{\eta_a \eta_b} G_b G_a. \quad (4.61)$$

We now subtract to $S(\delta\alpha)S(\delta\beta)$ the product of these two supersymmetric transformations applied in the reverse order. The result must itself be a supersymmetric transformation:

$$S(\delta\alpha)S(\delta\beta) - S(\delta\beta)S(\delta\alpha) = S(\delta\gamma) \quad \text{for some } \delta\gamma. \quad (4.62)$$

With a few computations this $\delta\gamma$ is shown to be

$$\delta\gamma^c G_c = -i\delta\beta^b \delta\alpha^a [G_a, G_b], \quad (4.63)$$

where, for two operators A and B , $[\cdot, \cdot]$ is defined to be the following generalization of the commutator and anti-commutator:

$$[A, B] \equiv AB - (-1)^{\eta_A \eta_B} BA. \quad (4.64)$$

Equation (4.63) implies that $[G_a, G_b]$ must be a linear combination of the generators G_c , so in this way we are lead to the concept of structure constants c_{ab}^c of a \mathbb{Z}_2 -graded Lie algebra:

$$[G_a, G_b] \equiv ic_{ab}^c G_c. \quad (4.65)$$

The generators are either bosonic ($\eta_A = 0$) or fermionic ($\eta_A = 1$), and according to equation (4.64), apart from relations between fermionic generators, which are anticommutating, all other relations between the \mathbb{Z}_2 -graded Lie algebra are given by commutators.

Returning now to the extension of the Poincaré symmetry, we note that the generators P_μ and $J_{\mu\nu}$ are bosonic operators, transforming under the proper Lorentz group as $(1/2, 1/2)$ and $(1, 0) \oplus (0, 1)$, respectively. The Haag-Łopuszański-Sohnius theorem states that the fermionic generators Q^I , $I = 1, \dots, N$ of supersymmetries must be either in the $(1/2, 0)$ representation of the proper Lorentz group or its conjugate $(0, 1/2)$. Therefore, without loss of generality, such Q^I can be taken to be left-handed Weyl spinors, while their hermitian conjugate operators $Q^{I\dagger}$ are right-handed Weyl spinors. Both have therefore two components: Q_α^I , $Q_\alpha^{I\dagger}$ with $\alpha = 1, 2$. It can be shown that the (anti)commutation relations between these fermionic charges and the generators P_μ and $J_{\mu\nu}$ of the Poincaré symmetry are the following:

$$[P_\mu, Q_\alpha^I] = 0, \quad [P_\mu, Q_\alpha^{I\dagger}] = 0, \quad (4.66)$$

$$[J_{\mu\nu}, Q_\alpha^I] = i(\sigma_{\mu\nu})_{\alpha\beta} Q_\beta^I, \quad [J_{\mu\nu}, Q_\alpha^{I\dagger}] = i(\bar{\sigma}_{\mu\nu})_{\alpha\beta} Q_\beta^{I\dagger}, \quad (4.67)$$

$$\{Q_\alpha^I, Q_\beta^J\} = \varepsilon_{\alpha\beta} Z^{IJ}, \quad \{Q_\alpha^{I\dagger}, Q_\beta^{J\dagger}\} = \varepsilon_{\alpha\beta} Z^{IJ*}, \quad (4.68)$$

$$\{Q_\alpha^I, Q_\beta^{J\dagger}\} = 2(\sigma^\mu)_{\alpha\beta} P_\mu \delta^{IJ}. \quad (4.69)$$

These relations complement the ones in equations (4.49)–(4.51). In terms of notation, we used $\sigma^{\mu\nu} = -\bar{\sigma}_{\mu\nu}^\dagger \equiv 1/4(\sigma^\mu \bar{\sigma}^\nu - \sigma^\nu \bar{\sigma}^\mu)$, where $\sigma^0 = \bar{\sigma}^0 \equiv \mathbb{1}$ and $\bar{\sigma}^{1,2,3} = -\sigma^{1,2,3} \equiv \sigma_{1,2,3}$ are the usual Pauli matrices. As for the Z^{IJ} in equations (4.68), they are bosonic symmetry generators which commute with all generators (including themselves) and for that reason they are called *central charges*. Note that in the important case where there is just a single pair of fermionic generators $\{Q, Q^\dagger\}$ ($N = 1$) then, since $Z^{IJ} = -Z^{JI}$, we conclude that there are no central charges. The $N = 1$ case is known as *simple supersymmetry*, while $N > 1$ is sometimes called *N -extended supersymmetry*. With the exception of the present section, this thesis discusses only $N = 1$ supersymmetric models; more fermionic charges lead to a bigger symmetry group and also to bigger irreducible representations, which in turn means that such theories are very restrictive.

In general, when $Z^{IJ} = 0$, one can perform any unitary transformation $U^{(R)}$ on the charges,

$$Q^I \rightarrow Q'^I = U_{IJ}^{(R)} Q^J, Q^{I\dagger} \rightarrow Q'^{I\dagger} = U_{IJ}^{(R)*} Q^{\dagger J}, \quad (4.70)$$

and the new $\{Q^I, Q^{\dagger I}\}$ will generate the same supersymmetry as before, since relations (4.66)–(4.69) are preserved. If $N = 1$ then, this so-called *R-symmetry* is a $U(1)$ global symmetry of the super-Poincaré algebra, which nonetheless does not need to be a symmetry of the action. Nevertheless, as explained in chapter 2, in physically interesting models where supersymmetry is softly broken, the Lagrangian and the action are made to be invariant under a discrete \mathbb{Z}_2 subgroup of this continuous R-symmetry (*R-parity*) in order to avoid dangerous couplings which would lead to rapid proton decay.

We note that the generators of internal symmetries are missing from equations (4.49)–(4.51) and (4.66)–(4.69). By definition, the generators T_i of such symmetries commute with P_μ , $J_{\mu\nu}$ (and also with the central charges Z^{IJ}), but they do not necessarily commute with the fermionic generators:

$$[T_i, T_j] = ic_{ij}^k T_k, \quad (4.71)$$

$$[T_i, Q_\alpha^I] = s_{iJ}^I Q_\alpha^J, \quad [T_i, Q_\alpha^{\dagger I}] = -s_{iJ}^{I*} Q_\alpha^{\dagger J}. \quad (4.72)$$

The c_{ij}^k are the structure constants of the internal symmetry algebra. The T_i are Lorentz scalars (by definition of internal symmetry) so their commutator with Q^I must be a linear combination of these fermionic charges, and this is precisely the statement made by equation (4.72), for some coefficients $s_{iJ}^I = (s_{iI}^J)^*$. Since there are N charges Q^I and because the representations of the compact internal symmetry are unitary, we deduce that the Q^I transform under an internal symmetry transformation as a representation of a subgroup of $U(N)$. In simple supersymmetry then, where $N = 1$, the single Q is in a 1-dimensional representation of the internal symmetry group and since non-abelian Lie algebras do not have non-trivial 1-dimensional representations, $[T_i, Q]$ must be 0 for non-abelian internal symmetry subgroups. One practical consequence is that all generators of the SM gauge group must commute with the fermionic charges Q , Q^\dagger in $N = 1$ supersymmetric theories, with the possible exception of the hypercharge generator.⁸

To conclude this discussion about the theoretical aspects of supersymmetry, we shall make some remarks about the irreducible representations of the supersymmetry group—the supermultiplets.

1. As in the Poincaré subgroup, P_μ still commutes with everything, so $P_\mu P^\mu \equiv m^2$ is also a Casimir of the supersymmetry algebra. As a consequence, the mass of all components of a supermultiplet is the same [420]. Interestingly, this mass cannot be negative as it can be shown that there is the following lower bound:

$$m \geq \frac{1}{2N} \text{Tr} \sqrt{Z^\dagger Z}, \quad (4.73)$$

where $\sqrt{Z^\dagger Z}$ is the unique hermitian matrix satisfying $(\sqrt{Z^\dagger Z})_{IJ} (\sqrt{Z^\dagger Z})_{JK} = Z_{JI}^* Z_{JK}$. In simple supersymmetry, where no central charges Z_{IJ} exist, the bound is $m \geq 0$.

⁸ In the MSSM even the hypercharge generator commutes with Q , Q^\dagger though.

2. The contraction $W_\mu W^\mu$ of the Pauli-Lubański pseudo-vector does not commute with the fermionic charges, which means that it is not a Casimir of the supersymmetry algebra. This is somewhat obvious, since a supermultiplet will group different irreducible representations of the Poincaré group, with different spins, so it does not have a single spin associated to it. However, for $N = 1$ supersymmetry (see also [421]) there is a new Casimir operator $C_{\mu\nu} C^{\mu\nu}$, with

$$C_{\mu\nu} \equiv B_\mu P_\nu - B_\nu P_\mu, \quad B_\mu \equiv W_\mu - \frac{1}{4} (\bar{\sigma}_\mu)_{\alpha\beta} Q_\alpha^\dagger Q_\beta, \quad (4.74)$$

which generalizes $W_\mu W^\mu$. For a massive particle, $C_{\mu\nu} C^{\mu\nu} = 2j(j+1)m^4$ where $j(j+1)$ is the eigenvalue of the operator $\sum_{i=1,2,3} \tilde{J}_i^2$ with

$$\tilde{J}_i \equiv J_i - \frac{1}{4m} Q_\alpha^\dagger Q_\beta (\bar{\sigma}_\mu)_{\alpha\beta}. \quad (4.75)$$

These \tilde{J}_i obey the same $SU(2)$ algebras as the rotation generators: $[\tilde{J}_i, \tilde{J}_k] = i\varepsilon_{ijk} \tilde{J}_j$.

3. Simple calculations reveal that a massless supermultiplet will contain particles with helicities $\lambda_0, \lambda_0 + 1/2, \dots, \lambda_0 + N/2$ for some half-integer λ_0 , and the number of states with helicity $\lambda_0 + i/2$ is $N!/i!(N-i)!$. On the other hand, a massive supermultiplet is composed of states with spins $\max(0, s_0 - N/2), \max(0, s_0 - N/2) + 1/2, \dots, s_0 + N/2$. In either case, the supermultiplets contain states with spins/helicities differing by as much as $N/2$ and this means that particles with spin/helicity modulus equal or bigger than $N/4$ will be present. Since renormalizable field theories without (with) gravity⁹ cannot describe particles with spins or helicities higher than 1(2) we can have at most $N = 4(8)$.
4. It can be shown that the trace of the operator $(-1)^{2s}$ (s is the spin or helicity) over each supermultiplet, times P_μ , is null. This means that for the physically known cases where the 4-momentum vector is non-null, the number of fermionic and bosonic degrees of freedom in a supersymmetric theory is the same.

⁹ Gravity can be incorporated in these theories by promoting supersymmetry to a local symmetry, instead of leaving it as global one, as we have tacitly been assuming. Supergravity [422–429] however will not be addressed in this thesis.

Part II

TOPICS ON THE RENORMALIZATION OF SUSY
MODELS

CALCULATING THE RENORMALIZATION GROUP EQUATIONS OF A SUSY MODEL WITH SUSYNO

5.1 INTRODUCTION

The analysis of the theoretical and phenomenological implications of SUSY GUT models requires a careful study of the evolution of the fundamental parameters from the high-energy scale down to the electroweak one, at which observables are computed and constraints applied. As such, knowledge of the renormalization group equations is necessary. Although the RGEs of several models (for example the MSSM and the NMSSM) are already known [430, 431], for other SUSY extensions of the SM complicated general equations must be used [430, 432].

In this chapter we describe `SusyNo`, a Mathematica-based package that addresses this issue. The program takes as input the gauge group, the representations (i.e., the chiral superfield content), the number of flavors/copies of each representation, and any abelian discrete symmetries (e.g., R-parity). `SusyNo` then computes the form of the most general superpotential and soft SUSY breaking Lagrangian consistent with the field content and symmetries imposed. Once these elements have been derived, `SusyNo` calculates the 2-loop β -functions of all the parameters of the model, which is its main output. The program also contains a variety of group theoretical functions which may be of interest on their own (see also the Mathematica application `LieART` [433]).

There is another Mathematica package, `SARAH` [434–437], which provides an extensive list of functions which can be used to automate many of the computations necessary to build and analyze supersymmetric models (including the RGEs).¹ Given that it worked originally for models based on $SU(n)$ gauge factor only and that `SusyNo` is prepared to accept any gauge group as working input, the two programs were linked as of `SARAH4`.

This chapter is organized as follows. Section 5.2 explains how to install version 2 of the program and run a first, simple example (MSSM based). Sections 5.3 and 5.4 explain how to prepare the input and how to read and interpret the output, also using as examples the MSSM case. Section 5.5 summarizes the tests conducted to validate the code, and finally section 5.6 lists some of the functions available to the end user.

Note that the theoretical concepts related to Lie algebras which are detailed in chapter 4 are fundamental for the functioning of the program. Because of their technical nature, these implementation details have been placed separately in appendix B.

¹ Also, see [438] for non-SUSY models.

5.2 INSTALLATION AND QUICK START

Susyno works on Windows, Linux and Mac OS provided that Mathematica 7 (or a latter version) is installed. The program is obtainable from

<http://web.ist.utl.pt/renato.fonseca/susyno.html>

The files *IO.m*, *LieGroups.m*, *ModelBuilding.m*, *Models.m*, *SimplifyEinstein-Notation.m*, and *SusyRGEs.m* are the core of the program. These and other auxiliary files can be found inside the folder *Susyno*, which must be extracted from the downloaded *Susyno-2.0.zip* file to a location that is visible to Mathematica. Typing `$Path` in Mathematica will show a complete list of acceptable locations. One possibility is to place the whole folder (not just its contents) in

(Mathematica base directory)/AddOns/Applications

(note that in a Windows system the slashes “/” must be replaced by backslashes “\”). The package can be loaded by typing

```
<< Susyno`
```

in Mathematica’s front end. A text message is returned, informing that a built-in help system provides a detailed description of the program and its functions (see also section 5.6). A tutorial is also included.

The `Susyno` lines below allow a simple and easy first run: the example consists in a possible way of writing the MSSM input (we shall call this model `myMSSM` because MSSM is already defined in the program by default).

```
group[myMSSM] ^= {U1, SU2, SU3};

fieldNames[myMSSM] ^= {u, d, Q, e, L, Hu, Hd};
normalization = Sqrt[3/5];
reps[myMSSM] ^= {{-2/3 normalization, {0}, {0, 1}},
{1/3 normalization, {0}, {0, 1}}, {1/6 normalization, {1}, {1, 0}},
{normalization, {0}, {0, 0}}, {-1/2 normalization, {1}, {0, 0}},
{1/2 normalization, {1}, {0, 0}}, {-1/2 normalization, {1}, {0,
0}}};

nFlavs[myMSSM] ^= {3, 3, 3, 3, 3, 1, 1};
discreteSym[myMSSM] ^= {-1, -1, -1, -1, -1, 1, 1};

GenerateModel[myMSSM]
```

Evaluation of this simple code generates the 2-loop β -functions of the model (MSSM in this case). Notice that no external input or output files are used—everything happens on Mathematica’s front end.

5.3 THE INPUT OF `SUSYNO`: DEFINING A MODEL

A SUSY model contains two building blocks: a superpotential and a soft SUSY breaking Lagrangian (see equations (2.8) and (2.14)). `Susyno` works as follows: it requires as input the gauge group, the representations/fields, the number of flavors of each representation/field and the discrete abelian symmetries (if there are any) of the model. With this information the program then internally builds the superpotential and the soft SUSY breaking Lagrangian using an algorithm to automatically name the parameters of the model (see the next section). Once this information has been assigned to a `model` variable, the user must then call the function `GenerateModel` as follows:

```
GenerateModel[model]
```

We shall focus now on each of the elements that characterize a model. We will take the Minimal Supersymmetric Standard Model as an example.

5.3.1 *Gauge group*

The program needs a complete list of all the abelian and simple Lie groups of the model.² For the MSSM this would correspond to ($U(1)$ factors must come first)

```
group[myMSSM] ^= {U1, SU2, SU3};
```

Note that this code assigns to the variable `myMSSM` (instead of `group`) the information on the right, therefore the use of `^=` is important.

Any simple group can be given as a factor: the simple gauge factor groups, as well as their corresponding `Susyno` input are collected in table (10)—see also chapter 4 for an explanation on how one arrives at this list of simple gauge factor groups.

Simple gauge factor group	<code>Susyno</code> input
$SU(n)$	SU2, SU3, SU4, SU5, ...
$SO(n)$	S03, S05, S06, S07, ...
$Sp(2n)$	SP2, SP4, SP6, ...
G_2	G2
F_4	F4
E_6, E_7, E_8	E6, E7, E8

Table 10: Simple gauge factor groups

² We emphasize here that we are actually dealing with algebras, not groups (see chapter 4). Nevertheless, we will adopt the common practice in high-energy physics of using the word *group* for both these concepts.

5.3.2 Representations/fields: the content of the model

As mentioned before, `SusyNo` is designed to accept an arbitrary field content. An input must be provided in the form of two lists

```
fieldNames[model] ^= {fieldName1, fieldName2,...};
reps[model] ^= {rep1,rep1,...};
```

The first one should simply contain a list of names chosen by the user for each field. It is important to note that the ordering of the fields is arbitrary. However, the user must consistently adhere to the chosen ordering when inputting lists composed of field attributes (for example the number of flavors). In our example

```
fieldNames[myMSSM] ^= {u, d, Q, e, L, Hu, Hd};
```

The other list must contain all the gauge group irreducible representations present in the model. Each of these `rep` should be a list with representations of the gauge factor groups:

```
rep={hChrg1,hChrg2,...,hChrgM,rep_simplegroup1,rep_simplegroup2,...};
```

The first entries correspond to the hypercharges of `rep` (if any), which are just real numbers. After the hypercharges one must declare the representations of `rep` under each of the simple gauge factor groups mentioned above. These representations must be specified by their Dynkin coefficients (see subsection 4.3.5 of chapter 4 for details). In table (11) we list some of the representations of $SU(2)$, $SU(3)$, $SU(5)$ and $SO(10)$ (Dynkin coefficients and corresponding dimensions). There are functions in `SusyNo` that compute properties of the representations (e.g., `DimR` calculates the dimension of a representation, `ReduceRepProduct` reduces products of representations) and they are documented in the built-in help files (see also section 5.6). These should be enough to identify a representation by its Dynkin coefficients; however, should the user wish to consult lists of representations, these are available in the literature (see for example [401]).

To understand how the MSSM was specified in the example of section 5.2, we just need the following information from table (11):

- the Dynkin coefficients of the trivial and fundamental representations of $SU(2)$: $\{0\}$ and $\{1\}$.
- the Dynkin coefficients of the trivial, fundamental (**3**) and anti-fundamental ($\bar{\mathbf{3}}$) representations of $SU(3)$: $\{0,0\}$, $\{1,0\}$, $\{0,1\}$.

For the MSSM each field must then be cast in the format

```
rep={U1_charge,SU(2)_rep,SU(3)_rep};
```

Group	Representation		
	<i>Dynkin coefficients</i>	<i>Dimension</i>	<i>Name</i>
$SU(2)$	{0}	1	Trivial/Singlet
	{1}	2	Fundamental/Doublet
	{2}	3	Adjoint/Triplet
$SU(3)$	{0,0}	1	Trivial/Singlet
	{1,0}	3	Fundamental
	{0,1}	$\bar{\mathbf{3}}$	Anti-fundamental
	{1,1}	8	Adjoint
$SU(5)$	{0,0,0,0}	1	Trivial/Singlet
	{1,0,0,0}	5	Fundamental
	{0,0,0,1}	$\bar{\mathbf{5}}$	Anti-fundamental
	{0,1,0,0}	10	
	{2,0,0,0}	15	
	{0,0,0,2}	$\bar{\mathbf{15}}$	
	{1,0,0,1}	24	Adjoint
$SO(10)$	{0,0,0,0,0}	1	Trivial/Singlet
	{1,0,0,0,0}	10	Fundamental
	{0,0,0,0,1}	16	Spinor
	{0,0,0,1,0}	$\bar{\mathbf{16}}$	Spinor's conjugate
	{0,1,0,0,0}	45	Adjoint
	{2,0,0,0,0}	54	
	{0,0,1,0,0}	120	
	{0,0,0,0,2}	126	
	{0,0,0,2,0}	$\bar{\mathbf{126}}$	
	{0,0,0,1,1}	210	
{3,0,0,0,0}	210'		

Table 11: List of some frequently used representations of $SU(2)$, $SU(3)$, $SU(5)$ and $SO(10)$

Further normalizing the hypercharges with the usual $\sqrt{\frac{3}{5}}$ factor (from an embedding of the MSSM in an $SU(5)$ based model),³ we can then write the following:

```

normalization = Sqrt[3/5];
reps[myMSSM] ^= {{-2/3 normalization, {0}, {0, 1}},
{1/3 normalization, {0}, {0, 1}}, {1/6 normalization, {1}, {1, 0}},
{normalization, {0}, {0, 0}}, {-1/2 normalization, {1}, {0, 0}},

```

³ Notice however that `Susyno` accepts any choice for the normalization of the hypercharges.

```
{1/2 normalization, {1}, {0, 0}}, {-1/2 normalization, {1}, {0, 0}}};
```

We must emphasize here that although the user is free to choose the ordering of the simple factor groups, $SU(2)$ and $SU(3)$, once this is set (e.g., `group[myMSSM] ^= {U1, SU2, SU3}`) one must adhere to the (user-established) convention, and define the representations of the fields accordingly:

```
rep={U1_charge,SU(2)_rep,SU(3)_rep};
```

5.3.3 *Number of flavors and abelian discrete symmetries*

`SusyNo` needs two more input lists: one containing the number of flavors of each field and another defining its abelian discrete symmetries. The ordering of both these lists must be consistent with the representations list we have just discussed. In our `myMSSM` example we used the ordering `{u,d,Q,L,e,Hu,Hd}`, so

```
nFlavs[myMSSM] ^= {3, 3, 3, 3, 3, 1, 1};
discreteSym[myMSSM] ^= {-1, -1, -1, -1, -1, 1, 1};
```

In this particular case, it is clear that the discrete symmetry imposed corresponds to R-parity. For the most general (R-parity violating) MSSM we have

```
discreteSym[RPVMSSM] ^= {1, 1, 1, 1, 1, 1, 1};
```

Let us consider another example: for instance, if we were to modify the MSSM to include m copies of \hat{H}_u and \hat{H}_d , we would write

```
nFlavs[myMSSMmod] ^= {3, 3, 3, 3, 3, m, m};
```

5.3.4 *Calling the function `GenerateModel`*

Once the `model` variable has been defined (`=myMSSM` in our case), the `GenerateModel` function can be invoked as follows:

```
GenerateModel[myMSSM]
```

There are two Boolean optional parameters which can be passed to this function: `CalculateEverything->False,True` (default value is `False`) and `Verbose->False,True` (default value is `True`). The first one, `CalculateEverything`, can be used to force the program to compute explicitly the most general superpotential and soft SUSY breaking Lagrangian consistent with the definitions of the model. On the other hand, the option `Verbose`

can be used to suppress the printing of the results on the screen. In any case, the RGEs are always saved to the variable `betaFunctions[myMSSM]`, and the model parameters are saved to `parameters[myMSSM]`: for properly bounded indices i, j , the 1- and 2-loop β functions of `parameters[myMSSM][[i,j]]` are `betaFunctions[myMSSM][[i,1,j]]` and `betaFunctions[myMSSM][[i,2,j]]` respectively.

5.4 THE OUTPUT OF `SUSYNO`

Once all the definitions have been provided, `Susyno` automatically computes the form of the most general superpotential and soft SUSY breaking Lagrangian consistent with them. In particular, parameter names are generated by the program (they are not given by the user). The advantage of this approach is that inputting a model becomes very easy, since it is not even necessary to know the exact number of its parameters.⁴ On the other hand, this notation renders the output harder to read (and hence not particularly user-friendly), since the names of the parameters are chosen by the program. There is nonetheless a built-in function—`RenameParametersWithRule`—which provides a way for the user to change `Susyno`'s default notation (see below).

We note that `Susyno` does not have custom built-in functions to export the results. Users who wish to do so must do it manually or with the help of Mathematica's built-in functions `CForm` and `FortranForm`.

5.4.1 *Naming of parameters*

`Susyno` assigns names to the parameters of a model in such a way that the user can identify which representations/fields they are multiplying:

```
y[{{field1,field2,field3}, <InvIndex>, {<flav1>,<flav2>,<flav3>}}]
μ[{{field1,field2}, {<flav1>,<flav2>}}]
l[{{field1}, {<flav1>}}]
h[{{field1,field2,field3}, <InvIndex>, {<flav1>,<flav2>,<flav3>}}]
b[{{field1,field2}, {<flav1>,<flav2>}}]
s[{{field1}, {<flav1>}}]
m2[{{field1,field2}, {<flav1>,<flav2>}}]
```

A few comments concerning the above (output) tensors are in order:

- `y`, `μ`, `l`, `h`, `b`, `s` and `m2` can easily be identified with the different types of couplings and dimensionful parameters of the superpotential and the soft SUSY breaking Lagrangian (see equations (2.8) and (2.9));

⁴ The parameters considered throughout this chapter are the fundamental degrees of freedom of a model, with no experimental input taken into consideration (such as the requirement of EWSB, for example).

- `field1`, `field2`, `field3` are the fields entering a given coupling. In our example above, where we used `fieldNames[myMSSM] = {u,d,Q,e,L,Hu,Hd}`, the up-quark Yukawa couplings would be `y[{u,Q,Hu},...]`;
- There is the possibility that the product of 3 representations, $R_1 \otimes R_2 \otimes R_3$, contains more than one invariant. Therefore an additional label `InvIndex=1,2,...` might be necessary to distinguish them. This is rare though, so in most cases (e.g., the MSSM) this index is omitted. Notice that in linear and bilinear terms, R_1 and $R_1 \otimes R_2$, this problem does not arise since there is at most one invariant;
- `<flav1>`, `<flav2>`, `<flav3>` are the flavor indices of `field1`, `field2`, `field3`. If any of these fields has only one flavor, the corresponding index is omitted. Consider again the example of the up-quark Yukawa couplings: we would have `y[{u,Q,Hu},{i,j,k}]` where `i` = flavor of \hat{u} , `j` = flavor of \hat{Q} , `k` = flavor of \hat{H}_u . Yet \hat{H}_u only has one flavor so the correct parameter name is `y[{u,Q,Hu},{i,j}]`.

Additionally, there are also the gauge coupling constants and the gaugino masses:⁵

`g[1]`, `g[2]`, ...
`M[1]`, `M[2]`, ...

5.4.2 Normalization of the parameters

Consider for example the MSSM's μ parameter. According to the discussion in the previous subsection, `SusyNo`'s name for μ will be `μ [{Hu,Hd}]`, but this identification is only valid up to some multiplicative factor, since we do not know how the doublet indices of \hat{H}_u and \hat{H}_d are being contracted. In principle the program could be assuming that the μ term is `μ [{Hu,Hd}] $\hat{H}_u \cdot \hat{H}_d$` , `$-\mu$ [{Hu,Hd}] $\hat{H}_u \cdot \hat{H}_d$` , `$2\mu$ [{Hu,Hd}] $\hat{H}_u \cdot \hat{H}_d$` or any other multiple of these expressions. Therefore with the generic description that `μ [{Hu,Hd}]` is the parameter that multiplies the contraction of \hat{H}_u and \hat{H}_d in the superpotential, we can only say that `$\mu \propto \mu$ [{Hu,Hd}]`.

Version 2 of the program no longer computes explicitly a Lagrangian in order to get the RGEs (although the user can still ask the program to compute it), but even with two explicit Lagrangians written with different conventions and notations, it is not straightforward to compare them, because they may differ by irrelevant/unphysical unitary transformations of the gauge representations. Fortunately, there is a simple way to compare the normalization of their parameters. First, we describe the parameter normalization convention used by `SusyNo`:

1. The trilinear superpotential couplings of a generic superpotential can be encoded in a tensor Y^{ijk} (see equation (2.8)). The program uses the

⁵ With more than one $U(1)$ gauge factor group, according to the discussion in chapter 6 there is $U(1)$ -mixing and both the gauge coupling constants and the gaugino masses should be seen as matrices in $U(1)$ space. As a consequence, parameters `g[1,1]`, `g[1,2]`, ... , `M[1,1]`, `M[1,2]`, ... are necessary.

normalization $Y^{ijk}Y_{ijk} = \sum_y \sqrt{\dim(R_1) \dim(R_2) \dim(R_3)} y^{\alpha\beta\gamma} y_{\alpha\beta\gamma}$, where the sum is over all trilinear superpotential parameters y , and R_1 , R_2 and R_3 are the participating representation/fields. Note that the flavor indices α, β, γ contract between $y^{\alpha\beta\gamma}$ and $y_{\alpha\beta\gamma} = (y^{\alpha\beta\gamma})^*$. Consider the MSSM's case, where there are three such parameters: $y[\{\mathbf{u}, \mathbf{Q}, \mathbf{Hu}\}, \{i, j\}]$, $y[\{\mathbf{d}, \mathbf{Q}, \mathbf{Hd}\}, \{i, j\}]$ and $y[\{\mathbf{e}, \mathbf{L}, \mathbf{Hd}\}, \{i, j\}]$. The dimensions of the \hat{u} , \hat{d} , \hat{Q} , \hat{e} , \hat{L} , \hat{H}_u and \hat{H}_d representations are 3, 3, 6, 1, 2, 2 and 2, respectively, therefore the Yukawa parameters are normalized in such a way that $Y^{ijk}Y_{ijk} = 6 y[\{\mathbf{u}, \mathbf{Q}, \mathbf{Hu}\}, \{m, n\}] y[\{\mathbf{u}, \mathbf{Q}, \mathbf{Hu}\}, \{m, n\}]^* + 6 y[\{\mathbf{d}, \mathbf{Q}, \mathbf{Hd}\}, \{m, n\}] y[\{\mathbf{d}, \mathbf{Q}, \mathbf{Hd}\}, \{m, n\}]^* + 3 y[\{\mathbf{e}, \mathbf{L}, \mathbf{Hd}\}, \{m, n\}] y[\{\mathbf{e}, \mathbf{L}, \mathbf{Hd}\}, \{m, n\}]^*$;

2. If there is a singlet representation \hat{S} , **Susyno** assumes that a bilinear term $R_1 \otimes R_2$ is written in the same way as the trilinear one $R_1 \otimes R_2 \otimes \hat{S}$, the only difference being that the singlet field is eliminated and, of course, a different parameter name must be given. In the NMSSM for example, if there is a term (parameter) $\hat{S} \hat{H}_u \cdot \hat{H}_d$ in the superpotential, then the bilinear one must be written as (parameter') $\hat{H}_u \cdot \hat{H}_d$, with no relative phases or factors. The same is true for a linear term so, given the normalization in the condition 1, this means that a linear term is of the form (parameter) \hat{S} ;
3. The trilinear, bilinear and linear terms in the soft SUSY breaking Lagrangian ($-\mathcal{L}_{\text{soft}}$) are obtained by copying the ones in the superpotential W and simply renaming the parameters: $y[\dots] \rightarrow \mathbf{h}[\dots]$, $\mu[\dots] \rightarrow \mathbf{b}[\dots]$ and $\mathbf{1}[\dots] \rightarrow \mathbf{s}[\dots]$. In particular, notice that there are no relative phases or factors between the parameters in W and the equivalent ones in $-\mathcal{L}_{\text{soft}}$;
4. The soft scalar masses m^2 are assumed to be, as usual, of the trivial form (mass parameter of R_i) $(R_i^1 R_i^{1*} + R_i^2 R_i^{2*} + \dots)$ for a representation R_i of the gauge group with components R_i^1, R_i^2, \dots .

The crucial statement is the following one: the RGEs of the parameters of any other Lagrangian, possibly written in a different form and with different parameter names, are the same as the ones provided by **Susyno** as long as these conditions are obeyed. Note that these conditions are necessary and sufficient. As an example, the RGEs of the MSSM would not change even if the μ parameter was doubled everywhere ($\mu \rightarrow 2\mu$), as long as we also doubled the b parameter in the soft SUSY breaking Lagrangian (condition 3).

In conclusion, the user must see how his/her own way of writing the model parameters compares with conditions 1-4 above and, according to the result of such comparison, make adequate adaptations of **Susyno**'s output (if necessary). Since conditions 2, 3 and 4 are reasonably standard, the only non-trivial one is the first.

5.4.3 Changing the default notation

The user can change the default notation by providing a list of substitution rules for the parameter names:

```
parameterRenamingRules[model]^=substitutionRules;
```

In our myMSSM example, from the previous subsections we know what are the parameters names used by Susyno, and how they are normalized. As such, we can derive table (12), which compares the program's notation with the more standard one in equations (2.15) and (2.16). Then, it is possible to match the two

Parameter	Susyno's default notation
g_1, g_2, g_3	$g[1], g[2], g[3]$
M_1, M_2, M_3	$M[1], M[2], M[3]$
$(Y_u)_{ij}$	$y[\{u, Q, Hu\}, \{i, j\}]$
$(Y_d)_{ij}$	$y[\{d, Q, Hd\}, \{i, j\}]$
$(Y_e)_{ij}$	$y[\{e, L, Hd\}, \{i, j\}]$
μ	$\text{mu}[\{Hu, Hd\}]$
$(h_u)_{ij}$	$h[\{u, Q, Hu\}, \{i, j\}]$
$(h_d)_{ij}$	$h[\{d, Q, Hd\}, \{i, j\}]$
$(h_e)_{ij}$	$h[\{e, L, Hd\}, \{i, j\}]$
b	$b[\{Hu, Hd\}]$
$(m_u^2)_{ij}$	$m2[\{u, u\}, \{i, j\}]$
$(m_d^2)_{ij}$	$m2[\{d, d\}, \{i, j\}]$
$(m_{\tilde{Q}}^2)_{ij}$	$m2[\{Q, Q\}, \{j, i\}]$
$(m_e^2)_{ij}$	$m2[\{e, e\}, \{i, j\}]$
$(m_{\tilde{L}}^2)_{ij}$	$m2[\{L, L\}, \{j, i\}]$
$m_{H_u}^2$	$m2[\{Hu, Hu\}]$
$m_{H_d}^2$	$m2[\{Hd, Hd\}]$

Table 12: Parameters of the MSSM assuming a field ordering $\{u, d, Q, e, L, Hu, Hd\}$ and the gauge factor group ordering $\{U1, SU2, SU3\}$.

with the following code:

```
parameterRenamingRules[myMSSM]^={g[i_]:>g_i, M[i_]:>M_i,
y[{x_,_},{i_,j_}]>Y_x[i,j], mu[{_}]:>mu, h[{x_,_},{i_,j_}]>h_x[i,j],
b[{_}]:>b, m2[{Q,Q},{i_,j_}]>m2_Q[j,i], m2[{L,L},{i_,j_}]>m2_L[j,i],
m2[{x_,_},{i_,j_}]>m2_x[i,j], m2[{x_,_}]:>m2_x,
f[i_]:>FromCharCode[104+i], Conjugate[x_]:>x*};
```

myMSSM

The last two rules change the default flavor indices $f[1], f[2], \dots$ ($f[i_]:>FromCharCode[104+i]$), and compactify the notation of the

conjugation operation (`Conjugate[x_]>x*`). Note that by simply running the model's name in the console (`myMSSM`), the program will detect that it is a `Susyno` model and print all relevant information, in the new notation.

5.5 TESTS/VALIDATION OF `SUSYNO`

The output of `Susyno` was confronted with the analysis of some models available in the literature. In particular, the RGEs generated by `Susyno` were compared with the results of [430] (MSSM), [439] (RPV-MSSM), [431] (general NMSSM) as well as [440] ($SU(5)$ -based models). The program's RGEs are consistent with the results collected in the latest version of these publications.

5.6 LIST OF AVAILABLE FUNCTIONS

`Susyno`'s code is spread over many functions. Due to their nature, some of these functions may be useful on their own, and they were thus built in a user-friendly way, and are documented.

Below is a list of functions that can be called directly by the user in Mathematica's front-end, followed by a brief description. The package's built-in help system describes in detail how to use them. Extensive use is made of the Lie algebra concepts mentioned in chapter 4 (see also appendix B for some implementation details of some of these functions).

- **Adjoint**: Computes the Dynkin coefficients of the adjoint representation of a group.
- **CartanMatrix**: Computes the Cartan matrix of a group.
- **Casimir**: Computes the quadratic Casimir of a representation.
- **CMtoName**: Returns the name of the group with a given a Cartan matrix.
- **ConjugateIrrep**: Computes the Dynkin coefficients of the conjugate of a representation.
- **DecomposeSnProduct**: Decomposes the product of an arbitrary number of representations of the discrete S_n group in its irreducible parts.
- **DimR**: Computes the dimension of a representation.
- **DynkinIndex**: Computes the Dynkin index of a representation.
- **GenerateModel**: Computes the 1- and 2-loop RGEs of a SUSY model, among other things.
- **HookContentFormula**: Counts the number of semi-standard Young tableaux of shape given by a partition λ and with the cells filled with the numbers $1, \dots, n$ [441].

- **Invariants:** Computes (in some basis) the invariant combination(s) of an arbitrary number of representations. These are essentially generalized Clebsch–Gordan coefficients (see also the similar function `IrrepInProduct`).
- **IrrepInProduct:** Computes (in some basis) the combination(s) of two representations which transforms according to a particular irreducible representation of the group. For the $SU(2)$ group, these are known as the Clebsch–Gordan coefficients.
- **PermutationSymmetryOfTensorProductParts:** Computes the transformation properties of the irreducible parts of a product of fields/representations (of the gauge group) under a permutation of the fields being multiplied. The related function `PermutationSymmetryOfInvariants` only returns the gauge invariant parts in these products of fields.
- **Plethysms:** Computes the plethysms in a product of an arbitrary number of representations of a group [442]. The related function `InvariantsPlethysms` only returns those plethysms which are invariants under the (Lie) group. See also appendix B for a description of what are plethysms and why do they need to be computed by the program.
- **PositiveRoots:** Computes the positive roots of a group.
- **ReduceRepProduct:** Decomposes a direct product representation in its irreducible parts [443, 444].
- **RepMatrices:** Computes (in some basis) the explicit matrices of any representation.
- **RepMinimalMatrices:** Computes (in some basis) the explicit representation matrices of the generators appearing in the Chevalley-Serre relations (4.25)–(4.27).
- **RepsUpToDimN:** Computes all representations of a given group up to some dimension.
- **RepsUpToDimNNoConjugates:** Computes all representations of a given group up to some dimension, returning for each pair of conjugate representations only one of them.
- **SimplifyEinsteinNotation:** Simplifies an expression written in Einstein’s notation.
- **SnClassCharacter:** Computes for a given representation of the discrete S_n group the character of a conjugacy class [445].
- **SnClassOrder:** Computes the dimension of a conjugacy class of the discrete S_n group (see for example [446]).
- **SnIrrepDim:** Computes the dimension of a representation of the discrete S_n group.

- `TriangularAnomalyValue`: Computes the contribution of a representation for the triangular gauge anomalies [50].
- `Weights`: Computes the weights of a representation, including degeneracy.

Unless otherwise stated, in the above list, *group* and *representation* refers to a simple Lie group and a representation of a simple Lie group, respectively (not to be confused with the discrete S_n group and its representations). We note that the functions `RepMatrices`, `Invariants`, `Plethysms`, `SimplifyEinsteinNotation` and related functions are discussed in some detail in appendix B.

5.7 SUMMARY

In this chapter, the Mathematica package `Susyno` was described. Given only the defining elements of a softly broken SUSY model—the gauge group, the representations, the number of flavors/copies of each representation, and any abelian discrete symmetries (such as R-parity)—it calculates the 2-loop RGEs. For each model, this is a long and complicated calculation which should be automated, otherwise it is very likely that mistakes will be made.

The program also contains several group theoretical functions (related to both Lie groups and to the discrete permutation group S_n) which may be of interest on their own. In other words, even if there is no intention of computing renormalization group equations, these functions can still be used. It should be pointed out that there is an almost complete absence of Mathematica packages with this kind of functionality (a notable exception is `LieART` [433], which has since been published precisely with the aim of filling this gap). In fact, even beyond Mathematica, at a theoretical level, the problem of calculating with all generality the representation matrices and Clebsch-Gordon coefficients appearing in gauge theories had not received much attention (see appendix B).

RUNNING SOFT PARAMETERS IN SUSY MODELS WITH MULTIPLE $U(1)$ GAUGE FACTORS

6.1 INTRODUCTION

The two-loop RGEs for a generic softly broken SUSY model have been known for quite some time [430, 432]. However, these expressions are not completely general. For instance, in the presence of one $U(1)$ factor group, it is possible to form a Fayet-Iliopoulos term κD in the superpotential with the non-dynamical D field of the $U(1)$ group, because it is gauge invariant. As such, there is one extra free parameter κ in the theory and the corresponding RGEs were given in [447–449]. Another issue is the potential presence of Dirac gaugino mass terms $m_D^{iA} \psi_i \lambda_A$ if there are superfields in the adjoint representation of one of the gauge factor groups (see [450–452]). Yet another problem occurs when there are multiple $U(1)$ factor groups, a situation that leads to something that is known as $U(1)$ -mixing [453, 454]. A two-loop renormalization group analysis for non-SUSY theories with this feature is available in [455], while the SUSY case was addressed in [2]. The discussion summarized in this chapter, as well as the contents of appendix D, are mostly taken from this last work. In [430, 432] the RGEs are given in a first stage for a single gauge group and then a list of substitution rules of certain terms is provided, which can be used to generalize the expressions for multiple gauge groups. In this chapter we shall see how these rules can be changed to account for the $U(1)$ -mixing effects.

The practical applications of these results are extensive. For instance, in SUSY GUTs featuring an extended intermediate $U(1)_R \times U(1)_{B-L}$ phase, see e.g. [271], the $U(1)$ -mixing effects can shift the effective MSSM bino soft mass by several per cent with respect to the naive estimate where such effects are neglected. In principle, this can have non-negligible effects for the low-energy phenomenology. In this respect, let us just mention that theories with a gauged $U(1)_{B-L}$ surviving to the proximity of the soft SUSY-breaking scale have become rather appealing recently due to their interesting implications for R-parity and the mechanism of its spontaneous violation [456–458], for leptogenesis [459, 460], etc.

6.2 $U(1)$ MIXING

Consider then that the gauge group of a given model is $U(1)^n$ and that there are m supermultiplets Φ_i , $i = 1, \dots, m$. At this point, it should be stressed that if the number of supermultiplets m is smaller than the number of $U(1)$ factors n , the $U(1)$'s may be redefined such that $n - m$ of them (or more) are rotated away. To see this, first define Q_i^a as the charge of Φ_i under the a -th $U(1)$ group, which we can

see as component a for a vector \mathbf{Q}_i . We can then make a rotation¹ \mathcal{O}_1 in $U(1)$ space such that $\mathbf{Q}_i \rightarrow \mathcal{O}_1 \mathbf{Q}_i$ for every index i , in such a way that $(\mathcal{O}_1 \mathbf{Q}_i)^{a=m+1, \dots, n} = 0$. In other words, all the Φ_i 's can be made to have vanishing charges under at least $n - m$ of the new, rotated $U(1)$'s, making them invisible.

Assuming henceforth that $m \geq n$, we now look for the most general Lagrangian invariant under this $U(1)^n$ gauge group. To do that we must introduce, as usual, n gauge bosons A_μ^a which are to be seen also as components of a vector \mathbf{A}_μ . Under a gauge transformation with parameters α^a we have the following:

$$\Phi_i \rightarrow \exp(iQ_i^a \alpha^a) \Phi_i \equiv \exp(i\mathbf{Q}_i^T \boldsymbol{\alpha}) \Phi_i, \quad (6.1)$$

$$\mathbf{A}_\mu \rightarrow \mathbf{A}_\mu + \mathbf{G}^{-1} \partial_\mu \boldsymbol{\alpha}, \quad (6.2)$$

where once more $\boldsymbol{\alpha}$ is defined as a vector in $U(1)$ space with α^a components ($a = 1, \dots, n$). In the last equation, a \mathbf{G} matrix shows up. In the spirit of making the most general gauge transformation, \mathbf{G} can be any real $n \times n$ matrix. In particular, this means that the transformation of A_μ^a may depend on some gauge transformation parameter α^b with $b \neq a$. It is straightforward to see that the Lagrangian will be invariant under this transformation if the covariant derivative for the supermultiplet Φ_i has the form

$$D_\mu \Phi_i = \left(\partial_\mu - i\mathbf{Q}_i^T \mathbf{G} \mathbf{A}_\mu \right) \Phi_i, \quad (6.3)$$

which supports the idea that \mathbf{G} is a $U(1)$ gauge couplings matrix. Notice that even though it is a square matrix in $U(1)$ space, its left and right indices contract with different vectors: on the left we have the vector with the hypercharges of Φ_i , while on the right there is the $U(1)$ gauge bosons vector. There is a generic gauge kinetic term to be considered,²

$$- \frac{1}{4} \mathbf{F}_{\mu\nu}^T \boldsymbol{\xi} \mathbf{F}^{\mu\nu}, \quad (6.4)$$

and also, in a softly broken supersymmetric theory, the $U(1)$ gaugino mass term

$$- \frac{1}{2} \boldsymbol{\lambda}^T \mathbf{M} \boldsymbol{\lambda} + \text{h.c.} \quad (6.5)$$

Here we have introduced more vectors in $U(1)$ space: $\mathbf{F}_{\mu\nu}$ is a vector whose components are $F_{\mu\nu}^a \equiv \partial_\mu A_\nu^a - \partial_\nu A_\mu^a$, while the a component of $\boldsymbol{\lambda}$ is the gaugino field λ^a associated with $U(1)^a$. Therefore we have new $n \times n$ matrices $\boldsymbol{\xi}$ and \mathbf{M} to consider, which are free parameters of the theory, containing $\frac{1}{2}n(n-1)$ extra real degrees of freedom. The advantage of having $\boldsymbol{\xi} \neq \mathbb{1}$ is that the gauge coupling matrix can be made diagonal with a rotation of the gauge boson and gaugino fields. As far as the renormalization group analysis is concerned, it is now necessary to include both the effect of $\boldsymbol{\xi}$ on the evolution of the other parameters and also to describe the evolution of $\boldsymbol{\xi}$ itself. This is indeed the method adopted in some of the first studies of the subject (see for example [455]). But there is an alternative: the fact

¹ Strictly speaking this \mathcal{O}_1 matrix does not need to be a rotation matrix; it is only necessary for it to be invertible.

² The same mixing parameter $\boldsymbol{\xi}$ appears in the gaugino kinetic term and also in the $1/2 D^a D^a$ term.

that $\xi \neq 1$ means that the gauge boson fields (as well as the gaugino fields) are not canonically normalized and we can therefore rotate and rescale these fields such that in the new basis one always has $\xi = 1$. In this way, the $U(1)$ -mixing in the kinetic term is completely encoded in a matrix of gauge couplings \mathbf{G} and in a matrix of gaugino masses \mathbf{M} . This latter approach is the one adopted in the rest of this chapter.

We have discussed above that the hypercharges \mathbf{Q}_i can be rotated by a transformation \mathcal{O}_1 and that the same can be done to the gauge bosons. Indeed, in general we may perform two rotations, \mathcal{O}_1 and \mathcal{O}_2 , which affect the different parameters and fields in the following way:

$$\mathbf{Q}_i \rightarrow \mathcal{O}_1 \mathbf{Q}_i, \quad (6.6)$$

$$\mathbf{A}_\mu(\lambda) \rightarrow \mathcal{O}_2 \mathbf{A}_\mu(\lambda), \quad (6.7)$$

$$\mathbf{G} \rightarrow \mathcal{O}_1 \mathbf{G} \mathcal{O}_2^T, \quad (6.8)$$

$$\mathbf{M} \rightarrow \mathcal{O}_2 \mathbf{M} \mathcal{O}_2^T. \quad (6.9)$$

As a result of this freedom, it is not straightforward to count the true number of degrees of freedom in the \mathbf{G} and \mathbf{M} matrices. We may proceed as follows: an \mathcal{O}_2 rotation is used to diagonalize \mathbf{M} and then, with the so-called QR matrix decomposition [461], it is possible to put \mathbf{G} in an upper or a lower triangular form with a particular choice of \mathcal{O}_1 . Another possibility is to use the so-called polar matrix decomposition to cast \mathbf{G} in a symmetric form, while keeping \mathbf{M} diagonal. In both these situations, and up to some discrete transformations, we exhaust the freedom to rotate \mathbf{Q}_i and \mathbf{A}_μ so we can count in these particular bases the number of degrees of freedom in \mathbf{G} and \mathbf{M} as being $\frac{1}{2}n(n+3)$.

Naturally, these symmetries must be reflected at the RGE level. Thus, for instance, only those combinations C of \mathbf{G} and $\gamma \propto \sum_i \mathbf{Q}_i \mathbf{Q}_i^T$ that transform as $C \rightarrow \mathcal{O}_1 C \mathcal{O}_2^T$ are allowed to enter the right-hand side of the renormalization group equation for \mathbf{G} . However, at the one-loop level, there is only one structure involving a third power of \mathbf{G} and one power of γ that can arise from a matter-field loop in the gauge propagator, namely $\mathbf{G} \mathbf{G}^T \gamma \mathbf{G}$, so one immediately concludes that

$$\beta_{\mathbf{G}}^{(\text{one loop})} \propto \mathbf{G} \mathbf{G}^T \gamma \mathbf{G}. \quad (6.10)$$

The proportionality coefficient is trivially obtained by matching this to the single $U(1)$ case. However, at the two loop level the same exercise becomes more complicated because the increased complexity of the underlying Feynman diagrams means that more matrices enter each term. In particular, and unlike in equation (6.10), it is possible that specific terms in [430, 432] need to be expanded into multiple terms because now, instead of dealing with numbers which always commute, we have to deal with matrices which do not.

It might be tempting to think that without the gaugino mass matrix \mathbf{M} in non-SUSY theories, we can diagonalize \mathbf{G} and therefore get rid of the $U(1)$ -mixing effects. However this is not the case, as radiative effects will reintroduce off-diagonalities in the gauge couplings matrix. In fact, already at one loop level, the anomalous dimension γ which controls the RGE of \mathbf{G} is in general a non-diagonal

matrix in $U(1)$ space and as such, even if \mathbf{G} is diagonal at a given energy scale, non-diagonal entries will be radiatively generated.

It turns out that there are exceptions to this rule. For instance, it can be that all the relevant $U(1)$ couplings originate from a common gauge factor and thus, barring threshold effects, all of them happen to be equal at a certain scale. In such a case, the charges and the gauge fields can be simultaneously rotated at the one-loop level so that no off-diagonalities appear in γ [430, 462] and one can use the simple form of the RGEs for individual gauge couplings. Note again that this will only work in the non-SUSY case where only the gauge sector has to be taken into account. Also, at two loops, Yukawa couplings and trilinear soft SUSY breaking couplings appear in the RGEs, rendering this approach useless.

6.3 TWO LOOP RGEs

In this section, we describe the generic method of constructing the fully general two-loop RGEs for softly-broken supersymmetric gauge theories out of the results of [430, 432] relevant to the case of (at most) a single abelian gauge-group factor. For the sake of completeness, the relevant formulae for the cases of (i) a simple gauge group and (ii) the product of several simple factors with at most a single $U(1)$ are reproduced in appendix C. The computation has been done using the \overline{DR}' scheme defined in [463].

6.3.1 Notation and conventions

The gauge group is taken to be $G_A \times G_B \times \dots \times U(1)^n$, where the G_X 's are simple groups. We shall use uppercase indices for simple group-factors only; lowercase indices are used either for all groups or, in some specific cases, for $U(1)$'s only.³ As mentioned before, the $U(1)$ sector should be treated as a whole and described in terms of a general real $n \times n$ gauge couplings matrix \mathbf{G} , a $n \times n$ symmetric soft SUSY breaking gaugino mass matrix \mathbf{M} and a column vector of charges \mathbf{Q}_i for each chiral supermultiplet Φ_i . Notice, however, that $\mathbf{V}_i \equiv \mathbf{G}^T \mathbf{Q}_i$ for each i are the only combinations of \mathbf{Q}_i and \mathbf{G} which appear in the Lagrangian (recall the \mathcal{O}_1 rotation freedom discussed in the previous section) and thus, all the general RGEs can be written in terms of \mathbf{V} 's and \mathbf{M} only. We shall follow this convention with a single exception—the evolution equations for the gauge couplings—which are traditionally written in terms of $d\mathbf{G}/dt$ rather than $d\mathbf{V}/dt$. Here, we shall adhere to the usual practice and as a consequence we expect an isolated \mathbf{G} in these equations.

Before proceeding any further we shall define some of the expressions that are used in the RGEs:

- $C_a(i)$: quadratic Casimir invariant of the representation of superfield Φ_i under the group G_a .

³ This will be evident from the context; we follow as closely as possible [430] and when quoting results contained therein, the a and b indices go over all groups (simple and $U(1)$ groups). On other occasions, when referring to particular components of the $U(1)$ -related \mathbf{G} , \mathbf{M} and \mathbf{V} matrices and vectors, a and b stretch over the $U(1)$ groups only.

- $C(G_a)$: quadratic Casimir invariant of the adjoint representation of group G_a .
- $S_a(i)$: Dynkin index of the representation of superfield Φ_i under the group G_a .
- $d_a(i)$: Dimension of the representation of Φ_i under the group G_a .
- $d(G_a)$: dimension of group G_a .
- $S_a(R)$: Dynkin index of group G_a summed over all chiral supermultiplets—
 $S_a(R) = \sum_i \frac{S_a(i)}{d_a(i)}$.
- $S_a(R) C_b(R)$: defined as $\sum_i \frac{S_a(i) C_b(i)}{d_a(i)}$.
- $S_a(R) \mathbf{V}_R^T \mathbf{V}_R$: defined as $\sum_i \frac{S_a(i) \mathbf{V}_i^T \mathbf{V}_i}{d_a(i)}$.
- $S_a(R) \mathbf{V}_R^T \mathbf{M} \mathbf{V}_R$: defined as $\sum_i \frac{S_a(i) \mathbf{V}_i^T \mathbf{M} \mathbf{V}_i}{d_a(i)}$.

In addition, sometimes one has to deal with the explicit representation matrices of the gauge groups (denoted in [430] by \mathbf{t}_i^{Aj}). Notice that here A is not a group index but rather a coordinate in the adjoint representation of the corresponding Lie algebra (for example, $A = 1, \dots, 3$ in $SU(2)$, and $A = 1, \dots, 8$ in $SU(3)$).

Naturally, whenever we refer to results of [430, 432] for a simple gauge group (collected in section C.1 of appendix C), the a and b indices will be omitted. In all cases, repeated indices are not implicitly summed over.

6.3.2 Strategy for the constructing the general substitution rules

Let us now describe in more detail the strategy for upgrading the “product” substitution rules of section III in reference [430] to the most general case of an arbitrary gauge group. For the moment we shall focus on a limited number of terms; later on, in section 6.4, a more elaborate discussion addresses all remaining situations.

Let us begin with the term $g^2 C(r)$ appearing for instance in equation (C.3) and, subsequently, in the substitution rules of [430] for product groups, equation (C.38). It is clear that this has to be replaced by $\sum_A g_A^2 C_A(r) + \text{‘}U(1)\text{ part’}$. For a single $U(1)$, $g^2 C(r) = g^2 y_r^2 \sim \mathbf{V}_r \mathbf{V}_r$ so this ‘ $U(1)$ part’ can only take the form⁴ $\mathbf{V}_r^T \mathbf{V}_r = \mathbf{Q}_r^T \mathbf{G} \mathbf{G}^T \mathbf{Q}_r$. There is no other way to obtain a number from two vectors \mathbf{V}_r . This expression automatically sums the contributions of all the $U(1)$ ’s.

Similarly, $M g^2 C(r)$ (in equation (C.12) for example) is replaced by $\sum_A M_A g_A^2 C_A(r) + \text{‘}U(1)\text{ part’}$; the ingredients for the construction of the ‘ $U(1)$ part’ are two vectors \mathbf{V}_r and the gaugino mass matrix \mathbf{M} . Only $\mathbf{V}_r^T \mathbf{M} \mathbf{V}_r$ forms a number.

In fact, this simple procedure allows us to generalize many of the terms in the RGEs of [430, 432], section II (reproduced in appendix C). As a more involved

⁴ If there is a single abelian factor group, we denote by y_i the (hyper)charge of chiral superfield Φ_i , which is just a number

example, consider for instance the $g^4 \mathbf{t}_i^{Aj} \text{Tr} [\mathbf{t}^A C(r) m^2]$ structure appearing in equation (C.25). It is not difficult to see that all terms where the representation matrices \mathbf{t}^A appear explicitly are zero unless A corresponds to an abelian group. Hence, if for a single $U(1)$ one has⁵

$$g^4 \mathbf{t}_i^{Aj} \text{Tr} [\mathbf{t}^A C(r) m^2] = g^2 \delta_i^j y_i \sum_p y_p \left[\sum_B g_B^2 C_B(p) + g^2 y_p^2 \right] (m^2)_p^p, \quad (6.11)$$

it can be immediately deduced that, in the general case,

$$g^4 \mathbf{t}_i^{Aj} \text{Tr} [\mathbf{t}^A C(r) m^2] \rightarrow \delta_i^j \sum_p (\mathbf{V}_i^T \mathbf{V}_p) \left[\sum_B g_B^2 C_B(p) + (\mathbf{V}_p^T \mathbf{V}_p) \right] (m^2)_p^p. \quad (6.12)$$

The RGEs of \mathbf{G} and \mathbf{M} represent a bigger challenge, because they are matrix equations (in other words, there are uncontracted gauge indices). On the other hand, this should be viewed as an advantage because all the relevant equations must then respect the reparametrization symmetries (6.6)–(6.9). Notice that these equations imply that the \mathbf{V} 's transform as $\mathbf{V}_i \rightarrow \mathcal{O}_2 \mathbf{V}_i$. These symmetries are especially powerful in the β -functions for the gauge couplings which, due to equation (6.8), inevitably take the generic form $\mathbf{G} \mathbf{V}_i (\dots) \mathbf{V}_j^T$ for some chiral indices i, j . For example, $g^3 S(R) \sim g^3 \sum_p y_p^2$ can only take the form $\mathbf{G} \sum_p \mathbf{V}_p \mathbf{V}_p^T$.

Concerning the gaugino soft masses M , let us for instance consider the $2g^2 S(R) M$ term appearing in equation (C.21). Its generalized variant should be built out of a pair of \mathbf{V}_p vectors and the \mathbf{M} matrix. However, there are only two combinations of these objects that transform correctly under \mathcal{O}_2 , namely, $\mathbf{M} \mathbf{V}_p \mathbf{V}_p^T$ and $\mathbf{V}_p \mathbf{V}_p^T \mathbf{M}$. Thus, due to the symmetry of \mathbf{M} , one obtains $2g^2 S(R) M \rightarrow \mathbf{M} \sum_p \mathbf{V}_p \mathbf{V}_p^T + \sum_p \mathbf{V}_p \mathbf{V}_p^T \mathbf{M}$.

Another important ingredient of the analysis is provided by the existing substitution rules linking the case of a simple gauge group (section II in [430] or section C.1 of appendix C) to the settings with group products (section III in [430] or section C.2 of appendix C). Consider, for example, the $g^5 S(R) C(R)$ term in equation (C.4) which, according to [430], is replaced by $\sum_b g_a^3 g_b^2 S_a(R) C_b(R)$; see formula (C.30) for the product groups. Let us recall that the expression $S(R) C(R)$ has a very particular meaning: it is the sum of the Dynkin indices weighted by the quadratic Casimir invariant, so $\sum_b g_a^3 g_b^2 S_a(R) C_b(R) = \sum_{b,p} g_a^3 g_b^2 \frac{S_a(p) C_b(p)}{d_a(p)}$. With this in mind, whenever a refers to the abelian part of the gauge group, one should replace $g_a^3 S_a(p) \rightarrow \mathbf{G} \mathbf{V}_p \mathbf{V}_p^T$ ($d_a(p) = 1$), while $\sum_b g_b^2 C_b(p) \rightarrow \sum_B g_B^2 C_B(p) + \mathbf{V}_p^T \mathbf{V}_p$. Therefore, for the abelian sector, $g^5 S(R) C(R) \rightarrow \sum_p \mathbf{G} \mathbf{V}_p \mathbf{V}_p^T \left[\sum_B g_B^2 C_B(p) + \mathbf{V}_p^T \mathbf{V}_p \right]$.

However, sometimes even a detailed inspection of the underlying expressions does not allow an unambiguous identification of its generalized form. When this happens, a careful analysis of the structure of the contributing Feynman diagrams

⁵ In this context, g is the $U(1)$ gauge coupling.

is necessary. However, remarkably, the number of such cases is small, as shown in section 6.4.

6.3.3 Substitution rules

Depending on the group sector (abelian or simple), we get different RGEs for the gauge couplings and the gaugino masses. The parameters are then either the matrices \mathbf{G} , \mathbf{M} or the numbers g_A , M_A . For the abelian sector, one obtains:

$$C(G) \rightarrow 0, \quad (6.13)$$

$$g^3 S(R) \rightarrow \mathbf{G} \sum_p \mathbf{V}_p \mathbf{V}_p^T, \quad (6.14)$$

$$g^5 S(R) C(R) \rightarrow \sum_p \mathbf{G} \mathbf{V}_p \mathbf{V}_p^T \left[\sum_B g_B^2 C_B(p) + \mathbf{V}_p \mathbf{V}_p^T \right], \quad (6.15)$$

$$\frac{g^3 C(k)}{d(G)} \rightarrow \mathbf{G} \mathbf{V}_k \mathbf{V}_k^T, \quad (6.16)$$

$$2g^2 S(R) M \rightarrow \mathbf{M} \sum_p \mathbf{V}_p \mathbf{V}_p^T + \sum_p \mathbf{V}_p \mathbf{V}_p^T \mathbf{M}, \quad (6.17)$$

$$g^2 C(k) \rightarrow \mathbf{V}_k \mathbf{V}_k^T, \quad (6.18)$$

$$2g^2 C(k) M \rightarrow \mathbf{M} \mathbf{V}_k \mathbf{V}_k^T + \mathbf{V}_k \mathbf{V}_k^T \mathbf{M}, \quad (6.19)$$

$$16g^4 S(R) C(R) M \rightarrow \sum_p \left\{ 4 \left(\mathbf{M} \mathbf{V}_p \mathbf{V}_p^T + \mathbf{V}_p \mathbf{V}_p^T \mathbf{M} \right) \left[\sum_B g_B^2 C_B(p) + \mathbf{V}_p \mathbf{V}_p^T \right] \right. \\ \left. + 8 \mathbf{V}_p \mathbf{V}_p^T \left[\sum_B M_B g_B^2 C_B(p) + \mathbf{V}_p^T \mathbf{M} \mathbf{V}_p \right] \right\}. \quad (6.20)$$

For a simple group factor G_A , the substitution rules of [430] do not need to be changed except for two cases:

$$g^5 S(R) C(R) \rightarrow g_A^3 S_A(R) \left[\sum_B g_B^2 C_B(R) + \mathbf{V}_R^T \mathbf{V}_R \right], \quad (6.21)$$

$$16g^4 S(R) C(R) M \rightarrow 8g_A^2 M_A S_A(R) \left[\sum_B g_B^2 C_B(R) + \mathbf{V}_R^T \mathbf{V}_R \right] \\ + 8g_A^2 S_A(R) \left[\sum_B M_B g_B^2 C_B(R) + \mathbf{V}_R^T \mathbf{M} \mathbf{V}_R \right]. \quad (6.22)$$

As for the rest of the parameters in a SUSY model, the relevant substitution rules read:

$$g^2 C(r) \rightarrow \sum_A g_A^2 C_A(r) + \mathbf{V}_r^T \mathbf{V}_r, \quad (6.23)$$

$$M g^2 C(r) \rightarrow \sum_A M_A g_A^2 C_A(r) + \mathbf{V}_r^T \mathbf{M} \mathbf{V}_r, \quad (6.24)$$

$$M^* g^2 C(r) \rightarrow \sum_A M_A^* g_A^2 C_A(r) + \mathbf{V}_r^T \mathbf{M}^\dagger \mathbf{V}_r, \quad (6.25)$$

$$MM^*g^2C(r) \rightarrow \sum_A M_A M_A^* g_A^2 C_A(r) + \mathbf{V}_r^T \mathbf{M} \mathbf{M}^\dagger \mathbf{V}_r, \quad (6.26)$$

$$g^4C(r)S(R) \rightarrow \sum_A g_A^4 C_A(r) S_A(R) + \sum_p \left(\mathbf{V}_r^T \mathbf{V}_p \right)^2, \quad (6.27)$$

$$Mg^4C(r)S(R) \rightarrow \sum_A M_A g_A^4 C_A(r) S_A(R) + \sum_p \left(\mathbf{V}_r^T \mathbf{M} \mathbf{V}_p \right) \left(\mathbf{V}_r^T \mathbf{V}_p \right), \quad (6.28)$$

$$g^4C^2(r) \rightarrow \left[\sum_A g_A^2 C_A(r) + \mathbf{V}_r^T \mathbf{V}_r \right]^2, \quad (6.29)$$

$$Mg^4C^2(r) \rightarrow \left[\sum_A M_A g_A^2 C_A(r) + \mathbf{V}_r^T \mathbf{M} \mathbf{V}_r \right] \left[\sum_A g_A^2 C_A(r) + \mathbf{V}_r^T \mathbf{V}_r \right], \quad (6.30)$$

$$g^4C(G)C(r) \rightarrow \sum_A g_A^4 C(G_A) C_A(r), \quad (6.31)$$

$$Mg^4C(G)C(r) \rightarrow \sum_A M_A g_A^4 C(G_A) C_A(r), \quad (6.32)$$

$$MM^*g^4C(G)C(r) \rightarrow \sum_A M_A M_A^* g_A^4 C(G_A) C_A(r), \quad (6.33)$$

$$g^2 \mathbf{t}_i^{Aj} \text{Tr} \left(\mathbf{t}^A m^2 \right) \rightarrow \delta_i^j \sum_p \mathbf{V}_i^T \mathbf{V}_p \left(m^2 \right)_p^p, \quad (6.34)$$

$$g^2 \mathbf{t}_i^{Aj} \left(\mathbf{t}^A m^2 \right)_r^l \rightarrow \delta_i^j \mathbf{V}_l^T \mathbf{V}_i \left(m^2 \right)_r^l, \quad (6.35)$$

$$g^4 \mathbf{t}_i^{Aj} \text{Tr} \left[\mathbf{t}^A C(r) m^2 \right] \rightarrow \delta_i^j \sum_p \mathbf{V}_i^T \mathbf{V}_p \left[\sum_B g_B^2 C_B(p) + \mathbf{V}_p^T \mathbf{V}_p \right] \left(m^2 \right)_p^p, \quad (6.36)$$

$$g^4C(i) \text{Tr} \left[S(r) m^2 \right] \rightarrow \sum_A g_A^4 C_A(i) \text{Tr} \left[S_A(r) m^2 \right] + \sum_p \left(\mathbf{V}_i^T \mathbf{V}_p \right)^2 \left(m^2 \right)_p^p, \quad (6.37)$$

$$\begin{aligned} 24g^4MM^*C(i)S(R) &\rightarrow 24 \sum_A g_A^4 M_A M_A^* C_A(i) S_A(R) \\ &+ 8 \sum_p \left[\left(\mathbf{V}_i^T \mathbf{M} \mathbf{V}_p \right) \left(\mathbf{V}_i^T \mathbf{M}^\dagger \mathbf{V}_p \right) + \left(\mathbf{V}_i^T \mathbf{M} \mathbf{M}^\dagger \mathbf{V}_p \right) \left(\mathbf{V}_i^T \mathbf{V}_p \right) \right. \\ &\left. + \left(\mathbf{V}_i^T \mathbf{M}^\dagger \mathbf{M} \mathbf{V}_p \right) \left(\mathbf{V}_i^T \mathbf{V}_p \right) \right], \end{aligned} \quad (6.38)$$

$$\begin{aligned} 48g^4MM^*C(r)^2 &\rightarrow \sum_{A,B} g_A^2 g_B^2 C_A(r) C_B(r) (32M_A M_A^* + 16M_A M_B^*) \\ &+ \sum_A g_A^2 C_A(r) \left(32M_A M_A^* \mathbf{V}_r^T \mathbf{V}_r + 16M_A \mathbf{V}_r^T \mathbf{M}^\dagger \mathbf{V}_r \right. \\ &\left. + 32\mathbf{V}_r^T \mathbf{M} \mathbf{M}^\dagger \mathbf{V}_r + 16M_A^* \mathbf{V}_r^T \mathbf{M} \mathbf{V}_r \right) \\ &+ 32 \left(\mathbf{V}_r^T \mathbf{M} \mathbf{M}^\dagger \mathbf{V}_r \right) \left(\mathbf{V}_r^T \mathbf{V}_r \right) + 16 \left(\mathbf{V}_r^T \mathbf{M} \mathbf{V}_r \right) \left(\mathbf{V}_r^T \mathbf{M}^\dagger \mathbf{V}_r \right). \end{aligned} \quad (6.39)$$

6.4 OBTAINING THE SUBSTITUTION RULES

We discuss now in more detail the methods used throughout the derivation of the substitution rules given in section 6.3, with particular emphasis on the few cases where this is not straightforward.

6.4.1 The role of the \mathbf{V}_i vectors and the \mathbf{M} matrix

As mentioned before, the $U(1)$ gauge coupling matrix \mathbf{G} and the charge vectors \mathbf{Q}_i of the chiral superfields Φ_i appear always through the combination $\mathbf{V}_i = \mathbf{G}^T \mathbf{Q}_i$. The only exception are the RGEs of \mathbf{G} , where there should be a leading free \mathbf{G} . For example, the $\psi^{i\dagger} \psi^i A_\mu^a$ vertex is proportional to V_i^a (component a of the vector \mathbf{V}_i)—figure (7).

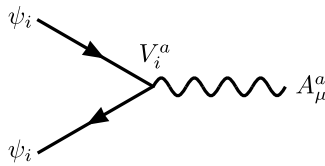


Figure 7: The vertex $\psi^{i\dagger} \psi^i A_\mu^a$ is proportional to V_i^a .

Similarly the vertices $\phi^{*i} \phi^i A_\mu^a$, $\phi^{*i} \phi^i A_\mu^a A_\nu^b$, $\phi^{i*} \psi^i \lambda^a$ and the Yukawa independent part of $\phi^{i*} \phi^i \phi^{j*} \phi^j$ are proportional to V_i^a , $V_i^a V_i^b$, V_i^a and $\mathbf{V}_i^T \mathbf{V}_j$ respectively. In addition, one must consider the $U(1)$ gaugino mass matrix \mathbf{M} (see figure (8)).

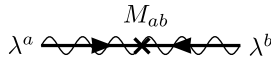


Figure 8: The $U(1)$ gaugino mass matrix \mathbf{M} mixes gaugino fields. M_{ab} is the a, b component of \mathbf{M} .

6.4.2 RGEs with no $U(1)$ indices

Diagrams needed to compute the RGEs of \mathbf{G} and \mathbf{M} are the only ones with external $U(1)$ gauge bosons/gauginos. In all other equations, while vectors \mathbf{V}_i and the matrix \mathbf{M} may be present, they must form scalar combinations, so no free $U(1)$ indices exist. Consider the $Mg^2 C(i)$ appearing in the one-loop RGE of the bilinear scalar soft terms b^{ij} , which is to be replaced by $\sum_A M_A g_A^2 C_A(i) + \mathbf{V}_i^T \mathbf{M} \mathbf{V}_i$. The simple groups contribution, $\sum_A M_A g_A^2 C_A(i)$, can safely be neglected in this discussion. We can see that $\mathbf{V}_i^T \mathbf{M} \mathbf{V}_i$ is the only structure that can generalize the expression $Mg^2 C(i) = Mg^2 y_i^2$ for one $U(1)$ group only. Notice also the contraction of the $U(1)$ indices in the expression—it comes from the possibility of having any of the $U(1)$ gauginos in the internal lines of the contributing diagram in figure (9). The amplitude is proportional to $\sum_{a,b} V_i^a M_{ab} V_j^b \mu^{ij} = \mu^{ij} \mathbf{V}_i^T \mathbf{M} \mathbf{V}_j$. Note that for any pair of values i, j the gauge symmetry forces $\mu^{ij} = 0$ unless $\mathbf{V}_i + \mathbf{V}_j = 0$, which means that $\mu^{ij} \mathbf{V}_j = -\mu^{ij} \mathbf{V}_i$ so the amplitude of the diagram is indeed proportional to $\mathbf{V}_i^T \mathbf{M} \mathbf{V}_i$.

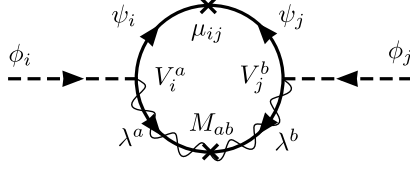


Figure 9: Diagram contributing to the one-loop RGE of the bilinear scalar soft terms b^{ij} . Notice the contraction of the a and b indices between the \mathbf{V} 's and \mathbf{M} .

This requirement that expressions with \mathbf{V} 's and \mathbf{M} 's must form scalars is enough to derive equations (6.21)–(6.26), (6.29)–(6.36) and (6.39) from the existing substitution rules for gauge groups with multiple factors. We are left with the terms $g^4 C(r) S(R)$, $M g^4 C(r) S(R)$, $g^4 C(i) \text{Tr}[S(r) m^2]$ and $24 g^4 M M^* C(i) S(R)$. Note that one can write $S(R)$ as $\text{Tr}[S(r)]$ in the notation of reference [430], so in all four cases there is a sum over field components of chiral superfields. For diagrams with up to two-loops and with no external gauginos nor gauge bosons, the factors $S(R)$ and $\text{Tr}[S(r) m^2]$ can only come from the sub-diagrams in figure (10).⁶ Take

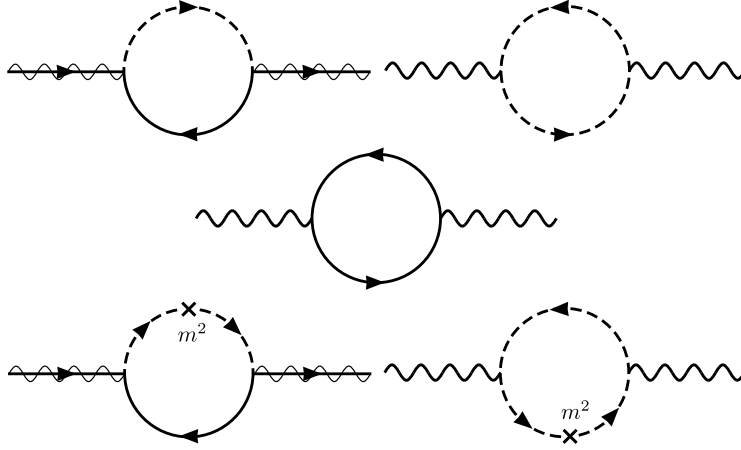


Figure 10: Sub-diagrams which give rise to $S(R)$ and $\text{Tr}[S(r) m^2]$ factors in the RGEs.

for example $g^4 C(r) S(R) \sim \sum_p g^4 y_r^2 y_p^2$. One cannot immediately generalize this expression to include $U(1)$ -mixing effects because in theory it could take the form $\sum_p (\mathbf{V}_r^T \mathbf{V}_p) (\mathbf{V}_r^T \mathbf{V}_p)$ or $\sum_p (\mathbf{V}_r^T \mathbf{V}_r) (\mathbf{V}_p^T \mathbf{V}_p)$. But looking at the diagrams in figure (10), such ambiguities disappear because in all cases the \mathbf{V} 's which are summed over (the \mathbf{V}_p 's) do not contract with each other; they contract with something else at the other end of the gauge boson/gaugino lines. As such, there are no $\mathbf{V}_p^T \mathbf{V}_p$'s in these expressions; with this piece of information, combined with the known rules for a gauge group with multiple factors, equations (6.27), (6.28) and (6.37) follow. The substitution rule given in equation (6.38) for $24 g^4 M M^* C(r) S(R)$ appearing in the two-loop equation of the soft scalar masses is more complicated since the placement of the \mathbf{M} , \mathbf{M}^\dagger gaugino mass matrices between these \mathbf{V} 's is relevant. Nevertheless, from the diagrams in figure (11) we can infer that the $U(1)$'s contri-

⁶ It is conceivable that they could come also from diagrams with one $\phi^* \phi^* \phi \phi$ vertex, but we may choose an appropriate gauge, the Landau gauge, where these vanish because an external scalar line always couples to a gauge bosons at a three point vertex.

bution to this term is $8 \sum_p \left[(\mathbf{V}_i^T \mathbf{M} \mathbf{V}_p) (\mathbf{V}_i^T \mathbf{M}^\dagger \mathbf{V}_p) + (\mathbf{V}_i^T \mathbf{M} \mathbf{M}^\dagger \mathbf{V}_p) (\mathbf{V}_i^T \mathbf{V}_p) + (\mathbf{V}_i^T \mathbf{M}^\dagger \mathbf{M} \mathbf{V}_p) (\mathbf{V}_i^T \mathbf{V}_p) \right]$.

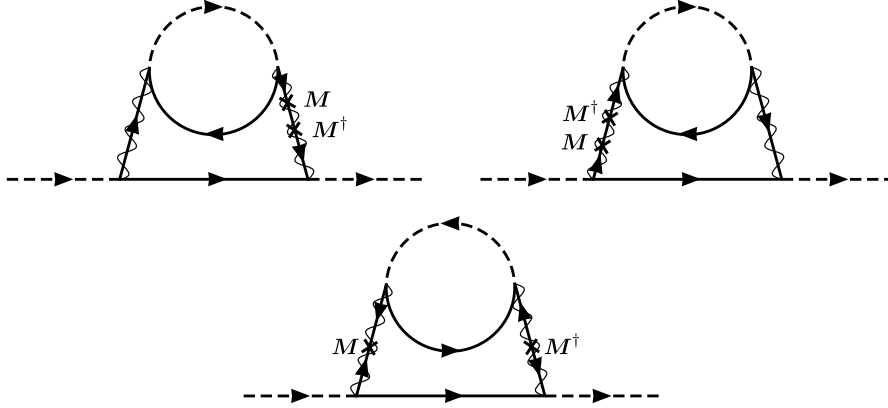


Figure 11: The three contribution from $U(1)$ groups to the term $24g^4 M M^* C(r) S(R)$.

6.4.3 RGEs with $U(1)$ indices

The RGEs for \mathbf{G} and \mathbf{M} are the only ones with free $U(1)$ indices. For the β functions of the gaugino masses, we will be interested in diagrams with two incoming gauginos. As for the coupling constant, due to the Ward identities, the contributing diagrams are those with two external gauge bosons. From the amplitude of these diagrams we still have to add a \mathbf{G} factor in order to obtain $\beta_{\mathbf{G}}$ (see figure (12)). Note that all the terms in $\beta_{\mathbf{G}}$ must be of the form $\mathbf{G} \mathbf{V}_i^T (\dots) \mathbf{V}_j$ for some

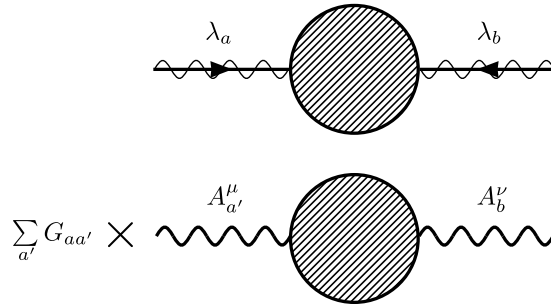


Figure 12: Diagrams from which the β functions of $U(1)$ gaugino masses and gauge couplings are calculated. Notice the isolated \mathbf{G} which appears in the RGEs of \mathbf{G} itself.

i, j as mentioned before, and also

1. the RGEs are invariant under the set of transformations $\mathbf{G} \rightarrow \mathcal{O}_1 \mathbf{G} \mathcal{O}_2^T$, $\mathbf{V}_i \rightarrow \mathcal{O}_2 \mathbf{V}_i$, $\mathbf{M} \rightarrow \mathcal{O}_2 \mathbf{M} \mathcal{O}_2^T$ for any orthogonal matrices $\mathcal{O}_1, \mathcal{O}_2$;
2. \mathbf{M} is a symmetric matrix, therefore $\frac{d\mathbf{M}}{dt}$ must be so as well.

Taken together, these considerations allow us to deduce equations (6.14)–(6.19) (equation (6.13) is trivial).

We shall exemplify this for the case of $16g^4 S(R) C(R) M$ which for multiple factor groups is replaced by $8 \sum_b g_a^2 g_b^2 S_a(R) C_b(R) (M_a + M_b)$ in the RGEs of M_a . This is the same as $8 \sum_{p,b} g_a^2 g_b^2 \frac{S_a(p) C_b(p)}{d_a(p)} (M_a + M_b)$. Groups a and b are independent so the expressions $\sum_b g_b^2 C_b(p)$, $\sum_b M_b g_b^2 C_b(p)$ are decoupled from $g_a^2 \frac{S_a(p)}{d_a(p)}$, $M_a g_a^2 \frac{S_a(p)}{d_a(p)}$. Inclusion of $U(1)$ mixing effects in the first pair of expressions is easy because there are no free $U(1)$ indices: $\sum_b g_b^2 C_b(p) \rightarrow \sum_B g_B^2 C_B(p) + \mathbf{V}_p^T \mathbf{V}_p$ and $\sum_b M_b g_b^2 C_b(p) \rightarrow \sum_B M_B g_B^2 C_B(p) + \mathbf{V}_p^T \mathbf{M} \mathbf{V}_p$. If the group a is a $U(1)$, then in the single $U(1)$ case this corresponds to $g_a^2 \frac{S_a(p)}{d_a(p)} = g^2 y_p^2$, which generalizes to $g_a^2 \frac{S_a(p)}{d_a(p)} \rightarrow \mathbf{V}_p \mathbf{V}_p^T$. Similarly, the only symmetric matrix expression which respects the \mathcal{O}_2 symmetry that can generalize $M_a g_a^2 \frac{S_a(p)}{d_a(p)}$ is $\frac{1}{2} (\mathbf{M} \mathbf{V}_p \mathbf{V}_p^T + \mathbf{V}_p \mathbf{V}_p^T \mathbf{M})$.

Assembling these pieces gives equation (6.20) for $16g^4 S(R) C(R) M$. The structure of the final expression is verifiable by considering the relevant diagrams (figure (13)).

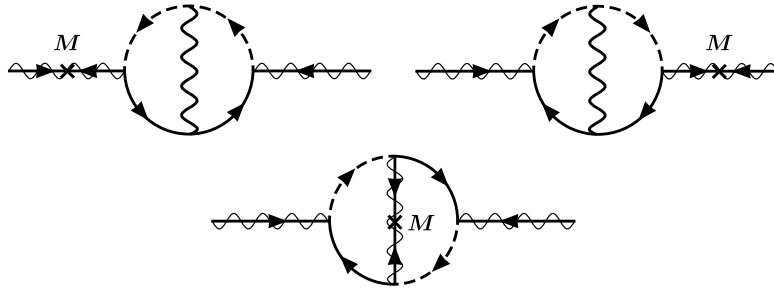


Figure 13: Diagrams contributing to the term $16g^4 S(R) C(R) M$ in the RGEs.

6.5 COMPARISON WITH OTHER METHODS OF INCLUDING $U(1)$ -MIXING EFFECTS

6.5.1 General discussion

So far, several approaches to the SUSY $U(1)$ -mixing problem have been proposed in the literature. In the following, we discuss some of them and comment on their limitations when compared to the complete two-loop treatment presented in this chapter.

As we have already mentioned, one can attempt to choose a convenient pair of bases in the $U(1)$ -charge and gauge field spaces for which the situation might simplify [430, 462]. For instance, it is always possible to diagonalize the one-loop anomalous dimensions

$$\gamma = \sum_i \mathbf{Q}_i \mathbf{Q}_i^T \quad (6.40)$$

by means of a suitable \mathcal{O}_1 rotation $\mathbf{Q}_i \rightarrow \mathcal{O}_1 \mathbf{Q}_i \equiv \mathbf{Q}'_i$ (cf. equation (6.6)), so that $\gamma' = \mathcal{O}_1 \gamma \mathcal{O}_1^T$ is diagonal. This changes the gauge coupling matrix as well: $\mathbf{G} \rightarrow \mathcal{O}_1 \mathbf{G}$. However, if all the relevant $U(1)$ gauge couplings arise at a single scale, or in other words $\mathbf{G} \propto \mathbb{1}$, this \mathcal{O}_1 matrix commutes with \mathbf{G} and can be absorbed

by a suitable redefinition of the gauge fields (equation (6.7)) where now $\mathcal{O}_2 = \mathcal{O}_1$. In this way, the one-loop evolution of \mathbf{G} is driven by a diagonal $\boldsymbol{\gamma}'$ and the initial condition $\mathbf{G} \propto \mathbb{1}$ remains intact. Thus, no off-diagonalities emerge in this case and it is consistent to work with the usual RGEs for individual gauge couplings, one for each $U(1)$ factor.

This approach, however, is generally limited to situations where there is a complete $U(1)$ unification. This is very often not the case in practice, in particular for GUTs in which the hypercharge is a non-trivial linear combination of diagonal generators of the higher energy gauge group, such as in left-right models based on $SU(3)_c \times SU(2)_L \times SU(2)_R \times U(1)_{B-L}$ (see the next section and also chapter 7). Moreover, we should take into consideration the $U(1)$ gaugino soft masses, which should also be universal at the unification scale; otherwise the method fails in the soft sector already at the one-loop level. The crucial point is that only then the generalized one-loop relation

$$\mathbf{G}M^{-1}\mathbf{G}^T = \text{constant} \quad (6.41)$$

between the gauge couplings and the gaugino masses ensures the gaugino mass diagonality along the unification trajectory.

At the two-loop level more complicated structures such as higher powers of charges, gauge couplings and Yukawa couplings enter the anomalous dimensions and therefore, in general, there is no way to diagonalize simultaneously all the evolution equations. Though there is still a technique one can implement in the gauge sector if the $U(1)$ couplings do not unify [462], in the supersymmetric case there is no general way out for the gauginos, as also discussed in [464]. Thus, a full-fledged two-loop approach as presented in this work is necessary and, in fact, it turns out to be even technically indispensable if there happen to be more than two abelian gauge groups as, for instance, in [465], [466] and many string-inspired constructions.

6.5.2 Quantifying $U(1)$ -mixing effects with simple examples

In this section, we shall see through some examples the importance of the kinetic mixing effects in simple scenarios which exhibit all the prominent features discussed above.

One-loop effects

GAUGE COUPLING CONSTANTS: We shall consider the one-loop evolution of the gauge couplings in the SUSY $SO(10)$ model of [271], in which the unified gauge symmetry is broken down to the MSSM in three steps, namely, $SO(10) \rightarrow SU(3)_c \times SU(2)_L \times SU(2)_R \times U(1)_{B-L} \rightarrow SU(3)_c \times SU(2)_L \times U(1)_R \times U(1)_{B-L} \rightarrow \text{MSSM}$; the corresponding breaking scales shall be denoted by m_G , m_R and m_{B-L} , respectively. Further details including the field contents at each of the symmetry breaking stages can be found in [271] (see also “class-III models” in chapter 7).

For our purpose, it is crucial that in this model the ratio m_R/m_{B-L} can be as large as 10^{10} and, hence, the $U(1)$ -mixing effects become important. Note that even a short $SU(3)_c \times SU(2)_L \times SU(2)_R \times U(1)_{B-L}$ stage is sufficient to split the g_R and the g_{B-L} gauge couplings such that the extended gauge-coupling matrix \mathbf{G} at the m_R scale is somewhat far from being proportional to the unit matrix. Thus, there is no way to choose the \mathcal{O}_1 and \mathcal{O}_2 rotation matrices such that both \mathbf{G} and

$$\gamma = \mathbf{N} \begin{pmatrix} \frac{15}{2} & -1 \\ -1 & 18 \end{pmatrix} \mathbf{N} \quad (6.42)$$

are simultaneously diagonalized. Here $\mathbf{N} = \text{diag}(1, \sqrt{3/8})$ ensures the canonical normalization of the $B-L$ charge within the $SO(10)$ framework. Therefore, the one-loop evolution equation relevant to the $U(1)_R \times U(1)_{B-L}$ stage has to be matrix-like. In the abelian sector it reads

$$\frac{d}{dt} \mathbf{A}^{-1} = -\gamma, \quad (6.43)$$

where $\mathbf{A}^{-1} = 4\pi(\mathbf{G}\mathbf{G}^T)^{-1}$ and $t = \log(E/E_0)/2\pi$.

The reason why the $U(1)_R \times U(1)_{B-L}$ phase can be spread over a broad energy range has to do with the fact that this gauge symmetry is broken by neutral components of an $SU(2)_R$ doublet pair, namely, $(1, 1, +\frac{1}{2}, -1) + (1, 1, -\frac{1}{2}, +1) = \chi_R^0 + \bar{\chi}_R^0$ which are SM singlets and, as such, they do not affect the low-energy value of α_Y^{-1} . Indeed, the would-be change inflicted on α_Y^{-1} by the presence or absence of $\chi_R^0 + \bar{\chi}_R^0$ is given by

$$\Delta\alpha_Y^{-1} = p_Y^T \cdot \Delta\mathbf{A}^{-1}(m_{B-L}) \cdot p_Y \propto p_Y^T \cdot \Delta\gamma \cdot p_Y = 0, \quad (6.44)$$

where $p_Y^T = (\sqrt{3/5}, \sqrt{2/5})$ is the vector describing the combination of $U(1)_R \times U(1)_{B-L}$ charges which constitutes the MSSM hypercharge, and $\Delta\gamma$ denotes the relevant change of the γ matrix. Therefore, at the one-loop level, the m_{B-L} scale is not constrained by the low-energy data and hence, barring other phenomenological constraints, it can be pushed as close to the MSSM scale (m_{SUSY}) as desired.

However, this simple argument only works if the $U(1)$ -mixing effects are properly taken into account. Remarkably, if they are neglected, $\Delta\gamma$ contains only diagonal non-null entries and $\alpha_Y^{-1}(m_Z)$ becomes a function of m_{B-L} . Moreover, by stretching the $m_{B-L}-m_R$ range to the maximum, the value of $\alpha_Y^{-1}(m_Z)$ can be incorrectly shifted by as much as 4%, as can be seen by comparing figures (14) and (15). Alternatively, in order to retain the desired value of $\alpha_Y^{-1}(m_Z)$, one would have to re-adjust m_R by several orders of magnitude. However, this could have a large impact on the MSSM soft spectrum [3, 467], and, in more general constructions, also on m_G and α_G , with potential consequences for $d = 6$ proton decay.

Finally, let us note that the *rotated-basis* method discussed previously is only partially successful because the g_R and g_{B-L} gauge couplings do not coincide at the m_R scale. In fact, the value of $\alpha_Y^{-1}(m_Z)$ obtained in this way is 60.93, which is $\sim 2\%$ off the correct value, but still this number is closer to the correct value than the one obtained by considering no mixing at all.

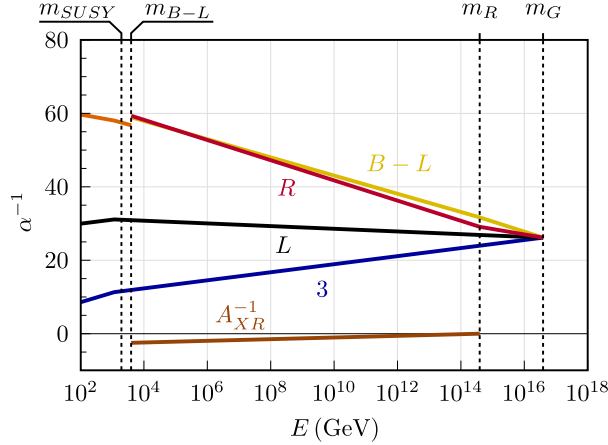


Figure 14: One-loop gauge-coupling evolution in the MRV model [271]. The position of the GUT scale, the unified gauge coupling and the intermediate symmetry-breaking scale m_R were chosen in such a way as to fit the electroweak data with $\alpha_Y^{-1}(m_Z) = 59.73$. The close-to-zero brown line in the $[m_{B-L}, m_R]$ energy range depicts the evolution of the off-diagonal entries of the $\mathbf{A}^{-1} = 4\pi (\mathbf{GG}^T)^{-1}$ matrix which, at the one-loop level, scales linearly with $\log E$. Likewise, in this energy range the red and yellow lines are the (1, 1) and (2, 2) diagonal entries of this matrix. The apparent discontinuity in α_Y^{-1} at the m_{B-L} scale is due to the generalized matching condition (see appendix D for details).

GAUGINO MASSES: The full impact of the method presented in this chapter can be understood by considering the interplay between the gauge and the soft sectors. At one loop-level, we can use equation (6.41) which relates the gauge couplings \mathbf{G} with the gaugino soft masses \mathbf{M} in an invariant combination. As a consequence, at low energies the bino mass is given by

$$M_Y(m_{SUSY}) = \frac{\alpha_Y(m_{SUSY})}{\alpha_G} p_Y^T \mathbf{M}_{1/2} p_Y, \quad (6.45)$$

where $\mathbf{M}_{1/2}$ is the GUT-scale gaugino soft mass matrix. From equation (6.45) we see that the ratio $M_Y(m_{SUSY})/\alpha_Y(m_{SUSY})$ depends on whether the mixing effects are included or not, as was already noticed in [468]. Note that if $\mathbf{M}_{1/2}$ is not proportional to the unit matrix at the GUT scale, the $p_Y^T \mathbf{M}_{1/2} p_Y$ term will mix all entries of $\mathbf{M}_{1/2}$. Moreover, in the special case in which the abelian gauge couplings unify, even the one-loop gaugino sector evolution can be fully accounted for by the *rotated-basis* technique.

Two-loop effects

At the two-loop level this method becomes important in cases with gauge coupling unification at a certain scale. We illustrate this by taking as an example the model presented in reference [457] where an intermediate $SU(3)_c \times SU(2)_L \times U(1)_Y \times U(1)_{B-L}$ gauge symmetry is assumed to originate from a grand unified framework. We consider two cases: (i) full gauge coupling unification at 2×10^{16} GeV and (ii) a small difference of 5% between the two $U(1)$ couplings caused by possible

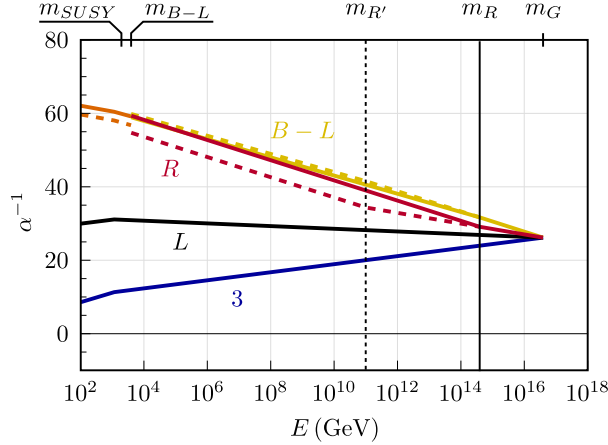


Figure 15: The same as in figure (14) but without the kinetic mixing effects taken into account. With the same GUT-scale boundary condition and m_R , the low-energy value of α_Y^{-1} is 62.51 (orange solid line) and it differs from the one obtained in the full calculation by as much as 4%. Alternatively, if one attempts to obtain the right value of $\alpha_Y^{-1}(m_Z)$ by adjusting the $SU(2)_R$ breaking scale, the new m'_R scale must be shifted with respect to the correct m_R by as much as 4 orders of magnitude (vertical solid and dashed lines).

GUT-scale threshold effects. In the gaugino sector we assume universal boundary conditions in both cases, but the effect gets even stronger if in addition one considers threshold effects in the gaugino sector as well.

The results are given in table (13). Interestingly, besides the expected equivalence of the *rotated-basis* method and the full-fledged calculation at the one-loop level, the relevant effective hypercharge gauge coupling turns out to be identical to the one obtained even at two loop-level if exact gauge coupling unification is assumed. The reason is that all additional states not present in the MSSM are charged only with respect to $U(1)_{B-L}$ and are neutral under the MSSM gauge group. In the gaugino sector, the first deviations show up already in this case, even though they are only of the per-mile order. If one includes also threshold corrections at the GUT-scale the effects are at the percent level leading to shifts in sparticle masses potentially measurable at the LHC.

Lastly, it should be kept in mind that the effects would be even larger if the $U(1)_Y$ would result from the breaking of $U(1)_R \times U(1)_{B-L}$ as discussed in the previous example.

6.6 CONCLUSIONS AND OUTLOOK

In this chapter we have discussed the structure of the renormalization group equations in softly broken supersymmetric models with more than a single abelian gauge factor group. In such models there are $U(1)$ -mixing effects which must be taken into consideration, as explained in section 6.1.

Although the evolution equations available in the literature do not formally exhibit any obvious pathologies if such subtleties are not taken into account, the calculations based on these formulas are in general incomplete and thus, the re-

	One-loop results			Two-loop results			
	No kinetic mixing	Rotated basis method	Complete RGEs	No kinetic mixing	Complete RGEs	No kinetic mixing	Complete RGEs
g_{YY}	0.4511	0.4700	0.4700	0.4487	0.4677	0.4487	0.4686
g_{BLBL}	0.4083	0.4243	0.4243	0.4070	0.4231	0.4131	0.4298
g_{BLY}, g_{YBL}	0.0	-0.0723	-0.0723	0.0	-0.0725	0.0	-0.0725
g_Y	0.4511	0.4511	0.4511	0.4487	0.4487	0.4487	0.4500
M_{YY}	196.34	218.13	218.13	185.82	207.96	185.80	208.71
M_{BLBL}	160.83	178.67	178.67	154.88	173.19	144.26	161.97
M_{BLY}, M_{YBL}	0.0	- 62.39	- 62.39	0.0	-63.10	0.0	-62.15
M_Y	196.34	196.34	196.34	185.82	185.96	185.80	187.04
Exact unification						$g_{BL}^{\text{GUT}} = 1.05 g_Y^{\text{GUT}}$	

Table 13: Low energy values of the entries of the gauge coupling and gaugino mass matrices (g_{ab} and M_{ab} with $a, b = Y, BL$) and the correctly fitted MSSM parameters (g_Y, M_Y)—see equations (D.12) and (D.17). All gaugino mass parameters are in GeV. We have set the GUT scale at 2×10^{16} with $g_G = 0.72$ and imposed an mSUGRA boundary condition taking $\mathbf{M}_{1/2} = \mathbb{1} \times 500$ GeV. At the one-loop level, we compare the case with no kinetic mixing effects included, the *rotated basis* and the full-fledged calculation. At the two-loop level, we include the case where g_Y and g_{BL} are split at the GUT scale due to threshold corrections.

sults are internally inconsistent. This is even more pronounced in the context of SUSY models because it affects also the evolution of the soft SUSY parameters, in particular the evolution of the gaugino mass parameters.

Remarkably enough, the issue of $U(1)$ -mixing in softly broken supersymmetric gauge theories has never been addressed in full generality, even at one loop. The main aim of reference [2], which is reprinted here, was to fill this gap and provide a fully self-consistent method of dealing with the renormalization group evolution of all the parameters in such models, up to two loops. To this end, the existing two-loop renormalization group equations valid for models with at most a single abelian gauge factor were extended.

In particular, we have argued that all the $U(1)$ -mixing effects can be consistently included if the gauge couplings and the soft SUSY-breaking gaugino masses associated to the individual abelian gauge-group factors are generalized to matrices and these are then substituted into the formulae in [430, 432] in a specific manner. However, this is a non-trivial task because the new matrix-like structures do not commute, and as a consequence the generalization of some expressions can be ambiguous. In this respect, the residual reparametrization invariance of the covariant derivative associated to the redefinition of the abelian gauge fields turned out to be a very useful tool, yet in many cases one had to resort to a detailed analysis of the relevant Feynman diagrams.

The general method has been illustrated for two cases: at the one loop level, for a model with different gauge coupling strengths due to a breaking of the original simple group in two steps; and at the two loop level, in a model where gauge coupling unification occurs in a single step, but only with threshold corrections

taken into consideration. In both case we obtain effects in the percent range which none of the previously proposed partial treatments can fully account for.

Lastly, let us stress again that our results are generic and, as such, they do not require any specific assumptions about the charges of the chiral multiplets in the theory and/or the boundary conditions applied to the relevant gauge couplings. This makes the framework suitable for implementation into computer algebraic codes calculating two-loop renormalization group equations in softly-broken supersymmetric gauge theories such as **SARAH** [434, 435, 437, 469] and **SusyNo** [1] (see chapter 5).

7.1 INTRODUCTION

In the MSSM gauge couplings unify at an energy scale of about $m_G \approx 2 \times 10^{16}$ GeV (see chapter 2). Arbitrarily adding particles to the MSSM easily destroys this attractive feature. Thus, relatively few SUSY models have been discussed in the literature which have a particle content larger than MSSM at experimentally accessible energies. However, neutrino oscillation experiments [61, 470, 471] have shown that at least one neutrino must have a mass bigger than 0.05 eV (confer with Δm^2 on table (4)). A Majorana neutrino mass of this order hints at the existence of a new energy scale below m_G . For models with renormalizable interactions and perturbative couplings, as for example in the classical seesaw models [264–266, 472], this new scale should lie below 10^{15} GeV, approximately.

From the theoretical point of view, GUT models based on the group $SO(10)$ [43] offer a number of advantages compared to the simpler models based on $SU(5)$. For example, several of the chains through which $SO(10)$ can be broken to the SM gauge group contain the left-right symmetric group $SU(3)_c \times SU(2)_L \times SU(2)_R \times U(1)_{B-L}$ as an intermediate step [473] (see also chapter 4), thus potentially explaining the observed left-handedness of the weak interactions. However, probably the most interesting aspect of $SO(10)$ is that it automatically contains the necessary ingredients to generate a seesaw mechanism [472]: (i) the right-handed neutrino is included in the **16** which forms a fermion family; and (ii) $(B - L)$ is one of the generators of $SO(10)$.

Left-right (LR) symmetric models usually break the LR symmetry at a rather large energy scale, m_R . For example, if LR is broken in the SUSY LR model by the VEV of $(B - L) = 2$ triplets [474, 475] or by a combination of $(B - L) = 2$ and $(B - L) = 0$ triplets [476, 477], $m_R \approx 10^{15}$ GeV is the typical scale consistent with gauge coupling unification (GCU). The authors of [478] find a lower limit of $m_R \gtrsim 10^9$ GeV from GCU for models where the LR symmetry is broken by triplets, even if one allows additional non-renormalizable operators or sizable GUT-scale thresholds to be present. On the other hand, in models with an extended gauge group it is possible to formulate sets of conditions on the β -coefficients for the gauge couplings, which allow to enforce GCU independently of the energy scale at which the extended gauge group is broken. This was called the *sliding mechanism* in [467].¹ However, reference [467] was not the first to present examples of sliding scale models in the literature. In [271] it was shown that, if the left-right group is

¹ A different (but related) approach to enforcing GCU is taken by the authors of [479] with what they call *magic fields*.

broken to $SU(2)_L \times U(1)_R \times U(1)_{B-L}$ by the VEV of a scalar field $\Phi_{1,1,3,0}$ then² the resulting $U(1)_R \times U(1)_{B-L}$ can be broken to the SM $U(1)_Y$, in agreement with experimental data at any energy scale. In [478] the authors demonstrated that in fact a complete LR group can be lowered to the TeV-scale, if certain carefully chosen fields are added and the LR-symmetry is broken by right doublets. A particularly simple model of this kind was discussed in [480]. Finally, the authors of [467] also discussed an alternative way of constructing a sliding LR scale by relating it to an intermediate Pati-Salam stage. We note in passing that these papers are not in contradiction with earlier works [474–477], all of which have a large m_R : as discussed briefly in the next section, it is not possible to construct a sliding scale *variant* of an LR model including pairs of $\Phi_{1,1,3,-2}$ and $\Phi_{1,3,1,-2}$.

Three different constructions, based on different $SO(10)$ breaking chains, were considered in [467]:

- In chain-I $SO(10)$ is broken in exactly one intermediate (LR symmetric) step to the Standard Model group;
- In chain-II $SO(10)$ is broken first to the Pati-Salam group [41] and at lower energies to the LR group;
- In chain-III there is a LR symmetric phase, which then breaks into a phase where instead of the full $SU(2)_R$ group there is only a $U(1)_R$ gauge symmetry.

In other words,

$$\text{chain I:} \quad SO(10) \rightarrow SU(3)_c \times SU(2)_L \times SU(2)_R \times U(1)_{B-L} \rightarrow \text{MSSM}, \quad (7.1)$$

$$\begin{aligned} \text{chain II:} \quad SO(10) &\rightarrow SU(4) \times SU(2)_L \times SU(2)_R \\ &\rightarrow SU(3)_c \times SU(2)_L \times SU(2)_R \times U(1)_{B-L} \rightarrow \text{MSSM}, \end{aligned} \quad (7.2)$$

$$\begin{aligned} \text{chain III:} \quad SO(10) &\rightarrow SU(3)_c \times SU(2)_L \times SU(2)_R \times U(1)_{B-L} \\ &\rightarrow SU(3)_c \times SU(2)_L \times U(1)_R \times U(1)_{B-L} \rightarrow \text{MSSM}. \end{aligned} \quad (7.3)$$

In all cases, the last symmetry breaking scale before reaching the SM group can be as low as $\mathcal{O}(1 \text{ TeV})$ maintaining nevertheless GCU.³ References [271, 467, 478, 480] mentioned above give at most one or two sample models for each chain; in other words they present a “proof of principle” that models with the stipulated conditions can indeed be constructed in agreement with experimental constraints. It is then perhaps natural to ask: how unique are the models discussed in these papers? In reference [3] we set out to address this question, and the discussion contained in this chapter (as well as in appendix E) is taken from it.

Predictably perhaps, we found that there is a huge number of variants in each class. Even in the simplest class, corresponding to the symmetry breaking chain I,

² The indices denote the transformation properties under the LR group, see next section and appendix E for notation.

³ In fact, the *sliding mechanism* would also work at even lower energy scales. However, this possibility is excluded phenomenologically.

there is a total of 53 variants (up to 5324 configurations, see next section) which can have perturbative GCU and a LR scale below 10 TeV, consistent with experimental data. For the two other classes, chain-II and chain-III, we have found literally thousands of variants.

With such a huge number of variants corresponding essentially to equivalent constructions, an immediate concern is whether there is any way of experimentally distinguishing among all of these constructions. Tests could be either direct or indirect. Direct tests are possible, because of the sliding scale feature of the classes of models we discuss—see section 7.2. Different variants predict different additional (s)particles, some of which (being colored) could give rise to spectacular resonances at the LHC. However, even if the new gauge symmetry and all additional fields are outside the reach of the LHC, all variants have different β -coefficients and thus different running of MSSM parameters, both the gauge couplings and the SUSY soft masses. Thus, if one assumes the validity of a certain SUSY breaking scheme, such as for example mSUGRA, indirect traces of the different variants remain in the SUSY spectrum, potentially measurable at the LHC and a future linear collider (ILC/CLIC). This was discussed earlier in the context of indirect tests for the SUSY seesaw mechanism in [333, 350, 481] and for extended gauge models in [467]. We generalize the discussion of [467] and show how the *invariants*, which are certain combinations of SUSY soft breaking parameters, can themselves be organized into a few classes, which in principle allow to distinguish class-II models from class-I or class-III and, if sufficient precision could be reached experimentally, even select specific variants within a class and provide indirect information about the new energy scale(s).

In the rest of this chapter, we first lay out the general conditions for the construction of the models we are interested in (next section), and afterwards we discuss variants and examples of configurations for all of the three classes we consider. Section 7.3 then addresses the *invariants*, which are combinations of SUSY soft parameters in the different model classes. A short summary and discussion of the main results can also be found at the end of this chapter. Finally, appendix E contains the lists of chiral superfields considered, as well as a quick discussion on the necessary ones to achieve a given symmetry breaking sequence.

7.2 MODELS

7.2.1 *Supersymmetric SO(10) models: General considerations*

Before entering into the details of the different model classes, we first list some general requirements which we use in all constructions. These requirements are the basic conditions any *proto-model*, as we shall call them for now, has to fulfill to guarantee that a phenomenologically realistic model based on it exists. We use the following conditions:

- **Perturbative SO(10) unification:** gauge couplings unify (at least) as successfully as in the MSSM and the value of α_G is in the perturbative regime.

- **The GUT scale should lie above $\sim 10^{16}$ GeV:** this bound is motivated by the limit on the proton decay half-life.
- **Sliding mechanism:** this requirement translates into a set of conditions (different conditions for the different classes of models) on the allowed β -coefficients of the gauge couplings, which ensures that the additional gauge group structure can be broken at any energy scale, while still achieving GCU.
- **Renormalizable symmetry breaking:** at each intermediate step we assume that there is a minimal number of scalar fields needed for symmetry breaking.
- **Fermion masses and in particular neutrino masses:** the field content of the extended gauge groups must be rich enough to account for experimental data, although we will not attempt detailed fits of all data. In particular, we require the presence of the fields necessary to generate Majorana neutrino masses through seesaw, either ordinary seesaw or inverse/linear seesaw.
- **Anomaly cancellation:** we accept as valid proto-models only field configurations which are anomaly free.
- **$SO(10)$ completion:** all fields used in a lower energy phase must be parts of a multiplet present at the next higher symmetry phase. In particular, all fields should come from the decomposition of one of the $SO(10)$ irreducible representations that we consider, which are the ones up to **126**.
- **Correct MSSM limit:** all proto-models must have a rich particle content, so that at low energies the MSSM can emerge as an effective theory.

A few more words on our naming convention and notations is necessary. We consider the three different $SO(10)$ breaking chains, equations (7.1)–(7.3), and we will call these *model classes*. In each class there are fixed sets of β -coefficients, all leading to GCU, but with different values of α_G and different values of α_R and α_{B-L} at low energies. These different sets are called *variants* in the following. Finally, (nearly) all of the variants can be created by more than one possible set of superfields. We will call such a set of superfields a *configuration*. Configurations are what usually is called *model* by model builders, although we prefer to think of these as *proto-models*, in other words constructions fulfilling all our basic requirements. These are only proto-models (and not full-fledged models), since for each configuration we do not check in a detailed calculation that all the fields required in that configuration can remain light. We believe that for many (but probably not all of the configurations) one can find conditions for the required field combinations being “light”, following conditions similar to those discussed in the prototype class-I model of [480]. Having said this, and for the sake of simplicity, we will henceforth call *proto-models* just *models*.

All superfields are named as $\Phi_{3_c, 2_L, 2_R, 1_{B-L}}$ (in the left-right symmetric stage), $\Psi_{4, 2_L, 2_R}$ (in the Pati-Salam regime) and $\Phi'_{3_c, 2_L, 1_R, 1_{B-L}}$ (in the $U(1)_R \times U(1)_{B-L}$ regime), with the indices giving the transformation properties under the group. The conjugate of a field is distinguished by an overbar ($\bar{\Phi}$, $\bar{\Psi}$, $\bar{\Phi}'$) as in $\bar{\Phi}_{3_c, 2_L, 2_R, 1_{B-L}}$,

for example, but note that no overbar or minus sign is added to the indices. In appendix E we list all fields used, together with their transformation properties and their $SO(10)$ origin, complete up to the **126** representation of $SO(10)$.

7.2.2 Model class-I: One intermediate (left-right) scale

We start our discussion with the simplest class of models with only one new intermediate scale (LR):

$$SO(10) \rightarrow SU(3)_c \times SU(2)_L \times SU(2)_R \times U(1)_{B-L} \rightarrow \text{MSSM}. \quad (7.4)$$

We do not discuss the first symmetry breaking step in detail, since it is not relevant for the following discussion; we only mention that $SO(10)$ can be broken to the LR group either via the interplay of VEVs from a **45** and a **54**, as done for example in [480], or via a **45** and a **210**, an approach followed in [271]. In the left-right symmetric stage we consider all irreducible representations which can be constructed from $SO(10)$ multiplets up to dimension **126**. This allows for a total of 24 different representations (plus conjugates), whose transformation properties under the LR group and their $SO(10)$ origin are summarized in table (22) of appendix E.

First, consider gauge coupling unification. If we take the MSSM particle content as a starting point, the β -coefficients in the different regimes are given as:⁴

$$\left(b_3^{SM'}, b_2^{SM'}, b_Y^{SM'}\right) = \left(-7, -3, \frac{21}{5}\right), \quad (7.5)$$

$$\left(b_3^{MSSM}, b_2^{MSSM}, b_Y^{MSSM}\right) = \left(-3, 1, \frac{33}{5}\right), \quad (7.6)$$

$$\left(b_3^{LR}, b_2^{LR}, b_R^{LR}, b_{B-L}^{LR}\right) = (-3, 1, 1, 6) + \left(\Delta b_3^{LR}, \Delta b_2^{LR}, \Delta b_R^{LR}, \Delta b_{B-L}^{LR}\right), \quad (7.7)$$

where we have used the canonical normalization for $B - L$, which is related to the usual one⁵ as follows: $(B - L)^c = \sqrt{\frac{3}{8}}(B - L)$. Here, Δb_i^{LR} stands for the contributions of chiral superfields which are not present in the MSSM.

As is well known, in contrast to the MSSM, putting an additional LR scale below the GUT scale with all Δb_i^{LR} equal to zero destroys unification. Nevertheless GCU can be maintained if some simple conditions on the Δb_i^{LR} are fulfilled. First, since in the MSSM $\alpha_3 = \alpha_2$ at roughly 2×10^{16} GeV one has that $\Delta b_2^{LR} = \Delta b_3^{LR} \equiv \Delta b$ in order to preserve this situation for an arbitrary LR scale (sliding condition). Next, recall the matching condition

$$\alpha_Y^{-1}(m_R) = \frac{3}{5}\alpha_R^{-1}(m_R) + \frac{2}{5}\alpha_{B-L}^{-1}(m_R) \quad (7.8)$$

which, by substitution of the LR scale by an arbitrary one above m_R , allows the definition of an artificial continuation of the hypercharge coupling constant α_Y

⁴ For $b_1^{SM'}$ and $b_2^{SM'}$ we use the SM particle content plus one additional Higgs doublet.

⁵ The canonical normalization comes from the requirement that all generators T^a of $SO(10)$, including therefore $B - L$, share the same norm $\text{Tr}(T^a T^a)$, while the usual normalization assumes that $B - L$ for the left quarks Q and left leptons L is $1/3$ and -1 respectively.

into the LR stage. The β -coefficient of this dummy coupling constant for $E > m_R$ is $\frac{3}{5}b_R^{LR} + \frac{2}{5}b_{B-L}^{LR}$ and it should be compared with b_Y^{MSSM} ($E < m_R$); the difference is $\frac{3}{5}\Delta b_R^{LR} + \frac{2}{5}\Delta b_{B-L}^{LR} - \frac{18}{5}$, which must be equal to Δb in order for the difference between this α_Y coupling and $\alpha_3 = \alpha_2$ at the GUT scale to be independent of the scale m_R . These are the two conditions imposed by the sliding requirement of the LR scale on the β -coefficients—see equations (7.9) and (7.10). Note, however, that we did not require (approximate) unification of α_R and α_{B-L} with α_3 and α_2 ; it is sufficient to require that $\alpha_2^{-1} = \alpha_3^{-1} \approx \frac{3}{5}\alpha_R^{-1} + \frac{2}{5}\alpha_{B-L}^{-1}$. In any case, we can always achieve the desired unification because the splitting between α_R and α_{B-L} at the m_R scale is a free parameter, so it can be used to force $\alpha_R = \alpha_{B-L}$ at the scale where α_3 and α_2 unify, which leads to an almost perfect unification of the four couplings. Also, we require that unification is perturbative, i.e. the value of the common coupling constant at the GUT scale is $\alpha_G^{-1} > 0$. From the experimental value of $\alpha_3(m_Z)$ [105] one can easily calculate the maximal allowed value of Δb as a function of the scale at which the LR group is broken to the SM group. This is shown in figure (16) for three different values of α_G^{-1} . The smallest value of $\max \Delta b$ is obtained when m_R is smallest as well (and α_G^{-1} is largest). For α_G^{-1} in the interval $[0, 3]$ one obtains $\max \Delta b$ in the range $[4.7, 5.7]$, which motivates us to consider Δb up to 5 (however, see the discussion below).

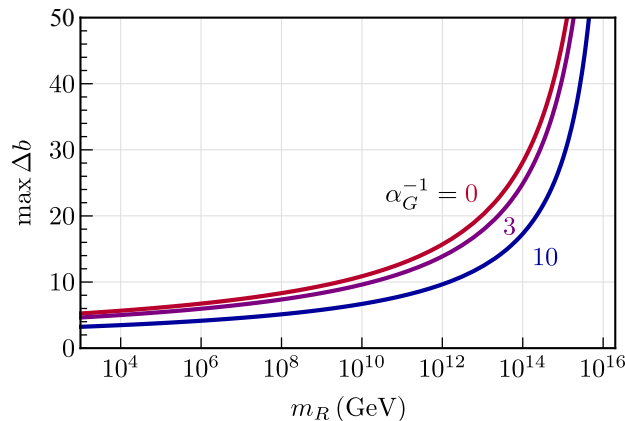


Figure 16: Maximum value of Δb allowed by perturbativity as function of the scale m_R (in GeV). The three different lines have been calculated for three different values for the unified coupling α_G^{-1} , namely $\alpha_G^{-1} = 0, 3, 10$. A LR scale below 10 TeV (1 TeV) requires $\Delta b_3 \lesssim 5.7$ (5.2) if the extreme value of $\alpha_G^{-1} = 0$ is chosen, and $\Delta b_3 \lesssim 5.1$ (4.7) for $\alpha_G^{-1} = 3$.

Altogether, these considerations result in the following constraints on the allowed values for the Δb_i^{LR} :

$$\Delta b_2^{LR} = \Delta b_3^{LR} \equiv \Delta b \leq 5, \quad (7.9)$$

$$\Delta b_{B-L}^{LR} + \frac{3}{2}\Delta b_R^{LR} - 9 = \frac{5}{2}\Delta b \leq \frac{25}{2}. \quad (7.10)$$

Given equations (7.9) and (7.10), one can calculate all allowed variants of sets of Δb_i^{LR} , guaranteed to give GCU. Two examples are shown in figure (17). The figure displays the running of the inverse gauge couplings as a function of the

energy scale, for an assumed value of $m_R = 10$ TeV and a SUSY scale of 1 TeV and $(\Delta b_3^{LR}, \Delta b_2^{LR}, \Delta b_R^{LR}, \Delta b_{B-L}^{LR}) = (0, 0, 1, 15/2)$ (left) or $(4, 4, 10, 4)$ (right). The example on the left has $\alpha_G^{-1} \approx 25$ as in the MSSM, while the example on the right has $\alpha_G^{-1} \approx 6$. Note that while both examples lead by construction to the same value of $\alpha_Y(m_Z)$, they have very different values for $\alpha_R(m_R)$ and $\alpha_{B-L}(m_R)$, and thus predict different couplings for the gauge bosons W_R and Z' of the extended gauge group.

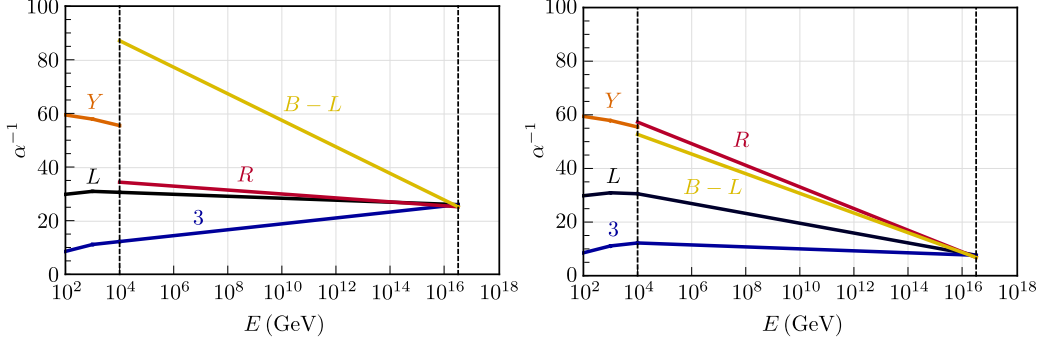


Figure 17: Gauge coupling unification in LR models with $m_R = 10^4$ GeV. The left panel is for $(\Delta b_3^{LR}, \Delta b_2^{LR}, \Delta b_R^{LR}, \Delta b_{B-L}^{LR}) = (0, 0, 1, 15/2)$ while the right one is for $(4, 4, 10, 4)$.

With the constraints in equations (7.9) and (7.10), we find that a total of 65 different variants can be built. However, after requiring that at least one of the fields that breaks correctly the $SU(2)_R \times U(1)_{B-L}$ symmetry to $U(1)_Y$ is indeed present, either a $\Phi_{1,1,3,-2}$ or a $\Phi_{1,1,2,-1}$ (and/or their conjugates), the number of variants is reduced to 53. We list them in table (14), together with one example of a field configuration for each variant.

Table 14: List of the 53 variants with a single LR scale. In each case, the fields shown are the extra ones, which are not part of the MSSM (the 2 Higgs doublets are assumed to come from one bi-doublet $\Phi_{1,2,2,0}$). The $\Delta b_3, \Delta b_2, \Delta b_R, \Delta b_{B-L}$ values can be obtained from the first column through equations (7.9) and (7.10).

$(\Delta b, \Delta b_R)$	Sample field combination
(0, 1)	$\bar{\Phi}_{1,1,2,-1} + 2\bar{\Phi}_{1,1,1,2} + \Phi_{1,1,2,-1} + 2\Phi_{1,1,1,2}$
(0, 2)	$2\bar{\Phi}_{1,1,2,-1} + \bar{\Phi}_{1,1,1,2} + 2\Phi_{1,1,2,-1} + \Phi_{1,1,1,2}$
(0, 3)	$\bar{\Phi}_{1,1,2,-1} + \bar{\Phi}_{1,1,1,2} + \Phi_{1,1,2,-1} + \Phi_{1,1,3,0} + \Phi_{1,1,1,2}$
(0, 4)	$2\bar{\Phi}_{1,1,2,-1} + 2\Phi_{1,1,2,-1} + \Phi_{1,1,3,0}$
(0, 5)	$\bar{\Phi}_{1,1,2,-1} + \Phi_{1,1,2,-1} + 2\Phi_{1,1,3,0}$
(1, 1)	$\bar{\Phi}_{1,2,1,1} + \bar{\Phi}_{1,1,2,-1} + 2\bar{\Phi}_{1,1,1,2} + \bar{\Phi}_{3,1,1,-\frac{2}{3}} + \Phi_{1,2,1,1} + \Phi_{1,1,2,-1} + 2\Phi_{1,1,1,2} + \Phi_{3,1,1,-\frac{2}{3}}$
(1, 2)	$\bar{\Phi}_{1,1,2,-1} + 2\bar{\Phi}_{1,1,1,2} + \bar{\Phi}_{3,1,1,-\frac{2}{3}} + \Phi_{1,1,2,-1} + \Phi_{1,2,2,0} + 2\Phi_{1,1,1,2} + \Phi_{3,1,1,-\frac{2}{3}}$
(1, 3)	$2\bar{\Phi}_{1,1,2,-1} + \bar{\Phi}_{1,1,1,2} + \bar{\Phi}_{3,1,1,-\frac{2}{3}} + 2\Phi_{1,1,2,-1} + \Phi_{1,2,2,0} + \Phi_{1,1,1,2} + \Phi_{3,1,1,-\frac{2}{3}}$
(1, 4)	$\bar{\Phi}_{1,1,2,-1} + \bar{\Phi}_{1,1,1,2} + \bar{\Phi}_{3,1,1,-\frac{2}{3}} + \Phi_{1,1,2,-1} + \Phi_{1,1,3,0} + \Phi_{1,2,2,0} + \Phi_{1,1,1,2} + \Phi_{3,1,1,-\frac{2}{3}}$
(1, 5)	$2\bar{\Phi}_{1,1,2,-1} + \bar{\Phi}_{3,1,1,-\frac{2}{3}} + 2\Phi_{1,1,2,-1} + \Phi_{1,1,3,0} + \Phi_{1,2,2,0} + \Phi_{3,1,1,-\frac{2}{3}}$

($\Delta b, \Delta b_R$) Sample field combination

(5, 2)	$\bar{\Phi}_{1,1,2,-1} + 5\bar{\Phi}_{1,1,1,2} + 2\bar{\Phi}_{3,1,1,-\frac{2}{3}} + \Phi_{1,1,2,-1} + 2\Phi_{1,3,1,0} + \Phi_{1,2,2,0} + \Phi_{8,1,1,0} + 5\Phi_{1,1,1,2}$ $+ 2\Phi_{3,1,1,-\frac{2}{3}}$
(5, 3)	$2\bar{\Phi}_{1,1,2,-1} + 4\bar{\Phi}_{1,1,1,2} + 2\bar{\Phi}_{3,1,1,-\frac{2}{3}} + 2\Phi_{1,1,2,-1} + 2\Phi_{1,3,1,0} + \Phi_{1,2,2,0} + \Phi_{8,1,1,0} + 4\Phi_{1,1,1,2}$ $+ 2\Phi_{3,1,1,-\frac{2}{3}}$
(5, 4)	$\bar{\Phi}_{1,2,1,1} + \bar{\Phi}_{1,1,1,2} + 2\bar{\Phi}_{3,1,1,-\frac{2}{3}} + \bar{\Phi}_{1,1,3,-2} + \Phi_{1,2,1,1} + 2\Phi_{1,3,1,0} + \Phi_{8,1,1,0}$ $+ \Phi_{1,1,1,2} + 2\Phi_{3,1,1,-\frac{2}{3}}$
(5, 5)	$\bar{\Phi}_{1,1,1,2} + 2\bar{\Phi}_{3,1,1,-\frac{2}{3}} + \bar{\Phi}_{1,1,3,-2} + 2\Phi_{1,3,1,0} + \Phi_{1,2,2,0} + \Phi_{8,1,1,0} + \Phi_{1,1,1,2} + 2\Phi_{3,1,1,-\frac{2}{3}}$ $+ \Phi_{1,1,3,-2}$
(5, 6)	$\bar{\Phi}_{1,1,2,-1} + 2\bar{\Phi}_{3,1,1,-\frac{2}{3}} + \bar{\Phi}_{1,1,3,-2} + \Phi_{1,1,2,-1} + 2\Phi_{1,3,1,0} + \Phi_{1,2,2,0} + \Phi_{8,1,1,0} + 2\Phi_{3,1,1,-\frac{2}{3}}$ $+ \Phi_{1,1,3,-2}$
(5, 7)	$2\bar{\Phi}_{3,1,1,-\frac{2}{3}} + \bar{\Phi}_{1,1,3,-2} + \Phi_{1,3,1,0} + 3\Phi_{1,2,2,0} + \Phi_{8,1,1,0} + 2\Phi_{3,1,1,-\frac{2}{3}} + \Phi_{1,1,3,-2}$
(5, 8)	$\bar{\Phi}_{3,1,2,\frac{1}{3}} + \bar{\Phi}_{1,1,3,-2} + 2\Phi_{1,3,1,0} + \Phi_{1,2,2,0} + \Phi_{8,1,1,0} + \Phi_{3,1,2,\frac{1}{3}} + \Phi_{1,1,3,-2}$
(5, 9)	$2\bar{\Phi}_{1,1,2,-1} + \bar{\Phi}_{1,1,1,2} + 2\bar{\Phi}_{3,1,1,-\frac{2}{3}} + 2\Phi_{1,1,2,-1} + \Phi_{1,1,3,0} + 5\Phi_{1,2,2,0} + \Phi_{8,1,1,0} + \Phi_{1,1,1,2}$ $+ 2\Phi_{3,1,1,-\frac{2}{3}}$
(5, 10)	$\bar{\Phi}_{1,1,2,-1} + \bar{\Phi}_{1,1,1,2} + 2\bar{\Phi}_{3,1,1,-\frac{2}{3}} + \Phi_{1,1,2,-1} + 2\Phi_{1,1,3,0} + 5\Phi_{1,2,2,0} + \Phi_{8,1,1,0} + \Phi_{1,1,1,2}$ $+ 2\Phi_{3,1,1,-\frac{2}{3}}$
(5, 11)	$2\bar{\Phi}_{1,1,2,-1} + 2\bar{\Phi}_{3,1,1,-\frac{2}{3}} + 2\Phi_{1,1,2,-1} + 2\Phi_{1,1,3,0} + 5\Phi_{1,2,2,0} + \Phi_{8,1,1,0} + 2\Phi_{3,1,1,-\frac{2}{3}}$
(5, 12)	$\bar{\Phi}_{1,1,2,-1} + 2\bar{\Phi}_{3,1,1,-\frac{2}{3}} + \Phi_{1,1,2,-1} + 3\Phi_{1,1,3,0} + 5\Phi_{1,2,2,0} + \Phi_{8,1,1,0} + 2\bar{\Phi}_{3,1,1,-\frac{2}{3}}$
(5, 13)	$\bar{\Phi}_{1,1,2,-1} + \bar{\Phi}_{3,1,2,\frac{1}{3}} + \Phi_{1,1,2,-1} + 2\Phi_{1,1,3,0} + 5\Phi_{1,2,2,0} + \Phi_{8,1,1,0} + \Phi_{3,1,2,\frac{1}{3}}$

We give only one example for each configuration in table (14), although we went through the exercise of finding all possible configurations for the 53 variants with the field content of table (22). In total there are 5324 anomaly-free configurations [482]. The variants (0,1), (0,2), (0,4) and (0,5) are the only ones which have a single configuration; for the other variants, in particular those with larger values of Δb_3^{LR} , there are many configurations.

Not all the fields in table (22) can lead to valid configurations: the fields which never give an anomaly-free configuration are $\Phi_{8,2,2,0}$, $\Phi_{3,2,2,\frac{4}{3}}$, $\Phi_{3,3,1,-\frac{2}{3}}$, $\Phi_{3,1,3,-\frac{2}{3}}$, $\Phi_{6,3,1,\frac{2}{3}}$, $\Phi_{6,1,3,\frac{2}{3}}$ and $\Phi_{1,3,3,0}$. Also, the field $\Phi_{3,2,2,-\frac{2}{3}}$ appears exactly once, in the configuration $4\Phi_{1,2,1,1} + \bar{\Phi}_{3,1,1,-\frac{2}{3}} + \Phi_{3,2,2,-\frac{2}{3}} + 4\Phi_{1,1,2,1} + 2\Phi_{1,1,1,2} + 5\bar{\Phi}_{3,1,1,-\frac{2}{3}}$ which is a (5,5) variant. Note that the examples we give for variants (1,3) and (1,4) are not the model-II and model-I discussed in [467].

Many of the 53 variants only have configurations with $\Phi_{1,1,2,-1}$ (and conjugate) for the breaking of the LR-symmetry. To generate neutrino masses via a seesaw mechanism these variants need either the presence of $\Phi_{1,3,1,0}$, as for example in the configuration shown for variant (2,1), or $\bar{\Phi}_{1,1,3,0}$ (see, for instance variant (1,4)), or an additional singlet $\Phi_{1,1,1,0}$ (which is not shown in table (14) since it does not affect the Δb_i^{LR}). Using the $\Phi_{1,1,1,0}$ one could construct either an inverse [270] or a linear [483, 484] seesaw mechanism, while with $\Phi_{1,3,1,0}$ a type-III seesaw [269] is a possibility, and finally a $\Phi_{1,1,3,0}$ allows for an inverse type-III seesaw [467]. The first

example where a valid configuration with $\Phi_{1,1,3,-2}$ appears is in the variant (3,4). The simplest configuration is $\Phi_{1,2,1,1} + \Phi_{1,3,1,0} + \Phi_{8,1,1,0} + \Phi_{1,1,3,-2} + \bar{\Phi}_{1,2,1,1} + \bar{\Phi}_{1,1,3,-2}$ (which is not the example given in table (14)). The VEV of the $\Phi_{1,1,3,-2}$ does not only break the LR symmetry, but it can also generate a Majorana mass term for the right-handed neutrino fields, i.e. configurations with $\Phi_{1,1,3,-2}$ can generate a type-I seesaw, in principle. Finally, the simplest possibility with a valid configuration including $\Phi_{1,3,1,-2}$ is found in variant (4,1) with $\Phi_{1,1,2,-1} + \Phi_{8,1,1,0} + \Phi_{1,1,1,2} + \Phi_{3,1,1,\frac{4}{3}} + \Phi_{1,3,1,-2} + \bar{\Phi}_{1,1,2,-1} + \bar{\Phi}_{1,1,1,2} + \bar{\Phi}_{3,1,1,\frac{4}{3}} + \bar{\Phi}_{1,3,1,-2}$. The presence of $\Phi_{1,3,1,-2}$ allows the construction of a type-II seesaw mechanism for the neutrinos.

As mentioned in the beginning of this chapter, it is not possible to construct a sliding scale model in which the LR symmetry is broken by two pairs of triplets: $\Phi_{1,3,1,-2} + \bar{\Phi}_{1,3,1,-2} + \Phi_{1,1,3,-2} + \bar{\Phi}_{1,1,3,-2}$. The sum of the Δb 's for these fields adds up to $(\Delta b_3^{LR}, b_L^{LR}, \Delta b_R^{LR}, \Delta b_{B-L}^{LR}) = (0, 4, 4, 18)$ and so, because $\Delta b_{B-L}^{LR} + \frac{3}{2}\Delta b_R^{LR} - 9 = 15 > \frac{25}{2}$ (confer with equation (7.10)), there are no configurations with this combination of fields. This observation is consistent with the analysis done in [478], where the authors have shown that a supersymmetric LR-symmetric model, where the LR symmetry is broken by two pairs of triplets, requires a minimal LR scale of at least 10^9 GeV (and, actually, a much larger scale in minimal renormalizable models, if GUT scale thresholds are small).

Regarding the variants with $\Delta b_2^{LR} = \Delta b_3^{LR} = 0$, strictly speaking none of these variants is guaranteed to give a valid model in the sense defined in subsection 7.2.1, as they contain only one $\Phi_{1,2,2,0} \rightarrow (H_u, H_d)$ and no vector-like quarks ($\Phi_{3,1,1,\frac{4}{3}}$ or $\Phi_{3,1,1,-\frac{2}{3}}$). With such a minimal configuration, the CKM matrix is trivial at the energy scale where the LR symmetry is broken. We nevertheless list these variants, since in principle a CKM matrix for quarks consistent with experimental data could be generated at 1-loop level from flavor violating soft terms, as discussed in [485].

7.2.3 Model class-II: Additional intermediate Pati-Salam scale

In the second class of supersymmetric $SO(10)$ models that we are considering, $SO(10)$ is broken first to the Pati-Salam (PS) group. The complete breaking chain is thus

$$\begin{aligned} SO(10) &\rightarrow SU(4) \times SU(2)_L \times SU(2)_R \\ &\rightarrow SU(3)_c \times SU(2)_L \times SU(2)_R \times U(1)_{B-L} \rightarrow \text{MSSM}. \end{aligned} \quad (7.11)$$

The representations available from the decomposition of $SO(10)$ multiplets up to **126** are listed in table (23) of appendix E, together with their possible $SO(10)$ origin. Breaking $SO(10)$ to the PS group requires that $\Psi_{1,1,1}$ from the **54** develops a VEV. The subsequent breaking of the PS group to the LR group requires that the LR singlet in $\Psi_{15,1,1}$, originally from the **45** of $SO(10)$, acquires a VEV. And finally, as before in the LR-class, the breaking of LR to $SU(3)_c \times SU(2)_L \times U(1)_Y$ can be done either with a $\Phi_{1,1,2,-1}$ or $\Phi_{1,1,3,-2}$ (and/or conjugates).

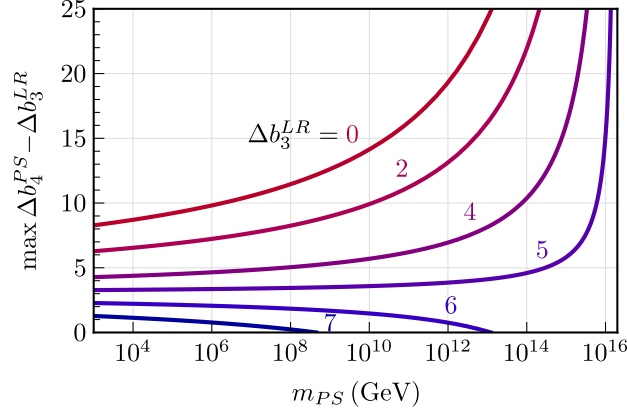


Figure 18: Maximum value of $\Delta b_4^{PS} - \Delta b_3^{LR}$ allowed by perturbativity as function of the scale m_{PS} in GeV. The different lines have been calculated for six different values of Δb_3^{LR} . For this plot we assumed that $m_R = 1$ TeV.

The additional b_i coefficients for the regime $[m_{PS}, m_{GUT}]$ are given by:

$$(b_4^{PS}, b_2^{PS}, b_R^{PS}) = (-6, 1, 1) + (\Delta b_4^{PS}, \Delta b_2^{PS}, \Delta b_R^{PS}) \quad (7.12)$$

where, as before, the Δb_i^{PS} include contributions from superfields which are not part of the MSSM field content.

In this class of models, the unification scale is independent of the LR one if the following condition is satisfied:

$$0 = \begin{pmatrix} \Delta b_3^{LR} - \Delta b_2^{LR} \\ \frac{3}{5} \Delta b_R^{LR} + \frac{2}{5} \Delta b_{B-L}^{LR} - \Delta b_2^{LR} - \frac{18}{5} \end{pmatrix}^T \cdot \begin{pmatrix} 2 & 3 \\ -5 & 0 \end{pmatrix} \cdot \begin{pmatrix} \Delta b_4^{PS} - \Delta b_2^{PS} - 3 \\ \Delta b_R^{PS} - \Delta b_2^{PS} - 12 \end{pmatrix}. \quad (7.13)$$

It is worth noting that also requiring m_{PS} to be independent of the LR scale would lead to the conditions (7.9)–(7.10), which are the sliding conditions for LR models. This must be so, and we can see it as follows: for some starting values of the three gauge couplings at m_{PS} , the scales m_{PS} and m_G can be adjusted such that the two splittings between the three gauge couplings are reduced to zero at m_G . This fixes these scales, which must not change even if m_R is varied. As such $\alpha_3^{-1}(m_{PS}) - \alpha_2^{-1}(m_{PS})$ and $\alpha_3^{-1}(m_{PS}) - \alpha_R^{-1}(m_{PS})$ are also fixed, and they can be determined by running the MSSM up to m_{PS} . The situation is therefore equal to the one that led to the equalities in (7.9)–(7.10), namely the splittings between the gauge couplings at some fixed scale must be independent of m_R .

Since there are now two unknown scales in the problem, the maximum Δb_i^X allowed by perturbativity in one regime do not depend only on the new scale X , but on the Δb_i^Y in the other regime Y as well. As an example, in figure (18) we show the maximum Δb_4^{PS} allowed by $\alpha_G^{-1} \geq 0$ for different values of Δb_3^{LR} and assuming that $m_R = 10^3$ GeV and $m_G \geq 10^{16}$ GeV. The dependence of $\max \Delta b_4^{PS}$ on m_R is rather weak, as long as m_R does not approach the GUT scale.

If all the Δb 's are to be bounded, an upper limit must be placed on the PS scale. For example, if $m_{PS} \leq 10^6$ GeV it is possible to derive the following bounds:⁶

$$\Delta b_2^{PS} + \frac{3}{10} \Delta b_2^{LR} < 7.2, \quad (7.14)$$

$$\Delta b_4^{PS} + \frac{3}{10} \Delta b_3^{LR} < 10, \quad (7.15)$$

$$\frac{2}{5} \Delta b_4^{PS} + \frac{3}{5} \Delta b_R^{PS} + \frac{3}{10} \left(\frac{2}{5} \Delta b_{B-L}^{LR} + \frac{3}{5} \Delta b_R^{LR} \right) < 17. \quad (7.16)$$

The large values of $\max \Delta b^{LR}$ and $\max \Delta b^{PS}$ allow, in principle, a huge number of class-II variants to be constructed. This is demonstrated in figure (19), where we show the number of variants for an assumed $m_R \approx 1$ TeV as a function of the scale m_{PS} (up to $m_{PS} = 10^{15}$ GeV). For larger values of the PS scale we have only scanned a finite (though large) set of possible variants. Also note that these are variants and not configurations. As in the case of class-I models, almost all variants can be realized through several anomaly-free configurations. The exhaustive list of variants (up to $m_{PS} = 10^{15}$ GeV) containing a total of 105909 possibilities can be found in [482].

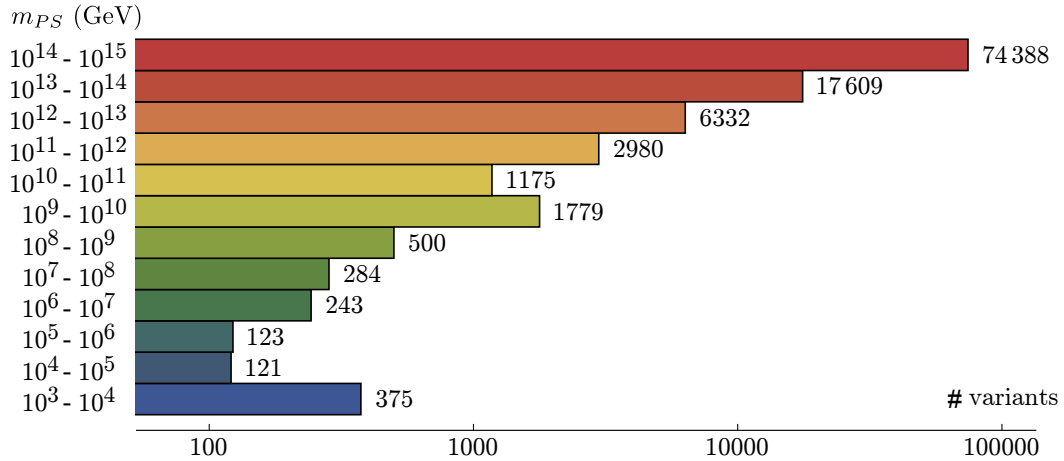


Figure 19: The number of possible variants of class-II models as a function of m_{PS} , assuming $m_R \approx 1$ TeV and 10^{16} GeV $\lesssim m_G \lesssim 2 \times 10^{18}$ GeV.

With such a huge number of possible variants, we can discuss only some general features. First of all, within the exhaustive set of models with $m_{PS} = 10^{15}$ GeV, there are a total of 1570 different sets of Δb_i^{LR} , each of which can be completed by more than one set of Δb_i^{PS} . Variants with the same set of Δb_i^{LR} but different completion of Δb_i^{PS} have the same configuration in the LR-regime, but are associated to a different value for m_{PS} for fixed m_R . Thus, they have in general different values for α_{B-L} and α_R at the LR scale and, as discussed in the following section,

⁶ In fact, the bounds shown here exclude a few variants with $m_{PS} < 10^6$ GeV. This is because of the following: while in most cases the most conservative assumption is to assume m_{PS} as large as possible in deriving these bounds ($= 10^6$ GeV, leading to a smaller running in the PS regime), there are some cases where this is not true. This is a minor complication which nonetheless was taken into account in our computation.

different values of the invariants. For example, for the smallest possible values of Δb_i^{LR} , $\Delta b_i^{LR} = (0, 0, 1, 3/2)$, there are 342 different completing sets of Δb_i^{PS} .

The simplest possible set of Δb_i^{LR} , $\Delta b_i^{LR} = (0, 0, 1, 3/2)$, corresponds to the configuration $\Phi_{1,1,2,-1} + \bar{\Phi}_{1,1,2,-1}$. These fields are necessary to break $SU(2)_R \times U(1)_{B-L} \rightarrow U(1)_Y$. Their presence in the LR regime requires that in the PS-regime we have at least one set of copies of $\Psi_{4,1,2} + \bar{\Psi}_{4,1,2}$. In addition, to break the PS group to the LR one, we need at least one copy of $\Psi_{15,1,1}$. However, the combination $\Psi_{4,1,2} + \bar{\Psi}_{4,1,2} + \Psi_{15,1,1}$ is not sufficient to generate a sliding scale mechanism and the simplest configuration that can do so is $3\Psi_{1,2,2} + 4\Psi_{1,1,3} + \Psi_{4,1,2} + \bar{\Psi}_{4,1,2} + \Psi_{15,1,1}$, leading to $\Delta b_i^{PS} = (6, 3, 15)$ and a very low possible value of $m_{PS} = 8.2$ TeV for $m_R = 1$ TeV (see, however, the discussion on leptoquarks below). The next possible completion for $\Phi_{1,1,2,-1} + \bar{\Phi}_{1,1,2,-1}$ is $3\Psi_{1,2,2} + 5\Psi_{1,1,3} + \Psi_{4,1,2} + \bar{\Psi}_{4,1,2} + \Psi_{15,1,1}$, with $\Delta b_i^{PS} = (6, 3, 17)$ and $m_{PS} = 1.3 \times 10^8$ GeV (for $m_R = 1$ TeV), and so forth.

As noted already in subsection 7.2.2, one copy of $\Phi_{1,2,2,0}$ is not sufficient to produce a realistic CKM matrix at tree-level. Thus, the minimal configuration of $\Phi_{1,1,2,-1} + \bar{\Phi}_{1,1,2,-1}$ relies on the possibility of generating all the departure of the CKM matrix from unity with flavor violating soft masses [485]. There are at least two possibilities to generate a non-trivial CKM at tree-level, either by adding another $\Phi_{1,2,2,0}$ plus (at least) one copy of $\Phi_{1,1,3,0}$, or with one copy of “vector-like quarks” $\Phi_{3,1,1,\frac{4}{3}}$ or $\Phi_{3,1,1,-\frac{2}{3}}$. First consider the configuration $\Phi_{1,1,2,-1} + \bar{\Phi}_{1,1,2,-1} + \Phi_{1,2,2,0} + \Phi_{1,1,3,0}$, which leads to $\Delta b_i^{LR} = (0, 1, 4, 3/2)$. Since $\Phi_{1,2,2,0}$ and $\Phi_{1,1,3,0}$ must come from $\Psi_{1,2,2}$ (or $\Psi_{15,2,2}$) and $\Psi_{1,1,3}$, respectively, the simplest completion for this set of Δb_i^{LR} is again $3\Psi_{1,2,2} + 4\Psi_{1,1,3} + \Psi_{4,1,2} + \bar{\Psi}_{4,1,2} + \Psi_{15,1,1}$, leading to $\Delta b_i^{PS} = (6, 3, 15)$ and $m_{PS} = 5.4$ TeV, for $m_R = 1$ TeV. Again, many completions with different Δb_i^{PS} exist for this set of Δb_i^{LR} .

The other possibility for generating CKM at tree-level, adding for example a pair of $\Phi_{3,1,1,-\frac{2}{3}} + \bar{\Phi}_{3,1,1,-\frac{2}{3}}$, corresponds to $\Delta b_i^{LR} = (1, 0, 1, 5/2)$ and its simplest PS-completion is $4\Psi_{1,2,2} + 4\Psi_{1,1,3} + \Psi_{4,1,2} + \bar{\Psi}_{4,1,2} + \Psi_{6,1,1} + \Psi_{15,1,1}$, with $\Delta b_i^{PS} = (7, 4, 16)$ and a $m_{PS} = 4.6 \times 10^6$ TeV for $m_R = 1$ TeV. In this case one can also find very low values of m_{PS} . For example, adding a $\Phi_{1,2,2,0}$ to this LR-configuration yields $\Delta b_i^{LR} = (1, 1, 2, 5/2)$, and one finds that, with the same Δb_i^{PS} , the PS scale is now $m_{PS} = 8.3$ TeV, for $m_R = 1$ TeV.

We note in passing that in our notation the original PS-class model of [467] corresponds to $\Delta b_i^{LR} = (1, 2, 10, 4)$ and $\Phi_{1,1,2,-1} + \bar{\Phi}_{1,1,2,-1} + \Phi_{1,2,1,1} + \bar{\Phi}_{1,2,1,1} + \Phi_{1,2,2,0} + 4\Phi_{1,1,3,0} + \Phi_{3,1,1,-\frac{2}{3}} + \bar{\Phi}_{3,1,1,-\frac{2}{3}}$, completed by $\Delta b_i^{PS} = (9, 5, 13)$ with $\Psi_{4,1,2} + \bar{\Psi}_{4,1,2} + \Psi_{4,2,1} + \bar{\Psi}_{4,2,1} + \Psi_{1,2,2} + 4\Psi_{1,1,3} + \Psi_{6,1,1} + \Psi_{15,1,1}$. The lowest possible m_{PS} , corresponding to $m_R = 1$ TeV, is $m_{PS} = 2.4 \times 10^8$ GeV. Obviously, this example is not the simplest construction in class-II. We also mention that, although this would not have an impact in the β -coefficients, the superfield $\Phi_{1,1,3,0}$ can be interpreted either as a “Higgs” field or as a “matter” field, and in the original construction [467] the 4 copies of $\Phi_{1,1,3,0}$ were viewed as one $\Omega = \Phi_{1,1,3,0}$ (“Higgs”) and three $\Sigma^c = \Phi_{1,1,3,0}$ (“matter”). In this way, Ω^c can be used to generate the CKM matrix at tree-level (together with the extra bi-doublet $\Phi_{1,2,2,0}$), while the Σ^c can be used to generate an inverse type-III seesaw accounting for neutrino masses.

As figure (19) shows, there are more than 600 variants in which m_{PS} can in principle be lower than 10^6 GeV. However, such low PS scales are already constrained by searches for rare decays, such as $B_s \rightarrow \mu^+ \mu^-$. This is because $\Psi_{15,1,1}$, which must be present in all our constructions for the breaking of the PS group, contains two leptoquark states. We will not study in detail leptoquark phenomenology [486], but it is worth mentioning that in a recent work [487] an absolute lower bound ≈ 40 TeV on the mass of leptoquarks within PS models was derived. There are 426 variants for which we find m_{PS} lower than this bound, provided that $m_R = 1$ TeV. Due to the sliding scale nature of our construction, this does not mean that these models are ruled out by the lower limit found in [487]. Instead, for these models one can calculate a lower limit on m_R from the requirement that $m_{PS} = 40$ TeV. It turns out that from this requirement, and depending on the model, the minimum m_R must be in the range [1.3, 27.7] TeV for these 426 variants.

Two variants can be seen in figure (20): we have chosen one example with a very low m_{PS} (left) and another with an intermediate m_{PS} (right). In both graphs m_R was chosen to be 1 TeV, and we note that in the example on the left this leads to $m_{PS} < 40$ TeV, therefore the scale m_R must be higher. Note also that, unlike in class-I models, in class-II models the GUT scale is no longer fixed to the MSSM value $m_G \approx 2 \times 10^{16}$ GeV.

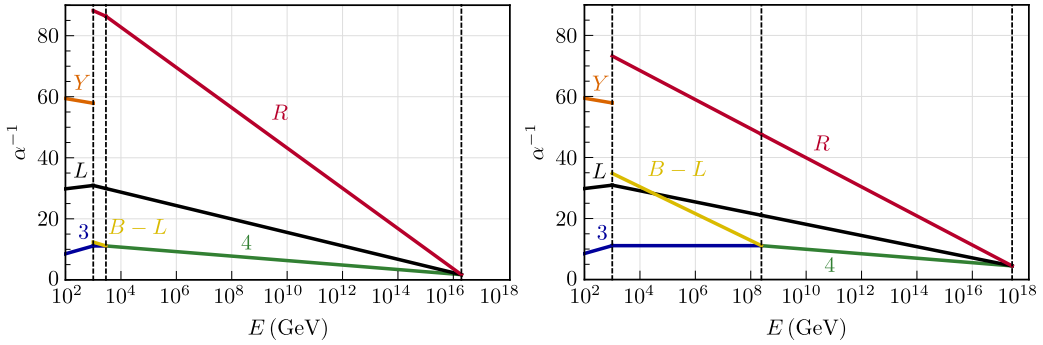


Figure 20: Gauge coupling unification for PS models with $m_R = 1$ TeV. In the plot to the left $(\Delta b_3^{LR}, \Delta b_L^{LR}, \Delta b_R^{LR}, \Delta b_{B-L}^{LR}, \Delta b_4^{PS}, \Delta b_L^{PS}, \Delta b_R^{PS}) = (3, 5, 10, 3/2, 8, 5, 17)$, while the plot to the right corresponds to $\Delta b's = (3, 4, 12, 6, 8, 4, 12)$. Note that in the left plot m_{PS} is lower than 40 TeV therefore, in order to respect leptoquark mass bounds, the m_R scale must be raised.

7.2.4 Models with an $U(1)_R \times U(1)_{B-L}$ intermediate scale

Finally, we consider models where there is an additional intermediate $U(1)_R \times U(1)_{B-L}$ phase that follows the $SU(2)_R \times U(1)_{B-L}$ stage. The field content relevant to this model is given in table (24) of appendix E. In this case, the original $SO(10)$ is broken down to the MSSM in three steps:

$$\begin{aligned} SO(10) &\rightarrow SU(3)_c \times SU(2)_L \times SU(2)_R \times U(1)_{B-L} \\ &\rightarrow SU(3)_c \times SU(2)_L \times U(1)_R \times U(1)_{B-L} \rightarrow \text{MSSM}. \end{aligned} \quad (7.17)$$

The first step is achieved in the same way as in class-I models. The subsequent breaking $SU(2)_R \times U(1)_{B-L} \rightarrow U(1)_R \times U(1)_{B-L}$ is triggered by $\Phi_5 = \Phi_{1,1,3,0}$ and the last one requires $\Phi'_4 = \Phi'_{1,1,\frac{1}{2},-1}$, $\Phi'_{20} = \Phi'_{1,1,1,-2}$ or their conjugates.

As mentioned previously in chapter 6, theories with more than one $U(1)$ gauge factor give rise to $U(1)$ -mixing, and to account for it the $U(1)$ gauge couplings should be seen as a matrix. In the present case,

$$\mathbf{G} = \begin{pmatrix} g_{RR} & g_{RX} \\ g_{XR} & g_{XX} \end{pmatrix}, \quad (7.18)$$

where an X is used instead of $B-L$ because of the $\sqrt{3/8}$ normalization factor mentioned previously. From section 6.5.2, we recall that we can build a generalization of α , which is $\mathbf{A} = \mathbf{G}\mathbf{G}^T/4\pi$, and whose evolution under the renormalization group is controlled by the anomalous dimensions matrix γ (see equations (6.40) and (6.43), as well as [467]). Taking the MSSM's field content, we find that

$$\gamma = \begin{pmatrix} 7 & 0 \\ 0 & 6 \end{pmatrix}. \quad (7.19)$$

Note again that to ensure the canonical normalization of the $B-L$ charge within the $SO(10)$ framework, γ should be normalized as $\gamma^{\text{can}} = \mathbf{N}\gamma^{\text{usual}}\mathbf{N}$, where $\mathbf{N} = \text{diag}(1, \sqrt{3/8})$ —compare with equation (6.42). The gauge coupling g_Y of the $U(1)_Y$ group of the MSSM is obtainable from the following expression, which is valid at the m_{B-L} energy scale:

$$\alpha_Y^{-1} = \mathbf{p}_Y^T \cdot \mathbf{A}^{-1} \cdot \mathbf{p}_Y. \quad (7.20)$$

For completeness, we recall here that $\mathbf{p}_Y^T = (\sqrt{3/5}, \sqrt{2/5})$; for generic details of the matching procedure in models with multiple $U(1)$'s, see appendix D.

The additional β -coefficients for the running step $[m_{B-L}, m_R]$ are given by

$$\begin{aligned} (b_3^{B-L}, b_2^{B-L}, \gamma_{RR}^{B-L}, \gamma_{XR}^{B-L}, \gamma_{XX}^{B-L}) &= (-3, 1, 6, 0, 7) \\ &+ (\Delta b_3^{B-L}, \Delta b_2^{B-L}, \Delta\gamma_{RR}, \Delta\gamma_{XR}, \Delta\gamma_{XX}). \end{aligned} \quad (7.21)$$

Similarly to what was done in the previous class of models, we consider $m_{B-L} = 10^3$ GeV, $m_G \geq 10^{16}$ GeV, $m_R \leq 10^6$ GeV, and extract bounds for the Δb :

$$\Delta b_2^{LR} + \frac{3}{10} \Delta b_2^{B-L} < 7.1, \quad (7.22)$$

$$\Delta b_3^{LR} + \frac{3}{10} \Delta b_3^{B-L} < 6.9, \quad (7.23)$$

$$\frac{3}{5} \Delta b_R^{LR} + \frac{2}{5} \Delta b_{B-L}^{LR} + \frac{3}{10} \mathbf{p}_Y^T \cdot \Delta\gamma \cdot \mathbf{p}_Y < 10.8. \quad (7.24)$$

Even with this restriction in the scales, we found 15610 solutions, more than in the PS case with similar conditions, due to the fact that there are more $\Delta b'$ s that can be varied to obtain solutions. The qualitative features of the running of the gauge couplings are shown for two cases in figure (21). In these two examples, $(\Delta b_3^{LR}, \Delta b_L^{LR}, \Delta b_R^{LR}, \Delta b_{B-L}^{LR}, \Delta b_3^{B-L}, \Delta b_L^{B-L}, \Delta \gamma_{RR}, \Delta \gamma_{XR}, \Delta \gamma_{XX})$ is equal to $(0, 1, 3, 3, 0, 0, 1/2, -\sqrt{3}/8, 3/4)$ (left) and $(2, 2, 4, 8, 2, 2, 1/2, -\sqrt{3}/8, 11/4)$ (right). The former corresponds to the minimal configuration $\Phi'_{1,1,1/2,-1} + \bar{\Phi}'_{1,1,1/2,-1}$, in the lower energy regime, and $\Phi_{1,1,2,-1} + \bar{\Phi}_{1,1,2,-1} + \Phi_{1,1,3,0} + \Phi_{1,2,1,1} + \bar{\Phi}_{1,2,1,1}$ in the higher one (the LR-symmetric regime). The latter corresponds to $\Phi'_{1,1,1/2,-1} + \bar{\Phi}'_{1,1,1/2,-1} + \Phi'_{1,3,0,0} + 2\bar{\Phi}'_{3,1,1,-2/3} + 2\bar{\Phi}'_{3,1,1,-2/3}$ and $2\Phi_{1,1,2,-1} + 2\bar{\Phi}_{1,1,2,-1} + \Phi_{1,1,3,0} + \Phi_{1,3,1,0} + \Phi_{1,1,1,2} + \bar{\Phi}_{1,1,1,2} + 2\Phi_{3,1,1,-2/3} + 2\bar{\Phi}_{3,1,1,-2/3}$, respectively.

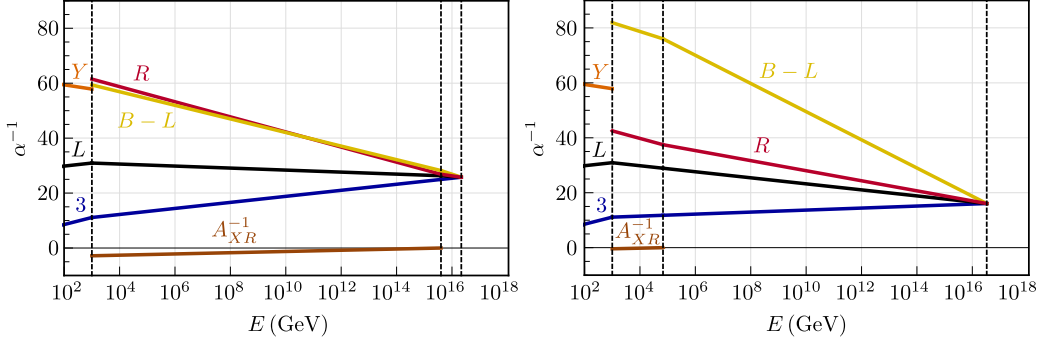


Figure 21: Gauge coupling unification in models with an $U(1)_R \times U(1)_{B-L}$ intermediate scale, for $m_R = 10^3$ GeV. Left: $(\Delta b_3^{LR}, \Delta b_L^{LR}, \Delta b_R^{LR}, \Delta b_{B-L}^{LR}, \Delta b_3^{B-L}, \Delta b_L^{B-L}, \Delta \gamma_{RR}, \Delta \gamma_{XR}, \Delta \gamma_{XX}) = (0, 1, 3, 3, 0, 0, 1/2, -\sqrt{3}/8, 3/4)$; Right: $(2, 2, 4, 8, 2, 2, 1/2, -\sqrt{3}/8, 11/4)$. The brown line, which appears close to zero in the $U(1)_R \times U(1)_{B-L}$ regime, is the running of the off-diagonal element of the matrix A^{-1} , measuring the size of the $U(1)$ -mixing in the model. The running of the diagonal components (1, 1) and (2, 2) of this matrix in the $U(1)_R \times U(1)_{B-L}$ regime are given by the red and yellow lines, respectively.

For models in this class, the sliding condition requires that the unification scale is independent of m_{B-L} , and this happens only if

$$0 = \begin{pmatrix} \Delta b_3^{B-L} - \Delta b_2^{B-L} \\ \mathbf{p}_Y^T \cdot \Delta \gamma \cdot \mathbf{p}_Y - \Delta b_2^{B-L} \end{pmatrix}^T \cdot \begin{pmatrix} 0 & 1 \\ -1 & 0 \end{pmatrix} \cdot \begin{pmatrix} \Delta b_3^{LR} - \Delta b_2^{LR} \\ \frac{3}{5} \Delta b_R^{LR} + \frac{2}{5} \Delta b_{B-L}^{LR} - \Delta b_2^{LR} - \frac{18}{5} \end{pmatrix}. \quad (7.25)$$

Similarly to PS models, in this class of models the higher intermediate scale (m_R) depends in general on the lower one (m_{B-L}). However, there is also a special condition in the present case which makes both m_R and m_G simultaneously independent of m_{B-L} :

$$\Delta b_3^{LR} = \Delta b_2^{LR} = \mathbf{p}_Y^T \cdot \Delta \gamma \cdot \mathbf{p}_Y. \quad (7.26)$$

Models of this kind are, for example, those with $\Delta b_3 = 0$ and large m_R ($\gtrsim 10^{13}$ GeV). One such case is given in [467], where $m_R \approx 4 \times 10^{15}$ GeV.

7.3 INVARIANTS

7.3.1 Leading-Log RGE Invariants

In this subsection we briefly recall the basic definitions [467] for the calculation of the *invariants* [333, 350, 481]. In mSUGRA, since gaugino masses scale with the square of the gauge couplings, the requirement of GCU fixes the gaugino masses at the low scale:

$$M_i(m_{SUSY}) = \frac{\alpha_i(m_{SUSY})}{\alpha_G} M_{1/2}. \quad (7.27)$$

Neglecting the Yukawa and soft trilinear couplings for the soft mass parameters of the first two sfermions generations, one can write

$$m_f^2 - m_0^2 = \frac{M_{1/2}^2}{2\pi\alpha_G^2} \sum_{R_j} \sum_{i=1}^N c_i^{f,R_j} \alpha_{i-}^{R_j} \alpha_{i+}^{R_j} (\alpha_{i-}^{R_j} + \alpha_{i+}^{R_j}) \log \frac{m_+^{R_j}}{m_-^{R_j}}. \quad (7.28)$$

	MSSM			LR			PS			
	c_Y	c_L	c_3	c_{B-L}	c_R	c_L	c_3	c_R	c_L	c_4
\tilde{Q}	$\frac{1}{30}$	$\frac{3}{2}$	$\frac{8}{3}$	$\frac{1}{12}$	0	$\frac{3}{2}$	$\frac{8}{3}$	0	$\frac{3}{2}$	$\frac{15}{4}$
\tilde{U}	$\frac{8}{15}$	0	$\frac{8}{3}$	$\frac{1}{12}$	$\frac{3}{2}$	0	$\frac{8}{3}$	$\frac{3}{2}$	0	$\frac{15}{4}$
\tilde{D}	$\frac{2}{15}$	0	$\frac{8}{3}$	$\frac{1}{12}$	$\frac{3}{2}$	0	$\frac{8}{3}$	$\frac{3}{2}$	0	$\frac{15}{4}$
\tilde{L}	$\frac{3}{10}$	$\frac{3}{2}$	0	$\frac{3}{4}$	0	$\frac{3}{2}$	0	0	$\frac{3}{2}$	$\frac{15}{4}$
\tilde{E}	$\frac{6}{5}$	0	0	$\frac{3}{4}$	$\frac{3}{2}$	0	0	$\frac{3}{2}$	0	$\frac{15}{4}$

Table 15: Values of the c_i^{f,R_j} coefficients entering equation (7.28), for $R_j =$ MSSM, LR, PS and $f = \tilde{E}, \tilde{L}, \tilde{D}, \tilde{U}, \tilde{Q}$. Values for the $U(1)_R \times U(1)_{B-L}$ regime are not shown, since equation (7.29) should be used instead.

Here, the sum over R_j runs over the different regimes in the models under consideration, while the sum over i runs over all gauge groups in a given regime; $m_+^{R_j}$ and $m_-^{R_j}$ are the upper and lower boundaries of the R_j regime and $\alpha_{i+}^{R_j}, \alpha_{i-}^{R_j}$ are the values of the gauge coupling of group i , α_i , at these scales. As for the coefficients c_i , they are twice the quadratic Casimir of the field representations under each gauge group i —see table (15). As discussed in chapter 6, in the presence of multiple $U(1)$ gauge groups the RGEs are different, and this leads to a generalization of equation (7.28) for the $U(1)$ -mixing phase [467]. Here we just quote the final result (with a minor correction to the one shown in this last reference), ignoring the non- $U(1)$ groups:

$$m_{f-}^2 - m_{f+}^2 = \frac{M_{1/2}^2}{\pi\alpha_G^2} \mathbf{Q}_f^T \mathbf{A}_- (\mathbf{A}_- + \mathbf{A}_+) \mathbf{A}_+ \mathbf{Q}_f \log \frac{m_+}{m_-}, \quad (7.29)$$

where m_+ and m_- are the boundary scales of the $U(1)$ -mixing regime, and \mathbf{A}_+ , \mathbf{A}_- are the \mathbf{A} matrix which generalizes α , evaluated in these two limits. Likewise, $\tilde{m}_{\tilde{f}_+}^2$ and $\tilde{m}_{\tilde{f}_-}^2$ are the values of the soft mass parameter of the sfermion \tilde{f} at these two energy scales. The equation above is a good approximation to the result obtained by integration of the following 1-loop RGE for the soft masses, which assumes unification of gaugino masses and gauge coupling constants:

$$\frac{d}{dt}m_{\tilde{f}}^2 = -\frac{4M_{1/2}^2}{\alpha_G^2}\mathbf{Q}_{\tilde{f}}^T\mathbf{A}^3\mathbf{Q}_{\tilde{f}}, \quad (7.30)$$

where $t = \log(E/E_0)/2\pi$. Note that in the limit where the $U(1)$ -mixing phase extends all the way up to m_G , the \mathbf{A} matrices measured at different energy scales will always commute amongst themselves, and therefore equation (7.29) presented here matches the one in [467] since both are exact integrations of (7.30). However, if this is not the case, it is expected that there will be a small discrepancy between the two approximations, which is nevertheless numerically small and therefore negligible.

From the five soft sfermion mass parameters of the MSSM and one of the gaugino masses, it is possible to form four different combinations that, at 1-loop level in the leading-log approximation, do not depend on the values of m_0 and $M_{1/2}$, and are therefore called invariants:

$$LE \equiv \frac{m_L^2 - m_E^2}{M_1^2}, \quad QE \equiv \frac{m_Q^2 - m_E^2}{M_1^2}, \quad (7.31)$$

$$DL \equiv \frac{m_D^2 - m_L^2}{M_1^2}, \quad QU \equiv \frac{m_Q^2 - m_U^2}{M_1^2}. \quad (7.32)$$

These are 4 numbers which carry information on the particle content and the gauge group of intermediate stages between the low energy MSSM and full unification, as shown by equations (7.28) and (7.29). We will not discuss in detail errors in the calculation of these quantities, referring instead to [467], and for classical $SU(5)$ based SUSY seesaw models to [333, 481].

We close this section by asserting that some model variants which were presented in the previous section will not be testable by measurements involving invariants at the LHC. According to [488], the LHC at $\sqrt{s} = 14$ TeV will be able to explore SUSY masses up to $m_{\tilde{g}} \sim 3.2$ TeV (3.6 TeV) for $m_{\tilde{q}} \approx m_{\tilde{g}}$ and of $m_{\tilde{g}} \sim 1.8$ TeV (2.3 TeV) for $m_{\tilde{q}} \gg m_{\tilde{g}}$ with 300 fb^{-1} (3000 fb^{-1}). The LEP limit on the chargino, $m_{\chi^\pm} > 105$ GeV [105], translates into a lower bound for $M_{1/2}$, with the precise value depending on Δb . For the class-I models with $\Delta b = 5$, this leads to $M_{1/2} \gtrsim 1.06$ TeV. One can assume conservatively $m_0 = 0$ GeV and calculate from this lower bound on $M_{1/2}$ a lower limit on the expected squark masses in the different variants. All variants with squark masses above the expected reach of the LHC-14 will then not be testable via measurements of the invariants, and this means that all single scale models with $\Delta b = 5$, for example, will be untestable.

For completeness we mention that if we take the present LHC limit on the gluino, $m_{\tilde{g}} \gtrsim 1.1$ TeV [489], this will translate into a lower limit $M_{1/2} \gtrsim 4.31$ TeV for $\Delta b = 5$. We have also checked that models with $\Delta b = 4$ can still have squarks

with masses testable at LHC, even for the more recent LHC bound on the gluino mass (see figure (4)).

7.3.2 Classification of invariants

For a given model, the invariants defined in equations (7.31)–(7.32) differ from the mSUGRA values, and the deviations can be either positive or negative once new superfields (and/or gauge groups) are added to the MSSM. The mSUGRA limit is reached in our models when the intermediate scales are equal to m_G . However, it should be noted that, in general, when there are two intermediate scales, the smallest one (henceforth called m_-) cannot be pushed all the way up to the unification scale. Therefore, in those cases, the invariants measured at the highest possible m_- are slightly different from the mSUGRA invariants.

With this in mind, for each variant of our models, we considered whether the invariants for $\min m_- (=m_{SUSY})$ are larger or smaller than for $\max m_-$, which tends to be within one or two orders of magnitude of m_G . With four invariants there are a priori $2^4 = 16$ possibilities, and in table (16) each of them is assigned a number.

Set #	1	2	3	4	5	6	7	8	9	10	11	12	13	14	15	16
ΔLE	+	+	+	+	+	+	+	+	-	-	-	-	-	-	-	-
ΔQE	+	+	+	-	+	-	-	-	+	+	+	-	+	-	-	-
ΔDL	+	+	-	+	-	+	-	-	+	+	-	+	-	+	-	-
ΔQU	+	-	+	+	-	-	+	-	+	-	+	+	-	-	+	-
Class-I	✓	✓	✗	✗	✗	✗	✗	✗	✗	✓	✗	✗	✗	✓	✗	✗
Class-II	✓	✓	✓	✗	✗	✓	✓	✓	✗	✓	✗	✗	✗	✓	✗	✓
Class-III	✓	✓	✓	✗	✗	✓	✓	✓		✓		✗	✗	✓		

Table 16: The 16 different combinations of signs for 4 invariants. We assign a “+” if the corresponding invariant, when the lowest intermediate scale is set to m_{SUSY} , is larger than its value when this scale is maximized, and “-” otherwise. As discussed in the text, only 9 of the 16 different sign combinations can be realized in the class-I and class-II models (sets 1, 2, 3, 6, 7, 8, 10, 14 and 16). In fact, class-I models always fall on sets 1, 2, 10 and 14, and this can be proven with simple arguments (see text). On the other hand, there are class-II models will all 9 invariant sign combinations. Class-III models can conceivably achieve three more sign combinations (sets 9, 11, 15), but we did not find any such case in a non-exhaustive search (also, no models in set 16 were found).

However, it is easy to demonstrate that not all of the 16 sets can be realized in the three classes of models we consider. This can be understood as follows. If all sfermions have a common mass at the GUT scale (m_0), then one can show that

$$m_Q^2 - 2m_U^2 + m_D^2 - m_L^2 + m_E^2 = 0 \quad (7.33)$$

holds independent of the energy scale at which soft masses are evaluated. This relation is general, regardless of the combination of intermediate scales that we may consider. It is a straightforward consequence of the charge assignments of the Standard Model fermions and can be easily checked by calculating the Dynkin coefficients of the Q, U, D, L and E representation in the different regimes. To be precise, the combination (row 1) $- 2$ (row 2) $+ (row 3) - (row 4) + (row 5)$ of table (15) yields the null row.⁷ In terms of the invariants, this relation becomes

$$QE = DL + 2QU, \quad (7.34)$$

which means that only three of the four invariants are independent. From equation (7.34) it is clear that if ΔDL and ΔQU are both positive (negative), then ΔQE must be also positive (negative). This immediately excludes the sets 4, 5, 12 and 13.

Equation (7.33) is extremely general, in the sense that any unified model with a combination of stages $\{\text{MSSM}, \text{BL}, \text{LR}, \text{PS}\}$ will obey it.⁸ However, given a restricted set of these stages, one can calculate other relations among the Dynkin indices of the MSSM sfermions. In particular, if we ignore the $U(1)$ -mixing in the BL regime, and the MSSM as well, we get one additional relation:

$$QU = LE. \quad (7.35)$$

On one hand, the fact that this relation is broken by $U(1)$ -mixing does not appear to be very important here, since the effect is somewhat small (see figure (23) below); On the other hand, the MSSM also breaks the relation, but we can account for this since the field content of the MSSM is known. In particular, the correction to equation (7.35) is independent of the variant/ Δb 's under consideration:

$$QU = LE + f(m_R), \quad (7.36)$$

with

$$f(m_R) = \frac{2}{33} \left\{ \left[\frac{33}{10\pi} \alpha_1^{MSSM} \log \left(\frac{m_R}{m_{SUSY}} \right) - 1 \right]^{-2} - 1 \right\}. \quad (7.37)$$

Here, α_1^{MSSM} is the value of α_1 at m_{SUSY} . It is easy to see that $f(m_R)$ is always small (< 0.3), positive and that it vanishes when $m_R \rightarrow m_{SUSY}$. Note that m_R should be seen as the upper energy limit of validity of the MSSM as an effective field theory; for simplicity we assumed with this nomenclature that the stage to follow is a LR regime, but this needs not be the case: in the class-III models it is m_{B-L} .

Equation (7.36) can be used to eliminate three more cases from table (16). Since $f(m_R)$ is non-negative and an increasing function of m_R , it follows that one always

⁷ Models with a $U(1)_R \times U(1)_{B-L}$ stage also obey this relation: to prove this, we observe that if table (15) is extended to include 3 more columns, with q_R^2, q_X^2 and q_{Rq_X} of the different MSSM fields in this regime, we still have (row 1) $- 2$ (row 2) $+ (row 3) - (row 4) + (row 5) = 0$.

⁸ Even models with a $SU(5)$ gauge group follow it (assuming the usual representations assignment of Q, U, D, L and E).

has $\Delta QU \leq \Delta LE$, so it is not possible to have $\Delta LE = -$ and $\Delta QU = +$. This excludes three additional sets from table (16): 9, 11 and 15, leaving a total of 9 possible sets. This last statement might conceivably not apply to some models with $U(1)$ -mixing, but it should be noted that for this to happen the somewhat small mixing effect must break relation (7.36) with a term which decreases with m_R on its left side, such that $\Delta QU > \Delta LE$. In other words, the small $U(1)$ -mixing effect must dominate over the MSSM's effect which is encoded by the monotonic increasing function f , and QU , LE should be almost constant with variations of m_R . See figure (24) below for two examples where this clearly does not happen. For completeness, using some simplifications we can write down an approximate expression which corrects equation (7.36) with this $U(1)$ -mixing effect in class-III models:

$$QU \approx LE + f(m_{B-L}) - \frac{1}{\pi\sqrt{6}} \frac{\mathbf{A}_{RX}^{-1}(m_{B-L})}{\mathbf{A}_{RR}^{-1}(m_{LR}) \mathbf{A}_{XX}^{-1}(m_{LR})} \times \left[1 + 2 \frac{\mathbf{A}_{RR}^{-1}(m_{LR}) + \mathbf{A}_{XX}^{-1}(m_{LR})}{\mathbf{A}_{RR}^{-1}(m_{B-L}) + \mathbf{A}_{XX}^{-1}(m_{B-L})} \right] \log \left(\frac{m_R}{m_{B-L}} \right). \quad (7.38)$$

The expression $[\dots]$ can be taken to be ≈ 1 if the $U(1)$ gauge couplings at m_{B-L} are much weaker than at m_{LR} , and in that case we can see that the magnitude of the $U(1)$ -mixing effect on relation (7.35) is roughly proportional to $\mathbf{A}_{RX}^{-1}(m_{B-L}) \log \left(\frac{m_R}{m_{B-L}} \right) / \mathbf{A}_{RR}^{-1}(m_{LR}) \mathbf{A}_{XX}^{-1}(m_{LR})$: a large running region $[m_{B-L}, m_R]$, a large \mathbf{A}_{RX}^{-1} at m_{B-L} , as well as large coupling constants α_R and α_{B-L} at the matching scale m_{LR} will increase the effect.

Finally, in class-I models it is possible to eliminate four more sets, namely all of those with $\Delta DL < 0$. It is easy to see with the help of equation (7.28) that this is the case; in the LR case, the c_i^L are non-zero for $U(1)_{B-L}$ and $SU(2)_L$ with the values $3/4$ and $3/2$, respectively. Since their sum is smaller than c_3^D (and α_3 is larger than the other couplings), D must run faster than L in the LR-regime.

By this reasoning, set 6 seems to be possible in class-I, but is not realized in our complete scan. However, we found a few examples in class-II; see below. In fact, it is quite straightforward to understand why set 6 variants are rare: from equations (7.34) and (7.36) we know that $\Delta QE > \Delta DL + 2\Delta LE - 0.3$ and set 6 requires that $\Delta LE, \Delta DL > 0$ but with $\Delta QE < 0$. This is possible, but it requires that $0.1 \gtrsim \Delta LE, \Delta DL > 0$, which is difficult to achieve given that typically $|\Delta LE| \sim \mathcal{O}(10^0, 10^1)$. This should also remind us that this classification of the variants into sets can easily suffer changes if a more accurate calculation of the invariants is performed. We also note in passing that in the high-scale seesaw models of type-II [481] and seesaw type-III [333] with running only within the MSSM group, all invariants run towards larger values, in other words only set 1 is realized in these cases.

The above discussion serves only as a qualitative classification of the invariants which are realizable in the different classes of models. Much of the numerical information contained in these invariants is therefore ignored by it. To mitigate this issue, in the following we shall look at some particular variants in each class

of models, and see how the Δb 's and the intermediate scales affect the values of the invariants.

7.3.3 Invariants in class-I model

Figure (22) shows examples of the m_R dependence of the invariants corresponding to the four cases indicated in table (16): sets 1, 2, 10 and 14. Note that we have scaled down the invariants QE and DL for practical reasons. Note also the different scales in the different plots.

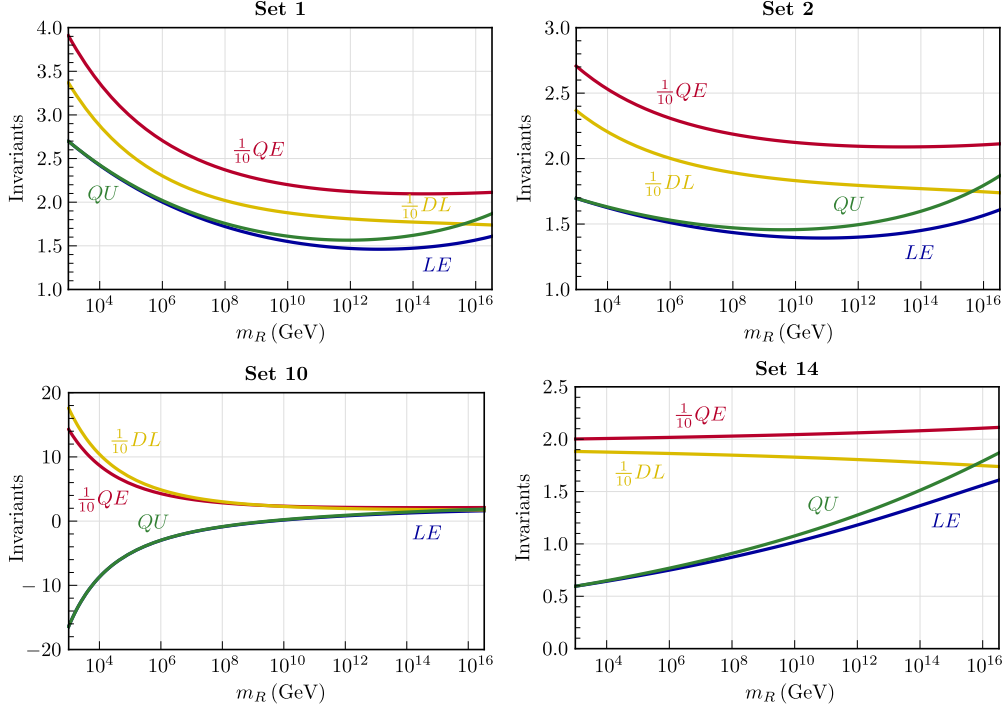


Figure 22: The m_R dependence of the invariants in class-I models. The values $\Delta b_i^{LR} = (\Delta b_3^{LR}, b_L^{LR}, \Delta b_R^{LR}, \Delta b_{BL}^{LR})$ are as follows: $(2, 2, 9, 1/2)$ in the set 1 plot, $(1, 1, 7, 1)$ in the set 2 plot, $(4, 4, 3, 29/2)$ in the set 10 plot, and $(0, 0, 2, 6)$ in the set 14 plot. For a discussion, see the main text.

In all cases $QU \approx LE$ if the LR regime extends to very low energies. As explained above, this is a general feature of this class of models: the separation between the QU and LE is model independent and thus, experimentally a non-zero measurement of $QU - LE$ allows, in principle, to determine the scale at which the LR symmetry is broken.

Sets 1 and 2 show a quite similar overall behavior in these examples. Set 1, however, can also be found in variants of class-I with larger β -coefficients, which induce larger quantitative changes with respect to the mSUGRA values. Note that while it is possible to find variants within class-I which fall into set 2, due to the similarity between QU and LE this set can be realized only if both QU and LE are numerically very close to their mSUGRA values. Graphically, this means that the left endpoint of the LE curve must be higher than its right endpoint and, at the

same time, the opposite must happen to the QU line. Similarly, since usually QU in equation (7.34) is significantly smaller than both QE and DL , set 14 typically implies that ΔQE and ΔDL , which necessarily have opposite signs, must be small. Therefore in set 14 QE and DL are close to their mSUGRA values.

In general, when Δb_3^{LR} is large the invariants vary strongly with the intermediate scale, as can be seen in the plot shown for set 10 (figure (22)). The large change is mainly due to the rapid running of the gaugino masses in these variants, but also the sfermion spectrum is very “deformed” with respect to mSUGRA expectations. For example, a negative LE means of course that left sleptons are lighter than right sleptons, a feature that can never be found in the “pure” mSUGRA model. Recall that for solutions with $\Delta b_3^{LR} = 5$, the value of the squark masses lies beyond the reach of the LHC.

7.3.4 Model class-II

Figure (23) shows the invariants of class-II models, corresponding to those cases which are not covered by class-I models.

The example shown in figure (23) for set 3 is similar to the one of the original prototype model constructed in [467]. For set 6 we have found only a few examples, all of them showing invariants which hardly change with respect to the mSUGRA values, as expected. The example for set 7 shows that in some variants QE can also decrease considerably with respect to its mSUGRA value. Set 8 is quantitatively similar to set 2, and set 16 is numerically similar to set 14. To distinguish these, highly accurate SUSY mass measurements would be necessary.

Again we note that larger values of Δb^{LR} , especially large Δb_3^{LR} , usually lead to numerically larger changes in the invariants, making these models in principle easier to test.

7.3.5 Model class-III

Here, the invariants depend on m_{B-L} , mildly or strongly depending on the value of $\Delta b_3^{B-L, LR}$. For almost all the solutions with $\Delta b_3^{B-L, LR} = 0$, the values of QU , DL , QE are constant and only LE shows a mild variation with m_{B-L} . This was already pointed out in [467]. However, we have found that class-III models can be made with $\Delta b_3^{B-L, LR} > 0$ and, in general, these lead to invariants which are qualitatively similar to the case of class-I discussed above. In figure (24) we show two examples of invariants for class-III, one with $\Delta b_3^{B-L, LR} = 0$ and one with $\Delta b_3^{B-L, LR} = 2$.

7.3.6 Comparison of classes of models

The classification of the variants that we have discussed in subsection 7.3.2 only takes into account what happens when the lowest intermediate scale is very low, $\mathcal{O}(m_{SUSY})$. When one varies continuously the lowest intermediate scale (m_R in class-I and class-II models, or m_{B-L} in class-III models), each variant draws a

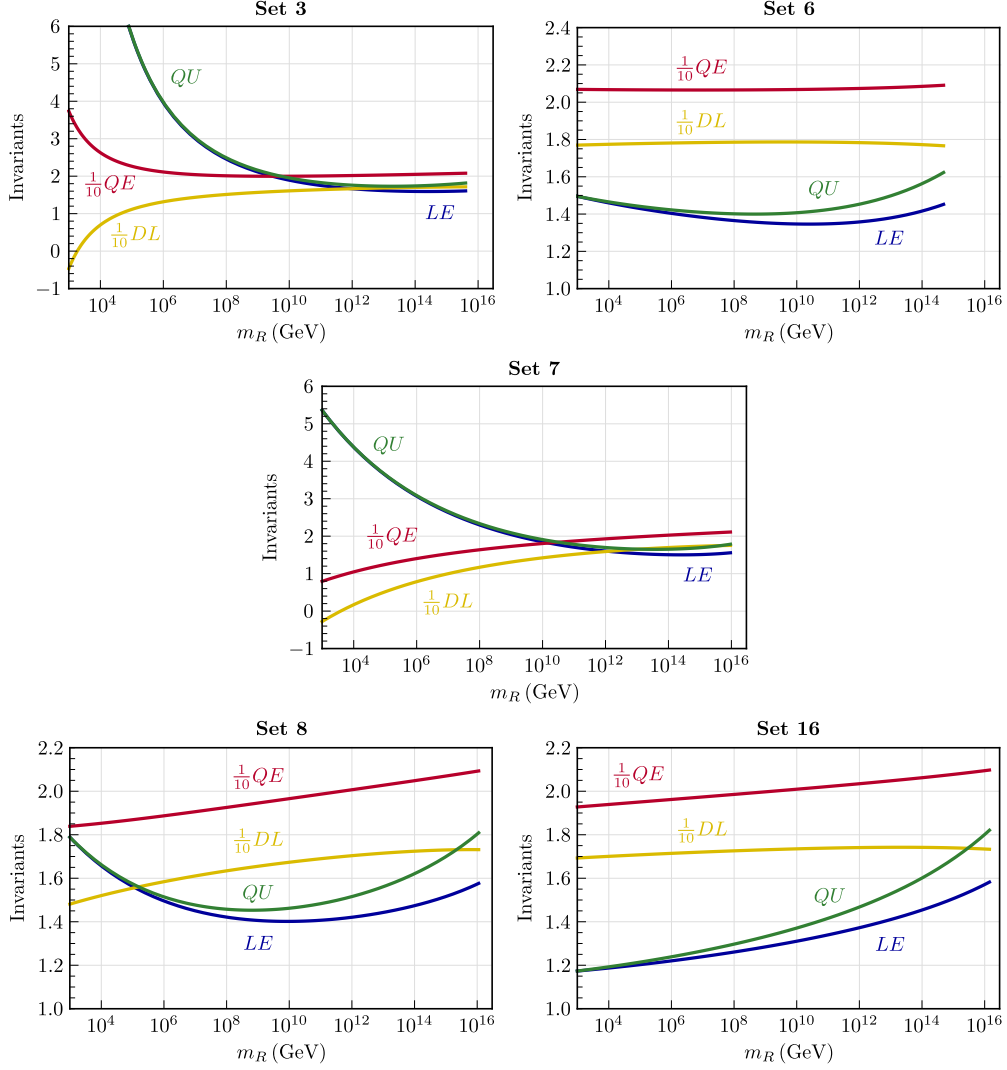


Figure 23: The m_R dependence of the invariants in class-II model. The examples shown correspond to the following $\Delta b = (\Delta b_3^{LR}, \Delta b_L^{LR}, \Delta b_R^{LR}, \Delta b_{BL}^{LR}, \Delta b_4^{PS}, \Delta b_L^{PS}, \Delta b_R^{PS})$: (0, 1, 10, $3/2$, 14, 9, 13) in the set 3 plot, (0, 0, 1, $9/2$, 63, 60, 114) in the set 6 plot, (0, 3, 12, $3/2$, 6, 3, 15) in the set 7 plot, (0, 0, 9, $3/2$, 11, 8, 12) in the set 8 plot, and (0, 0, 7, $3/2$, 11, 8, 10) in the set 16 plot.

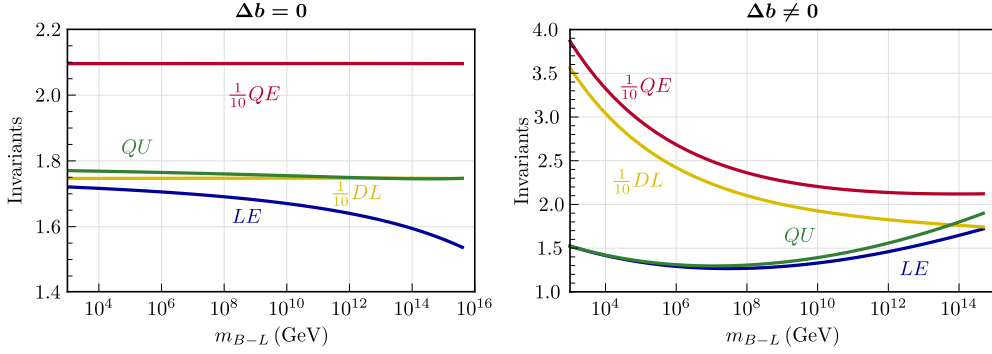


Figure 24: The m_{B-L} dependence of the invariants in two class-III models. The examples shown correspond to the following $(\Delta b_3^{LR}, \Delta b_L^{LR}, \Delta b_R^{LR}, \Delta b_{BL}^{LR}, \Delta b_3^{B-L}, \Delta b_L^{B-L}, \Delta\gamma_{RR}, \Delta\gamma_{XR}, \Delta\gamma_{XX})$: $(0, 1, 3, 3, 0, 0, 1/2, -\sqrt{3}/8, 3/4)$ in the left plot, and $(2, 2, 4, 8, 2, 2, 1/2, -\sqrt{3}/8, 11/4)$ in the one on the right. By comparing the endpoints of the QU and LE lines we can measure the relative effects of the MSSM and $U(1)$ -mixing in breaking the relation $QU = LE$; with m_{B-L} at its highest, the models are identical to the MSSM almost up to the unification scale, so the splitting of the lines QU and LE on the right of each plot measures the MSSM effect at its maximum. Analogously, the splitting of the lines QU and LE on the left of each plot measures the $U(1)$ -mixing breaking of the relation $QU = LE$ at its maximum, without the MSSM's contribution. Clearly, in these two examples the MSSM effect is bigger.

line in the 4-dimensional space (LE, QU, DL, QE) . The dimensionality of such a plot can be lowered if we use the (approximate) relations between the invariants shown above, namely $QU \approx LE$ and $QE = DL + 2QU$. We can then choose two independent ones, for example LE and QE , so that the only non-trivial information between the 4 invariants is encoded in a (LE, QE) plot. In this way, it is possible to simultaneously display the predictions of different variants. This was done in figure (25), where LR-, PS- and BL-variants are drawn together. The plot is exhaustive in the sense that it includes all LR-variants, as well as all PS- and BL-variants which can have the highest intermediate scale below 10^6 GeV. In all cases, we required that at unification α^{-1} is larger than $1/2$ when the lowest intermediate scale is equal to m_{SUSY} .

There is a dot in the middle of the figure—the mSUGRA point—which corresponds to the prediction of mSUGRA models, in the approximation used. It is expected that every model will draw a line with one end close to this point. This end-point corresponds to the limit where the intermediate scales are close to the GUT scale and therefore the running in the LR, PS and BL phases is small, so the invariants should be similar to those in mSUGRA models. The general picture is that lines tend to start (when the lowest intermediate scale is of the order of 10^3 GeV) outside or at the periphery of the plot, away from the mSUGRA point and, as the intermediate scales increase, they converge towards the region of the mSUGRA point, in the middle of the plot. In fact, note that all the blue lines of LR-class models do touch this point, because we can slide the LR scale all the way to m_G , as mentioned before. But in PS- and BL- models there are two intermediate scales and often the lowest one cannot be increased all the way up to m_G

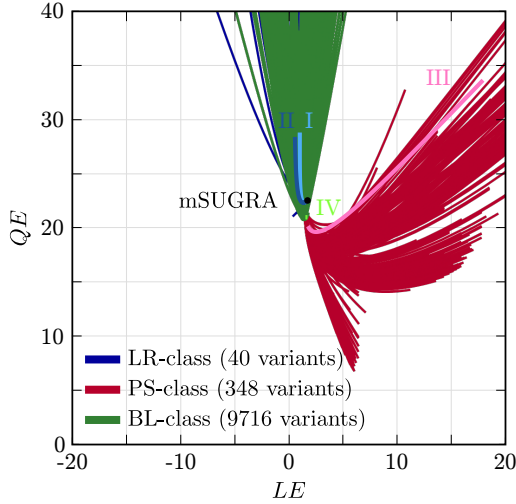


Figure 25: Parametric (LE, QE) plot for the different variants (see text). The thicker lines labeled with I, II, III and IV indicate the result for the four prototype models presented in [467].

(either because that would make the highest intermediate scale bigger than m_G or because it would invert the natural ordering of the two intermediate scales).

It is interesting to note that the BL-class with low m_R can produce the same imprint in the sparticle masses as LR-models. This is to be expected because with m_R close to m_{B-L} , the running in the $U(1)$ -mixing phase is small, leading to predictions similar to LR-models. The equivalent limit for PS-class models is reached for very high m_{PS} , close to the GUT scale (see below). On the other hand, from figure (25) we can see that a low m_{PS} actually leads to a very different signal on the soft sparticle masses. For example, a measurement of $LE \approx 10$ and $QE \approx 15$, together with compatible values for the other two invariants ($QU \approx 10$ and $DL \approx -5$) would immediately exclude all classes of models except PS-models, and in addition it would strongly suggest low PS and LR scales.

Figure (26) illustrates the general behavior of PS-models as we increase the separation between the m_{LR} and m_{PS} scales. The red region in the (LE, QE) plot tends to rotate anti-clockwise until it reaches, for very high m_{PS} , the same region of points which is predicted by LR-models. Curiously, we also see in figure (26) that some of these models actually predict different invariant values from the ones of LR models. What happens in these cases is that since the PS phase is very short, it is possible to have many active fields in it which decouple at lower energies. As such, even though the running is short, the values of the different gauge couplings actually get very large corrections in this regime, and these are uncommon in other settings. For example, in this special subclass of PS-models it is possible for α_R to get bigger than α_3/α_4 before unification! One can see from figure (26) that many (although not all) PS-models can lead to large values of LE . This can happen for both low and high values of m_{PS} , and is a rather particular feature of class-II which is not found for the other ones.

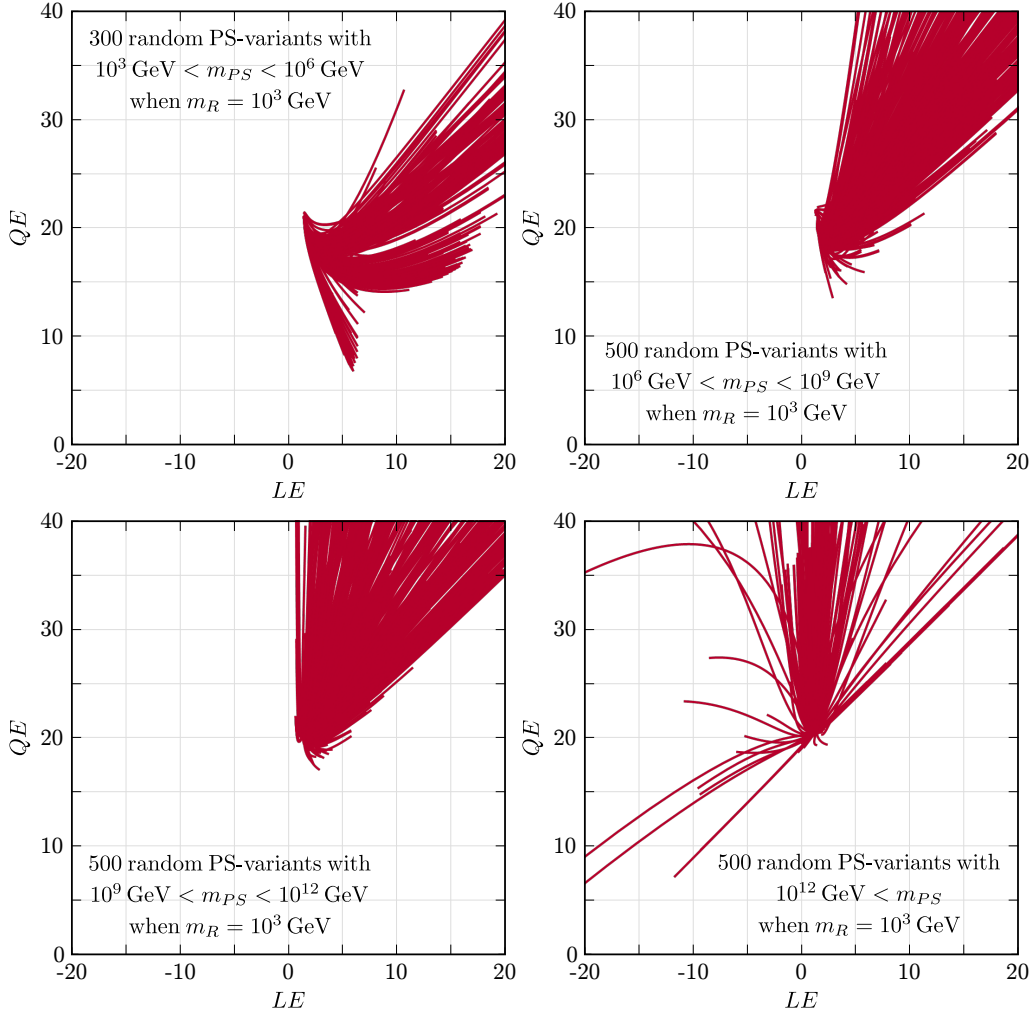


Figure 26: Parametric (LE, QE) plots for different PS-variants showing the effect of the PS scale.

7.4 SUMMARY

In this chapter, we have discussed $SO(10)$ inspired supersymmetric models with an extended gauge group near the electroweak scale, consistent with gauge coupling unification due to a sliding scale mechanism. We have discussed three different setups, which we call classes of models. The first and simplest chain breaks $SO(10)$ through a left-right symmetric stage to the SM group, class-II uses an additional intermediate Pati-Salam stage, while in class-III we discuss models which break the LR-symmetric group first into a $U(1)_R \times U(1)_{B-L}$ group before reaching the SM group. We have shown that in each case many different variants and many configurations (or *proto-models*) for each variant can be constructed.

We have discussed that one can construct sliding models in which an inverse or linear seesaw is consistent with GCU, as done in earlier works [271, 467, 480], as well as all other known types of seesaws, in principle. We found configurations for

type-I, type-II, type-III seesaw, and even inverse type-III (for which one example limited to class-II was previously discussed in [467]).

Due to the sliding scale property, the different configurations predict potentially rich and distinctive phenomenology at the LHC, although by the same reasoning the discovery of any of the additional particles predicted by the models is not guaranteed. However, even if all the new particles, including the gauge bosons of the extended gauge group, lie outside the reach of the LHC, indirect tests of the models are possible from measurements of SUSY particle masses and couplings. We have discussed certain combinations of soft parameters, called *invariants*, and shown that they could be used to gain indirect information not only on the class of model and its variant realized in Nature, but also give hints on the scale of beyond-MSSM physics, which is the energy scale at which the extended gauge group is broken.

We add a few words of caution however. First of all, our analysis is done completely at the one loop level. It is known from numerical calculations for seesaw type-II [481] and seesaw type-III [333] that numerically the invariants receive important shifts at the two loop level. In addition, there are also uncertainties in the calculation from GUT-scale thresholds and from uncertainties in the input parameters. For the latter, the most important is most likely the error on α_3 [467]. With the huge number of models we have considered, taking into account all of these effects is impractical and, thus, our numerical results should be considered as approximate. However, should any signs of supersymmetry be found in the future, improvements in the calculations along these lines could be easily made, it necessary. More important for the calculation of the invariants is, of course, the assumption that SUSY breaking is indeed mSUGRA-like. Tests of the validity of this assumption can be made also only indirectly. Many of the spectra we find, especially in class-II models, are actually quite different from standard mSUGRA expectations and thus pure mSUGRA would give a bad fit to experimental data, if one of these models is realized in nature. Also, it is important to keep in mind that by construction our models obey a certain sliding condition (see the discussion in subsection 7.3.2), which means that in principle it is possible that there are other models that do not satisfy this condition, and yet exhibit the other interesting features such as low intermediate $B - L$ or LR scales.

So far no signs of supersymmetry have been seen at the LHC, but with the planned increase of \sqrt{s} for the next run of the accelerator there is still quite a lot of parameter space to be explored. We note in this respect that a heavy Higgs with a mass of $m_h \sim (125 - 126)$ GeV, as suggested by the new resonance found by the ATLAS [27] and CMS [28] collaborations,⁹ does not necessarily imply a heavy sparticle spectra for the models studied here. While for a pure MSSM with mSUGRA boundary conditions it is well-known [157, 160, 165, 492] that such a hefty Higgs requires multi-TeV scalars,¹⁰ all our models have an extended gauge symmetry which means that new D -terms contribute to the Higgs mass [493, 494],

⁹ See also the ATLAS [490] and CMS [491] collaborations' websites for more up-to-date results and analysis.

¹⁰ Multi-TeV scalars are also required if the MSSM with mSUGRA boundary conditions is extended to include a high-scale seesaw mechanism [167].

alleviating the need for large soft SUSY breaking terms, as has been explicitly shown in [495, 496] for one particular realization of a class-III model [271, 467].

Finally, many of the configurations (or *proto-models*) which we have discussed here contain exotic superfields, which might show up in the LHC. Therefore it might be interesting to do a more detailed study of the phenomenology of at least some of the models that were constructed in this chapter.

THE $\Gamma(K \rightarrow e\nu)/\Gamma(K \rightarrow \mu\nu)$ RATIO IN SUPERSYMMETRIC UNIFIED MODELS

8.1 THE R_K RATIO, LEPTON FLAVOR UNIVERSALITY, AND LEPTON FLAVOR VIOLATION

In chapter 3 it was mentioned that LFV has only been observed in the neutral sector, through neutrino oscillation experiments. In the charged sector there is no evidence yet that lepton flavor is violated and, from a theoretical point of view, even the minimally extended Standard Model with massive neutrinos does not predict it to happen at experimentally detectable rates. Even so, there is an ongoing effort by different collaborations to look at such effects in different observables, because in many extensions of the SM, in particular supersymmetric ones, the flavor of charged leptons is violated in some processes at rates which are within reach of present or near future experiments.

In this chapter, following closely reference [4], we will look at the ratio

$$R_K \equiv \frac{\Gamma(K^+ \rightarrow e^+\nu[\gamma])}{\Gamma(K^+ \rightarrow \mu^+\nu[\gamma])}, \quad (8.1)$$

and see how it relates to cLFV in supersymmetric models, both constrained and unconstrained, even though we will be particularly interested in unified models. The B meson decay observables $\text{BR}(B_u \rightarrow \tau\nu)$ and $\text{BR}(B_s \rightarrow \mu\mu)$, as well as $\text{BR}(\tau \rightarrow e\gamma)$, depend on some of the supersymmetric parameters in the same way as R_K and therefore we will take them into consideration in our analysis. On the other hand, as we shall see later on, a lightest Higgs with a mass 125 – 126 GeV does not affect things considerably, even though, as pointed out previously in this thesis, it does point to a heavy SUSY spectrum.

In the SM, at tree level a charged meson P^\pm decays into leptons through the exchange of a W boson (figure (27)), and the decay width is given by

$$\Gamma^{\text{SM}}(P^\pm \rightarrow \ell^\pm\nu) = \frac{G_F^2 m_P m_\ell^2}{8\pi} \left(1 - \frac{m_\ell^2}{m_P^2}\right)^2 f_P^2 |V_{qq'}|^2. \quad (8.2)$$

Here P can be a π , K , D or a B meson, with mass m_P and decay constant f_P , and G_F is the Fermi constant, m_ℓ the lepton mass and $V_{qq'}$ the corresponding Cabibbo-Kobayashi-Maskawa matrix element. This decay width is approximately proportional to the square of the charged lepton's mass, which makes $R_K \sim m_e^2/m_\mu^2$ very small, even though the phase space in $K^+ \rightarrow e^+\nu$ is bigger than in $K^+ \rightarrow \mu^+\nu$. The reason for this is well known: this type of decay, mediated by weak interactions, is helicity suppressed. This means the following: in its rest frame the spin 0 meson decays into an almost massless neutrino with left helicity and consequently a charged anti-lepton with left helicity as well. However, this last

particle is only allowed to have right chirality by the $W_\mu^+ \bar{\nu} P_L \gamma^\mu \ell$ interaction, so in the limit where $m_\ell \rightarrow 0$ the amplitude of the process vanishes.

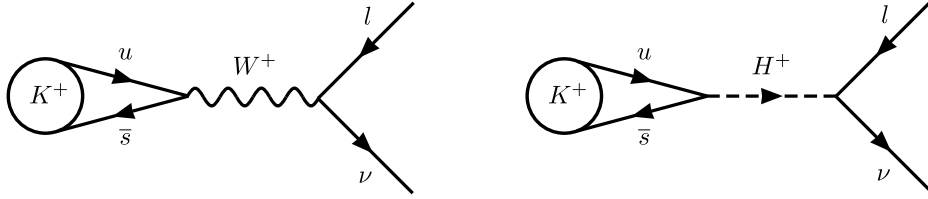


Figure 27: Tree level contributions to R_K —through the W boson, and through a charged Higgs.

As is usually the case, amplitudes of processes involving bound states of quarks are hampered by hadronic uncertainties in the meson decay constants. That is the reason why often it is better to work with ratios, such as R_K in equation (8.1), as they are independent of f_P to a very good approximation, and the SM prediction can then be computed very precisely. Once corrections beyond tree level are taken into consideration, the SM prediction (inclusive of internal bremsstrahlung radiation) can be expressed as [497]

$$R_K^{\text{SM}} = \left(\frac{m_e}{m_\mu} \right)^2 \left(\frac{m_K^2 - m_e^2}{m_K^2 - m_\mu^2} \right)^2 (1 + \delta R_{\text{QED}}), \quad (8.3)$$

where $\delta R_{\text{QED}} = (-3.60 \pm 0.04)\%$ is a small electromagnetic correction accounting for internal bremsstrahlung and structure-dependent effects. Note that a factor g_e^2/g_μ^2 is implicit in this expression, but since we assume that weak interactions couple with the same strength to all lepton flavors ($g_e = g_\mu$), such an expression is not needed. In any case, it is worth remembering that this observable also tests the universality of the weak interaction.

The most recent analysis has provided the following value [497]:

$$R_K^{\text{SM}} = (2.477 \pm 0.001) \times 10^{-5}. \quad (8.4)$$

On the experimental side, the NA62 collaboration has obtained stringent bounds [498]:

$$R_K^{\text{exp}} = (2.488 \pm 0.010) \times 10^{-5}, \quad (8.5)$$

which should be compared with the SM prediction (equation (8.4)). In order to do so, it is often useful to introduce the following parametrization,

$$R_K^{\text{exp}} = R_K^{\text{SM}} (1 + \Delta r), \quad \Delta r \equiv R_K/R_K^{\text{SM}} - 1, \quad (8.6)$$

where Δr is a quantity denoting potential contributions arising from scenarios of new physics. Comparing the theoretical SM prediction to the current bounds (equations (8.4) and (8.5)), one verifies that observation is compatible with the SM at 1σ :

$$\Delta r = (4 \pm 4) \times 10^{-3}. \quad (8.7)$$

Previous analyzes have investigated supersymmetric contributions to R_K in different frameworks, as for instance low-energy SUSY extensions of the SM (i.e., the unconstrained Minimal Supersymmetric Standard Model (MSSM)) [499–501], or non-minimal grand unified models (where higher dimensional terms contribute to fermion masses) [502]. These studies have also considered the interplay of R_K with other important low-energy flavor observables, magnetic and electric lepton moments and potential implications for leptonic CP violation. Distinct computations, based on an approximate parametrization of flavor violating effects—the mass insertion approximation (MIA) [307]—allowed to establish that SUSY LFV contributions can induce large contributions to the breaking of lepton universality, as parametrized by Δr . The dominant FV contributions are in general associated to charged-Higgs mediated processes, being enhanced due to non-holomorphic effects—the so-called “HRS” mechanism [503]—and require flavor violation in the RR block of the charged slepton mass matrix. It is important to notice that these Higgs contributions have been known to have an impact on numerous observables, and can become especially relevant for the large $\tan\beta$ regime [322, 503–513]. Also, it has recently been pointed out [514] that the modified $W\ell\nu$ vertex generated in models with sterile neutrinos can produce a large, measurable change in R_K .

In the following section, we will therefore explore supersymmetric contributions to Δr , and in particular we shall review the connection between this observable and charged lepton flavor violation.

8.2 R_K IN SUPERSYMMETRIC MODELS

In type-II two Higgs doublet models, such as the MSSM, the extended Higgs sector can play an important role in lepton flavor violating transitions and decays (see [322, 503–513]). The effects of the additional Higgs are also sizable in meson decays through a charged Higgs boson, as schematically depicted in figure (27). In particular, for kaons, one finds [504]

$$\Gamma(K^\pm \rightarrow \ell^\pm \nu) = \Gamma^{\text{SM}}(K^\pm \rightarrow \ell^\pm \nu) \left(1 - \tan^2 \beta \frac{m_K^2}{m_{H^+}^2} \frac{m_s}{m_s + m_u} \right)^2 ; \quad (8.8)$$

yet, despite this new tree-level contribution, R_K is unaffected as the extra factor does not depend on the (flavored) leptonic part of the process.

New contributions to R_K only emerge at higher order: at one-loop level, there are box and vertex contributions, wave function renormalization, which can be both lepton flavor conserving (LFC) and lepton flavor violating. Flavor conserving contributions arise from loop corrections to the W^\pm propagator, through heavy Higgs exchange (neutral or charged) as well as from chargino/neutralino-sleptons (in the latter case stemming from non-universal slepton masses, in other words, a selectron-smuon mass splitting). As concluded in [499], in the framework of SUSY models where lepton flavor is conserved, the new contributions to Δr^{SUSY} are too small to be within experimental reach.

On the other hand, Higgs mediated LFV processes are capable of providing an important contribution when the kaon decays into an electron plus a tau-neutrino.

For such LFV Higgs couplings to arise, the leptonic doublet (L) must couple to more than one Higgs doublet. However, at tree level in the MSSM, L can only couple to H_d , and therefore such LFV Higgs couplings arise only at loop level, due to the generation of an effective non-holomorphic coupling between L and H_u^* —the HRS mechanism [503]—which is a crucial ingredient in enhancing the Higgs contributions to LFV observables.

From an effective theory approach, the HRS mechanism can be accounted for by additional terms, corresponding to the higher-order corrections to the Higgs-neutrino-charged lepton interaction (schematically depicted in figure (28)). At tree-level, the Lagrangian describing the $\nu\ell H^\pm$ interaction is given by

$$\begin{aligned}\mathcal{L}_0^{H^\pm} &= \bar{\nu}_L Y^{\ell\dagger} \ell_R H_d^{-*} + \text{h.c.} \\ &= \left(2^{3/4} G_F^{1/2}\right) \tan\beta \bar{\nu}_L M^\ell \ell_R H^+ + \text{h.c.},\end{aligned}\quad (8.9)$$

with $M^\ell = \text{diag}(m_e, m_\mu, m_\tau)$. At loop level, two new terms are generated:

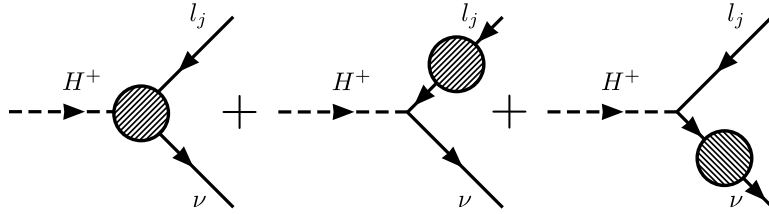


Figure 28: Corrections to the $\nu\ell H^+$ vertex, as discussed in the text.

$\bar{\nu}_L \Delta^+ \ell_R H_u^+ - \bar{\ell}_L \Delta^0 \ell_R H_d^0 + \text{h.c.}$. The second one, with Δ^0 , forces a redefinition of the charged lepton Yukawa couplings, $Y^{\ell\dagger} = M^\ell/v_d \rightarrow Y^{\ell\dagger} \approx M^\ell/v_d - \Delta^0 \tan\beta$, which in turn implies a redefinition of the charged lepton propagator; the term with Δ^+ corrects the Higgs-neutrino-charged lepton vertex¹. Once these terms are taken into account, the interaction Lagrangian in equation (8.9) becomes

$$\begin{aligned}\mathcal{L}^{H^\pm} &= \left(2^{3/4} G_F^{1/2}\right) \tan\beta \bar{\nu}_L M^\ell \ell_R H^+ \\ &\quad + \cos\beta \bar{\nu}_L \left(\Delta^+ - \Delta^0 \tan^2\beta\right) \ell_R H^+ + \text{h.c.}\end{aligned}\quad (8.10)$$

Since in the $SU(2)_L$ -preserving limit we have $\Delta^+ = \Delta^0$, it is reasonable to assume that, after electroweak (EW) symmetry breaking, both terms remain approximately of the same order of magnitude. Hence, it is clear that the contribution associated with Δ^0 (the loop contribution to the charged lepton mass term) will be enhanced by a factor of $\tan^2\beta$ when compared to the one associated with Δ^+ . This simple discussion elucidates the origin of the dominant SUSY contribution² to R_K .

¹ An extensive discussion on the radiatively induced couplings which are at the origin of the HRS effect can be found in [515].

² There are additional corrections to the $\bar{q}q'H^\pm$ vertex, which are mainly due to a similar modification of the the quark Yukawa couplings—especially that of the strange quarks. This amounts to a small multiplicative effect on Δr which we will not discuss here (see [501] for details).

To quantify the effect encoded in Δ^+ and Δ^0 , higher-order effects on the vertex $\bar{\nu}_L Z^H \ell_R H^+$ must be considered in a systematic way (see [516]). The Z^H matrix depends on the following loop-induced quantities:

- η_L^ℓ and η_L^ν (corrections to the kinetic terms of ℓ_L and ν_L);
- η_m^ℓ (correction to the charged lepton mass term);
- η^H (correction to the $\nu\ell H$ vertex).

The expressions for the distinct η -parameters can be found in appendix F. Instead of Z^H , which includes both tree and loop level effects, it is more convenient to use the following combination,

$$-\frac{\tan\beta}{2^{3/4}G_F^{1/2}}\left(\frac{m_K}{m_{H^+}}\right)^2\frac{m_s}{m_s+m_u}Z^H(M^\ell)^{-1}\equiv\epsilon\mathbf{1}+\Delta, \quad (8.11)$$

where

$$\epsilon=-\tan^2\beta\left(\frac{m_K}{m_{H^+}}\right)^2\frac{m_s}{m_s+m_u}, \quad (8.12)$$

$$\Delta=\epsilon\left[\frac{\eta_L^\ell}{2}-\frac{\eta_L^\nu}{2}+\left(\frac{\eta^H}{2^{3/4}G_F^{1/2}\tan\beta}-\eta_m^\ell\right)(M^\ell)^{-1}\right]. \quad (8.13)$$

In the above, ϵ encodes the tree level Higgs mediated amplitude (which does not change the SM prediction for R_K), while Δ , a matrix in lepton flavor space, encodes the 1-loop effects. From the simplified approach that led to equation (8.10), we expect that the main contribution comes from η_m^ℓ , which corrects the charged lepton mass term. This, however, is only true if the SUSY parameters are such that Δr is highly enhanced; if this is not the case, the remaining η 's should be taken into consideration, as we shall do in the numerical calculations shown in this chapter.

The Δr observable is then related to ϵ and Δ as follows:

$$\Delta r\equiv\frac{R_K}{R_K^{\text{SM}}}-1=\frac{\left[\left(\mathbf{1}+\frac{\Delta^\dagger}{1+\epsilon}\right)\left(\mathbf{1}+\frac{\Delta}{1+\epsilon}\right)\right]_{ee}}{\left[\left(\mathbf{1}+\frac{\Delta^\dagger}{1+\epsilon}\right)\left(\mathbf{1}+\frac{\Delta}{1+\epsilon}\right)\right]_{\mu\mu}}-1. \quad (8.14)$$

If the slepton mixing is sufficiently large, this expression can be approximated as

$$\Delta r\approx 2\text{Re}(\Delta_{ee})+\left(\Delta^\dagger\Delta\right)_{ee}. \quad (8.15)$$

In the above, the first (linear) term on the right hand-side is due to an interference with the SM process, and is thus lepton flavor conserving. As shown in [499], this contribution can be enhanced through both large RR and LL slepton mixing. On the other hand, the quadratic term $(\Delta^\dagger\Delta)_{ee}$ can be augmented mainly through a large LFV contribution from $\Delta_{\tau e}$, which can only be obtained in the presence of significant RR slepton mixing.

8.2.1 The LFV in the slepton mass matrices as the source of an enhanced Δr

In order to understand the dependence of Δr on the SUSY parameters, and the origin of the dominant contributions to this observable, an approximate expression for Δ is required. Firstly, we remind that the previous discussion leading to equation (8.10) suggests that the η_m^ℓ term is responsible for the dominant contributions to Δr . Thus, in what follows, and for the purpose of obtaining simple analytical expressions, we shall neglect the contributions of the other terms (although these are included in the numerical analysis of section 8.3). A fairly simple analytical insight can be obtained when working in the limit in which the virtual particles in the loops (sleptons and gauginos) are assumed to have similar masses, so that their relative mass splittings are small. In this limit, one can Taylor-expand the loop functions entering η_m^ℓ (see appendix F); working to third order in this expansion, and keeping only the terms enhanced by a factor of $m_\tau \tan \beta \frac{m_{SUSY}}{m_{EW}}$, we obtain

$$\Delta r \sim \left[1 + X \left(1 - \frac{9}{10} \frac{\delta}{\bar{m}_{\ell, \chi^0}^2} \right) (m_L^2)_{e\tau} \right]^2 - 1 + X^2 \left[-\mu^2 + \delta \left(3 - \frac{3}{10} \frac{\mu^2 + 2M_1^2}{\bar{m}_{\ell, \chi^0}^2} \right) \right]^2, \quad (8.16)$$

where μ , M_1 and $(m_L^2)_{e\tau}$ denote the low-energy values of the Higgs bilinear term, bino soft breaking mass, and off-diagonal entry of the soft breaking left-handed slepton mass matrix, respectively (see chapter 2). We have also introduced $\bar{m}_{\ell, \chi^0}^2 = \frac{1}{2} (\langle m_\ell^2 \rangle + \langle m_{\chi^0}^2 \rangle)$, the average mass squared of sleptons and neutralinos ($\approx m_{SUSY}^2$), and $\delta = \frac{1}{2} (\langle m_\ell^2 \rangle - \langle m_{\chi^0}^2 \rangle)$, the corresponding splitting. The quantity X is given by

$$X \equiv \frac{1}{192\pi^2} m_K^2 g'^2 \mu M_1 \frac{\tan^3 \beta}{m_{H^+}^2} \frac{m_\tau}{m_e} \frac{(m_e^2)_{\tau e}}{(\bar{m}_{\ell, \chi^0}^2)^3}, \quad (8.17)$$

and it illustrates in a transparent (albeit approximate) way the origin of the terms contributing to the enhancement of R_K : in addition to the factor $\tan^3 \beta / m_{H^+}^2$ usually associated with Higgs exchanges, the crucial flavor violating source emerges from the off-diagonal (τe) entry of the right-handed slepton soft breaking mass matrix.

Using the above analytical approximation, one easily recovers the results in the literature, usually obtained using the MIA. For instance, equation (11) of reference [499] amounts to

$$\Delta r \sim 2X (m_L^2)_{e\tau} + X^2 (m_L^2)_{e\tau}^2 + X^2 \delta^2, \quad (8.18)$$

which stems from having kept the dominant (crucial) second and third order contributions in the expansion: $X^2 \delta^2$ and $2X (m_L^2)_{e\tau} + X^2 (m_L^2)_{e\tau}^2$, respectively.

Regardless of the approximation considered, it is thus clear that the LFV effects on kaon decays into a $e\nu$ or $\mu\nu$ pair can be enhanced in the large $\tan \beta$ regime

(especially in the presence of low values of m_{H^+}), and via a large RR slepton mixing $\left(m_e^2\right)_{\tau e}$. Although the latter is indeed the privileged source, notice that, as can be seen from equation (8.18), a strong enhancement can be obtained from sizable flavor violating entries of the left-handed slepton soft breaking mass, $\left(m_L^2\right)_{e\tau}$. This is in fact a globally flavor conserving effect (which can also account for negative contributions to R_K). Previous experimental measurements of R_K appeared to favor values smaller than the SM theoretical estimation, thus motivating the study of regimes leading to negative values of Δr [499], but these regimes have now become disfavored in view of the present bounds in equation (8.7).

Clearly, these Higgs mediated exchanges, as well as the FV terms at the origin of the strong enhancement to R_K , will have an impact on a number of other low-energy observables, as can be easily inferred from the structure of equations (8.16)–(8.18). This has been extensively addressed in the literature [499–502], and here we will only briefly discuss the most relevant observables: electroweak precision data on the anomalous electric and magnetic moments of the electron, as well as the naturalness of the electron mass, directly constrain the η_m^ℓ corrections (and η_L^ℓ, η^H); low-energy cLFV observables, such as $\tau \rightarrow \ell\gamma$ and $\tau \rightarrow 3\ell$ decays are also extremely sensitive probes of Higgs mediated exchanges, and in the case of $\tau - e$ transitions, depend on the same flavor violating entries. It has been suggested that positive and negative values of Δr can be of the order of 1%, still in agreement with data on the electron’s electric dipole moment and on $\tau \rightarrow \ell\gamma$ [499, 500, 502]. Finally, other meson decays, such as $B \rightarrow \ell\ell$ (and $B \rightarrow \ell\nu$), exhibit a similar dependence on $\tan\beta$, $\tan^n\beta/m_{H^+}^4$ [517, 518] (n ranging from 2 to 6, depending on the other SUSY parameters), and may also lead to indirect bounds on Δr . In particular, the strict bounds on $\text{BR}(B_u \rightarrow \tau\nu)$ [519] and the recent measurement of $\text{BR}(B_s \rightarrow \mu\mu)$ [391] might severely constrain the allowed regions in SUSY parameter space for large $\tan\beta$. Although we will come to this issue in greater detail when discussing the numerical results, it is clear from the similar nature of the $K^+ \rightarrow \ell\nu$ and $B_u \rightarrow \tau\nu$ processes (easily inferred from a generalization of equation (8.8), see for example [504, 520]) that light charged Higgs masses, which saturate the bounds on R_K , lead to a tension.

Supersymmetric models of neutrino mass generation (such as the SUSY seesaw) naturally induce sizable cLFV contributions, via radiatively generated off-diagonal terms in the LL (and to a lesser extent LR) slepton soft breaking mass matrices [309]. In addition to explaining neutrino masses and mixing, such models can also easily account for values of $\text{BR}(\mu \rightarrow e\gamma)$, within the reach of the MEG experiment. In view of the recent confirmation of a large value for the Chooz angle ($\theta_{13} \sim 8.8^\circ$) [521–523] and on the impact it might have on $\left(m_L^2\right)_{e\tau}$, in the numerical analysis of the following section we will also consider different realizations of the SUSY seesaw (type-I [264–268], type-II [257–263], and inverse [270]), embedded in the framework of constrained SUSY models. We will also revisit semi-constrained scenarios allowing for light values of m_{H^+} , re-evaluating the predictions for R_K under a full, one loop-computation, and in view of recent experimental data. Finally, we confront these (semi-)constrained scenarios with general, low-energy realizations, of the MSSM.

8.3 PROSPECTS FOR R_K : UNIFIED VS UNCONSTRAINED SUSY MODELS

In this section we evaluate the SUSY contributions to R_K , with the results obtained via the full expressions for Δr , as described in section (8.2) [4]. These were implemented into the `SPheno` public code [524, 525], which was modified to allow the different studies. It is important to stress that even though some approximations were used (as previously discussed), the results of the present computation strongly improve upon those so far reported in the literature (mostly obtained using the MIA). Although the different contributions cannot be easily disentangled in a full computation, our results automatically include all one-loop lepton flavor violating and lepton flavor conserving contributions (in association with charged Higgs mediation, see footnote 2). As mentioned before, we evaluate R_K in the framework of constrained (the cMSSM), semi-constrained (the NUHM) and unconstrained SUSY models (the general MSSM)—see chapter 2 for details on these models. We will also consider the supersymmetrization of several mechanisms for neutrino mass generation. More specifically, we have considered the type-I and type-II SUSY seesaw (as detailed in chapter 3). We shall briefly comment on the inverse SUSY seesaw, and discuss a LR model.

In our numerical analysis, we took into account LHC bounds on the SUSY spectrum [526–549], as well as the constraints from low-energy flavor dedicated experiments [519], and neutrino data [550, 551]. In particular, concerning lepton flavor violation, we have considered [519, 552]:

$$\text{BR}(\tau \rightarrow e\gamma) < 3.3 \times 10^{-8} \quad (90\% \text{ C.L.}), \quad (8.19)$$

$$\text{BR}(\tau \rightarrow 3e) < 2.7 \times 10^{-8} \quad (90\% \text{ C.L.}), \quad (8.20)$$

$$\text{BR}(\mu \rightarrow e\gamma) < 2.4 \times 10^{-12} \quad (90\% \text{ C.L.}), \quad (8.21)$$

$$\text{BR}(B_u \rightarrow \tau\nu) > 9.7 \times 10^{-5} \quad (2\sigma). \quad (8.22)$$

Also relevant are the following B meson bounds from LHCb [553]

$$\text{BR}(B_s \rightarrow \mu\mu) < 4.5 \times 10^{-9} \quad (95\% \text{ C.L.}), \quad (8.23)$$

$$\text{BR}(B \rightarrow \mu\mu) < 1.03 \times 10^{-9} \quad (95\% \text{ C.L.}). \quad (8.24)$$

It is worth mentioning that, since this analysis was first performed, the LHCb [391] and the MEG collaborations [378] has released new results; in particular there is now evidence for the decay $B_s \rightarrow \mu\mu$ (see chapter 3).³ Nevertheless we find that this does have a significant impact in our findings.

³ The 1σ upper bound for $\text{BR}(B_s \rightarrow \mu\mu)$ obtained recently [391] is close to the value in equation (8.23).

When addressing models for neutrino mass generation, we take the following values for the neutrino mixing angles [551] (where θ_{13} is already in good agreement with the recent results from [521–523]),

$$\sin^2 \theta_{12} = 0.312_{-0.015}^{+0.017}, \quad \sin^2 \theta_{23} = 0.52_{-0.07}^{+0.06}, \quad \sin^2 \theta_{13} \approx 0.013_{-0.005}^{+0.007}, \quad (8.25)$$

$$\Delta m_{12}^2 = (7.59_{-0.18}^{+0.20}) \times 10^{-5} \text{ eV}^2, \quad \Delta m_{13}^2 = (2.50_{-0.16}^{+0.09}) \times 10^{-3} \text{ eV}^2, \quad (8.26)$$

$$(8.27)$$

and all CP violating phases are set to zero.⁴ See however chapter 3 for more up-to-date numbers [189, 190].

8.3.1 *mSUGRA inspired scenarios: cMSSM and the SUSY seesaw*

We begin by re-evaluating, through a full computation of the one-loop corrections, the maximal amount of supersymmetric contributions to R_K in constrained SUSY scenarios.

As could be expected from equations (8.16)–(8.18), in a strict cMSSM scenario (in agreement with the experimental bounds above referred to) the SUSY contributions to R_K are extremely small; motivated by the need to accommodate neutrino data, and at the same time accounting for values of $\text{BR}(\mu \rightarrow e\gamma)$ within MEG reach, we implement type-I and type-II seesaws in mSUGRA-inspired models. Regarding the heavy-scale mediators, we considered degenerate right-handed neutrinos, as well as degenerate scalar triplets. We set the seesaw scale aiming at maximizing the low-energy, non-diagonal entries of the soft breaking slepton mass matrices, while still in agreement with the current low-energy bounds (see equations (8.19)–(8.24)). In particular, we tried to maximize the LL contributions to Δr , i.e., $(m_L^2)_{e\tau}$, and to obtain $\text{BR}(\mu \rightarrow e\gamma)$ within MEG reach (i.e. $10^{-13} \lesssim \text{BR}(\mu \rightarrow e\gamma) \lesssim 2.4 \times 10^{-12}$).⁵ However, and due to the fact that both seesaw realizations fail to account for radiatively induced LFV in the right-handed slepton sector, one finds values $|\Delta r| \lesssim 2 \times 10^{-8}$. It is worth emphasizing that if one further requires m_h to lie close to 125 GeV, then one is led to regions in mSUGRA parameter space where, due to the much heavier sparticle masses and typically lower values of $\tan \beta$, the SUSY contributions to R_K become even further suppressed.

Thus, and even under a full computation of the corrections to the $\nu\ell H^+$ vertex, we nevertheless confirm that, as firstly put forward in the analyzes of [499, 500] strictly constrained SUSY and SUSY seesaw models indeed fail to account for values of R_K close to the present limits.

Clearly, new sources of flavor violation, associated to the right-handed sector are required: in what follows, we maintain universality of soft breaking terms allowing, at the grand unified (GUT) scale, for a single $\tau - e$ flavor violating entry in m_e^2 . This

⁴ We will assume that we are in a strictly CP conserving framework, where all terms are taken to be real. This implies that there will be no contributions to observables such as electric dipole moments, or CP asymmetries.

⁵ Indeed, the more recent bound from MEG is 5.7×10^{-13} [378].

approach is somewhat closer to the lines of [499–502], although in our computation we will still conduct a full evaluation of the distinct contributions to Δr , and we consider otherwise universal soft breaking terms. Without invoking a specific framework/scenario of SUSY breaking that would account for such a pattern, we thus set

$$\delta_{\tau e}^{RR} = \frac{(m_e^2)_{\tau e}}{m_0^2} \neq 0. \quad (8.28)$$

As discussed above, low-energy constraints on LFV observables (especially $\tau \rightarrow e\gamma$), severely constrain this entry.

In figure (29), we present our results for Δr scanning the $m_0 - M_{1/2}$ plane for a regime of large $\tan\beta$. We have set $\delta_{\tau e}^{RR} = 0.1$, $\tan\beta = 40$, and taken $A_0 = -500$ GeV. The surveys displayed in the panels correspond to having embedded a type-I (left) or type-II (right) seesaw onto this near-mSUGRA framework.

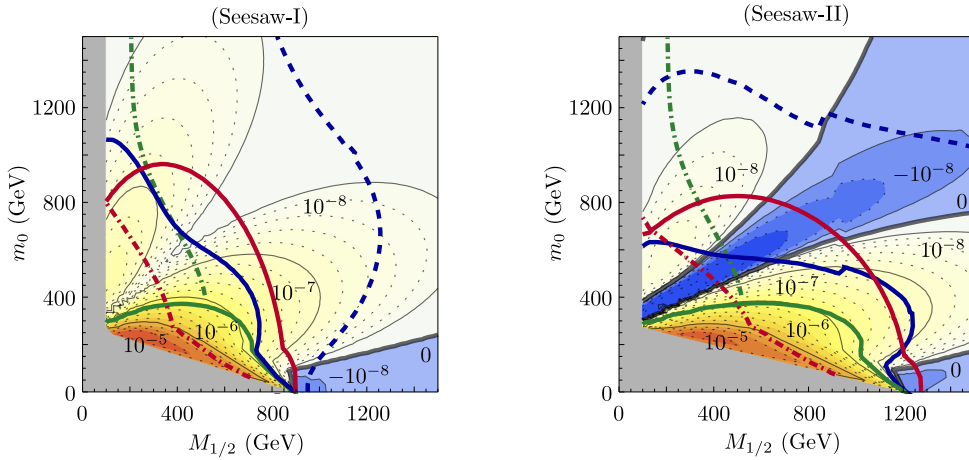


Figure 29: $m_0 - M_{1/2}$ plane for $\tan\beta = 40$ and $A_0 = -500$ GeV, with $\delta_{\tau e}^{RR} = 0.1$. On the left (right) panel, a type-I (II) SUSY seesaw, considering degenerate heavy mediators. Contour lines denote values of Δr (decreasing values: positive—in association with an orange-yellow-white color gradient; negative—blue gradients); solid (gray) regions are excluded due to the requirement of having the correct EWSB. A green dot-dashed line corresponds to the present LHC bounds on the cMSSM [554]. A full green line delimits the $\text{BR}(\tau \rightarrow e\gamma)$ exclusion region, while full (dot-dashed) red lines correspond to the bounds on $\text{BR}(B_s \rightarrow \mu\mu)$ [$\text{BR}(B_u \rightarrow \tau\nu)$]. Finally, the region delimited by blue lines corresponds to having $\text{BR}(\mu \rightarrow e\gamma)$ within MEG reach (current bound—solid line, future sensitivity—dashed line).

As can be readily seen from figure (29), once the constraints from low-energy observables have been applied, in the type-I SUSY seesaw, the maximum values for Δr are $\mathcal{O}(10^{-7})$, associated to the region with a lighter SUSY spectra (which is in turn disfavored by a “heavy” light Higgs). Even for the comparatively small non-universality, $\delta_{\tau e}^{RR} = 0.1$, a considerable region of the parameter space is excluded due to excessive contributions to $\text{BR}(B_u \rightarrow \tau\nu)$ and $\text{BR}(\tau \rightarrow e\gamma)$, thus precluding the possibility of large values of Δr . In a regime of large $\tan\beta$, the contributions to $\text{BR}(B_s \rightarrow \mu\mu)$ are also sizable, and LHCb results seem to exclude the regions of the parameter space where one could still have $\Delta r \sim \mathcal{O}(10^{-6,-7})$. The excessive

SUSY contributions to $\text{BR}(B_s \rightarrow \mu\mu)$ can be somewhat reduced by adjusting A_0 (in figure (29) we used $A_0 = -500$ GeV) and the values of Δr can be slightly augmented by increasing $\delta_{\tau e}^{RR}$; in the latter case, the $\tau \rightarrow e\gamma$ bound proves to be the most constraining, and values of Δr larger than $\mathcal{O}(10^{-6,-7})$ cannot be obtained in these constrained SUSY seesaw models.

The situation is somewhat different for the type-II case: first, notice that a sizable region in the $m_0 - M_{1/2}$ plane is associated to negative contributions to R_K , which are currently disfavored. In the remaining (allowed) parameter space, the values of Δr are slightly smaller than for the type-I case: this is a consequence of a non trivial interplay between a smaller value for the splitting $\delta = \frac{1}{2}(\langle m_\ell^2 \rangle - \langle m_{\chi^0}^2 \rangle)$ (induced by a lighter spectra), and a lighter charged Higgs boson.

Notice that in both SUSY seesaws it is fairly easy to accommodate a potential observation of $\text{BR}(\mu \rightarrow e\gamma) \sim 10^{-13}$ by MEG, taking for instance $M_{\text{seesaw}} \sim 10^{12}$ GeV for the type-I and II seesaw mechanisms.

In order to conclude this part of the analysis we provide a comprehensive overview of the constrained MSSM prospects regarding R_K , presenting in figure (30) a survey of the (type-I seesaw) mSUGRA parameter space, for two different regimes of $\delta_{\tau e}^{RR}$, taking all bounds (including the recent ones on m_h) into account. The panels of figure (30) allow to recover the information that could be expected from the discussion following figure (29): for fixed values of A_0 and $\tan \beta$, increasing $\delta_{\tau e}^{RR}$ indeed allows to augment the SUSY contributions to Δr although, as can be seen from the right-panel, the constraints from $\text{BR}(\tau \rightarrow e\gamma)$ become increasingly harder to accommodate. Notice that the latter could be avoided by increasing the SUSY scale (i.e., larger m_0 and/or $M_{1/2}$). However, and shown in figure (30), in a constrained SUSY framework this would lead to heavier charged Higgs masses, and in turn to suppressed contributions to Δr .

Although we do not display an analogous plot here, the situation is very similar for the type-II SUSY seesaw (even though accommodating $m_h \sim 125$ GeV is more difficult in these models [167]).

In view of the above discussion, it is clear that even taking into account all 1-loop corrections to the $\nu\ell H^+$ vertex, it is impossible to saturate Δr 's current experimental limit in the framework of constrained SUSY models (and its seesaw extensions accommodating neutrino data). In this sense, and even though we have followed a different approach, our results follow the conclusions of [502]. We also stress that recent experimental bounds (both from flavor observables and collider searches) add even more severe constraints to the maximal possible values of Δr .

8.3.2 mSUGRA inspired scenarios: inverse seesaw and LR models

We briefly comment here on the prospects of the inverse SUSY seesaw concerning R_K : it was pointed out in [555] that some flavor violating observables can be enhanced by as much as two orders of magnitude in a model with the inverse seesaw mechanism. Within such a framework, right-handed (s)neutrino masses can be relatively light, and as a consequence these $\nu_R, \tilde{\nu}_R$ states do not decouple from the theory until the TeV scale, hence potentially providing important contributions

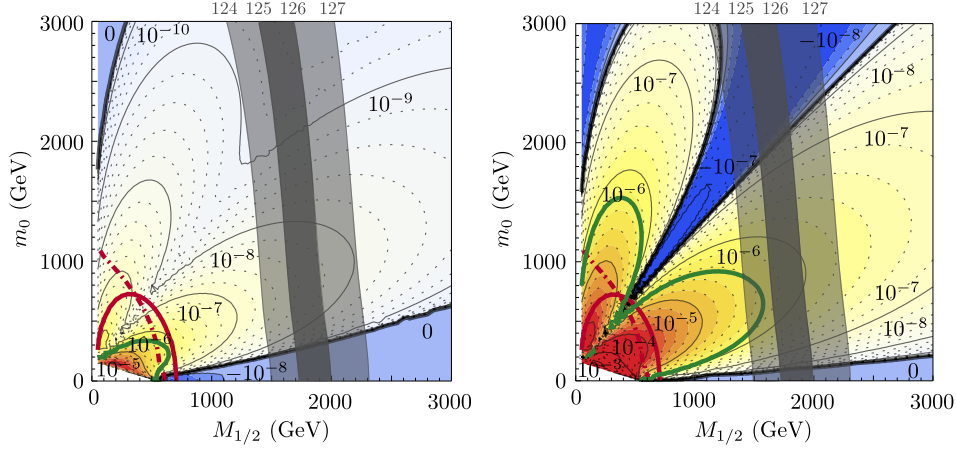


Figure 30: mSUGRA (type-I seesaw) $m_0 - M_{1/2}$ plane for $\tan\beta = 40$ and $A_0 = 0$ GeV, with $\delta_{\tau e}^{RR} = 0.1$ (left panel) and $\delta_{\tau e}^{RR} = 0.7$ (right panel). Contour lines denote values of Δr (decreasing values: positive—in association with an orange-yellow-white color gradient; negative—blue gradients). A full green line delimits the $\text{BR}(\tau \rightarrow e\gamma)$ exclusion region, while full (dot-dashed) red lines correspond to the bounds on $\text{BR}(B_s \rightarrow \mu\mu)$ ($\text{BR}(B_u \rightarrow \tau\nu)$). Superimposed are the regions for the Higgs boson mass: the dark band is for $125 \leq m_{h^0} \leq 126$ (GeV) and the lighter one marks the region where $124 \leq m_{h^0} \leq 127$ (GeV).

to different low-energy processes. Nevertheless, the specific contributions to Δr are suppressed by a factor $\frac{m_e^2}{m_\tau^2}$, with respect to those discussed above (see equation (8.17)), so that we do not expect a significant enhancement of SUSY 1-loop Higgs mediated effects to R_K due to the inverse seesaw mechanism. However, we note that it was shown in [514] that a change to the $W\ell\nu$ vertex in such models could potentially lead to a large Δr ($\sim \mathcal{O}(1)$).

For completeness (and although we do not provide specific details here), we have considered a specific LR seesaw model [556]. In this framework, non-vanishing values of $\delta_{\tau e}^{RR}$ can be dynamically generated. We have numerically verified that typically one finds $\delta_{\tau e}^{RR} \lesssim 0.01$ (we do not dismiss that larger values might be found, although certainly requiring a considerable amount of fine-tuning in the input parameters). We have not done a dedicated Δr calculation for this case, but considering that $\Delta r \propto (\delta_{\tau e}^{RR})^2$, we also expect the typical range of Δr to be far below the current experimental sensitivity.

8.3.3 mSUGRA inspired scenarios: NUHM

As can be seen from the approximate expression for Δr in equations (8.17) and (8.18), regimes associated with both large $\tan\beta$ and a light charged Higgs can greatly enhance this observable [502] ($\Delta r \propto \tan^6\beta/m_{H^+}^4$). By relaxing the mSUGRA-inspired universality conditions for the Higgs sector, as occurs in NUHM scenarios (see chapter 2), one can indeed have very low masses for the H^+ boson at low energies. This regime corresponds to a narrow strip in parameter space where $m_{H_1}^2 \approx m_{H_2}^2$, in particular when both are close to $-(2.2\text{TeV})^2$. In addition to favor-

ing electroweak symmetry breaking, since $m_{H^\pm}^2 \sim |m_{H_1}^2 - m_{H_2}^2|$ (even accounting for RG evolution of the parameters down to the weak scale), it is expected that the charged Higgs can be made very light with some fine tuning [502]. In order to explore the maximal values of Δr , a small scan was conducted around this region, where m_{H^\pm} changes very rapidly (see table (17)).

	m_0 (GeV)	$M_{1/2}$ (GeV)	$m_{H_1}^2, m_{H_2}^2$ (GeV ²)	$\tan \beta$	$\delta_{\tau e}^{RR}$
Min	0	100	-5.2×10^6	40	0.1
Max	1500	1500	-4.6×10^6	40	0.7

Table 17: Range of NUHM parameters leading to the scan of figure (31).

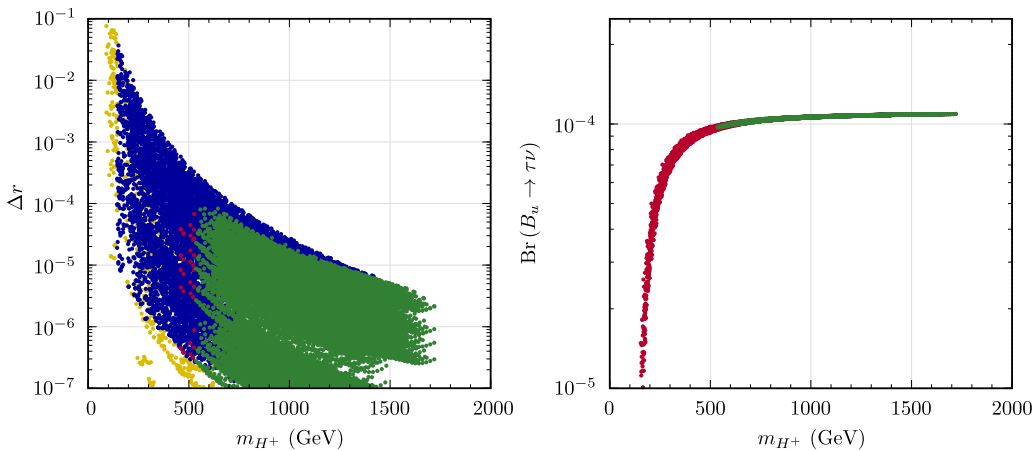


Figure 31: Left panel: Δr as a function of the charged Higgs mass, m_{H^\pm} (in GeV). Yellow points have been subject to no cuts, blue points comply with the bounds on the masses (LEP+LHC), red points satisfy all bounds except $\text{BR}(B_u \rightarrow \tau\nu)$ and green points satisfy all bounds. Right panel: $\text{BR}(B_u \rightarrow \tau\nu)$ versus m_{H^\pm} . Red points satisfy only the bounds on the masses (LEP+LHC) while green points comply with all bounds.

As can be verified from the left-hand panel of figure (31), one could in principle have semi-constrained regimes leading to sizable values of R_K , $\mathcal{O}(10^{-2})$. Once all (collider and low-energy) bounds have been imposed, one has at most $\Delta r \lesssim 10^{-4}$ (in association with $m_{H^\pm} \gtrsim 500$ GeV). Moreover, it is interesting to notice that SUSY contributions to $\text{BR}(B_u \rightarrow \tau\nu)$, which become non-negligible for lighter H^\pm , have a negative interference with those of the SM, lowering the latter branching ratio to values below the current experimental bound. This can be seen on the right-hand panel of figure (31). The following subsection addresses this topic in greater detail.

8.3.4 Unconstrained MSSM

To conclude the numerical discussion, and to allow for a better comparison between our approach and those usually followed in other analyzes (for instance [500, 501]), we conduct a final study of the unconstrained, low-energy MSSM. Thus, and in what follows, we make no hypothesis concerning the source of lepton flavor violation, nor on the underlying mechanism of SUSY breaking. Massive neutrinos are introduced by hand (no assumption being made on their nature), and although charged interactions do violate lepton flavor, as parametrized by the PMNS matrix U , no sizable contributions to $\text{BR}(\mu \rightarrow e\gamma)$ should be expected, as these would be suppressed by the light neutrino masses. At low-energies, no constraints (other than the relevant experimental bounds) are imposed on the SUSY spectrum (for simplicity, we will assume a common value for all sfermion trilinear couplings at the low-scale, $A_i = A_0$). The soft breaking slepton masses are allowed to be non-diagonal, so that *a priori* a non-negligible mixing in the slepton sector can occur. In order to better correlate the source of flavor violation at the origin of Δr with the different experimental bounds, we again allow for a single FV entry in the slepton mass matrices, $\delta_{\tau e}^{RR} \sim 0.5$, setting all other δ_{ij}^{XY} to zero.

	μ	m_A	$M_1,$ M_2	M_3	A_0	$m_{\tilde{L}}$	$m_{\tilde{e}}$	$m_Q, m_U,$ m_D	$\tan \beta$	$\delta_{\tau e}^{RR}$	other δ_{ij}^{XY}
Min	100	50	100	1100	-1000	100	100	1200	30	0.5	0
Max	3000	1500	2500	2500	1000	2200	2500	5000	60	0.5	0

Table 18: Range of variation of the unconstrained MSSM parameters (dimensionful parameters in GeVs). A_0 denotes the common value of the low-energy sfermion trilinear couplings.

In our scan we have varied the input parameters in the ranges collected in table (18). We have also applied all relevant constraints on the low-energy observables, equations (8.19)–(8.24), as well as the constraints on the SUSY spectrum [519, 526–549]. In particular we have assumed the limits

$$m_{\tilde{q}_{L,R}} > 1000 \text{ GeV}, \quad m_{\tilde{g}} > 1000 \text{ GeV}, \quad (8.29)$$

which nonetheless can be raised even further without affecting the R_K observable. Concerning the light Higgs boson mass, no constraint was explicitly imposed, but we note that values close to 125 GeV [33, 34], or even larger, are easily achievable due to the heavy squark masses.

This can be observed from the left panel of figure (32), where we display the output of the above scan, presenting the values of Δr versus the associated light Higgs boson mass, m_h . As expected, no explicit correlation between m_h and Δr is manifest, nor with the other (relevant) flavor-related low-energy bounds. For completeness, and to clarify the following discussion, we present on the right-hand panel of figure (32) the charged Higgs mass as a function of A_0 , again under a color scheme denoting the experimental bounds applied in each case. Identical to

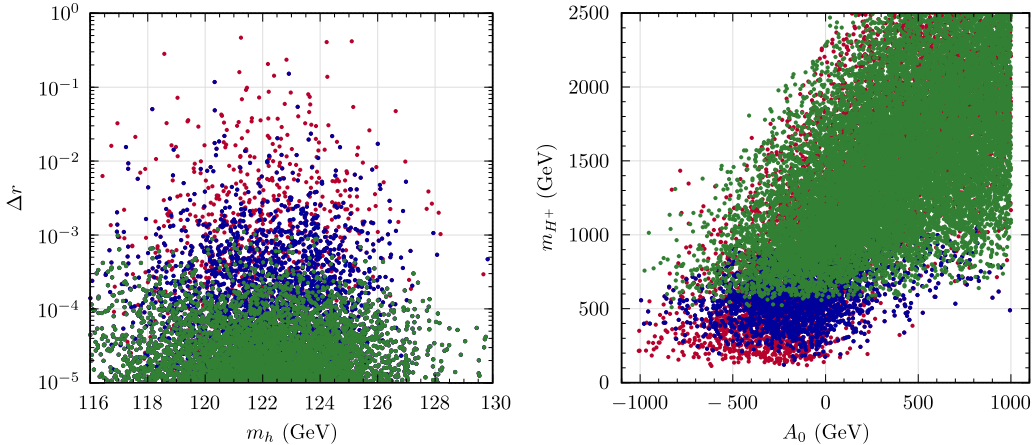


Figure 32: Left panel: Δr as a function of the lightest Higgs boson mass m_h (in GeV) for the range of parameters shown in table (18). Red points satisfy the bounds on the spectrum (LEP+LHC), blue points satisfy all bounds except $\text{BR}(B_u \rightarrow \tau\nu)$ and green points satisfy all bounds. Right panel: m_{H^+} versus A_0 , with the same color code. Both plots were produced by varying the different input parameters as in table (18).

what was observed in figure (31) (notice that NUHM models correspond, at low-energies, to a subset of these general cases), regimes of very light charged Higgs are indeed present, in association with small to moderate (negative) regimes for A_0 . Nevertheless, these regimes—which could potentially enhance Δr —are likewise excluded due to a conflict with $\text{BR}(B_u \rightarrow \tau\nu)$. This can be further confirmed from the left panel of figure (33), where we display the possible range of variation for Δr as a function of m_{H^+} , color-coding the different applied bounds.

As can be seen from both panels of figure (33), values $\Delta r \approx \mathcal{O}(10^{-2} - 10^{-1})$ could be obtainable, in agreement with references [499–502]. However, the situation is substantially altered when one takes into account the current experimental bounds on B decays ($B_u \rightarrow \tau\nu$ and $B_s \rightarrow \mu\mu$) and $\tau \rightarrow e\gamma$. As we can see from the left panel of figure (33), once experimental bounds—other than $B_u \rightarrow \tau\nu$ —are imposed, one could in principle have $\Delta r^{\text{max}} \approx \mathcal{O}(10^{-2})$; however, taking into account the limits from $\text{BR}(B_u \rightarrow \tau\nu)$, one is now led to $\Delta r \lesssim 10^{-3}$.

There are a few comments to be made regarding the impact of the different low-energy bounds from radiative τ decays and B -physics observables. Firstly, let us consider the $\tau \rightarrow e\gamma$ decay: although directly depending on $\delta_{\tau e}^{RR}$, its amplitude is (roughly) suppressed by the fourth power of the average SUSY scale, m_{SUSY} . From equations (8.17) and (8.18), Δr only depends on the charged Higgs mass: if the latter is assumed to be an EW scale parameter, Δr will be thus independent of m_{SUSY} in these unconstrained models. As such, it is possible to evade the $\tau \rightarrow e\gamma$ bound by increasing the soft SUSY masses, and this can indeed be seen from the right-hand panel of figure (33), where a number of blue points are to the left of the $\text{BR}(\tau \rightarrow e\gamma)$ bound line.

Secondly, the $B_s \rightarrow \mu\mu$ decay can be a severe constraint regarding the SUSY contributions to Δr in the case of constrained models (figures (29) and (30)). We note that $B_s \rightarrow \mu\mu$ is approximately proportional to A_0^2 (see for instance [520])

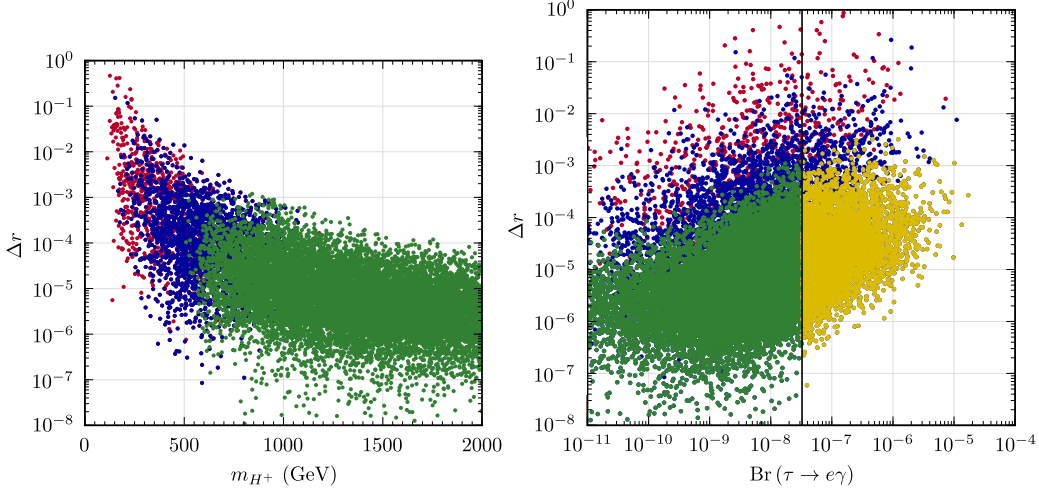


Figure 33: Ranges of variation of Δr in the unconstrained MSSM as a function of m_{H^+} (left panel), and as a function of $\text{BR}(\tau \rightarrow e\gamma)$ (right panel). The different input parameters were varied as in table (18) (notice that $\delta_{\tau e}^{RR} = 0.5$). On the left panel red points satisfy the bounds on the masses (LEP+LHC), blue points satisfy all bounds except $\text{BR}(B_u \rightarrow \tau\nu)$ and green points comply with all bounds. Similar color code on the right panel, except that blue points now comply with all bounds except $\text{BR}(B_u \rightarrow \tau\nu)$ and $\text{BR}(\tau \rightarrow e\gamma)$ while yellow denotes points only failing the bound on $\text{BR}(\tau \rightarrow e\gamma)$.

while Δr shows no such dependency, thus a regime of small trilinear couplings easily evades the $B_s \rightarrow \mu\mu$ bound.

Finally, there is the $B_u \rightarrow \tau\nu$ bound to consider. Notice that this is a process essentially identical to the charged kaon decays at the origin of the R_K ratio (the only difference being that the K^+ meson is to be replaced by a B_u and the e/μ in the decay products by a kinematically allowed τ), and hence its tree-level decay width can be inferred from equations (8.2) and (8.8). Due to a negative interference between the SM and the MSSM contributions, given by the term proportional to $\tan^2 \beta / m_{H^\pm}^2$ in equation (8.8), regimes of low m_{H^\pm} lead to excessively small values of $B_u \rightarrow \tau\nu$ (below the experimental bound), effectively setting a lower bound for $m_{H^\pm}^2$ (see right panel of figure (31), in relation to the discussion of NUHM models). In turn, this excludes regimes of m_{H^+} associated to sizable values of Δr , as is clear from the comparison of the blue and green regions of the left panel of figure (33).

8.4 SUMMARY

In this chapter we have revisited supersymmetric contributions to $R_K = \Gamma(K \rightarrow e\nu) / \Gamma(K \rightarrow \mu\nu)$, considering the potential of a broad class of constrained SUSY models to saturate the current measurement of R_K [4]. We based our analysis in a full computation of the one-loop corrections to the $\nu\ell H^+$ vertex; we have also derived (when possible) illustrative analytical approximations, which in addition to offering a more transparent understanding of the role of the different

parameters, also allow to establish a bridge between our results and previous ones in the literature. Our analysis further revisited the R_K observable in the light of new experimental data, arising from flavor physics as well as from collider searches.

We numerically evaluated the contributions to R_K arising in the context of different minimal supergravity inspired models which account for observed neutrino data, further considering the possibility of accommodating a near future observation of a $\mu \rightarrow e\gamma$ decay. As expected from the (mostly) LL nature of the radiatively induced charged lepton flavor violation, type-I and II seesaw mechanisms implemented in the cMSSM provide minimal contributions to R_K , thus implying that such cMSSM SUSY seesaws cannot saturate the present value for Δr .

We then considered unified models where the flavor-conserving hypothesis on the RR slepton sector is relaxed by allowing a non-vanishing $\delta_{\tau e}^{RR}$. In all models, special attention was given to experimental constraints, especially four observables which turn out to play a particularly relevant role: the recent interval for the lightest neutral Higgs boson mass provided by the CMS and ATLAS collaborations, $\text{BR}(B_s \rightarrow \mu\mu)$, $\text{BR}(B_u \rightarrow \tau\nu)$ and $\text{BR}(\tau \rightarrow e\gamma)$. These last two exhibit a dependence on m_{H^+} ($B_u \rightarrow \tau\nu$) and on $\delta_{\tau e}^{RR}$ ($\tau \rightarrow e\gamma$) similar to that of Δr . SUSY contributions to Δr are thus maximized in a regime in which m_{H^+} and $\delta_{\tau e}^{RR}$ are such that the experimental limits for $B_u \rightarrow \tau\nu$ and $\tau \rightarrow e\gamma$ are simultaneously saturated; in this regime one must then accommodate the bounds on other observables, such as m_h and $\text{BR}(B_s \rightarrow \mu\mu)$. For a minimal deviation from a pure cMSSM scenario allowing for non-vanishing values of $\delta_{\tau e}^{RR}$, we can have values for Δr at most of the order of 10^{-6} . In fact, the requirement of having a Higgs boson mass of 125-126 GeV is much more constraining on the cMSSM parameter space than, for instance $B_s \rightarrow \mu\mu$ (which is sub-dominant, and can be overcome by variations of the trilinear coupling, A_0). In order to have $\Delta r \sim \mathcal{O}(10^{-6})$, one must significantly increase $\delta_{\tau e}^{RR}$ so to marginally overlap the regions of $m_h \sim 125$ GeV, while still in agreement with $\tau \rightarrow e\gamma$.

SUSY contributions to Δr increase ($\sim 10^{-4}$) in models where the charged Higgs mass can be significantly lowered, as is the case of NUHM models; larger values are precluded due to $B_u \rightarrow \tau\nu$ decay constraints.

More general models, as the unconstrained MSSM realized at low-energies, offer more degrees of freedom, and the possibility to better accommodate/evade the different experimental constraints. In the unconstrained MSSM, one can find values of Δr one order of magnitude larger, $\sim 10^{-3}$. Again, any further augmentation is precluded due to incompatibility with the bounds on $B_u \rightarrow \tau\nu$.

However, $\Delta r \sim \mathcal{O}(10^{-3})$ still remains one order of magnitude shy of the current experimental sensitivity to R_K , and also substantially lower than some of the values previously found in the literature. As such, if SUSY is indeed discovered, and unless there is significant progress in the experimental sensitivity to R_K , it seems unlikely that the contributions to R_K of the SUSY models studied here will be testable in the near future. On the other hand, any near-future measurement of Δr larger than $\mathcal{O}(10^{-3})$ would unambiguously point towards a scenario different than those here addressed (mSUGRA-like seesaw, NUHM and the phenomenological MSSM).

It should be kept in mind that the analysis presented here focused on the impact of LFV interactions. Should the discrepancy between the SM and experimental

observations turn out to be much smaller than 10^{-4} , a more detailed approach and evaluation will then be necessary.

CONCLUSIONS

In this thesis we have analyzed radiative effects in supersymmetric models, with particular emphasis on supersymmetric grand unified theories (SUSY GUTs), based on [1–4]. If one attempts to supersymmetrize the SM in a minimal way, the gauge coupling constants unify in the resulting model (the MSSM). To study the evolution of these and other parameters in SUSY models, their renormalization group equations (RGEs) must be calculated. As pointed out in this thesis, such equations are known in a generic form for an arbitrary SUSY model to second order in perturbation theory. However, application of these generic RGEs to a specific model requires cumbersome computations involving the fully expanded Lagrangian, which are better performed by a computer. Otherwise, mistakes may jeopardize the very precision which is sought by using second order equations. In this work, following [1], the `Susyno` package for Mathematica was presented: given the gauge group and particle content, it computes the model Lagrangian and then applies the RGEs to its parameters. Testing of the program’s output showed incorrections in some of the results available in the literature (since then corrected by the authors), which emphasizes the importance of automatically calculating the RGEs of particular models, if true precision is to be achieved.

While the RGEs for a generic SUSY model were known to two loops or more, this did not include the important class of models where the gauge group contains more than a single $U(1)$ factor: for example the MSSM with an additional $U(1)$, and $SO(10)$ models with an intermediate $U(1)_R \times U(1)_{B-L}$ scale. Indeed, GUTs based on gauge groups with rank higher than four (such as $SO(10)$ and E_6) can have phases where the effective gauge group contains multiple $U(1)$ factors. In general, this leads to $U(1)$ mixing—gauge bosons and gauginos of different abelian factor groups can mix—and there were just some one-loop RGEs for such SUSY models. In [2] we have extended these results by deriving the two-loop renormalization group evolution of all parameters. We have also shown that failure to fully take into account these corrections can lead to errors of the percent level.

For several $SO(10)$ -inspired models, radiative effects on SUSY soft breaking masses were also analyzed [3]. In particular, we studied models where the lowest intermediate scale can be changed continuously without affecting the unification of the coupling constants. This sliding condition ensures that these supersymmetric models can have an extended gauge group near the electroweak scale, which potentially entails a rich phenomenology at the LHC. By the same reasoning, it is also conceivable that the intermediate scales of these $SO(10)$ -inspired models are beyond the reach of current direct detection experiments. If this is the case, it is still possible to indirectly test these models by measuring the masses of SUSY particles, since radiative effects imprint on them some of the higher energy behavior of the theory. In this way, we have showed that it is possible in principle not

only to gain indirect information on the type of intermediate phases of these SUSY GUT models, but also infer their energy scales.

The above analysis was done at the one-loop level only. Nevertheless, at the expense of lower precision we were able to analyze a broad range of $SO(10)$ -inspired models. A more precise computation would require the use of two-loop RGEs, as well as inclusion of threshold effects. Should any signs of supersymmetry be found in the future, such improvements in the calculations could easily be carried out.

In some cases, SUSY GUTs also lead to charged lepton flavor violation (cLFV). The reason why cLFV is so significant is because in the Standard Model we expect it to be negligible even if we add neutrino masses; any observation of lepton violating processes, $\ell \rightarrow \ell' \gamma$ for example, would clearly point to the presence of new Physics. These new Physics could well be SUSY and, in that case, due to the many new flavored parameters in the soft SUSY breaking Lagrangian, cLFV could be experimentally detectable. In fact, even assuming that SUSY is broken in a flavor blind way at some high scale, the SUSY-preserving neutrino Yukawa couplings are still able to generate cLFV interactions radiatively. There are many observables affected by this mechanism of generating cLFV—one of them, the ratio of decay amplitudes $\Gamma(K \rightarrow e\nu) / \Gamma(K \rightarrow \mu\nu) \equiv R_K$, was revisited in this thesis (based on [4]). We studied this ratio in the constrained MSSM with several seesaw realizations (type I, type II and inverse seesaw), in left-right symmetric models, and in non-universal Higgs mass models as well. To complete the analysis, we also considered the prospects of obtaining a large R_K in unconstrained low-energy SUSY models. We took into consideration LEP's bounds on slepton, chargino and neutralino masses, as well as LHC bounds on squark, gluino and the lightest Higgs masses. But more importantly for the saturation of the current experimental sensitivity on R_K , we also imposed the $BR(B_s \rightarrow \mu\mu)$, $BR(B_u \rightarrow \tau\nu)$ and $BR(\tau \rightarrow e\gamma)$ limits. We concluded that in light of these experimental constraints, SUSY contributions to the R_K observable cannot be as large as previously argued in the literature and in particular, the effects are (at least) an order of magnitude lower than the current experimental sensitivity. Therefore, it seems unlikely that these contributions to R_K will be testable in the near future, and if any near-future measurement of it does detect a discrepancy with the Standard Model value, it would unambiguously point towards different new Physics.

We conclude by noting that supersymmetry remains one of the most studied and attractive candidates to solve some of the Standard Model shortcomings, particularly in the context of grand unified theories, and radiative corrections are fundamental in the study of the phenomenology of these models. Even though no SUSY particles were observed yet at the LHC, the mass of the recently discovered Higgs boson is within the expected range if supersymmetry is to be the solution to the hierarchy problem and also provide a viable dark matter candidate particle. It does however point to a heavy SUSY spectrum, in the multi TeV range. However, there is hope that with the restart of the LHC at 13–14 TeV center of mass energy, as well as with a new generation of low energy experiments which have started or will start taking data in the near future, that we may uncover some of the fundamental Physics which lie beyond the Standard Model.

Part III

APPENDIX

STRUCTURE OF THE STANDARD MODEL

This appendix reviews the structure of the Standard Model, which is a gauge theory based on the group $U(1)_Y \times SU(2)_L \times SU(3)_c$ that is broken down into $U(1)_Q \times SU(3)_c$ by the Higgs mechanism, at low energies.

A.1 THE GAUGE THEORY

A representation Ψ in table (1) of the gauge group $U(1)_Y \times SU(2)_L \times SU(3)_c$ transforms as

$$\Psi \rightarrow \exp \left[i \left(\alpha T^Y + \alpha'^a T_a^L + \alpha''^b T_b^c \right) \right] \Psi \quad (\text{A.1})$$

under a local gauge transformation, where T^Y , T_a^L , T_b^c are representation matrices and α , α'^a , α''^b are some real parameters which can be space-time dependent (see [557–559] for example). The Standard Model contains $SU(2)_L$ singlets ($T_a^L = \mathbf{0}$) and doublets ($T_a^L = \frac{1}{2}\sigma_a$), as well as $SU(3)_c$ singlets ($T_a^c = \mathbf{0}$) and triplets ($T_a^c = \frac{1}{2}\lambda_a$).¹ Here, σ_a and λ_a are the Pauli and Gell-Mann matrices, respectively. On the other hand, the matrix T^Y is simply given by $Y\mathbb{1}$, where Y is the $U(1)_Y$ hypercharge of the representation.

The Lagrangian density itself must not change under gauge transformations and, in order to achieve this, some vector bosons must be introduced: one B_μ plus three W_μ^a (the electroweak gauge bosons), and eight G_μ^a (the gluons). These fields are in the adjoint representation of the gauge factor groups $U(1)_Y$, $SU(2)_L$, and $SU(3)_c$, respectively, changing as follows under infinitesimal transformations:

$$B_\mu \rightarrow B_\mu - \frac{1}{g'} \partial_\mu \alpha, \quad (\text{A.2})$$

$$W_\mu^a \rightarrow W_\mu^a - \varepsilon_{abc} \alpha'^b W_\mu^c - \frac{1}{g} \partial_\mu \alpha'^a, \quad (\text{A.3})$$

$$G_\mu^a \rightarrow G_\mu^a - f_{abc} \alpha''^b G_\mu^c - \frac{1}{g_s} \partial_\mu \alpha''^a. \quad (\text{A.4})$$

The tensors ε_{abc} and f_{abc} are structure constants of $SU(2)_L$ and $SU(3)_c$:

$$\begin{aligned} [\sigma_a, \sigma_b] &= i\varepsilon_{abc} \sigma_c, \\ [\lambda_a, \lambda_b] &= if_{abc} \lambda_c. \end{aligned}$$

¹ In the case of the left-handed quarks $Q = (u, d)^T$, which are neither singlets of $SU(2)_L$ nor singlets of $SU(3)_c$, $T_a^{SU(2)_L} = \frac{1}{2}\sigma_a \otimes \mathbb{1}_3$ and $T_a^{SU(3)_c} = \frac{1}{2}\mathbb{1}_2 \otimes \lambda_a$.

In order to make the Lagrangian density invariant under local gauge transformations, the partial derivative ∂_μ is replaced with the covariant one,

$$\partial_\mu \rightarrow D_\mu = \partial_\mu + ig'Y\mathbb{1}B_\mu + igT_a^L W_\mu^a + ig_s T_b^c G_\mu^b, \quad (\text{A.5})$$

and in this way interactions between the gauge bosons and matter/Higgs fields are generated. For the fermions we obtain

$$\begin{aligned} \mathcal{L}_{\text{kin } f} = & i \sum_f \bar{f} \gamma^\mu \partial_\mu f - \frac{g_s}{2} \sum_T \bar{T} \gamma^\mu \lambda_a T G_\mu^a - \frac{g}{\sqrt{2}} \sum_{(f_u, f_d)^T} \left(\bar{f}_u \gamma^\mu P_L f_d W_\mu^+ + \text{h.c.} \right) \\ & - e \sum_f q_f \bar{f} \gamma^\mu f A_\mu - \frac{g}{\cos \theta_W} \sum_f \bar{f} \gamma^\mu \left(g_f^V - g_f^A \gamma_5 \right) f Z_\mu, \end{aligned} \quad (\text{A.6})$$

where f are the fermionic field components, $(f_u, f_d)^T$ are the $SU(2)_L$ doublets, and T are the $SU(3)_c$ triplets. In preparation to the breaking of the electroweak symmetry, the gauge bosons B_μ and W_μ^3 have been rotated to the fields A_μ (the photon) and Z_μ ,

$$\begin{pmatrix} W_\mu^3 \\ B_\mu \end{pmatrix} = \begin{pmatrix} \cos \theta_W & \sin \theta_W \\ -\sin \theta_W & \cos \theta_W \end{pmatrix} \begin{pmatrix} Z_\mu \\ A_\mu \end{pmatrix}, \quad (\text{A.7})$$

where θ_W is the weak mixing angle:

$$e \equiv g \sin \theta_W \equiv g' \cos \theta_W. \quad (\text{A.8})$$

On the other hand,

$$W_\mu^+ = \frac{1}{\sqrt{2}} \left(W_\mu^1 - i W_\mu^2 \right). \quad (\text{A.9})$$

Lastly, the electric charge q_f and the vector/axial-vector coupling strengths g_f^V/g_f^A of fermions to the Z boson can be expressed as a function of the fermion weak isospin T_{3f}^L and hypercharge Y_f :

$$q_f = T_{3f}^L + Y_f, \quad (\text{A.10})$$

$$g_f^V = \left(\frac{1}{2} - \sin^2 \theta_W \right) T_{3f}^L - \sin^2 \theta_W Y_f, \quad (\text{A.11})$$

$$g_f^A = \frac{1}{2} T_{3f}^L. \quad (\text{A.12})$$

We note as well that in order for the gauge bosons to be dynamical entities, they need kinetic terms:

$$\mathcal{L}_{\text{kin } g} = -\frac{1}{4} B_{\mu\nu} B^{\mu\nu} - \frac{1}{4} W_{\mu\nu}^a W_a^{\mu\nu} - \frac{1}{4} G_{\mu\nu}^a G_a^{\mu\nu}, \quad (\text{A.13})$$

where

$$B_{\mu\nu} \equiv \partial_\mu B_\nu - \partial_\nu B_\mu, \quad (\text{A.14})$$

$$W_{\mu\nu}^a \equiv \partial_\mu W_\nu^a - \partial_\nu W_\mu^a - g\varepsilon_{abc} W_\mu^b W_\nu^c, \quad (\text{A.15})$$

$$G_{\mu\nu}^a \equiv \partial_\mu G_\nu^a - \partial_\nu G_\mu^a - gf_{abc} G_\mu^b G_\nu^c. \quad (\text{A.16})$$

A.2 ELECTROWEAK SYMMETRY BREAKING

Unless the gauge symmetry is broken, fermions will have no mass, as right- and left-handed matter fields are in different representations of the $U(1)_Y \times SU(2)_L$ group. Also, none of the gauge bosons can be massive. In the Standard Model, the breaking of the electroweak symmetry is achieved spontaneously through the Higgs mechanism: the scalar doublet H in table (1) acquires a non-vanishing vacuum expectation value $\langle H^\dagger H \rangle$ which is only invariant under one combination of the electroweak generators: it is usually chosen to be $T^Q \equiv T_3^L + T^Y$. Since $SU(3)_c$ is also preserved by this vacuum state, we have following breaking of the gauge group:

$$U(1)_Y \times SU(2)_L \times SU(3)_c \rightarrow U(1)_Q \times SU(3)_c. \quad (\text{A.17})$$

Considering the Higgs Lagrangian,

$$\mathcal{L}_H = (D^\mu H)^\dagger (D_\mu H) - V(H), \quad V(H) = \mu^2 H^\dagger H + \lambda (H^\dagger H)^2, \quad (\text{A.18})$$

one realizes that if the mass squared parameter μ^2 is negative and the quartic coupling λ is positive (to ensure vacuum stability), the potential is minimal when

$$\langle H^\dagger H \rangle = -\frac{\mu^2}{2\lambda} \equiv v^2. \quad (\text{A.19})$$

In a particular gauge—the so-called unitary gauge—one can write the Higgs doublet as

$$H = \begin{pmatrix} 0 \\ v + \phi/\sqrt{2} \end{pmatrix}, \quad (\text{A.20})$$

where v is just a number, and ϕ is a dynamical entity with a vanishing vacuum expectation value. Substituting this expression in equation (A.18) yields

$$\begin{aligned} \mathcal{L}_H = & \frac{1}{2} \partial^\mu \phi \partial_\mu \phi - \frac{1}{2} m_\phi^2 \phi^2 + \frac{1}{2} m_Z^2 Z^\mu Z_\mu + m_W^2 W^{+\mu} (W_\mu^+)^* \\ & - \frac{m_\phi^2}{2\sqrt{2}v} \phi^3 - \frac{m_\phi^2}{16v^2} \phi^4 + \sqrt{2} \frac{m_W^2}{v} W^{+\mu} (W_\mu^+)^* \phi + \frac{m_Z^2}{\sqrt{2}v} Z^\mu Z_\mu \phi \\ & + \frac{1}{2} \frac{m_W^2}{v^2} W^{+\mu} (W_\mu^+)^* \phi^2 + \frac{1}{4} \frac{m_Z^2}{v^2} Z^\mu Z_\mu \phi^2 \end{aligned} \quad (\text{A.21})$$

up to a constant term. The masses in this expression are the following:

$$m_W = \frac{gv}{\sqrt{2}}, \quad (\text{A.22})$$

$$m_Z = \frac{\sqrt{g'^2 + g^2}v}{\sqrt{2}}, \quad (\text{A.23})$$

$$m_\phi = 2\sqrt{\lambda}v. \quad (\text{A.24})$$

Importantly, the photon A_μ remains massless, in accordance with stringent experimental bounds [105].

The matter fields acquire mass by interacting with the Higgs doublet:

$$\mathcal{L}_{\text{Yukawa}} = -Y_{ij}^u \bar{u}_{Ri} Q_j \cdot H - Y_{ij}^d \bar{d}_{Ri} Q_j \cdot H - Y_{ij}^\ell \bar{e}_{Ri} L_j \cdot H + \text{h.c.}, \quad (\text{A.25})$$

where the flavor indices— i and j —are summed over. These are the Yukawa interactions. After EWSB,

$$\begin{aligned} \mathcal{L}_{\text{Yukawa}} = & -m_{ij}^u \bar{u}_{Li} u_{Rj} - m_{ij}^d \bar{d}_{Li} d_{Rj} - m_{ij}^\ell \bar{e}_{Li} e_{Rj} \\ & - \frac{m_{ij}^u}{\sqrt{2}v} \bar{u}_{Li} u_{Rj} \phi - \frac{m_{ij}^d}{\sqrt{2}v} \bar{d}_{Li} d_{Rj} \phi - \frac{m_{ij}^\ell}{\sqrt{2}v} \bar{e}_{Li} e_{Rj} \phi + \text{h.c.}, \end{aligned} \quad (\text{A.26})$$

with

$$m_{ij}^x = v Y_{ji}^{x*}, \quad x = u, d, \ell. \quad (\text{A.27})$$

There is no theoretical reason for the fermion mass matrices to be aligned with the charged interactions in equation (A.6). In fact, it has been experimentally established that this is not the case. Once the weak eigenstates $f_{L/R}$ are rotated to the mass eigenstates $f_{L/R}^m$ by some unitary matrices $U_{L/R}^f$,

$$\left(f_{L/R}\right)_i \equiv \left(U_{L/R}^f\right)_{ij} \left(f_{L/R}^m\right)_j, \quad \text{with } U_L^{f\dagger} m^f U_R^f = \text{diagonal}, \quad (\text{A.28})$$

the quark charged current ceases to be diagonal:

$$\mathcal{L}_{\text{kin } f} = \dots - \frac{g}{\sqrt{2}} \left(U_L^{u\dagger} U_L^d\right)_{ij} \left(\bar{u}_{Li}^m \gamma^\mu d_{Lj}^m W_\mu^+ + \text{h.c.}\right). \quad (\text{A.29})$$

The quark mixing matrix $V \equiv U_L^{u\dagger} U_L^d$ appearing in this equation is known as the Cabibbo-Kobayashi-Maskawa matrix [108]. There is no leptonic analogue in the SM because, in it, neutrinos do not have mass: since they are degenerate states, any rotation between the different flavors is physically meaningless (see chapter 3).

For completeness, it should be mentioned that, in order to perform the quantification of a gauge theory, it is also necessary to provide a gauge-fixing Lagrangian, \mathcal{L}_{GF} , as well as a ghost Lagrangian $\mathcal{L}_{\text{ghost}}$ (see [558] and references contained therein). Therefore, the complete Standard Model Lagrangian density is

$$\mathcal{L}_{\text{SM}} = \mathcal{L}_{\text{kin } f} + \mathcal{L}_{\text{kin } g} + \mathcal{L}_H + \mathcal{L}_{\text{Yukawa}} + \mathcal{L}_{\text{GF}} + \mathcal{L}_{\text{ghost}}. \quad (\text{A.30})$$

IMPLEMENTATION OF SOME FUNCTIONS IN THE SUSYNO PROGRAM

This appendix discusses how the main functions of the Mathematica program described in chapter 5 were implemented. These are almost exclusively group theoretical functions, since coding the RGEs themselves is a lengthy but simple process. Most of issues to be discussed below are rather technical, yet they are important for model building. Since the available literature does not seem to cover these topics thoroughly, they are discussed here.

Section B.1 below analyzes how the matrices of any representation of any simple Lie group can be constructed. Quantum mechanics textbooks often discuss how to do this for the simplest of simple groups, $SU(2)$, but the general case presents qualitative new features that complicate matters. We note that with the representation matrices of simple groups, the ones of products of simple groups (and possibly of abelian groups) are trivial to obtain, so effectively the method described here can be used to construct the matrices of any representation used in gauge theories. In `SusyNo`, this was implemented as the `RepMatrices` function. The code is quite efficient, since the 45 matrices with dimensions 1050×1050 of the representation $\{1, 0, 0, 2, 0\}$ of $SO(10)$,

```
RepMatrices[S010, {1, 0, 0, 2, 0}]
```

, are computed in less than one minute in a computer with an Intel Core i5-2300 CPU (see section B.5). We note that in the past some authors have analyzed other methods of computing the representation matrices of the classical Lie algebras $SU(n)$, $SO(n)$, $Sp(2n)$ [560–565] (for more references, see [564]).

Section B.2 discusses how to compute the combinations of product of fields which are gauge invariant, once their transformation/representation matrices are known. For the $SU(2)$ group, this is equivalent to finding the Clebsch-Gordan coefficients. Such computation is critical to the construction of the Lagrangian of a given model. In `SusyNo` this was implemented in the `Invariants` function (which is very similar to `IrrepInProduct`) and performance-wise, since the method discussed can reasonably be seen as a brute-force one, it can take many hours once the representations involved have dimensions above $\sim 100,200$. The references [566–571] also discuss the computation of such generalized Clebsch-Gordan coefficients for some groups/representations.¹

In section B.3, without entering into many details, we discuss briefly the complicated problem of simplifying the final expressions appearing in the RGEs.

Actually, version 2 of the `SusyNo` program does not compute an explicit form of the Lagrangian. In other words, the functions described in sections B.1 and B.2

¹ The `Clego` program [571] can only compute tensor products of non-degenerate or adjoint representations, but the authors suggest a work around this limitation.

are no longer used to calculate RGEs, but they are still part of the program. The aim of section B.4 is to discuss this Lagrangian-free approach to the computation of the RGEs. With it, the RGEs can be computed much quicker than with the traditional way that required building a superpotential and a soft SUSY breaking Lagrangian for each model. Section B.5 presents some reference running times.

We emphasize here once more that a detailed description on how to use these and other functions of the program (see the list in section 5.5) is provided in the built-in help system of `SusyNo`.

B.1 BUILDING THE MATRICES OF AN ARBITRARY REPRESENTATION OF A SIMPLE GROUP

In order to build the representation matrices of the algebra of a group acting on some vector space, a specific basis for both the algebra and the vector space must be chosen. In particular, once we arrive at a desired set of generator matrices $\{T_a\}$, performing the transformations $T_a \rightarrow \sum_b \mathcal{O}_{ab} T_b$ and/or $T_a \rightarrow U^\dagger T_a U$ for some orthogonal and unitary matrices \mathcal{O} and U , yields another valid set of generators, which obeys all the normalization requirements often used in Particle Physics (see subsection 4.3.7 of the group theory chapter). Because these matrices are basis dependent, some of the information they contain is not physically relevant. Even so, the explicit representation matrices are very useful, since many quantities can be computed from them. We shall then see how these can be built, for any representation of any simple group.

First, we review how the $SU(2)$ matrices are computed. In preparation for the general case, we shall use the generators e , f and h of equation (4.8). Henceforth denoted by E , F and H , their representation matrices obey the following relations

$$[E, F] = H, \quad [H, E] = 2E, \quad [H, F] = -2F. \quad (\text{B.1})$$

This should be compared with the Chevalley-Serre relations (4.25)–(4.27) for a generic simple group, taking into account that the Cartan matrix of $SU(2)$ is simply (2). We define the state $|2m\rangle$, with unit norm ($\langle 2m'|2m\rangle = \delta_{m,m'}$) and m a half-integer, to be such that

$$H |2m\rangle \equiv [2m] |2m\rangle, \quad (\text{B.2})$$

where $[2m] = 2m$ is presently only a number. Regarding the notation, notice that there is no sum over m here (summations will be indicated explicitly). We know that all weights of $SU(2)$ have multiplicity 1, meaning that the eigenspace of H associated to the eigenvalue $[2m]$ is always 1-dimensional. Applying $E(F)$ to $|2m\rangle$ raises(lower) $2m$ by two units:

$$H (E |2m\rangle) = (EH + 2E) |2m\rangle = ([2m] + 2) (E |2m\rangle), \quad (\text{B.3})$$

$$H (F |2m\rangle) = (FH - 2F) |2m\rangle = ([2m] - 2) (F |2m\rangle), \quad (\text{B.4})$$

Our construction procedure of the representation matrices shows that it is possible to take the simplest case, $[2m]_- = [2m - 2]^+ \in \mathbb{R}$, such that $E = F^T$ and $T_1, T_2 \propto E + F, i(E - F)$. As such,

$$[2m_{\max}]_- = [2m_{\max} - 2]^+ = \sqrt{2m_{\max}}, \quad (\text{B.11})$$

and recursive application of equation (B.8) yields all the remaining entries $[]_-$ and $[]^+$ of E and F :

$$[2m_{\max} - 2]_- [2m_{\max} - 4]^+ = [2m_{\max}]_- [2m_{\max} - 2]^+ + 2m_{\max} - 2 \quad (\text{B.12})$$

\Rightarrow

$$[2m_{\max} - 2]_- = [2m_{\max} - 4]^+ = \sqrt{4m_{\max} - 2} \quad (\text{B.13})$$

\vdots

In fact, $SU(2)$ is such a simple case that we can write down these values in a closed form:

$$[2m]_- = [2m - 2]^+ = \sqrt{(s + m)(s - m + 1)}, \quad (\text{B.14})$$

where $s \equiv m_{\max}$.

We move now to the general case of an arbitrary simple group of rank n . Our starting point will be the Chevalley-Serre relations (4.25)–(4.27) for the representation matrices E_i, F_i, H_i of the algebra elements e_i, f_i, h_i . These $3n$ matrices alone do not generate the whole algebra because there are more raising and lowering matrices \tilde{E}_x and \tilde{F}_x but, as noted in chapter 4, these can be obtained from the commutators of the elementary E_i and F_i , $i = 1, \dots, n$. So once the $3n$ matrices E_i, F_i, H_i are known, it is trivial to obtain the remaining generators, and then, as in $SU(2)$, for each pair of raising and lowering operators \tilde{E}_x and \tilde{F}_x , we can change basis so that all generators are hermitian by considering instead the combinations $\tilde{E}_x + \tilde{F}_x$ and $i(\tilde{E}_x - \tilde{F}_x)$.

Having dealt with these issues, the only step remaining in order to get the representation matrices is to actually build the elementary matrices E_i, F_i, H_i which obey the relations (4.25)–(4.27).² We will proceed in analogy to the $SU(2)$ case, and to do so two complications must be overcome:

1. As mentioned already, instead of just one set of matrices $\{E, F, H\}$, there are now n such sets $\{E_i, F_i, H_i\}$.
2. The space associated to a given weight is multi-dimensional. This means that, in general, the quantities $[]_-$, $[]^+$ and $[]$ in equation (B.7) are no longer numbers (1×1 matrices)—instead they are matrices, which are not even necessarily square.

Recall from chapter 4 that a state with weight ω , $|\omega\rangle$, is such that

$$H_i |\omega\rangle = \omega(i) |\omega\rangle, \quad (\text{B.15})$$

² The function `RepMinimalMatrices` in `Susyno` returns just these matrices.

with $\omega(i) = 2\langle\omega, \alpha_i\rangle/\langle\alpha_i, \alpha_i\rangle$,³ and α_i ($i = 1, \dots, n$) are the simple roots of the algebra. As mentioned above, in general there is more than a single state with weight ω , so we must introduce an extra label, $|\omega\rangle \rightarrow |\omega, \lambda\rangle$, such that

$$H_i |\omega, \lambda\rangle = \omega(i) |\omega, \lambda\rangle \quad (\text{B.16})$$

and $\langle\lambda', \omega'|\omega, \lambda\rangle = \delta_{\omega, \omega'} \delta_{\lambda, \lambda'}$. Denoting by n_ω the degeneracy of the space associated with the weight ω , then $\lambda = 1, \dots, n_\omega$. However, we find it more convenient to hide this extra label and instead view $|\omega\rangle$ as a n_ω -dimensional vector. Then, it is possible to define a diagonal matrix $[\omega(i)] \equiv \omega(i) \mathbb{1}$ such that

$$H_i |\omega\rangle = [\omega(i)] |\omega\rangle . \quad (\text{B.17})$$

Now, according to the Chevalley-Serre relations (4.25)–(4.27), applying $E_j(F_j)$ to $|\omega\rangle$ raises(lower) ω by the simple root α_j :

$$H_i (E_j |\omega\rangle) = (E_j H_i + A_{ji} E_j) |\omega\rangle = [(\omega + \alpha_j)(i)] (E_j |\omega\rangle) , \quad (\text{B.18})$$

$$H_i (F_j |\omega\rangle) = (F_j H_i - A_{ji} F_j) |\omega\rangle = [(\omega - \alpha_j)(i)] (F_j |\omega\rangle) . \quad (\text{B.19})$$

As such, we define the matrices $[\omega]^i$ and $[\omega]_i$ through the equations

$$E_i |\omega, \lambda\rangle \equiv \sum_{\lambda'} ([\omega]^i)_{\lambda'\lambda} |\omega + \alpha_i, \lambda'\rangle , \quad (\text{B.20})$$

$$F_i |\omega, \lambda\rangle \equiv \sum_{\lambda'} ([\omega]_i)_{\lambda'\lambda} |\omega - \alpha_i, \lambda'\rangle , \quad (\text{B.21})$$

or equivalently

$$E_i |\omega\rangle = ([\omega]^i)^T |\omega + \alpha_i\rangle , \quad (\text{B.22})$$

$$F_i |\omega\rangle = ([\omega]_i)^T |\omega - \alpha_i\rangle . \quad (\text{B.23})$$

The dimensions of $[\omega]^i$ and $[\omega]_i$ are $n_{\omega+\alpha_i} \times n_\omega$ and $n_{\omega-\alpha_i} \times n_\omega$, respectively. Based on this observation, we conclude that the set of matrices $\{E_i, F_i, H_i\}$ are almost entirely composed of null blocks, with a few exceptions:

$$E_i = \begin{pmatrix} \omega & & \\ \vdots & & \\ [\omega]^i & \dots & \end{pmatrix} \omega + \alpha_i \quad , \quad F_i = \begin{pmatrix} \omega & & \\ \vdots & & \\ [\omega]_i & \dots & \end{pmatrix} \omega - \alpha_i \quad ,$$

$$H_i = \begin{pmatrix} \omega & & \\ \vdots & & \\ [\omega(i)] & \dots & \end{pmatrix} \omega \quad . \quad (\text{B.24})$$

³ The Dynkin coefficients of a representation, which are used to identify it, are precisely these $\omega_{\max}(i)$ numbers (see chapter 4).

In order to build the diagonal matrices H_i , we only need the list of weights $\{\omega\}$, and this is easy to obtain for a given simple Lie algebra (see for example [399]). Also, with Freudenthal's formula, the dimension of the weight space associated to ω ($= n_\omega$) can be readily calculated, so we assume that this is known as well. The non-trivial part of the computation is calculating the ladder operators E_i and F_i , or equivalently, the matrix blocks $[\omega]^i$ and $[\omega]_i$ for all weights ω . To proceed we need the equation analogous to (B.8) of $SU(2)$. By applying $E_i F_j = F_j E_i + \delta_{ij} H_j$ to the vector $|\omega\rangle$, we get the desired relation:

$$[\omega - \alpha_j]^i [\omega]_j = [\omega + \alpha_i]_j [\omega]^i + \delta_{ij} [\omega(i)] . \quad (\text{B.25})$$

If all $[\omega + \alpha_i]_j$ and $[\omega]^i$ are known for all ω above some limit, then this equation can be used to recursively derive the remaining $[\]^i$ and $[\]_i$, with the right-hand side always known and the left-hand side unknown. For example, starting with the highest weight $\Lambda \equiv \omega_{\max}$ of the representation, $[\Lambda]^i = 0$ since we cannot raise it any further, and also $n_\Lambda = 1$ always [399], so $[\Lambda(j)]$ are simply the Dynkin indices of the representation Λ_j (not to be confused with the block matrices $[\Lambda]_j$ of the lowering operators F_j):

$$\begin{aligned} [\Lambda - \alpha_j]^i [\Lambda]_j &= \delta_{ij} \Lambda_j \\ &\vdots \end{aligned} \quad (\text{B.26})$$

Assuming that $E_i = F_i^\dagger$ and that these are real matrices, it follows that $[\omega + \alpha_i]_i = ([\omega]^i)^T$. Using this relation in equation (B.25), and also making the shift $\omega \rightarrow \omega + \alpha_j$, we find that

$$[\omega]^i ([\omega]^j)^T = ([\omega + \alpha_i]^j)^T [\omega + \alpha_j]^i + \delta_{ij} [(\omega + \alpha_i)(i)] . \quad (\text{B.27})$$

Then, to compute the unknown $[\omega]^i$ on the left-hand side, it is clear that we must simultaneously solve this equation for all $[\omega]^1, [\omega]^2, \dots, [\omega]^n$,⁴ since they all mix together. We can do this by defining a big matrix

$$\Omega(\omega) \equiv \begin{pmatrix} [\omega]^1 \\ \vdots \\ [\omega]^i \\ \vdots \end{pmatrix} \quad (\text{B.28})$$

which contains the $[\omega]^i$ ($i = 1, \dots, n$), for a weight ω . Then, the left-hand side of equation (B.27) is just the (ij) block of the matrix $\Omega(\omega) \Omega^T(\omega)$:

$$\Omega(\omega) \Omega^T(\omega) = X(\omega) , \quad (\text{B.29})$$

⁴ Note that some of these $[\omega]^i$ might not exist if $\omega + \alpha_i$ is not a weight, or equivalently $[\omega]^i$ is a matrix with size $0 \times n_\omega$ in these cases.

where $X(\omega)$ is a known matrix, because it depends on weights bigger than ω : its (ij) block is $\left([\omega + \alpha_i]^j\right)^T [\omega + \alpha_j]^i + \delta_{ij} [(\omega + \alpha_i)(i)]$. One must only break this symmetric $X(\omega)$ into some matrix $\Omega(\omega)$ times its transpose and then use this $\Omega(\omega)$ to build $X(\omega')$ for lower weights ω' , and repeat this process until the lowest weight is reached. There is always some arbitrariness in this process, since $\tilde{\Omega}(\omega) = \Omega(\omega) \mathcal{O}$, for some orthogonal matrix \mathcal{O} , also satisfies equation (B.29).⁵ In any case, with this algorithm, all the $[\]^i$ matrix blocks needed to build the matrices E_i, F_i are determined and, as previously explained, from there it is easy to build a complete list of hermitian generators $\{T_a\}$ of the algebra.

B.2 INVARIANT COMBINATIONS OF FIELDS TRANSFORMING UNDER SOME REPRESENTATION OF A SIMPLE GROUP AND GENERALIZED CLEBSCH-GORDAN COEFFICIENTS

Two $SU(2)$ doublets, $A \equiv (A^+, A^-)^T$ and $B = (A^+, A^-)^T$, transform as

$$A(B) \rightarrow \left(\mathbb{1} + i \sum_{a=1}^3 \varepsilon^a \sigma_a \right) A(B) \quad (\text{B.30})$$

under an infinitesimal transformation of the group. However, the bilinear combination $A^+ B^- - A^- B^+$ of the two fields does not change:

$$A^+ B^- - A^- B^+ \rightarrow A^+ B^- - A^- B^+. \quad (\text{B.31})$$

In order to write the Lagrangian of gauge theories, it is crucial that all such invariant combinations of the fields are known.⁶ For some combinations of the representations of certain groups ($SU(N)$, $SO(10)$, ...) there are clever techniques used in Particle Physics to write down these terms. However, they are usually only applicable to a few cases, and since *Susyno* aims at building the Lagrangian of a model based on any gauge group and with any field content (in theory at least), these approaches are not adequate. In this section, our aim is to describe the method used to solve this issue.

First, we should drop the $+/-$ notation for the components of fields, in favor of a more general one. As such, we assume that the components of a field A are labeled as A^i , such that $A = \sum_i A^i e_i^{(A)}$ where the $e_i^{(A)}$ form a basis of the vector space to which A belongs. Under the gauge symmetry, these basis vectors transform as

$$\delta e_j^{(A)} = i \sum_{a,j'} \varepsilon^a \left[T_a^{(A)} \right]_{j'j} e_{j'}^{(A)}, \quad (\text{B.32})$$

⁵ It is instructive to compare this general situation with the one encountered in $SU(2)$, which corresponds to the case where $\Omega(\omega)$ and $X(\omega)$ are numbers (1×1 matrices) for each weight ω .

⁶ The invariants of a Lie algebra can however be used to refer to something entirely different [572].

where the $T_a^{(A)}$ are the algebra generators, in A 's representation. Another perspective is to assume that the $\delta e_j^{(A)}$ do not change ($\delta e_j^{(A)} = 0$) and instead the components of the field A transform as follows:

$$\delta A^j = i \sum_a \varepsilon^a \left[T_a^{(A)} A \right]^j . \quad (\text{B.33})$$

Consider now the Kronecker product of two fields A and B given by

$$A \otimes B = \sum_{i,j} A^i B^j e_i^{(A)} \otimes e_j^{(B)} \equiv \sum_{i,j} (A \otimes B)^{ij} e_i^{(A)} \otimes e_j^{(B)} . \quad (\text{B.34})$$

Each component is specified by two indices, i and j , but to view $A \otimes B$ as a vector, we may combine the two indices into a single one: $\tilde{k} = 1, 2, 3 \dots, nm$ instead of $(i, j) = (1, 1), \dots, (1, m), (2, 1), \dots, (n, m)$. Then, each component of the Kronecker product of A and B transforms as

$$\delta (A \otimes B)^{\tilde{k}} = i \sum_a \varepsilon^a \left[\left(T_a^{(A)} \otimes \mathbb{1}^{(B)} + \mathbb{1}^{(A)} \otimes T_a^{(B)} \right) A \otimes B \right]^{\tilde{k}} . \quad (\text{B.35})$$

In other words, $A \otimes B$ transforms as a representation of the gauge symmetry, with generator matrices given by $T_a^{(A \otimes B)} = T_a^{(A)} \otimes \mathbb{1}^{(B)} + \mathbb{1}^{(A)} \otimes T_a^{(B)}$. In principle, this representation is reducible and, in fact, if there is an invariant combination of A and B , there must be a trivial representation in it. Then, consider that

$$\sum_{i,j} \kappa_{ij} A^i B^j = \sum_{\tilde{k}} \kappa_{\tilde{k}} (A \otimes B)^{\tilde{k}} \quad (\text{B.36})$$

is such a combination. Gauge invariance is verified if and only if

$$\sum_{\tilde{k}'} \kappa_{\tilde{k}'} \left[T_a^{(A \otimes B)} \right]_{\tilde{k}' \tilde{k}} = 0 \quad (\text{B.37})$$

for all \tilde{k} and all a . Equivalently, all invariant combinations of the A and B fields are given by vectors κ which belong to the nullspace of the matrix:

$$\begin{pmatrix} \left(T_1^{(A \otimes B)} \right)^T \\ \vdots \\ \left(T_a^{(A \otimes B)} \right)^T \\ \vdots \end{pmatrix} . \quad (\text{B.38})$$

As such, the number of independent invariants is given by the dimension of this space. We note that this method of finding the invariants will work for any representation of any group, provided that their matrices are known. Also, the extension of this method to combinations involving more than two fields is straightforward.

We now go through the example mentioned at the beginning of this section, namely A and B are two $SU(2)$ doublets. First, notice that

$$\sigma_a \otimes \mathbb{1}_2 = \begin{pmatrix} (\sigma_a)_{11} \mathbb{1}_2 & (\sigma_a)_{12} \mathbb{1}_2 \\ (\sigma_a)_{21} \mathbb{1}_2 & (\sigma_a)_{22} \mathbb{1}_2 \end{pmatrix}, \quad \mathbb{1}_2 \otimes \sigma_a = \begin{pmatrix} \sigma_a & 0 \\ 0 & \sigma_a \end{pmatrix}. \quad (\text{B.39})$$

Then, the components of $A \otimes B = (A^1 B^1, A^1 B^2, A^2 B^1, A^2 B^2)^T$ transform according to the generators

$$T_1^{(A \otimes B)} = \begin{pmatrix} 0 & 1 & 1 & 0 \\ 1 & 0 & 0 & 1 \\ 1 & 0 & 0 & 1 \\ 0 & 1 & 1 & 0 \end{pmatrix}, \quad (\text{B.40})$$

$$T_2^{(A \otimes B)} = \begin{pmatrix} 0 & -i & -i & 0 \\ i & 0 & 0 & -i \\ i & 0 & 0 & -i \\ 0 & i & i & 0 \end{pmatrix}, \quad (\text{B.41})$$

$$T_3^{(A \otimes B)} = \begin{pmatrix} 2 & 0 & 0 & 0 \\ 0 & 0 & 0 & 0 \\ 0 & 0 & 0 & 0 \\ 0 & 0 & 0 & -2 \end{pmatrix}. \quad (\text{B.42})$$

The invariants $\sum_{k=1}^4 \kappa_k (A \otimes B)^{\tilde{k}} = \kappa_1 A^1 B^1 + \kappa_2 A^1 B^2 + \kappa_3 A^2 B^1 + \kappa_4 A^2 B^2$ are given by the vectors $\kappa = (\kappa_1, \kappa_2, \kappa_3, \kappa_4)^T$ which are in the nullspace of the transpose of all three matrices in equations (B.40)–(B.42). One simple way to find them is to stack the transpose of these three matrices on top of each other in a single 12×4 matrix, and find its nullspace. In this case, we get a 1-dimensional nullspace generated by the vector $\kappa = (0, 1, -1, 0)^T$, which means that the only invariant combination of the fields A and B is $A^1 B^2 - A^2 B^1$ (and multiples of it).

As a slightly more elaborate example, consider a third field C , which is a triplet of $SU(2)$. Using as representation matrices of the generators

$$T_1^{(C)} = \frac{1}{\sqrt{2}} \begin{pmatrix} 0 & 1 & 0 \\ 1 & 0 & 1 \\ 0 & 1 & 0 \end{pmatrix}, \quad (\text{B.43})$$

$$T_2^{(C)} = \frac{1}{\sqrt{2}} \begin{pmatrix} 0 & -i & 0 \\ i & 0 & -i \\ 0 & i & 0 \end{pmatrix}, \quad (\text{B.44})$$

$$T_3^{(C)} = \begin{pmatrix} 1 & 0 & 0 \\ 0 & 0 & 0 \\ 0 & 0 & -1 \end{pmatrix}, \quad (\text{B.45})$$

the trilinear invariants involving the fields A and B and C are of the form

$$\sum_{\tilde{k}=1}^{12} \kappa_{\tilde{k}} (A \otimes B \otimes C)^{\tilde{k}} = \kappa_1 A^1 B^1 C^1 + \kappa_2 A^1 B^1 C^2 + \cdots + \kappa_{12} A^2 B^2 C^3, \quad (\text{B.46})$$

where the 12-dimensional vector κ must be in the nullspace of a 36×12 matrix made from the $T_a^{(A \otimes B \otimes C)}$ generators, which we shall not write down here. Again, it turns out that a single $\kappa = (0, 0, \sqrt{2}, 0, -1, 0, 0, -1, 0, \sqrt{2}, 0, 0)$ generates this vector space so, up to a multiplicative factor,

$$\sqrt{2} A^1 B^1 C^3 - A^1 B^2 C^2 - A^2 B^1 C^2 + \sqrt{2} A^2 B^2 C^1 \quad (\text{B.47})$$

is the only trilinear invariant involving two doublets A/B , and a triplet C . As a final example, if all A , B and C were triplets, a similar construction would require finding the nullspace of a 81×27 dimensional matrix; $\varepsilon_{ijk} A^i B^j C^k$ is the only invariant obtained.

A legitimate concern is the time needed to compute invariant combinations of larger representations with this method. The most demanding part of the algorithm consists in finding a basis of the nullspace of a potentially very large matrix: for a simple group with d generators, and representations of size n_A, n_B, \dots this matrix has $d \times n_A \times n_B \times \dots$ rows and $n_A \times n_B \times \dots$ columns. For example, the calculation of the invariant in $\mathbf{120} \otimes \mathbf{120} \otimes \mathbf{54}$ of $SO(10)$ involves a 29160000×648000 matrix. Even so, with a few simple tricks, this computation can be completed in less than a minute in a modern computer.

Consider the representation matrices $\{E_i, F_i, H_i\}$ obeying the Chevalley-Serre relations obtained in the previous section:

- The H_i are diagonal matrices, so $H_i \kappa = 0$ implies that $\kappa_j = 0$ unless the entries $(H_i)_{jj}$ for all i are null. This means that we should focus on the subspace of $A \otimes B \otimes \dots$ with null weights, which can be readily calculated.
- All the remaining generators \tilde{E}_x, \tilde{F}_x of a Lie algebra are given by commutators of the Chevalley-Serre elementary E_i or F_i , so if $E_i^T \kappa = F_i^T \kappa = 0$ for all i , then it follows that $\tilde{E}_x^T \kappa = \tilde{F}_x^T \kappa = 0$ for all x . Therefore, we only need to consider the nullspace of the matrices E_i^T and F_i^T .
- Since $F_i = E_i^T$, the nullspace of F_i^T is the same as $E_i^T F_i^T$, but $E_i^T F_i^T \kappa = (F_i^T E_i^T - H_i) \kappa = 0$ assuming that κ is in the nullspace of both E_i^T and H_i . As such, there is no need to compute the null space of the F_i^T matrices.

All things considered, for a rank n group, the matrix whose nullspace we must find has roughly $n \sqrt{n_A n_B \dots}$ rows and $\sqrt{n_A n_B \dots}$ columns, and most of its entries are null.

To conclude this discussion, we note that finding such invariant combinations is essentially equivalent to the computation of generalized (i.e., non- $SU(2)$) Clebsch-

Gordan coefficients. To see this, consider the following invariant combination of the fields/representations A , B and C of some group:

$$\sum_{ijk} \kappa_{ijk} A^i B^j C^k. \quad (\text{B.48})$$

Then, a vector D with components $D^k \equiv \kappa_{ijk} A^i B^j$ is in the irreducible representation conjugate to one of C . Therefore, by fixing A and B , and writing all such invariant combinations for different irreducible representations C , we get the explicit form of the decomposition of $A \otimes B$ in its irreducible parts (see also [566]).

B.3 EINSTEIN CONVENTION APPLIED TO FLAVOR INDICES

In this section, we discuss a difficulty in making a program such as `Susyno`, arising from the presence of multiple copies of a representation of the gauge group in a given model. These copies are usually considered as different flavors of the same field. Flavor is then an index, which must be carried not only by the fields but also by the parameters in the Lagrangian which multiply them. An example would be the Yukawa couplings.

The two-loop RGEs can be quite lengthy, so in most cases, it is preferable to write an expression such as

$$\text{Yu}[1,1]*\text{Yu}[1,1]+\text{Yu}[1,2]*\text{Yu}[1,2]+\dots+\text{Yu}[3,3]*\text{Yu}[3,3]$$

in Einstein notation:

$$\text{Yu}[i,j]*\text{Yu}[i,j]$$

This same expression could be expressed as $\text{Tr}[\text{Yu}^\dagger \text{Yu}]$, which is an even more compact notation. However, this last matrix form cannot handle parameters with more than two flavor indices, so instead `Susyno` uses the Einstein summation notation.

A problem then arises due to the presence of dummy indices: we know that $\text{Yu}[i,j]*\text{Yu}[i,j]$ is the same as $\text{Yu}[k,i]*\text{Yu}[k,i]$, but in general, computationally it is far from trivial to establish the equality of two such terms, particularly when there are parameters with more than two indices. In order to simplify the final expressions, this task must nevertheless be carried out. Here, we shall not go through the algorithm used in the program; we simply note that it is not perfect, since `Susyno` can sometimes fail to see that different forms of the same term are indeed identical.

To complicate matters further, some of these parameters have symmetries: for instance, some $\text{P}[i,j]$ might be the same as $\text{P}[j,i]$, which means that $\text{P}[i,j]*\text{P}[i,j]+\text{P}[i,j]*\text{P}[j,i]$ equals $2\text{P}[i,j]*\text{P}[i,j]$. In general, a set of m

parameters $P_{f_1 f_2 \dots f_n}^1, \dots, P_{f_1 f_2 \dots f_n}^m$ with n flavor indices f_i , under a permutation σ of these, transforms as

$$P_{\sigma(f_1 f_2 \dots f_n)}^i = \sum_j S(\sigma)_{ij} P_{f_1 f_2 \dots f_n}^j, \quad (\text{B.49})$$

where the matrix $S(\sigma)$ is a representation of the symmetric group S_n . Usually, parameters have at most $n = 2$ flavor indices, and the S_2 group only has two 1-dimensional irreducible representations: the trivial one, $S(\sigma) = 1$, and the alternating one, $S(\sigma) = \text{sign}(\sigma)$. So

$$P_{f_2 f_1} = \pm P_{f_1 f_2}. \quad (\text{B.50})$$

In other words, exchanging the flavors of a 2-index parameter results at most in a sign change. But as shown in equation (B.49), more complex situations can arise—for example, two parameters $P_{f_1 f_2 f_3}^1$ and $P_{f_1 f_2 f_3}^2$ with three flavor indices may be such that $P_{\sigma(f_1 f_2 f_3)}^{1(2)}$ is actually a linear combination of both $P_{f_1 f_2 f_3}^1$ and $P_{f_1 f_2 f_3}^2$. In the next section, we return to this topic.

B.4 A LAGRANGIAN-FREE COMPUTATION OF THE RGEs

The RGEs of a model can be calculated in two main steps: first the model's gauge invariant Lagrangian is computed, and then the generic two-loop RGE formulae of [430, 432] are applied to it. Above, we have detailed how the first part can be carried out for any gauge group and for any field content; the second part is straightforward, with the exception of the simplification of expressions discussed in the previous section. Nevertheless, this procedure can be very time consuming:

- Calculating the model's Lagrangian requires the computation of all representation matrices and of all invariant combinations of the fields (see sections B.1 and B.2);
- Naive application of the RGEs of a generic SUSY model requires many summations of symbolic quantities. As an example, one of the terms in the RGEs of the soft masses is $h_{ilm} h^{jln} Y_{npq} Y^{mpq}$ (see equation (C.25)) where the tensors Y and h collect all the trilinear couplings in the superpotential and soft SUSY breaking Lagrangian, respectively. The free indices (i, j) , as well as the summed/dummy ones (l, m, n, p, q) , range over all the field components in a model; in the MSSM, ignoring different flavors, there are 19 (6 in \hat{Q} , 3 in both \hat{u} and \hat{d} , 2 in \hat{L} , \hat{H}_u , \hat{H}_d , and 1 in \hat{e}). This means that for each $i, j = 1, \dots, 19$ the expression $h_{ilm} h^{jln} Y_{npq} Y^{mpq}$ alone, appearing in $[\beta_{m^2}^{(2)}]_i^j$, represents $19^5 = 2476099$ terms. With some ingenuity, the fact that the tensors Y and h are very sparse (most of the entries are null) can be used to reduce the complexity of this calculation, allowing the MSSM's RGEs to be computed in a few seconds. Nevertheless, it is clear that the time needed will scale as some power law N^x of the number of field components N in the model. The expression $h_{ilm} h^{jln} Y_{npq} Y^{mpq}$ suggests that this exponent x is

roughly 7, but due to the increasing sparseness of the tensors as N increases, the true number is lower.

For example, minimalistic $SO(10)$ models contain hundreds of field components, which makes this approach impractical due to the time it would take to complete the computations. Given the large representations involved, there can be memory problems as well.

On the other hand, by inspection of the generic RGEs, it is indisputable that they do not depend on the explicit basis used for each gauge representation: a unitary transformation $\Phi_i \rightarrow U_{ij}\Phi_j$ of all superfields which does not mix different components of different irreducible representations of the gauge group will not affect the RGEs. This raises the following question: is it possible to calculate the basis-independent RGEs of a model, without actually building an unphysical/basis-dependent Lagrangian? It turns out that such a Lagrangian-free computation of the RGEs is feasible and also dramatically faster than the more conventional approach. Therefore, in version 2 of `SusyNo` this new method was introduced, leading to an extensive rewriting of the code. Even though there is no longer any need for methods such as `RepMatrices` and `Invariants`, these were kept (and in some cases extended) since they are useful on their own for other potential applications. It should be pointed out that the idea of avoiding altogether the construction of basis dependent quantities, such as the Lagrangian, is not new—see for example [573, 574].

Let us now analyze how this can be done. We recall that the information contained in the superpotential and soft SUSY-breaking scalar terms can be collected in the tensors $Y^{abc}, \mu^{ab}, L^a, h^{abc}, b^{ab}, s^a$ and $(m^2)_b^a$ (see equations (2.8) and (2.14)). Each of these indices runs over all fields in the model, and it will prove useful to expand each of them into 3 sub-indices:

1. A representation index, denoted by a roman lowercase letter (a, b, c, \dots);
2. A representation-component index, denoted by a roman uppercase letter (A, B, C, \dots);
3. A flavor index, denoted by a Greek lowercase letter ($\alpha, \beta, \xi, \dots$).

As such,

$$a \xrightarrow{\text{new notation}} (aA\alpha) \quad ; \quad b \xrightarrow{\text{new notation}} (bB\beta) \quad ; \quad c \xrightarrow{\text{new notation}} (cC\xi) . \quad (\text{B.51})$$

For example, the a in $(aA\alpha)$ could point to the left-handed leptons representation (L), $A = 1, 2$ would then specify the doublet's component, and $\alpha = 1, 2, 3$ would stand for one of the three possible lepton flavors. Consider now a trilinear term in the superpotential, for example: it involves three superfields, $\Phi_{(aA\alpha)}\Phi_{(bB\beta)}\Phi_{(cC\xi)}$, whose A, B, C indices must be contracted in a gauge invariant way: $\kappa^{ABC}\Phi_{(aA\alpha)}\Phi_{(bB\beta)}\Phi_{(cC\xi)}$. This tensor κ consists of numbers only, and it is specific to the combination of the representations a, b and c , so we shall use $\kappa(abc)$ instead of just κ . However, the product of three representations may contain more than one independent gauge invariant combination, so we introduce

an extra label λ to distinguish them. Finally, we note that the whole expression $\kappa(abc\lambda)^{ABC} \Phi_{(aA\alpha)} \Phi_{(bB\beta)} \Phi_{(cC\xi)}$ must be multiplied by a parameter $y(abc\lambda)^{\alpha\beta\xi}$ (such as Y_u, Y_d or Y_e in the MSSM) which contains flavor indices α, β, ξ . As such, we may write

$$[W]_{\text{trilinear part}} = \frac{1}{6} \sum_{\substack{a,b,c,\lambda \\ \alpha,\beta,\xi \\ A,B,C}} y(abc\lambda)^{\alpha\beta\xi} \kappa(abc\lambda)^{ABC} \Phi_{(aA\alpha)} \Phi_{(bB\beta)} \Phi_{(cC\xi)}, \quad (\text{B.52})$$

or equivalently,

$$\left[Y^{abc} \right]_{\text{old notation}} = Y^{(aA\alpha)(bB\beta)(cC\xi)} = \sum_{\lambda} y(abc\lambda)^{\alpha\beta\xi} \kappa(abc\lambda)^{ABC}. \quad (\text{B.53})$$

In this way, we have successfully separated the symbolic part, $y(abc\lambda)^{\alpha\beta\xi}$, from the numerical one, $\kappa(abc\lambda)^{ABC}$. Focusing on the latter one, we note that

$$\sum_{BC} \kappa(abc\lambda)^{ABC} \kappa(a'bc\lambda')^*_{A'BC} = f(a, \lambda, \lambda') \delta_{a'}^a \delta_{A'}^A. \quad (\text{B.54})$$

The $\delta_{a'}^a \delta_{A'}^A$ factor is explained by the fact that the expression on the left must be proportional to the $\kappa(aa')^{AA'}$ coefficients of a bilinear term $\kappa(aa')^{AA'} \Phi_{(aA)} \Phi_{(a'A')}^*$ (omitting the flavor indices and the parameter). As for the $f(a, \lambda, \lambda')$ factor in the above equation, we may reasonably orthonormalize the various invariants in a trilinear combination of the a, b and c representations, such that

$$\sum_{ABC} \kappa(abc\lambda)^{ABC} \kappa(abc\lambda')^*_{ABC} \equiv \delta_{\lambda'}^{\lambda}, \quad (\text{B.55})$$

and consequently

$$\sum_{BC} \kappa(abc\lambda)^{ABC} \kappa(a'bc\lambda')^*_{A'BC} = \frac{1}{\dim \phi_a} \delta_{a'}^a \delta_{\lambda'}^{\lambda} \delta_{A'}^A, \quad (\text{B.56})$$

where $\dim \phi_a$ is the dimension of the representation a of the gauge group ($A = 1, \dots, \dim \phi_a$). Consider now two generic trilinear tensors, T^{abc} and U^{abc} ,

$$\left[T^{abc} \right]_{\text{old notation}} = \sum_{\lambda} t(abc\lambda)^{\alpha\beta\xi} \kappa(abc\lambda)^{ABC}, \quad (\text{B.57})$$

$$\left[U^{abc} \right]_{\text{old notation}} = \sum_{\lambda} u(abc\lambda)^{\alpha\beta\xi} \kappa(abc\lambda)^{ABC}, \quad (\text{B.58})$$

and two bilinear ones, D_b^a and $D'_b{}^a$, which are diagonal in both representation and representation-component space:

$$[D_b^a]_{\text{old notation}} = d(a)_{\beta}^{\alpha} \delta_b^a \delta_B^A, \quad (\text{B.59})$$

$$[D'_b{}^a]_{\text{old notation}} = d'(a)_{\beta}^{\alpha} \delta_b^a \delta_B^A. \quad (\text{B.60})$$

Assuming that repeated indices are summed over from now on, after a few simple manipulations of the expressions we conclude that the generic quan-

tity $U^{amn} D_n^{n'} D_m^{m'} T_{bmn'}$ is also diagonal in representation and representation-component space:

$$T^{amn} D_n^{n'} D_m^{m'} U_{bmn'} = \frac{1}{\dim \phi_{\check{a}}} t(\check{a}mn\lambda)^{\alpha\mu\nu} d(n)_{\nu}^{n'} d'(m)_{\mu}^{m'} u(\check{a}mn\lambda)_{\beta\mu'\nu'}^* \delta_b^{\check{a}} \delta_B^A. \quad (\text{B.61})$$

An inverted hat “ $\check{\sim}$ ” was added to the a index to indicate that it is not to be summed over. This is the most important equation of this section: we are able to get the result of a multiple-summation expression without actually performing these sums over the representation-component indices A, B, \dots . It is not even required to know most of the group theoretical details such as the gauge group or representations involved; only $\dim \phi_{\check{a}}$ is needed. Substituting the generic tensors U, T, D, D' by appropriate ones we can compute essentially all the terms of the two loop RGEs in [430, 432].

Consider as an example the two-loop RGEs of the gauge couplings, which contain a term $Y^{ijk} Y_{ijk}$. Using $T = U = Y$ and $D_b^a = D_b'^a = \delta_b^a$ in the master equation (B.61) we get

$$\left[Y^{ijk} Y_{ijk} \right]_{\text{old notation}} = y(amn\lambda)^{\alpha\mu\nu} y(amn\lambda)_{\alpha\mu\nu}^*. \quad (\text{B.62})$$

To fully appreciate the simplicity of this formula, if the Yukawa couplings in the MSSM were normalized according to equation (B.55) we would immediately conclude that $Y^{ijk} Y_{ijk} \stackrel{*}{=} \text{Tr} \left(Y^{u\dagger} Y^u + Y^{d\dagger} Y^d + Y^{\ell\dagger} Y^{\ell} \right)$.⁷ As a more complex example, consider the term $Y^{acd} Y_{dmn} Y^{d'mn} Y_{bcd'}$, which appears in the two-loop RGEs of the anomalous dimensions of the chiral superfields (equation (C.4)). Setting $D_d^{d'} = Y_{dmn} Y^{d'mn}$ and $D_b'^a = \delta_b^a$ in equation (B.61) yields

$$Y^{acd} Y_{dmn} Y^{d'mn} Y_{bcd'} = \frac{1}{\dim \phi_{\check{a}} \dim \phi_d} y(\check{a}cd\lambda)^{\alpha\xi\delta} y(dmn\lambda')_{\delta\mu\nu}^* y(dmn\lambda')^{\delta'\mu\nu} y(\check{a}cd\lambda)_{\beta\xi\delta'}^* \delta_b^{\check{a}} \delta_B^A. \quad (\text{B.63})$$

For bilinear terms the situation is similar; the entry μ^{ab} of the μ tensor is separated as (some μ parameter) \times (tensor κ with representation-component indices):

$$\left[\mu^{ab} \right]_{\text{old notation}} = \mu^{(aA\alpha)(bB\beta)} = \mu(ab)^{\alpha\beta} \kappa(ab)^{AB} \quad (\text{no sums}). \quad (\text{B.64})$$

Note that we do not use here a λ label because the product of two representations contains at most one invariant. Interestingly, in a model with no singlets, these $\kappa(ab)^{AB}$ numerical tensors do not need to be normalized (unlike the trilinear ones $\kappa(abc\lambda)^{ABC}$ —see equation (B.55)). In other words, as long as we use consistently the same $\kappa(ab)^{AB}$ throughout the Lagrangian, its normalization will not affect the RGEs. As an example of this statement, using $W = \dots + x\mu\hat{H}_u \cdot \hat{H}_d + \dots$ and

⁷ However, note that usually the normalization in equation (B.55) is not followed. Nevertheless, adaptation to other normalization schemes is trivial.

$-\mathcal{L}_{\text{soft}} = \dots + xB\widehat{H}_u \cdot \widehat{H}_d + \dots$ in the MSSM for any value of x yields the same RGEs for all the parameters in the model.

If there are singlets, combinations such as $Y_{amn}b^{mn}$ appearing in the one-loop RGEs of the tensor b^{ij} require that we relate b^{mn} with Y^{amn} when representation a is a singlet. The following convention seems reasonable: bilinear terms involving some representations m and n are obtained from the trilinear ones with m , n and the singlet representation \widehat{S} by just deleting the singlet field (and of course using a different parameter name): for example, from the NMSSM's trilinear term (parameter) $\widehat{S}\widehat{H}_u \cdot \widehat{H}_d$ we would write a bilinear one as (parameter') $\widehat{H}_u \cdot \widehat{H}_d$ instead of, for example, $-(\text{parameter}')\widehat{H}_u \cdot \widehat{H}_d$ or $2(\text{parameter}')\widehat{H}_u \cdot \widehat{H}_d$. With this convention,

$$[Y_{amn}b^{mn}]_{\text{old notation}} = y(\mathbf{s}mn)_{\alpha\mu\nu}^* b(mn)^{\mu\nu} \delta_a^{\mathbf{s}}, \quad (\text{B.65})$$

where \mathbf{s} refers to the singlet representation.

For completeness, we note that linear and soft mass terms always have a trivial representation-component structure,

$$[L^a]_{\text{old notation}} = L^{(aA\alpha)} = l(\mathbf{s})^\alpha \delta_{\mathbf{s}}^a, \quad (\text{B.66})$$

$$\left[\left(m^2 \right)_b^a \right]_{\text{old notation}} = \left(m^2 \right)_{(bB\beta)}^{(aA\alpha)} = m^2 (\check{a})_\beta^\alpha \delta_b^{\check{a}} \delta_B^A, \quad (\text{B.67})$$

so no complications arise from them.

In summary, it is possible to completely avoid doing sums over the components of representations of the gauge group. In fact, the only group theoretical quantities needed are the following:

- Dimension of the Lie algebras of each gauge factor group;
- Quadratic Casimirs and dimensions of the representations under each gauge factor group;
- The number of invariants of the gauge group in a given product of representations.

This last piece of information is necessary in order to compute which are the parameters of a given model. However, as we have already mentioned in the previous section, this discussion is complicated by the fact that parameters can have symmetries in their flavor indices. These symmetries appear only when a parameter multiplies repeated representations, and its precise nature is inherited from the way these representations combine to form a singlet. For example, in $SU(2)$, the combination of $\mathbf{3} \otimes \mathbf{3}$ is symmetric under a permutation of the two triplets, so introducing flavor indices α and β , the μ parameter in $\mu^{\alpha\beta} \mathbf{3}^\alpha \otimes \mathbf{3}^\beta$ must be symmetric under a permutation of its indices. On the other hand, $SU(2)$ doublets are pseudo-real representations, which means that the singlet in $\mathbf{2} \otimes \mathbf{2}$ changes sign if the doublets are permuted, so μ' in $\mu'^{\alpha\beta} \mathbf{2}^\alpha \otimes \mathbf{2}^\beta$ must be anti-symmetric under a permutation of its flavor indices. Crucially, because of this antisymmetry, if there is just one flavor such a term cannot be formed!

Therefore, in order to determine the parameters in the Lagrangian it is not enough to know if a given product of representations contains a singlet state; it is also necessary to know if those combinations are symmetric, antisymmetric or of mixed symmetry. In general, the product of n copies of the gauge group G breaks into irreducible representations of $G \times S_n$, where S_n is the permutation group of n objects, and these irreducible representations are sometimes known as **plethysms**. If the G invariants are calculated explicitly, as in section B.2, then their S_n transformation properties can be accessed explicitly. However, in a Lagrangian-free approach there is no such option. As such, we have implemented in Mathematica a `Plethysms` function,⁸ following the algorithm in the manual of the LiE program [442, 575]. Details can be found in the built-in documentation of `SusyNo` and also in reference [442].

Version 2 of `SusyNo` therefore writes the RGEs without computing basis invariant quantities, such as a Lagrangian, even though all necessary functions to do so remain in the program. Finally, we must mention that the canonical normalization assumed in the text above (equation (B.55) in particular) does not match the usual one in the MSSM. To make it match, the actual normalization used by `SusyNo` is

$$\sum_{ABC} \kappa(abc\lambda)^{ABC} \kappa(abc\lambda')^*_{ABC} \equiv \sqrt{\dim \phi_a \dim \phi_b \dim \phi_c \delta_{\lambda\lambda'}}, \quad (\text{B.68})$$

and matching the program’s default parameter normalization with the user’s preferred one is easy. In fact, the Lagrangian-free approach presented here clarifies which are the exact requirements for two notations to be equivalent, as far as the RGEs of the parameters are concerned—see subsection (5.4.2).

B.5 RUNNING TIME

For reference, this section provides the time needed to run some of `SusyNo`’s functions in a computer with an Intel Core i5-2300 CPU. In particular, tables (19), (20) and (21) contain information on the functions `GenerateModel`, `Invariants` and `RepMatrices`, respectively.

⁸ There are also other, more complex functions—`PermutationSymmetryOfInvariants` and `PermutationSymmetryOfTensorProductParts`—which are more practical and closer to a model builder’s needs. Details can be found on the built-in documentation.

Model	MSSM	RPV MSSM	NMSSM	$SO(10)$ #1	$SO(10)$ #2
Time 1 (s)	1.1	38	1.7	2.9	2.9
Time 2 (s)	1.2	39	1.8	3584	166

Table 19: Running time of the command `GenerateModel` without (“Time 1”) and with (“Time 2”) the option `CalculateEverything->True` (output was suppressed in both cases). Five models are presented: MSSM [430], R-parity violating MSSM (RPV MSSM) [439], NMSSM [431], and two $SO(10)$ models. Model “ $SO(10)$ #1” contains three **16** multiplets together with the representations **210**, **126**, $\overline{\mathbf{126}}$, **10** (one copy each). In model “ $SO(10)$ #2”, the representation **210** is replaced by the **45** plus the **54**. Note that `GenerateModel` will always compute the RGEs, regardless of the optional parameters; using `CalculateEverything->True` forces the program to calculate the Lagrangian explicitly (superpotential and soft SUSY breaking Lagrangian). In this last case, Clebsch-Gordan coefficients must be computed, and that is why “Time 2” can be significantly larger than “Time 1”. Note as well that the RPV MSSM, with or without optional parameters, takes a substantial amount of time to be computed essentially because the model contains equal representations, L and H_d , which are to be treated differently (in other words, the running time would be smaller if H_d was erased and instead we considered 4 flavors of L).

Input	$\mathbf{3} \otimes \mathbf{6} \otimes \mathbf{10} \otimes \mathbf{15} \otimes \mathbf{15}' \otimes \mathbf{42}$ in $SU(3)$	$\mathbf{16} \otimes \mathbf{16} \otimes \overline{\mathbf{126}}$ in $SO(10)$	$\mathbf{27} \otimes \mathbf{27} \otimes \mathbf{27} \otimes \mathbf{650}$ in E_6
Time (s)	1574	2.0	1230

Table 20: Running time of the command `Invariants` which calculates generalized Clebsch-Gordan coefficients of arbitrary representations of an arbitrary gauge group. Note that there are fifty seven $SU(3)$ invariants in $\mathbf{3} \otimes \mathbf{6} \otimes \mathbf{10} \otimes \mathbf{15} \otimes \mathbf{15}' \otimes \mathbf{42}$, 1 $SO(10)$ invariant in $\mathbf{16} \otimes \mathbf{16} \otimes \overline{\mathbf{126}}$, and 3 E_6 invariants in $\mathbf{27} \otimes \mathbf{27} \otimes \mathbf{27} \otimes \mathbf{650}$.

Representation	100 in $SU(2)$	324 in F_4	1050 in $SO(10)$	10560 in $SO(10)$	248 in E_8
Time (s)	0.2	128	48	5139	

Table 21: Running time of the command `RepMatrices` which calculates explicitly the matrices of arbitrary representations of an arbitrary simple gauge group.

TWO-LOOP RGEs FOR MODELS WITH GAUGE GROUPS
CONTAINING AT MOST ONE $U(1)$

In this appendix, the two-loop RGEs for a generic softly broken SUSY model are reproduced from [430, 432, 576]. However, these results do not take into account the presence of a Fayet-Iliopoulos term (see [447–449]) nor the presence of non-standard soft supersymmetric breaking terms $\phi_i^* \phi_j \phi_k$, $\psi_i \psi_j$, $\psi_i \lambda_a$ —see [450–452] for discussions and analyzes of the RGEs in these cases. With multiple $U(1)$ gauge groups, the adaptations described in chapter 6 must also be carried out in order to include $U(1)$ -mixing effects.

C.1 SIMPLE GAUGE GROUP

Let us recall that for a general $N = 1$ supersymmetric gauge theory with a generic superpotential

$$W = \frac{1}{6} Y^{ijk} \Phi_i \Phi_j \Phi_k + \frac{1}{2} \mu^{ij} \Phi_i \Phi_j + L^i \Phi_i, \quad (\text{C.1})$$

the soft SUSY breaking scalar terms are written in a compact way as

$$-\mathcal{L}_{\text{soft}} = \left(\frac{1}{2} M_a \lambda^a \lambda^a + \frac{1}{6} h^{ijk} \phi_i \phi_j \phi_k + \frac{1}{2} b^{ij} \phi_i \phi_j + s^i \phi_i + \text{h.c.} \right) + (m^2)_j^i \phi_i \phi_j^*, \quad (\text{C.2})$$

as mentioned already in chapter 1. Here we will follow [430] and assume that repeated indices are summed over. The anomalous dimensions of the chiral superfields are given by

$$\gamma_i^{(1)j} = \frac{1}{2} Y_{ipq} Y^{jpq} - 2\delta_i^j g^2 C(i), \quad (\text{C.3})$$

$$\begin{aligned} \gamma_i^{(2)j} &= g^2 Y_{ipq} Y^{jpq} [2C(p) - C(i)] - \frac{1}{2} Y_{imn} Y^{npq} Y_{pqr} Y^{mrj} \\ &\quad + 2\delta_i^j g^4 [C(i)S(R) + 2C(i)^2 - 3C(G)C(i)], \end{aligned} \quad (\text{C.4})$$

and the β -functions for the gauge couplings are given by

$$\beta_g^{(1)} = g^3 [S(R) - 3C(G)], \quad (\text{C.5})$$

$$\begin{aligned} \beta_g^{(2)} &= g^5 \left\{ -6[C(G)]^2 + 2C(G)S(R) + 4S(R)C(R) \right\} \\ &\quad - g^3 Y^{ijk} Y_{ijk} C(k) / d(G). \end{aligned} \quad (\text{C.6})$$

The corresponding RGEs are defined as

$$\frac{d}{dt} g = \frac{1}{16\pi^2} \beta_g^{(1)} + \frac{1}{(16\pi^2)^2} \beta_g^{(2)}. \quad (\text{C.7})$$

We used in this expression $t = \log Q$, where Q is the renormalization scale. The β -functions for the superpotential parameters can be obtained by using the superfield technique. The expressions obtained are

$$\beta_Y^{ijk} = Y^{ijp} \left[\frac{1}{16\pi^2} \gamma_p^{(1)k} + \frac{1}{(16\pi^2)^2} \gamma_p^{(2)k} \right] + (k \leftrightarrow i) + (k \leftrightarrow j), \quad (\text{C.8})$$

$$\beta_\mu^{ij} = \mu^{ip} \left[\frac{1}{16\pi^2} \gamma_p^{(1)j} + \frac{1}{(16\pi^2)^2} \gamma_p^{(2)j} \right] + (j \leftrightarrow i), \quad (\text{C.9})$$

$$\beta_L^i = L^p \left[\frac{1}{16\pi^2} \gamma_p^{(1)i} + \frac{1}{(16\pi^2)^2} \gamma_p^{(2)i} \right]. \quad (\text{C.10})$$

The expressions for trilinear soft breaking terms are

$$\frac{d}{dt} h^{ijk} = \frac{1}{16\pi^2} [\beta_h^{(1)}]^{ijk} + \frac{1}{(16\pi^2)^2} [\beta_h^{(2)}]^{ijk}, \quad (\text{C.11})$$

with

$$\begin{aligned} [\beta_h^{(1)}]^{ijk} &= \frac{1}{2} h^{ijl} Y_{lmn} Y^{mnk} + Y^{ijl} Y_{lmn} h^{mnk} \\ &\quad - 2 \left(h^{ijk} - 2MY^{ijk} \right) g^2 C(k) + (k \leftrightarrow i) + (k \leftrightarrow j), \end{aligned} \quad (\text{C.12})$$

$$\begin{aligned} [\beta_h^{(2)}]^{ijk} &= -\frac{1}{2} h^{ijl} Y_{lmn} Y^{npq} Y_{pqr} Y^{mrk} \\ &\quad - Y^{ijl} Y_{lmn} Y^{npq} Y_{pqr} h^{mrk} - Y^{ijl} Y_{lmn} h^{npq} Y_{pqr} Y^{mrk} \\ &\quad + \left(h^{ijl} Y_{lpq} Y^{pqk} + 2Y^{ijl} Y_{lpq} h^{pqk} - 2MY^{ijl} Y_{lpq} Y^{pqk} \right) g^2 [2C(p) - C(k)] \\ &\quad + \left(2h^{ijk} - 8MY^{ijk} \right) g^4 \left[C(k)S(R) + 2C(k)^2 - 3C(G)C(k) \right] \\ &\quad + (k \leftrightarrow i) + (k \leftrightarrow j). \end{aligned} \quad (\text{C.13})$$

For the bilinear soft-breaking parameters, the expressions read

$$\frac{d}{dt} b^{ij} = \frac{1}{16\pi^2} [\beta_b^{(1)}]^{ij} + \frac{1}{(16\pi^2)^2} [\beta_b^{(2)}]^{ij}, \quad (\text{C.14})$$

with

$$\begin{aligned} [\beta_b^{(1)}]^{ij} &= \frac{1}{2} b^{il} Y_{lmn} Y^{mnj} + \frac{1}{2} Y^{ijl} Y_{lmn} b^{mn} + \mu^{il} Y_{lmn} h^{mnj} \\ &\quad - 2 \left(b^{ij} - 2M\mu^{ij} \right) g^2 C(i) + (i \leftrightarrow j), \end{aligned} \quad (\text{C.15})$$

$$\begin{aligned} [\beta_b^{(2)}]^{ij} &= -\frac{1}{2} b^{il} Y_{lmn} Y^{pqn} Y_{pqr} Y^{mrj} - \frac{1}{2} Y^{ijl} Y_{lmn} \mu^{mr} Y_{pqr} h^{pqn} \\ &\quad - \mu^{il} Y_{lmn} h^{npq} Y_{pqr} Y^{mrj} - \mu^{il} Y_{lmn} Y^{npq} Y_{pqr} h^{mrj} \\ &\quad - \frac{1}{2} Y^{ijl} Y_{lmn} b^{mr} Y_{pqr} Y^{pqn} + 2Y^{ijl} Y_{lpq} (b^{pq} - \mu^{pq} M) g^2 C(p) \\ &\quad + \left(b^{il} Y_{lpq} Y^{pqj} + 2\mu^{il} Y_{lpq} h^{pqj} - 2\mu^{il} Y_{lpq} Y^{pqj} M \right) g^2 [2C(p) - C(i)] \\ &\quad + \left(2b^{ij} - 8\mu^{ij} M \right) g^4 \left[C(i)S(R) + 2C(i)^2 - 3C(G)C(i) \right] + (i \leftrightarrow j). \end{aligned} \quad (\text{C.16})$$

The RGEs for the linear soft-breaking parameters are

$$\frac{d}{dt} s^i = \frac{1}{16\pi^2} [\beta_s^{(1)}]^i + \frac{1}{(16\pi^2)^2} [\beta_s^{(2)}]^i, \quad (\text{C.17})$$

with

$$[\beta_s^{(1)}]^i = \frac{1}{2} Y^{iln} Y_{pln} s^p + L^p Y_{pln} h^{iln} + \mu^{ik} Y_{kln} b^{ln} + 2Y^{ikp} (m^2)_p^l \mu_{kl} + h^{ikl} b_{kl}, \quad (\text{C.18})$$

$$\begin{aligned} [\beta_s^{(2)}]^i &= 2g^2 C(l) Y^{ikl} Y_{pkl} s^p - \frac{1}{2} Y^{ikq} Y_{qst} Y^{lst} Y_{pkl} s^p - 4g^2 C(l) Y_{jnl} (\mu^{nl} M - b^{nl}) \mu^{ij} \\ &\quad - [Y^{ikq} Y_{qst} h^{lst} Y_{pkl} + h^{ikq} Y_{qst} Y^{lst} Y_{pkl}] L^p - 4g^2 C(l) (Y^{ikl} M - h^{ikl}) Y_{pkl} L^p \\ &\quad - [Y_{jnl} h^{qst} Y_{lst} \mu^{nl} + Y_{jnl} Y^{qst} Y_{lst} b^{nl}] \mu^{ij} + 4g^2 C(l) [2Y^{ikl} \mu_{kl} |M|^2 \\ &\quad - Y^{ikl} b_{kl} M - h^{ikl} \mu_{kl} M^* + h^{ikl} b_{kl} + Y^{ipl} (m^2)_p^k \mu_{kl} + Y^{ikp} (m^2)_p^l \mu_{kl}] \\ &\quad - [Y^{ikq} Y_{qst} h^{lst} b_{kl} + h^{ikq} Y_{qst} Y^{lst} b_{kl} + h^{ikq} h_{qst} Y^{lst} \mu_{kl} + Y^{ikq} h_{qst} h^{lst} \mu_{kl} \\ &\quad + Y^{ipq} (m^2)_p^k Y_{qst} Y^{lst} \mu_{kl} + Y^{ikq} Y_{qst} Y^{pst} (m^2)_p^l \mu_{kl} \\ &\quad + Y^{ikp} (m^2)_p^q Y_{qst} Y^{lst} \mu_{kl} + 2Y^{ikq} Y_{qsp} (m^2)_t^p Y^{lst} \mu_{kl}]. \end{aligned} \quad (\text{C.19})$$

With these results, the list of the β -functions for all couplings is complete. Now, we consider the RGEs for the gaugino masses and squared masses of scalars. The result for the gaugino masses is

$$\frac{d}{dt} M = \frac{1}{16\pi^2} \beta_M^{(1)} + \frac{1}{(16\pi^2)^2} \beta_M^{(2)}, \quad (\text{C.20})$$

with

$$\beta_M^{(1)} = g^2 [2S(R) - 6C(G)] M, \quad (\text{C.21})$$

$$\begin{aligned} \beta_M^{(2)} &= g^4 [-24C(G)^2 + 8C(G)S(R) + 16S(R)C(R)] M \\ &\quad + 2g^2 (h^{ijk} - MY^{ijk}) Y_{ijk} C(k) / d(G). \end{aligned} \quad (\text{C.22})$$

The one- and two-loop RGEs for the scalar mass parameters read

$$\frac{d}{dt} (m^2)_i^j = \frac{1}{16\pi^2} [\beta_{m^2}^{(1)}]_i^j + \frac{1}{(16\pi^2)^2} [\beta_{m^2}^{(2)}]_i^j, \quad (\text{C.23})$$

with

$$\begin{aligned} [\beta_{m^2}^{(1)}]_i^j &= \frac{1}{2} Y_{ipq} Y^{pqn} (m^2)_n^j + \frac{1}{2} Y^{jpn} Y_{ipq} (m^2)_i^n + 2Y_{ipq} Y^{jpr} (m^2)_r^q + h_{ipq} h^{jpn} \\ &\quad - 8\delta_i^j |M|^2 g^2 C(i) + 2g^2 \mathbf{t}_i^A \text{Tr}[\mathbf{t}^A m^2], \end{aligned} \quad (\text{C.24})$$

$$[\beta_{m^2}^{(2)}]_i^j = -\frac{1}{2} (m^2)_i^l Y_{lmn} Y^{mrj} Y_{pqr} Y^{pqn} - \frac{1}{2} (m^2)_l^j Y^{lmn} Y_{mri} Y^{pqr} Y_{pqn}$$

$$\begin{aligned}
& - h_{ilm} Y^{jln} Y_{npq} h^{mpq} - Y_{ilm} Y^{jnm} (m^2)_n^r Y_{rpq} Y^{lpq} - Y_{ilm} Y^{jnr} (m^2)_n^l Y_{pqr} Y^{pqm} \\
& - Y_{ilm} Y^{jln} h_{npq} h^{mpq} - 2Y_{ilm} Y^{jln} Y_{npq} Y^{mpr} (m^2)_r^q - h_{ilm} h^{jln} Y_{npq} Y^{mpq} \\
& - Y_{ilm} Y^{jnm} (m^2)_r^l Y_{npq} Y^{rpq} - Y_{ilm} h^{jln} h_{npq} Y^{mpq} \\
& + \left[(m^2)_i^l Y_{lpq} Y^{jpa} + Y_{ipq} Y^{lpq} (m^2)_l^j + 4Y_{ipq} Y^{jpl} (m^2)_l^q + 2h_{ipq} h^{jpa} \right. \\
& - 2h_{ipq} Y^{jpa} M - 2Y_{ipq} h^{jpa} M^* + 4Y_{ipq} Y^{jpa} |M|^2 \left. \right] g^2 [C(p) + C(q) - C(i)] \\
& - 2g^2 \mathbf{t}_i^{Aj} \left(\mathbf{t}^A m^2 \right)_r^l Y_{lpq} Y^{rpq} + 8g^4 \mathbf{t}_i^{Aj} \text{Tr} \left[\mathbf{t}^A C(r) m^2 \right] \\
& + \delta_i^j g^4 |M|^2 \left[24C(i)S(R) + 48C(i)^2 - 72C(G)C(i) \right] \\
& + 8\delta_i^j g^4 C(i) \left\{ \text{Tr}[S(r)m^2] - C(G) |M|^2 \right\} . \tag{C.25}
\end{aligned}$$

Finally, partial expressions for the RGEs for a VEV v^i can be found in [577].

A few comments and clarifications concerning the variables appearing in the different β -functions are necessary:

- $Y_{ijk} = (Y^{ijk})^*$, $h_{ijk} = (h^{ijk})^*$, $\mu_{ij} = (\mu^{ij})^*$ and $b_{ij} = (b^{ij})^*$.
- $d(G)$ = Dimension of the adjoint representation of group G .
- $C(i)$ = Quadratic Casimir invariant of the representation of the chiral superfield with index i .
- $C(G)$ = Quadratic Casimir invariant of the adjoint representation of group G .
- $S(R)$ = Dynkin index summed over all chiral multiplets. However $S(R)C(R)$ should be interpreted as the sum of Dynkin indices weighted by the quadratic Casimir invariant.
- \mathbf{t}^A = Representation matrices under the gauge group G . Terms with \mathbf{t}^A are only relevant for $U(1)$ groups.
- In $\beta_{m^2}^{(1)}$ and $\beta_{m^2}^{(2)}$, the traces should be understood as traces over all chiral superfields.

C.2 PRODUCT GROUPS WITH AT MOST ONE $U(1)$

To generalize the formulae above to the case of a direct product of gauge groups, the following substitution rules are needed [430]. As long as there is at most one $U(1)$ gauge group, this procedure will yield the correct results; otherwise the rules must be generalized, as discussed in section 6.3.

$$g^3 C(G) \rightarrow g_a^3 C(G_a), \tag{C.26}$$

$$g^3 S(R) \rightarrow g_a^3 S_a(R), \tag{C.27}$$

$$g^5 C(G)^2 \rightarrow g_a^5 C(G_a)^2, \quad (\text{C.28})$$

$$g^5 C(G)S(R) \rightarrow g_a^5 C(G_a)S_a(R), \quad (\text{C.29})$$

$$g^5 S(R)C(R) \rightarrow \sum_b g_a^3 g_b^2 S_a(R)C_b(R), \quad (\text{C.30})$$

$$g^3 C(k)/d(G) \rightarrow g_a^3 C_a(k)/d(G_a), \quad (\text{C.31})$$

$$Mg^2 C(G) \rightarrow M_a g_a^2 C(G_a), \quad (\text{C.32})$$

$$Mg^2 S(R) \rightarrow M_a g_a^2 S_a(R), \quad (\text{C.33})$$

$$Mg^4 C(G)^2 \rightarrow M_a g_a^4 C(G_a)^2, \quad (\text{C.34})$$

$$Mg^4 C(G)S(R) \rightarrow M_a g_a^4 C(G_a)S_a(R), \quad (\text{C.35})$$

$$16Mg^4 S(R)C(R) \rightarrow 8 \sum_b (M_a + M_b) g_a^2 g_b^2 S_a(R)C_b(R), \quad (\text{C.36})$$

$$Mg^2 C(k)/d(G) \rightarrow M_a g_a^2 C_a(k)/d(G_a), \quad (\text{C.37})$$

$$g^2 C(r) \rightarrow \sum_a g_a^2 C_a(r), \quad (\text{C.38})$$

$$Mg^2 C(r) \rightarrow \sum_a M_a g_a^2 C_a(r), \quad (\text{C.39})$$

$$M^* g^2 C(r) \rightarrow \sum_a M_a^* g_a^2 C_a(r), \quad (\text{C.40})$$

$$|M|^2 g^2 C(r) \rightarrow \sum_a |M_a|^2 g_a^2 C_a(r), \quad (\text{C.41})$$

$$g^4 C(r)S(R) \rightarrow \sum_a g_a^4 C_a(r)S_a(R), \quad (\text{C.42})$$

$$Mg^4 C(r)S(R) \rightarrow \sum_a M_a g_a^4 C_a(r)S_a(R), \quad (\text{C.43})$$

$$g^4 C(r)^2 \rightarrow \sum_a \sum_b g_a^2 g_b^2 C_a(r)C_b(r), \quad (\text{C.44})$$

$$Mg^4 C(r)^2 \rightarrow \sum_a \sum_b M_a g_a^2 g_b^2 C_a(r)C_b(r), \quad (\text{C.45})$$

$$g^4 C(r)C(G) \rightarrow \sum_a g_a^4 C_a(r)C(G_a), \quad (\text{C.46})$$

$$Mg^4 C(r)C(G) \rightarrow \sum_a M_a g_a^4 C_a(r)C(G_a), \quad (\text{C.47})$$

$$|M|^2 g^4 C(r)C(G) \rightarrow \sum_a |M_a|^2 g_a^4 C_a(r)C(G_a), \quad (\text{C.48})$$

$$48 |M|^2 g^4 C(i)^2 \rightarrow \sum_a \sum_b (32M_a + 16M_b) M_a^* g_a^2 g_b^2 C_a(i)C_b(i), \quad (\text{C.49})$$

$$|M|^2 g^4 C(i)S(R) \rightarrow \sum_a |M_a|^2 g_a^4 C_a(i)S_a(R), \quad (\text{C.50})$$

$$g^2 \mathbf{t}_i^{Aj} \text{Tr} \left(\mathbf{t}^A m^2 \right) \rightarrow \sum_a g_a^2 \left(\mathbf{t}_a^A \right)_i^j \text{Tr} \left(\mathbf{t}_a^A m^2 \right), \quad (\text{C.51})$$

$$g^2 \mathbf{t}_i^{Aj} \left(\mathbf{t}^A m^2 \right)_r^l Y_{lpq} Y^{rpq} \rightarrow \sum_a g_a^2 \left(\mathbf{t}_a^A \right)_i^j \left(\mathbf{t}_a^A m^2 \right)_r^l Y_{lpq} Y^{rpq}, \quad (\text{C.52})$$

$$g^4 \mathbf{t}_i^{Aj} \text{Tr} \left[\mathbf{t}^A C(r) m^2 \right] \rightarrow \sum_a \sum_b g_a^2 g_b^2 \left(\mathbf{t}_a^A \right)_i^j \text{Tr} \left[\mathbf{t}_a^A C_b(r) m^2 \right], \quad (\text{C.53})$$

$$g^4 C(i) \text{Tr} [S(r)m^2] \rightarrow \sum_a g_a^4 C_a(i) \text{Tr} [S_a(r)m^2]. \quad (\text{C.54})$$

When there is an index a not summed over (equations (C.26)–(C.37)), this means that the corresponding rule is for the RGEs of a gauge coupling g_a or a gaugino mass M_a .

MATCHING CONDITIONS FOR GAUGE COUPLINGS AND GAUGINO MASSES IN MODELS WITH $U(1)$ -MIXING

As a complement to chapter 6, in this appendix we discuss how to proceed with the matching of gauge couplings and gaugino masses in models with a phase where the gauge group is $U(1)^n$ which spontaneously breaks down into $U(1)^m$ with $m < n$ [2]. We shall not deal with non-abelian factors since it is straightforward to take them into account. Note also that this is a one-loop discussion—at higher orders the situation becomes more involved, as there are non-trivial threshold effects to be considered [578, 579], yielding for example extra factors associated to non-abelian gauge groups, entering formulas such as equation (D.12) below—see for instance [580]. The specific shape of these terms is, however, renormalization scheme dependent.

D.1 GAUGE COUPLINGS

Here we assume the same setting as the one described in chapter 6, namely that there are scalar fields ϕ_i (we may ignore their fermionic partners) with charge vectors \mathbf{Q}_i , such that the covariant derivative is written as

$$D_\mu \phi_i = \left(\partial_\mu - i \mathbf{Q}_i^T \mathbf{G} \mathbf{A}_\mu \right) \phi_i. \quad (\text{D.1})$$

Therefore, if the scalar fields acquire a VEV, there will be a gauge boson mass term

$$\mathcal{L}_A = \frac{1}{2} \mathbf{A}_\mu^T \mathbf{M}_A^2 \mathbf{A}_\mu, \quad M_A^2 = \sum_i 2 |\langle \phi_i \rangle|^2 \mathbf{G}^T \mathbf{Q}_i \mathbf{Q}_i^T \mathbf{G}. \quad (\text{D.2})$$

Some of the $U(1)$ groups will be broken by these VEVs but in principle there will be m linearly independent combinations of the n original $U(1)$'s that remain unbroken. Thus, we should do a \mathcal{O}_1 rotation in $U(1)$ space such that the first m rotated $U(1)$'s are the unbroken ones. By doing this, for all i we find new charges

$$\mathbf{Q}'_i \equiv \mathcal{O}_1 \mathbf{Q}_i, \quad (\text{D.3})$$

and by construction

$$\forall_i \mathbf{Q}'_i{}^j \langle \phi_i \rangle = 0 \text{ for } j = 1, \dots, m, \quad (\text{D.4})$$

$$\exists_i \mathbf{Q}'_i{}^j \langle \phi_i \rangle \neq 0 \text{ for } j = m + 1, \dots, n. \quad (\text{D.5})$$

The gauge boson mass matrix is then of the following form:

$$M_A^2 = \mathbf{G}^T \mathcal{O}_1^T \begin{pmatrix} \mathbf{0} & \mathbf{0} \\ \mathbf{0} & \mathbf{X} \end{pmatrix} \mathcal{O}_1 \mathbf{G}, \quad (\text{D.6})$$

where \mathbf{X} is some non-null $(n-m) \times (n-m)$ matrix. M_A^2 will not be block diagonal unless we also rotate the gauge boson states in such a way that the first m rotated fields are massless,

$$A'_\mu \equiv \mathcal{O}_2 A_\mu. \quad (\text{D.7})$$

This gives rise to a new matrix of gauge couplings

$$\mathbf{G}' \equiv \mathcal{O}_1 \mathbf{G} \mathcal{O}_2^T, \quad (\text{D.8})$$

and, in this new basis, we have

$$M_{A'}^2 = \mathbf{G}'^T \begin{pmatrix} \mathbf{0} & \mathbf{0} \\ \mathbf{0} & \mathbf{X}' \end{pmatrix} \mathbf{G}' \equiv \begin{pmatrix} \mathbf{0} & \mathbf{0} \\ \mathbf{0} & \mathbf{X}' \end{pmatrix} \quad (\text{D.9})$$

for some \mathbf{X}' . Note that the last equality is true by construction: the first m gauge bosons are the massless ones, while the remaining ones are not (an additional rotation might be needed to bring \mathbf{X}' into a diagonal form). Equation (D.9) will only hold if

$$\mathbf{G}' = \begin{pmatrix} \mathbf{G}'_{SS} & \mathbf{G}'_{SB} \\ \mathbf{0} & \mathbf{G}'_{BB} \end{pmatrix}. \quad (\text{D.10})$$

The interpretation of this $\mathbf{0}$ in the $(2, 1)$ block is that the massless gauge bosons will only interact with the matter fields via the charges $\mathbf{Q}'_i{}^j$ with $j = 1, \dots, m$ as we would expect. To see this we only have to consider the covariant derivative in the rotated basis, which amounts to adding primes to equation (D.1):

$$\begin{aligned} D_\mu \phi_i &= \partial_\mu \phi_i - i \mathbf{Q}'_i{}^T \mathbf{G}' A'_\mu \phi_i \\ &= \partial_\mu \phi_i - i \sum_{a,b=1}^m \mathbf{Q}'_i{}^a (\mathbf{G}'_{SS})_{ab} A'_\mu{}^b \phi_i + \left(\text{interactions with heavy } A'_\mu{}^b \text{ s} \right). \end{aligned} \quad (\text{D.11})$$

Finally, notice that we are still free to rotate the light gauge bosons $A'_\mu{}^{1, \dots, m}$ among themselves, so we cannot predict completely \mathbf{G}'_{SS} since it is basis dependent. The solution to this problem is nonetheless clear: we should focus on $\mathbf{G}'_{SS} \mathbf{G}'_{SS}{}^T$ instead. Unfortunately, the $(1, 1)$ block of $\mathbf{G}' \mathbf{G}'^T$ is equal to the combination $\mathbf{G}'_{SS} \mathbf{G}'_{SS}{}^T +$

$\mathbf{G}'_{SB}\mathbf{G}'_{SB}{}^T$ so it cannot be used to extract directly this quantity, but on the other hand, the (1, 1) block of $(\mathbf{G}'\mathbf{G}'^T)^{-1}$ is suitable for this:

$$\left[(\mathcal{O}_1 \mathbf{G} \mathbf{G}^T \mathcal{O}_1^T)^{-1} \right]_{\text{block (1,1)}} = \left[(\mathbf{G}' \mathbf{G}'^T)^{-1} \right]_{\text{block (1,1)}} = (\mathbf{G}'_{SS} \mathbf{G}'_{SS}{}^T)^{-1}. \quad (\text{D.12})$$

As an example, consider the $U(1)_R \times U(1)_{B-L}$ symmetry of class-III models discussed in chapter 7, which breaks down into $U(1)_Y$. Before SSB there is a 2×2 $U(1)$ gauge couplings matrix

$$\mathbf{G} = \begin{pmatrix} g_{RR} & g_{RX} \\ g_{XR} & g_{XX} \end{pmatrix}, \quad (\text{D.13})$$

where $X \equiv \sqrt{3/5}(B-L)$ refers to the properly normalized $B-L$ abelian group. The hypercharge under $U(1)_Y$ is given by the relation $\sqrt{3/5}[U(1)_R \text{ hypercharge}] + \sqrt{2/5}[U(1)_{B-L} \text{ hypercharge}]$ (see appendix E), so according to equation (D.12) the gauge coupling matching condition is

$$\begin{aligned} g_Y^{-2} &= \begin{pmatrix} \sqrt{3/5} & \sqrt{2/5} \end{pmatrix} (\mathbf{G} \mathbf{G}^T)^{-1} \begin{pmatrix} \sqrt{3/5} \\ \sqrt{2/5} \end{pmatrix} \\ &= \frac{2(g_{RR}^2 + g_{RX}^2) + 3(g_{XX}^2 + g_{XR}^2) - 2\sqrt{6}(g_{RR}g_{XR} + g_{XX}g_{RX})}{5(g_{RR}g_{XX} - g_{RX}g_{XR})^2}. \end{aligned} \quad (\text{D.14})$$

Only in the limit $g_{RX}, g_{XR} \rightarrow 0$ do we recover the simplified relation $g_Y^{-2} = 3/5g_{RR}^{-2} + 2/5g_{XX}^{-2}$.

D.2 GAUGINO MASSES

Gauginos interact with the fermionic and scalar components of chiral superfields, so when the latter acquire VEVs, a mass term is generated, mixing fermions from chiral and vector superfields. In the rotated, primed basis we have

$$\mathcal{L} = \begin{pmatrix} \lambda & \psi_j \end{pmatrix} \begin{pmatrix} \mathbf{M}' & \sqrt{2}\mathbf{G}'^T \mathbf{Q}'_i \langle \phi_i \rangle \\ \sqrt{2}\mathbf{Q}'_j{}^T \mathbf{G}' \langle \phi_j \rangle & \frac{\delta^2 W}{\delta \Phi_i \delta \Phi_j} \end{pmatrix} \begin{pmatrix} \lambda \\ \psi_i \end{pmatrix} + \text{h.c.} + \dots, \quad (\text{D.15})$$

where $\mathbf{M}' = \mathcal{O}_2 \mathbf{M} \mathcal{O}_2^T$ is the rotated gaugino soft mass matrix and W refers to the superpotential. Now notice that together, equations (D.4), (D.5) and (D.10) imply that in block notation $\mathbf{G}'^T \mathbf{Q}'_i \langle \phi_i \rangle = \begin{pmatrix} \mathbf{0} & [\dots] \end{pmatrix}^T$. In other words, the first m rows and columns of the matrix in the previous equation, which correspond to the λ 's associated with the massless gauge bosons, only receive a non-null contribution from the \mathbf{M}' matrix itself. As such, if we define \mathbf{M}' in blocks,

$$\mathbf{M}' \equiv \begin{pmatrix} \mathbf{M}'_{SS} & \mathbf{M}'_{SB} \\ \mathbf{M}'_{SB}{}^T & \mathbf{M}'_{BB} \end{pmatrix}, \quad (\text{D.16})$$

the gaugino mass matrix in the broken phase $U(1)^m$ is given simply by the $m \times m$ block \mathbf{M}'_{SS} . Analogously to what happens to \mathbf{G} , here too we have a basis problem: firstly, we need the rotation matrix \mathcal{O}_2 in order to define \mathbf{M}' ; and secondly, we will always retain the freedom to perform rotations between the massless gauge bosons, which means that the exact form of the (1, 1) block \mathbf{M}'_{SS} of the full gaugino mass matrix \mathbf{M}' will always be basis dependent. Here the sensible solution is to consider a combination of \mathbf{M}' and \mathbf{G}' which is \mathcal{O}_2 invariant and from which it is easy to extract the (1, 1) block \mathbf{M}'_{SS} . The best solution seems to be the following:

$$\begin{aligned} \left[\mathcal{O}_1 \mathbf{G}^{-1T} \mathbf{M} \mathbf{G}^{-1} \mathcal{O}_1^T \right]_{\text{block (1,1)}} &= \left[\mathbf{G}'^{-1T} \mathbf{M}' \mathbf{G}'^{-1} \right]_{\text{block (1,1)}} \\ &= \mathbf{G}'_{SS}{}^{-1T} \mathbf{M}'_{SS} \mathbf{G}'_{SS}{}^{-1}. \end{aligned} \quad (\text{D.17})$$

We may consider the simple case $U(1)_R \times U(1)_{B-L} \rightarrow U(1)_Y$ once more. In the $U(1)$ -mixing phase, the gaugino mass matrix is 2×2 ,

$$\mathbf{M} = \begin{pmatrix} M_{RR} & M_{RX} \\ M_{RX} & M_{XX} \end{pmatrix}, \quad (\text{D.18})$$

and at the matching scale we have

$$\begin{aligned} \frac{M_Y}{g_Y^2} &= \frac{1}{5(g_{RR}g_{XX} - g_{RX}g_{XR})^2} \left[(3g_{XX}^2 + 2g_{RX}^2 - 2\sqrt{6}g_{XX}g_{RX}) M_{RR} \right. \\ &\quad + (2g_{RR}^2 + 3g_{XR}^2 - 2\sqrt{6}g_{RR}g_{XR}) M_{XX} \\ &\quad \left. + (-4g_{RR}g_{RX} - 6g_{XX}g_{XR} + 2\sqrt{6}g_{RR}g_{XX} + 2\sqrt{6}g_{RX}g_{XR}) M_{RX} \right]. \end{aligned} \quad (\text{D.19})$$

In the absence of mixing, this expression becomes $M_Y/g_Y^2 = 3/5 M_{RR}/g_{RR}^2 + 2/5 M_{XX}/g_{XX}^2$ or $M_Y = (3g_{XX}^2 M_{RR} + 2g_{RR}^2 M_{XX}) / (3g_{XX}^2 + 2g_{RR}^2)$ if we eliminate g_Y from the equation.

LISTS OF SUPERFIELDS IN LEFT-RIGHT MODELS

In chapter 7 we have considered $SO(10)$ -inspired models which may contain any irreducible representation up to dimension 126 (**1**, **10**, **16**, **$\overline{16}$** , **45**, **54**, **120**, **126**, **$\overline{126}$**) [3]. Once the gauge group breaks down to $SU(4) \times SU(2)_L \times SU(2)_R$ or $SU(3)_C \times SU(2)_L \times SU(2)_R \times U(1)_{B-L}$ these $SO(10)$ fields divide into a multitude of different irreducible representations of these groups. In addition, if $SU(2)_R$ is further broken down further to $U(1)_R$, the following branching rules apply: $\mathbf{3} \rightarrow -1, 0, +1$; $\mathbf{2} \rightarrow \pm\frac{1}{2}$; $\mathbf{1} \rightarrow 0$. The Standard Model's hypercharge, in the canonical normalization, is then equal to the combination $\sqrt{\frac{3}{5}}[U(1)_R \text{ hypercharge}] + \sqrt{\frac{2}{5}}[U(1)_{B-L} \text{ hypercharge}]$. In tables (22), (23) and (24) we present the list of relevant fields respecting the conditions above. In these tables we used an ordered naming of the fields but note that in chapter 7 we favor another, less compact, notation where the quantum numbers under the various groups are indicated explicitly (see for instance table (14)).

Finally, we point out here that in order for a group G to break into a subgroup $H \subset G$, there must be one or more fields transforming non-trivially under G which contain a singlet of H that acquires a vacuum expectation value. Non-trivial here means that the singlet(s) of H contained in this(these) field(s) must also break any group G' such that $H \subset G' \subseteq G$. From this observation alone we know that certain fields must be present in a fundamental model if we are to achieve a given breaking sequence—this is shown schematically in figure (34) for the groups considered in chapter 7.

		Subgroup		
		LR	BL	SM
Group	PS	Ψ_{10}	$\Psi_4 + \Psi_{10}$	Ψ_{13}, Ψ_{17} or conjugates
	LR		Φ_5	Φ_3, Φ_{17} or conjugates
	BL			Φ'_4, Φ'_{20} or conjugates

Figure 34: Specific fields which are needed to break a group (rows) into a given subgroup (columns).

	Φ_1	Φ_2	Φ_3	Φ_4	Φ_5	Φ_6	Φ_7	Φ_8	Φ_9	Φ_{10}	Φ_{11}	Φ_{12}	Φ_{13}	Φ_{14}
	χ	χ^c	Ω	Ω^c	Φ				δ_d	δ_u				
$SU(3)_C$	1	1	1	1	1	1	8	1	3	3	6	6	3	3
$SU(2)_L$	1	2	1	3	1	2	1	1	1	1	1	1	2	1
$SU(2)_R$	1	1	2	1	3	2	1	1	1	1	1	1	1	2
$U(1)_{B-L}$	0	+1	-1	0	0	0	0	+2	$-\frac{2}{3}$	$+\frac{4}{3}$	$+\frac{2}{3}$	$-\frac{4}{3}$	$+\frac{1}{3}$	$+\frac{1}{3}$
PS origin	Ψ_1 Ψ_{10}	$\bar{\Psi}_{12}$	Ψ_{13}	Ψ_3	Ψ_4	Ψ_2 Ψ_7	Ψ_{10} Ψ_{11}	$\bar{\Psi}_9$	Ψ_8 Ψ_9	Ψ_{10}	Ψ_9	Ψ_{11}	Ψ_{12}	Ψ_{13}

	Φ_{15}	Φ_{16}	Φ_{17}	Φ_{18}	Φ_{19}	Φ_{20}	Φ_{21}	Φ_{22}	Φ_{23}	Φ_{24}
	Δ	Δ^c								
$SU(3)_C$	8	1	1	3	3	3	6	6	1	3
$SU(2)_L$	2	3	1	2	3	1	3	1	3	2
$SU(2)_R$	2	1	3	2	1	3	1	3	3	2
$U(1)_{B-L}$	0	-2	-2	$+\frac{4}{3}$	$-\frac{2}{3}$	$-\frac{2}{3}$	$+\frac{2}{3}$	$+\frac{2}{3}$	0	$-\frac{2}{3}$
PS origin	Ψ_7	Ψ_{16}	Ψ_{17}	Ψ_7	Ψ_{14} Ψ_{16}	Ψ_{15} Ψ_{17}	Ψ_{16}	Ψ_{17}	Ψ_5	Ψ_6

Table 22: Naming conventions and transformation properties of fields in the left-right symmetric regime (excluding conjugates). The last row exhibits the Pati-Salam regime fields from which they may originate. The charges under the $U(1)_{B-L}$ group shown here were multiplied by a factor $\sqrt{\frac{8}{3}}$.

	Ψ_1	Ψ_2	Ψ_3	Ψ_4	Ψ_5	Ψ_6	Ψ_7	Ψ_8	Ψ_9	Ψ_{10}	Ψ_{11}	Ψ_{12}	Ψ_{13}	Ψ_{14}	Ψ_{15}	Ψ_{16}	Ψ_{17}
$SU(4)$	1	1	1	1	1	6	15	6	10	15	20'	4	4	6	6	10	10
$SU(2)_L$	1	2	3	1	3	2	2	1	1	1	1	2	1	3	1	3	1
$SU(2)_R$	1	2	1	3	3	2	2	1	1	1	1	1	2	1	3	1	3
$SO(10)$	1	10	45	45	54	45	120	10	120	45	54	16	$\bar{16}$	120	120	126	$\bar{126}$
Origin	54	120				54	126	126									

Table 23: Naming conventions and transformation properties of fields in the Pati-Salam regime (excluding conjugates). The last row exhibits the $SO(10)$ representations from which they may originate.

	Φ'_1	Φ'_2	Φ'_3	Φ'_4	Φ'_5	Φ'_6	Φ'_7	Φ'_8	Φ'_9	Φ'_{10}	Φ'_{11}	Φ'_{12}	Φ'_{13}	Φ'_{14}	Φ'_{15}	Φ'_{16}
$SU(3)_C$	1	1	1	1	1	1	1	8	1	3	3	6	6	3	3	3
$SU(2)_L$	1	2	1	1	3	1	2	1	1	1	1	1	1	2	1	1
$U(1)_R$	0	0	$-\frac{1}{2}$	$+\frac{1}{2}$	0	+1	$+\frac{1}{2}$	0	0	0	0	0	0	0	$-\frac{1}{2}$	$+\frac{1}{2}$
$U(1)_{B-L}$	0	+1	-1	-1	0	0	0	0	+2	$-\frac{2}{3}$	$+\frac{4}{3}$	$+\frac{2}{3}$	$-\frac{4}{3}$	$+\frac{1}{3}$	$+\frac{1}{3}$	$+\frac{1}{3}$
LR	Φ_1	Φ_2	Φ_3	Φ_3	Φ_4	Φ_5	Φ_6	Φ_7	Φ_8	Φ_9	Φ_{10}	Φ_{11}	Φ_{12}	Φ_{13}	Φ_{14}	Φ_{14}
origin	Φ_5				Φ_{23}				$\bar{\Phi}_{17}$	Φ_{20}		Φ_{22}				

	Φ'_{17}	Φ'_{18}	Φ'_{19}	Φ'_{20}	Φ'_{21}	Φ'_{22}	Φ'_{23}	Φ'_{24}	Φ'_{25}	Φ'_{26}	Φ'_{27}	Φ'_{28}	Φ'_{29}	Φ'_{30}	Φ'_{31}
$SU(3)_C$	8	1	1	1	3	3	3	3	3	6	6	6	1	3	3
$SU(2)_L$	2	3	1	1	2	2	3	1	1	3	1	1	3	2	2
$U(1)_R$	$+\frac{1}{2}$	0	-1	+1	$-\frac{1}{2}$	$+\frac{1}{2}$	0	-1	+1	0	-1	+1	+1	$-\frac{1}{2}$	$+\frac{1}{2}$
$U(1)_{B-L}$	0	-2	-2	-2	$+\frac{4}{3}$	$+\frac{4}{3}$	$-\frac{2}{3}$	$-\frac{2}{3}$	$-\frac{2}{3}$	$+\frac{2}{3}$	$+\frac{2}{3}$	$+\frac{2}{3}$	0	$-\frac{2}{3}$	$-\frac{2}{3}$
LR	Φ_{15}	Φ_{16}	Φ_{17}	Φ_{17}	Φ_{18}	Φ_{18}	Φ_{19}	Φ_{20}	Φ_{20}	Φ_{21}	Φ_{22}	Φ_{22}	Φ_{23}	Φ_{24}	Φ_{24}
origin															

Table 24: Naming conventions and transformation properties of fields in the $U(1)$ mixing regime (excluding conjugates). The last row exhibits the left-right regime fields from which they may originate. The charges under the $U(1)_{B-L}$ group shown here were multiplied by a factor $\sqrt{\frac{8}{3}}$.

RENORMALIZATION OF THE $\nu\ell H^+$ VERTEX

In what follows we detail the computation leading to equations (8.11)–(8.13) of chapter 8 (see also [4]), further referring to [516] for a similar analysis. As expected, loop effects contribute to both kinetic and mass terms of charged leptons as well as to the $\nu\ell H^+$ vertex:

$$\begin{aligned} \mathcal{L}_0^{H^\pm} &= i\bar{\ell}_L (\mathbb{1} + \eta_L^\ell) \not{\partial} \ell_L + i\bar{\ell}_R (\mathbb{1} + \eta_R^\ell) \not{\partial} \ell_R \\ &\quad + i\bar{\nu}_L (\mathbb{1} + \eta_L^\nu) \not{\partial} \nu_L - \left[\bar{\ell}_L (M^{\ell 0} + \eta_m^\ell) \ell_R + \text{h.c.} \right] \\ &\quad + \left[\bar{\nu}_L (2^{3/4} G_F^{1/2} \tan \beta M^{\ell 0} + \eta^H) \ell_R H^+ + \text{h.c.} \right]. \end{aligned} \quad (\text{F.1})$$

Here $M^{\ell 0}$ denotes the bare charged lepton mass and the η 's correspond to loop contributions to the various terms. The (new) kinetic terms can be recast into a canonical form by means of unitary rotations of the fields $(K_L^\ell, K_R^\ell, K_L^\nu)$, which are then renormalized by diagonal transformations $(\hat{Z}_L^\ell, \hat{Z}_R^\ell, \hat{Z}_L^\nu)$:

$$\ell_L^{\text{old}} = K_L^\ell (\hat{Z}_L^\ell)^{-\frac{1}{2}} \ell_L^{\text{new}}, \quad \hat{Z}_L^\ell = K_L^{\ell \dagger} (\mathbb{1} + \eta_L^\ell) K_L^\ell, \quad (\text{F.2})$$

$$\ell_R^{\text{old}} = K_R^\ell (\hat{Z}_R^\ell)^{-\frac{1}{2}} \ell_R^{\text{new}}, \quad \hat{Z}_R^\ell = K_R^{\ell \dagger} (\mathbb{1} + \eta_R^\ell) K_R^\ell, \quad (\text{F.3})$$

$$\nu_L^{\text{old}} = K_L^\nu (\hat{Z}_L^\nu)^{-\frac{1}{2}} \nu_L^{\text{new}}, \quad \hat{Z}_L^\nu = K_L^{\nu \dagger} (\mathbb{1} + \eta_L^\nu) K_L^\nu. \quad (\text{F.4})$$

Two unitary rotation matrices (R_L^ℓ, R_R^ℓ) are further required to diagonalize the charged lepton mass matrix, and one finally has

$$\ell_L^{\text{old}} = K_L^\ell (\hat{Z}_L^\ell)^{-\frac{1}{2}} R_L^\ell \ell_L^{\text{new}}, \quad (\text{F.5})$$

$$\ell_R^{\text{old}} = K_R^\ell (\hat{Z}_R^\ell)^{-\frac{1}{2}} R_R^\ell \ell_R^{\text{new}}, \quad (\text{F.6})$$

$$\nu_L^{\text{old}} = K_L^\nu (\hat{Z}_L^\nu)^{-\frac{1}{2}} R_L^\ell \nu_L^{\text{new}}. \quad (\text{F.7})$$

In the new basis, the mass terms now read

$$\begin{aligned} \mathcal{L}^{\text{mass}} &\equiv -\bar{\ell}_L M^\ell \ell_R + \text{h.c.} \\ &= -\bar{\ell}_L R_L^{\ell \dagger} \left[(\hat{Z}_L^\ell)^{-\frac{1}{2}} K_L^{\ell \dagger} (M^{\ell 0} + \eta_m^\ell) K_R^\ell (\hat{Z}_R^\ell)^{-\frac{1}{2}} \right] R_R^\ell \ell_R + \text{h.c.} \end{aligned} \quad (\text{F.8})$$

The above equation relates the unknown parameter $M^{\ell 0}$ with the physical mass matrix M^ℓ . Using the latter to rewrite the $\nu\ell H^+$ vertex, one finds

$$\mathcal{L}^{H^\pm} \equiv \bar{\nu}_L Z^H \ell_R H^+ + \text{h.c.}, \quad (\text{F.9})$$

where

$$Z^H = 2^{3/4} G_F^{1/2} \tan \beta R_L^{\ell \dagger} \left(\hat{Z}_L^\nu \right)^{-\frac{1}{2}} K_L^{\nu \dagger} K_L^\ell \left(\hat{Z}_L^\ell \right)^{\frac{1}{2}} R_L^\ell M^\ell \\ + R_L^{\ell \dagger} \left(\hat{Z}_L^\nu \right)^{-\frac{1}{2}} K_L^{\nu \dagger} \left(-2^{3/4} G_F^{1/2} \tan \beta \eta_m^\ell + \eta^H \right) K_R^\ell \left(\hat{Z}_R^\ell \right)^{-\frac{1}{2}} K_R^\ell. \quad (\text{F.10})$$

To one-loop order, this exact expression simplifies to

$$Z^H = 2^{3/4} G_F^{1/2} \tan \beta \left[\left(\mathbb{1} + \frac{\eta_L^\ell}{2} - \frac{\eta_L^\nu}{2} \right) M^\ell - \eta_m^\ell \right] + \eta^H. \quad (\text{F.11})$$

The expressions for the η 's can be computed from the relevant Feynman diagrams (assuming zero external momenta):

$$-(4\pi)^2 \left(\eta_m^\ell \right)_{ij} = N_{i\alpha\beta}^{R(\ell)} N_{j\alpha\beta}^{L(\ell)*} m_{\chi_\alpha^0} B_0 \left(0, m_{\chi_\alpha^0}^2, m_{\tilde{\ell}_\beta}^2 \right) + \\ + C_{i\alpha\beta}^{R(\ell)} C_{j\alpha\beta}^{L(\ell)*} m_{\chi_\alpha^\pm} B_0 \left(0, m_{\chi_\alpha^\pm}^2, m_{\tilde{\nu}_\beta}^2 \right), \quad (\text{F.12})$$

$$-(4\pi)^2 \left(\eta_R^\ell \right)_{ij} = N_{i\alpha\beta}^{L(\ell)} N_{j\alpha\beta}^{L(\ell)*} B_1 \left(0, m_{\chi_\alpha^0}^2, m_{\tilde{\ell}_\beta}^2 \right) \\ + C_{i\alpha\beta}^{L(\ell)} C_{j\alpha\beta}^{L(\ell)*} B_1 \left(0, m_{\chi_\alpha^\pm}^2, m_{\tilde{\nu}_\beta}^2 \right), \quad (\text{F.13})$$

$$-(4\pi)^2 \left(\eta_L^\ell \right)_{ij} = N_{i\alpha\beta}^{R(\ell)} N_{j\alpha\beta}^{R(\ell)*} B_1 \left(0, m_{\chi_\alpha^0}^2, m_{\tilde{\ell}_\beta}^2 \right) \\ + C_{i\alpha\beta}^{R(\ell)} C_{j\alpha\beta}^{R(\ell)*} B_1 \left(0, m_{\chi_\alpha^\pm}^2, m_{\tilde{\nu}_\beta}^2 \right), \quad (\text{F.14})$$

$$-(4\pi)^2 \left(\eta_L^\nu \right)_{ij} = N_{i\alpha\beta}^{R(\nu)} N_{j\alpha\beta}^{R(\nu)*} B_1 \left(0, m_{\chi_\alpha^0}^2, m_{\tilde{\nu}_\beta}^2 \right) \\ + C_{i\alpha\beta}^{R(\nu)} C_{j\alpha\beta}^{R(\nu)*} B_1 \left(0, m_{\chi_\alpha^\pm}^2, m_{\tilde{\ell}_\beta}^2 \right), \quad (\text{F.15})$$

$$-(4\pi)^2 \left(\eta^H \right)_{ij} = C_{i\beta\gamma}^{R(\nu)} N_{j\alpha\gamma}^{L(\ell)*} \left[D_{\beta\alpha 2}^{L(S^+)*} m_{\chi_\alpha^0} m_{\chi_\beta^\pm} C_0 \left(0, 0, 0, m_{\chi_\alpha^0}^2, m_{\chi_\beta^\pm}^2, m_{\tilde{\ell}_\gamma}^2 \right) \right. \\ \left. + D_{\beta\alpha 2}^{R(S^+)*} dC_{00} \left(0, 0, 0, m_{\chi_\alpha^0}^2, m_{\chi_\beta^\pm}^2, m_{\tilde{\ell}_\gamma}^2 \right) \right] \\ + N_{i\alpha\gamma}^{R(\nu)} C_{j\beta\gamma}^{L(\ell)*} \left[D_{\beta\alpha 2}^{L(S^+)*} m_{\chi_\alpha^0} m_{\chi_\beta^\pm} C_0 \left(0, 0, 0, m_{\chi_\alpha^0}^2, m_{\chi_\beta^\pm}^2, m_{\tilde{\nu}_\gamma}^2 \right) \right. \\ \left. + D_{\beta\alpha 2}^{R(S^+)*} dC_{00} \left(0, 0, 0, m_{\chi_\alpha^0}^2, m_{\chi_\beta^\pm}^2, m_{\tilde{\nu}_\gamma}^2 \right) \right] \\ + N_{i\alpha\beta}^{R(\nu)} N_{j\alpha\gamma}^{L(\ell)*} g_{2\gamma\beta}^{(S^+ \tilde{t}^*)} m_{\chi_\gamma^0} C_0 \left(0, 0, 0, m_{\tilde{\ell}_\gamma}^2, m_{\tilde{\nu}_\beta}^2, m_{\chi_\alpha^0}^2 \right), \quad (\text{F.16})$$

with $B_{0,1}$, C_0 , $C_{0,0}$ denoting the usual loop integral functions

$$B_0(0, x, y) = \Delta_\epsilon + 1 - \frac{x \log \frac{x}{\mu^2} - y \log \frac{y}{\mu^2}}{x - y}, \quad (\text{F.17})$$

$$B_1(0, x, y) = -\frac{1}{2} \left[\Delta_\epsilon + \frac{3x - y}{2(x - y)} - \log \frac{y}{\mu^2} + \left(\frac{x}{x - y} \right)^2 \log \frac{y}{x} \right], \quad (\text{F.18})$$

$$C_0(0, 0, 0, x, y, z) = \frac{xy \log \frac{x}{y} + yz \log \frac{y}{z} + zx \log \frac{z}{x}}{(x-y)(y-z)(z-x)}, \quad (\text{F.19})$$

$$dC_{00}(0, 0, 0, x, y, z) = \Delta_\varepsilon + 1 + \frac{x^2(y-z) \log \frac{x}{\mu^2} + y^2(z-x) \log \frac{y}{\mu^2} + z^2(x-y) \log \frac{z}{\mu^2}}{(x-y)(y-z)(z-x)}. \quad (\text{F.20})$$

Here $d = 4 - \varepsilon$, μ is the regularization parameter and $\Delta_\varepsilon = \frac{2}{\varepsilon} - \gamma + \log 4\pi$. For the couplings notation we followed [581].

The comparison of the above expressions with the corresponding ones derived in reference [516], reveals a fair agreement; we note nevertheless that the neutralino and chargino masses are absent from the analogous of equation (F.12), and that the order of the arguments of B_1 in equations (F.13), (F.14), (F.15) appears reversed. Moreover, we find small discrepancies (which cannot be accounted by the distinct notations) in the expressions for η_m^ℓ and η_H —compare with equations (F.12) and (F.16), respectively.

BIBLIOGRAPHY

- [1] R. M. Fonseca, *Comput.Phys.Commun.* **183** (2012) 2298–2306, [arXiv:1106.5016 \[hep-ph\]](#).
- [2] R. M. Fonseca, M. Malinský, W. Porod, and F. Staub, *Nucl.Phys.* **B854** (2012) 28–53, [arXiv:1107.2670 \[hep-ph\]](#).
- [3] C. Arbeláez, R. Fonseca, M. Hirsch, and J. Romão, *Phys.Rev.* **D87** (2013) 075010, [arXiv:1301.6085 \[hep-ph\]](#).
- [4] R. Fonseca, J. Romão, and A. Teixeira, *Eur.Phys.J.* **C72** (2012) 2228, [arXiv:1205.1411 \[hep-ph\]](#).
- [5] S. Glashow, *Nucl.Phys.* **22** (1961) 579–588.
- [6] S. Weinberg, *Phys.Rev.Lett.* **19** (1967) 1264–1266.
- [7] A. Salam, in *Elementary Particle Theory: Proceedings of the Eighth Nobel Symposium*, N. Svartholm, ed., pp. 367–377. Almqvist & Wiksell, 1968.
- [8] M. Gell-Mann, *Phys.Lett.* **8** (1964) 214–215.
- [9] G. Zweig, *CERN-TH-401* (1964) .
- [10] G. Zweig, *CERN-TH-412, NP-14146* (1964) .
- [11] J. Bjorken, *Phys.Rev.* **179** (1969) 1547–1553.
- [12] R. P. Feynman, *Phys.Rev.Lett.* **23** (1969) 1415–1417.
- [13] D. Gross and F. Wilczek, *Phys.Rev.Lett.* **30** (1973) 1343–1346.
- [14] H. D. Politzer, *Phys.Rev.Lett.* **30** (1973) 1346–1349.
- [15] O. Greenberg, *Phys.Rev.Lett.* **13** (1964) 598–602.
- [16] M. Han and Y. Nambu, *Phys.Rev.* **139** (1965) B1006–B1010.
- [17] H. Georgi and H. D. Politzer, *Phys.Rev.* **D9** (1974) 416–420.
- [18] **Gargamelle Neutrino Collaboration**, F. Hasert *et al.*, *Phys.Lett.* **B46** (1973) 138–140.
- [19] **UA1 Collaboration**, G. Arnison *et al.*, *Phys.Lett.* **B122** (1983) 103–116.
- [20] M. Breidenbach, J. I. Friedman, H. W. Kendall, E. D. Bloom, D. Coward, *et al.*, *Phys.Rev.Lett.* **23** (1969) 935–939.
- [21] E. D. Bloom, D. Coward, H. DeStaebler, J. Drees, G. Miller, *et al.*, *Phys.Rev.Lett.* **23** (1969) 930–934.

- [22] J. I. Friedman and H. W. Kendall, *Ann.Rev.Nucl.Part.Sci.* **22** (1972) 203–254.
- [23] F. Englert and R. Brout, *Phys.Rev.Lett.* **13** (1964) 321–323.
- [24] P. W. Higgs, *Phys.Lett.* **12** (1964) 132–133.
- [25] P. W. Higgs, *Phys.Rev.Lett.* **13** (1964) 508–509.
- [26] G. Guralnik, C. Hagen, and T. Kibble, *Phys.Rev.Lett.* **13** (1964) 585–587.
- [27] **ATLAS Collaboration**, G. Aad *et al.*, *Phys.Lett.* **B716** (2012) 1–29, [arXiv:1207.7214 \[hep-ex\]](#).
- [28] **CMS Collaboration**, S. Chatrchyan *et al.*, *Phys.Lett.* **B716** (2012) 30–61, [arXiv:1207.7235 \[hep-ex\]](#).
- [29] C.-N. Yang and R. L. Mills, *Phys.Rev.* **96** (1954) 191–195.
- [30] **ALEPH Collaboration, DELPHI Collaboration, L3 Collaboration, OPAL Collaboration, LEP Electroweak Working Group**, S. Schael *et al.*, [arXiv:1302.3415 \[hep-ex\]](#).
- [31] G. Giudice, P. Paradisi, and M. Passera, *JHEP* **1211** (2012) 113, [arXiv:1208.6583 \[hep-ph\]](#).
- [32] **ATLAS Collaboration**, G. Aad *et al.*, Tech. Rep. **ATLAS-CONF-2013-034**, March, 2013.
- [33] **CMS Collaboration**, S. Chatrchyan *et al.*, Tech. Rep. **CMS-PAS-HIG-13-005**, April, 2013.
- [34] **ATLAS Collaboration**, G. Aad *et al.*, Tech. Rep. **ATLAS-CONF-2013-014**, March, 2013.
- [35] L. Susskind, *Phys.Rev.* **D20** (1979) 2619–2625.
- [36] G. 't Hooft, *NATO Adv.Study Inst.Ser.B Phys.* **59** (1980) 135.
- [37] M. Veltman, *Acta Phys.Polon.* **B12** (1981) 437.
- [38] H. Murayama, in *Proceedings of INS Symposium*. World Scientific, 1994. [arXiv:hep-ph/9410285 \[hep-ph\]](#).
- [39] H. Murayama, *ICTP Summer School Lectures* (1999) 296–335, [arXiv:hep-ph/0002232 \[hep-ph\]](#).
- [40] H. Georgi and S. Glashow, *Phys.Rev.Lett.* **32** (1974) 438–441.
- [41] J. C. Pati and A. Salam, *Phys.Rev.* **D10** (1974) 275–289.
- [42] H. Georgi, H. R. Quinn, and S. Weinberg, *Phys.Rev.Lett.* **33** (1974) 451–454.

- [43] H. Fritzsch and P. Minkowski, *Annals Phys.* **93** (1975) 193–266.
- [44] A. Buras, J. R. Ellis, M. Gaillard, and D. V. Nanopoulos, *Nucl.Phys.* **B135** (1978) 66–92.
- [45] H. Georgi and C. Jarlskog, *Phys.Lett.* **B86** (1979) 297–300.
- [46] S. M. Barr, *Phys.Lett.* **B112** (1982) 219.
- [47] S. Dimopoulos and H. Georgi, *Nucl.Phys.* **B193** (1981) 150.
- [48] J. L. Hewett and T. G. Rizzo, *Phys.Rept.* **183** (1989) 193.
- [49] H. Georgi and S. L. Glashow, *Phys.Rev.* **D6** (1972) 429.
- [50] S. Okubo, *Phys.Rev.* **D16** (1977) 3528.
- [51] P. Langacker, *Phys.Rept.* **72** (1981) 185.
- [52] P. Langacker, in *Radiative Corrections: Status and Outlook*. World Scientific, 1995. [arXiv:hep-ph/9411247](#) [hep-ph].
- [53] **Super-Kamiokande**, H. Nishino *et al.*, *Phys.Rev.* **D85** (2012) 112001, [arXiv:1203.4030](#) [hep-ex].
- [54] D. Emmanuel-Costa and S. Wiesenfeldt, *Nucl.Phys.* **B661** (2003) 62–82, [arXiv:hep-ph/0302272](#) [hep-ph].
- [55] S. Raby, *Eur.Phys.J.* **C59** (2009) 223–247, [arXiv:0807.4921](#) [hep-ph].
- [56] G. R. Farrar and P. Fayet, *Phys.Lett.* **B76** (1978) 575–579.
- [57] N. Sakai and T. Yanagida, *Nucl.Phys.* **B197** (1982) 533.
- [58] S. Weinberg, *Phys.Rev.* **D26** (1982) 287.
- [59] M. Miura, p. 408. PoS, 2010.
- [60] H. Bethe and R. Peierls, *Nature* **133** (1934) 532.
- [61] **Super-Kamiokande Collaboration**, Y. Fukuda *et al.*, *Phys.Rev.Lett.* **81** (1998) 1562–1567, [arXiv:hep-ex/9807003](#) [hep-ex].
- [62] J. N. Bahcall, *Phys.Rev.Lett.* **12** (1964) 300–302.
- [63] R. Davis, *Phys.Rev.Lett.* **12** (1964) 303–305.
- [64] J. Davis, Raymond, D. S. Harmer, and K. C. Hoffman, *Phys.Rev.Lett.* **20** (1968) 1205–1209.
- [65] A. Belavin, A. M. Polyakov, A. Schwartz, and Y. Tyupkin, *Phys.Lett.* **B59** (1975) 85–87.
- [66] G. 't Hooft, *Phys.Rev.* **D14** (1976) 3432–3450.

- [67] G. 't Hooft, *Phys.Rev.Lett.* **37** (1976) 8–11.
- [68] F. R. Klinkhamer and N. Manton, *Phys.Rev.* **D30** (1984) 2212.
- [69] F. Zwicky, *Helv.Phys.Acta* **6** (1933) 110–127.
- [70] D. Clowe, M. Bradač, A. H. Gonzalez, M. Markevitch, S. W. Randall, *et al.*, *Astrophys.J.* **648** (2006) L109–L113, [arXiv:astro-ph/0608407](#) [[astro-ph](#)].
- [71] **Planck Collaboration**, P. Ade *et al.*, [arXiv:1303.5076](#) [[astro-ph.CO](#)].
- [72] G. Marx and A. Szalay, in *Proceedings of Neutrino '72*, vol. 1, p. 213. Technoinform, 1972.
- [73] R. Cowsik and J. McClelland, *Phys.Rev.Lett.* **29** (1972) 669–670.
- [74] R. Cowsik and J. McClelland, *Astrophys.J.* **180** (1973) 7–10.
- [75] G. Bertone, D. Hooper, and J. Silk, *Phys.Rept.* **405** (2005) 279–390, [arXiv:hep-ph/0404175](#) [[hep-ph](#)].
- [76] R. Bernabei, P. Belli, F. Cappella, R. Cerulli, F. Montecchia, *et al.*, *Riv.Nuovo Cim.* **26N1** (2003) 1–73, [arXiv:astro-ph/0307403](#) [[astro-ph](#)].
- [77] **DAMA LIBRA Collaboration**, R. Bernabei *et al.*, *Eur.Phys.J.* **C67** (2010) 39–49, [arXiv:1002.1028](#) [[astro-ph.GA](#)].
- [78] C. Aalseth, P. Barbeau, J. Colaresi, J. Collar, J. Diaz Leon, *et al.*, *Phys.Rev.Lett.* **107** (2011) 141301, [arXiv:1106.0650](#) [[astro-ph.CO](#)].
- [79] G. Angloher, M. Bauer, I. Bavykina, A. Bento, C. Bucci, *et al.*, *Eur.Phys.J.* **C72** (2012) 1971, [arXiv:1109.0702](#) [[astro-ph.CO](#)].
- [80] J. Kopp, T. Schwetz, and J. Zupan, *JCAP* **1203** (2012) 001, [arXiv:1110.2721](#) [[hep-ph](#)].
- [81] **CDMS-II Collaboration**, Z. Ahmed *et al.*, *Phys.Rev.Lett.* **106** (2011) 131302, [arXiv:1011.2482](#) [[astro-ph.CO](#)].
- [82] **CDMS Collaboration**, Z. Ahmed *et al.*, [arXiv:1203.1309](#) [[astro-ph.CO](#)].
- [83] **XENON100 Collaboration**, E. Aprile *et al.*, *Phys.Rev.Lett.* **109** (2012) 181301, [arXiv:1207.5988](#) [[astro-ph.CO](#)].
- [84] **CDMS Collaboration**, R. Agnese *et al.*, *Phys.Rev.Lett.* (2013) , [arXiv:1304.4279](#) [[hep-ex](#)].
- [85] M. Cirelli, *Pramana* **79** (2012) 1021–1043, [arXiv:1202.1454](#) [[hep-ph](#)].
- [86] **PAMELA Collaboration**, O. Adriani *et al.*, *Nature* **458** (2009) 607–609, [arXiv:0810.4995](#) [[astro-ph](#)].

- [87] **Fermi LAT Collaboration**, M. Ackermann *et al.*, *Phys.Rev.Lett.* **108** (2012) 011103, [arXiv:1109.0521](#) [[astro-ph.HE](#)].
- [88] **AMS Collaboration**, M. Aguilar *et al.*, *Phys.Rev.Lett.* **110** (2013) 141102.
- [89] J. Chang, J. Adams, H. Ahn, G. Bashindzhagyan, M. Christl, *et al.*, *Nature* **456** (2008) 362–365.
- [90] **PPB-BETS Collaboration**, S. Torii *et al.*, [arXiv:0809.0760](#) [[astro-ph](#)].
- [91] **Fermi LAT Collaboration**, A. A. Abdo *et al.*, *Phys.Rev.Lett.* **102** (2009) 181101, [arXiv:0905.0025](#) [[astro-ph.HE](#)].
- [92] **H.E.S.S. Collaboration**, F. Aharonian *et al.*, *Phys.Rev.Lett.* **101** (2008) 261104, [arXiv:0811.3894](#) [[astro-ph](#)].
- [93] **H.E.S.S. Collaboration**, F. Aharonian *et al.*, *Astron.Astrophys.* **508** (2009) 561, [0905.0105](#).
- [94] O. Adriani, G. Barbarino, G. Bazilevskaya, R. Bellotti, M. Boezio, *et al.*, *Phys.Rev.Lett.* **102** (2009) 051101, [arXiv:0810.4994](#) [[astro-ph](#)].
- [95] **PAMELA Collaboration**, O. Adriani *et al.*, *Phys.Rev.Lett.* **105** (2010) 121101, [arXiv:1007.0821](#) [[astro-ph.HE](#)].
- [96] T. Bringmann, X. Huang, A. Ibarra, S. Vogl, and C. Weniger, *JCAP* **1207** (2012) 054, [arXiv:1203.1312](#) [[hep-ph](#)].
- [97] C. Weniger, *JCAP* **1208** (2012) 007, [arXiv:1204.2797](#) [[hep-ph](#)].
- [98] **Supernova Cosmology Project**, S. Perlmutter *et al.*, *Astrophys.J.* **517** (1999) 565–586, [arXiv:astro-ph/9812133](#) [[astro-ph](#)].
- [99] **Supernova Search Team**, A. G. Riess *et al.*, *Astron.J.* **116** (1998) 1009–1038, [arXiv:astro-ph/9805201](#) [[astro-ph](#)].
- [100] S. M. Carroll, in *SNAP Yellow Book*. 2001. [arXiv:astro-ph/0107571](#) [[astro-ph](#)].
- [101] A. Ashtekar, in *Proceedings of 3rd Quantum Gravity and Quantum Geometry School*, p. 001. PoS, 2011. [arXiv:1201.4598](#) [[gr-qc](#)].
- [102] A. Riotto and M. Trodden, *Ann.Rev.Nucl.Part.Sci.* **49** (1999) 35–75, [arXiv:hep-ph/9901362](#) [[hep-ph](#)].
- [103] S. Davidson, E. Nardi, and Y. Nir, *Phys.Rept.* **466** (2008) 105–177, [arXiv:0802.2962](#) [[hep-ph](#)].
- [104] E. W. Kolb and M. S. Turner, *The Early universe*. Frontiers in physics. Sarat Book House, 1994.
- [105] **Particle Data Group**, J. Beringer *et al.*, *Phys.Rev.* **D86** (2012) 010001.

- [106] A. Sakharov, *Pisma Zh.Eksp.Teor.Fiz.* **5** (1967) 32–35.
- [107] V. Kuzmin, V. Rubakov, and M. Shaposhnikov, *Phys.Lett.* **B155** (1985) 36.
- [108] M. Kobayashi and T. Maskawa, *Prog.Theor.Phys.* **49** (1973) 652–657.
- [109] C. Jarlskog, *Z.Phys.* **C29** (1985) 491–497.
- [110] C. Jarlskog, *Phys.Rev.Lett.* **55** (1985) 1039.
- [111] M. Gavela, P. Hernández, J. Orloff, and O. Pène, *Mod.Phys.Lett.* **A9** (1994) 795–810, [arXiv:hep-ph/9312215](#) [hep-ph].
- [112] M. Gavela, P. Hernández, J. Orloff, O. Pène, and C. Quimbay, *Nucl.Phys.* **B430** (1994) 382–426, [arXiv:hep-ph/9406289](#) [hep-ph].
- [113] P. Huet and E. Sather, *Phys.Rev.* **D51** (1995) 379–394, [arXiv:hep-ph/9404302](#) [hep-ph].
- [114] A. Bochkarev and M. Shaposhnikov, *Mod.Phys.Lett.* **A2** (1987) 417.
- [115] K. Kajantie, M. Laine, K. Rummukainen, and M. E. Shaposhnikov, *Nucl.Phys.* **B466** (1996) 189–258, [arXiv:hep-lat/9510020](#) [hep-lat].
- [116] D. E. Morrissey and M. J. Ramsey-Musolf, *New J.Phys.* **14** (2012) 125003, [arXiv:1206.2942](#) [hep-ph].
- [117] D. Delepine, J. Gérard, R. González Felipe, and J. Weyers, *Phys.Lett.* **B386** (1996) 183–188, [arXiv:hep-ph/9604440](#) [hep-ph].
- [118] J. M. Cline and G. D. Moore, *Phys.Rev.Lett.* **81** (1998) 3315–3318, [arXiv:hep-ph/9806354](#) [hep-ph].
- [119] M. Laine and K. Rummukainen, *Nucl.Phys.* **B535** (1998) 423–457, [arXiv:hep-lat/9804019](#) [hep-lat].
- [120] M. Carena, G. Nardini, M. Quirós, and C. E. Wagner, *JHEP* **0810** (2008) 062, [arXiv:0806.4297](#) [hep-ph].
- [121] M. Carena, G. Nardini, M. Quirós, and C. Wagner, *Nucl.Phys.* **B812** (2009) 243–263, [arXiv:0809.3760](#) [hep-ph].
- [122] D. Curtin, P. Jaiswal, and P. Meade, *JHEP* **1208** (2012) 005, [arXiv:1203.2932](#) [hep-ph].
- [123] D. J. Chung, A. J. Long, and L.-T. Wang, *Phys.Rev.* **D87** (2013) 023509, [arXiv:1209.1819](#) [hep-ph].
- [124] W. Huang, J. Shu, and Y. Zhang, *JHEP* **1303** (2013) 164, [arXiv:1210.0906](#) [hep-ph].
- [125] T. Cohen, D. E. Morrissey, and A. Pierce, *Phys.Rev.* **D86** (2012) 013009, [arXiv:1203.2924](#) [hep-ph].

- [126] M. Fukugita and T. Yanagida, *Phys.Lett.* **B174** (1986) 45.
- [127] Y. Golfand and E. Likhtman, *JETP Lett.* **13** (1971) 323–326.
- [128] J. Wess and B. Zumino, *Phys.Lett.* **B49** (1974) 52.
- [129] J. Wess and B. Zumino, *Nucl.Phys.* **B70** (1974) 39–50.
- [130] L. Girardello and M. T. Grisaru, *Nucl.Phys.* **B194** (1982) 65.
- [131] S. P. Martin, [arXiv:hep-ph/9709356](#) [hep-ph].
- [132] H. K. Dreiner, in *Perspectives on Supersymmetry*, G. Kane, ed. World Scientific, 1997. [arXiv:hep-ph/9707435](#) [hep-ph].
- [133] G. Bhattacharyya, in *Beyond the desert 1997: Accelerator and non-accelerator approaches*, H. Klapdor-Kleingrothaus and H. Päs, eds. IOP, 1997. [arXiv:hep-ph/9709395](#) [hep-ph].
- [134] M. A. Díaz, J. C. Romão, and J. Valle, *Nucl.Phys.* **B524** (1998) 23–40, [arXiv:hep-ph/9706315](#) [hep-ph].
- [135] B. Allanach, A. Dedes, and H. K. Dreiner, *Phys.Rev.* **D60** (1999) 075014, [arXiv:hep-ph/9906209](#) [hep-ph].
- [136] M. Hirsch, M. Díaz, W. Porod, J. Romão, and J. Valle, *Phys.Rev.* **D62** (2000) 113008, [arXiv:hep-ph/0004115](#) [hep-ph].
- [137] R. Barbier, C. Bérat, M. Besançon, M. Chemtob, A. Deandrea, *et al.*, *Phys.Rept.* **420** (2005) 1–202, [arXiv:hep-ph/0406039](#) [hep-ph].
- [138] Y. Nambu, *Phys.Rev.* **117** (1960) 648–663.
- [139] J. Goldstone, *Nuovo Cim.* **19** (1961) 154–164.
- [140] K. Inoue, A. Kakuto, H. Komatsu, and S. Takeshita, *Prog.Theor.Phys.* **67** (1982) 1889.
- [141] R. A. Flores and M. Sher, *Annals Phys.* **148** (1983) 95.
- [142] **LEP Working Group for Higgs boson searches, ALEPH Collaboration, DELPHI Collaboration, L3 Collaboration, OPAL Collaboration**, R. Barate *et al.*, *Phys.Lett.* **B565** (2003) 61–75, [arXiv:hep-ex/0306033](#) [hep-ex].
- [143] Y. Okada, M. Yamaguchi, and T. Yanagida, *Prog.Theor.Phys.* **85** (1991) 1–6.
- [144] J. R. Ellis, G. Ridolfi, and F. Zwirner, *Phys.Lett.* **B257** (1991) 83–91.
- [145] H. E. Haber and R. Hempfling, *Phys.Rev.Lett.* **66** (1991) 1815–1818.
- [146] M. S. Carena and H. E. Haber, *Prog.Part.Nucl.Phys.* **50** (2003) 63–152, [arXiv:hep-ph/0208209](#) [hep-ph].

- [147] A. Djouadi, *Phys.Rept.* **459** (2008) 1–241, [arXiv:hep-ph/0503173 \[hep-ph\]](#).
- [148] **ATLAS Collaboration**, G. Aad *et al.*, “ATLAS exotics searches - 95% CL Lower Limits (Status: HCP 2012).” https://twiki.cern.ch/twiki/pub/AtlasPublic/CombinedSummaryPlots/AtlasSearches_exotics_hcp12.pdf, 2013. Retrieved April 14, 2013.
- [149] **CMS Collaboration**, S. Chatrchyan *et al.*, [arXiv:1301.2175 \[hep-ex\]](#).
- [150] S. Dimopoulos and D. W. Sutter, *Nucl.Phys.* **B452** (1995) 496–512, [arXiv:hep-ph/9504415 \[hep-ph\]](#).
- [151] H. E. Haber, *Nucl.Phys.Proc.Suppl.* **62** (1998) 469–484, [arXiv:hep-ph/9709450 \[hep-ph\]](#).
- [152] **MSSM Working Group**, A. Djouadi *et al.*, in *GDR-Supersymétrie*. 1998. [arXiv:hep-ph/9901246 \[hep-ph\]](#).
- [153] A. H. Chamseddine, R. L. Arnowitt, and P. Nath, *Phys.Rev.Lett.* **49** (1982) 970.
- [154] R. Barbieri, S. Ferrara, and C. A. Savoy, *Phys.Lett.* **B119** (1982) 343.
- [155] L. J. Hall, J. D. Lykken, and S. Weinberg, *Phys.Rev.* **D27** (1983) 2359–2378.
- [156] G. L. Kane, C. F. Kolda, L. Roszkowski, and J. D. Wells, *Phys.Rev.* **D49** (1994) 6173–6210, [arXiv:hep-ph/9312272 \[hep-ph\]](#).
- [157] A. Arbey, M. Battaglia, A. Djouadi, F. Mahmoudi, and J. Quevillon, *Phys.Lett.* **B708** (2012) 162–169, [arXiv:1112.3028 \[hep-ph\]](#).
- [158] M. Carena, S. Gori, N. R. Shah, and C. E. Wagner, *JHEP* **1203** (2012) 014, [arXiv:1112.3336 \[hep-ph\]](#).
- [159] S. Heinemeyer, O. Stål, and G. Weiglein, *Phys.Lett.* **B710** (2012) 201–206, [arXiv:1112.3026 \[hep-ph\]](#).
- [160] H. Baer, V. Barger, and A. Mustafayev, *Phys.Rev.* **D85** (2012) 075010, [arXiv:1112.3017 \[hep-ph\]](#).
- [161] P. Draper, P. Meade, M. Reece, and D. Shih, *Phys.Rev.* **D85** (2012) 095007, [arXiv:1112.3068 \[hep-ph\]](#).
- [162] M. Kadastik, K. Kannike, A. Racioppi, and M. Raidal, *JHEP* **1205** (2012) 061, [arXiv:1112.3647 \[hep-ph\]](#).
- [163] J. F. Gunion, Y. Jiang, and S. Kraml, *Phys.Lett.* **B710** (2012) 454–459, [arXiv:1201.0982 \[hep-ph\]](#).

- [164] L. Aparicio, D. Cerdeño, and L. Ibáñez, *JHEP* **1204** (2012) 126, [arXiv:1202.0822 \[hep-ph\]](#).
- [165] J. Ellis and K. A. Olive, *Eur.Phys.J.* **C72** (2012) 2005, [arXiv:1202.3262 \[hep-ph\]](#).
- [166] H. Baer, V. Barger, and A. Mustafayev, *JHEP* **1205** (2012) 091, [arXiv:1202.4038 \[hep-ph\]](#).
- [167] M. Hirsch, F. Joaquim, and A. Vicente, *JHEP* **1211** (2012) 105, [arXiv:1207.6635 \[hep-ph\]](#).
- [168] H. Baer, V. Barger, P. Huang, D. Mickelson, A. Mustafayev, *et al.*, [arXiv:1210.3019 \[hep-ph\]](#).
- [169] V. E. Mayes, [arXiv:1302.4394 \[hep-ph\]](#).
- [170] V. Berezhinsky, A. Bottino, J. R. Ellis, N. Fornengo, G. Mignola, *et al.*, *Astropart.Phys.* **5** (1996) 1–26, [arXiv:hep-ph/9508249 \[hep-ph\]](#).
- [171] P. Nath and R. L. Arnowitt, *Phys.Rev.* **D56** (1997) 2820–2832, [arXiv:hep-ph/9701301 \[hep-ph\]](#).
- [172] B. Pontecorvo, *Camb.Monogr.Part.Phys.Nucl.Phys.Cosmol.* **1** (1991) 25–31.
- [173] C. Cowan, F. Reines, F. Harrison, H. Kruse, and A. McGuire, *Science* **124** (1956) 103–104.
- [174] F. Close, *Neutrino*. OUP Oxford, 2010.
- [175] G. Danby, J. Gaillard, K. A. Goulianos, L. Lederman, N. B. Mistry, *et al.*, *Phys.Rev.Lett.* **9** (1962) 36–44.
- [176] **DONUT Collaboration**, K. Kodama *et al.*, *Phys.Lett.* **B504** (2001) 218–224, [arXiv:hep-ex/0012035 \[hep-ex\]](#).
- [177] B. Pontecorvo, *Sov.Phys.JETP* **6** (1957) 429.
- [178] Z. Maki, M. Nakagawa, and S. Sakata, *Prog.Theor.Phys.* **28** (1962) 870–880.
- [179] B. Pontecorvo, *Sov.Phys.JETP* **26** (1968) 984–988.
- [180] L. Wolfenstein, *Phys.Rev.* **D17** (1978) 2369–2374.
- [181] S. Mikheev and A. Y. Smirnov, *Sov.J.Nucl.Phys.* **42** (1985) 913–917.
- [182] S. Mikheev and A. Y. Smirnov, *Nuovo Cim.* **C9** (1986) 17–26.
- [183] **KAMIOKANDE-II Collaboration**, K. Hirata *et al.*, *Phys.Rev.Lett.* **63** (1989) 16.
- [184] A. Abazov, O. Anosov, E. Faizov, V. Gavrin, A. Kalikhov, *et al.*, *Phys.Rev.Lett.* **67** (1991) 3332–3335.

- [185] **GALLEX Collaboration**, P. Anselmann *et al.*, *Phys.Lett.* **B285** (1992) 376–389.
- [186] **SNO Collaboration**, Q. Ahmad *et al.*, *Phys.Rev.Lett.* **87** (2001) 071301, [arXiv:nucl-ex/0106015](#) [nucl-ex].
- [187] A. Balantekin and W. Haxton, [arXiv:1303.2272](#) [nucl-th].
- [188] S. M. Bilenky and S. Petcov, *Rev.Mod.Phys.* **59** (1987) 671.
- [189] D. V. Forero, M. Tórtola, and J. W. F. Valle, *Phys.Rev.* **D86** (2012) 073012, [arXiv:1205.4018](#) [hep-ph].
- [190] G. Fogli, E. Lisi, A. Marrone, D. Montanino, A. Palazzo, *et al.*, *Phys.Rev.* **D86** (2012) 013012, [arXiv:1205.5254](#) [hep-ph].
- [191] M. Gonzalez-Garcia, M. Maltoni, J. Salvado, and T. Schwetz, *JHEP* **1212** (2012) 123, [arXiv:1209.3023](#) [hep-ph].
- [192] C. Garcia, M. Maltoni, T. Schwetz, and J. Salvado, “Nufit.” [www.http://www.nu-fit.org/](http://www.nu-fit.org/), 2013. Retrieved June 21, 2013.
- [193] S. Pascoli, S. Petcov, and L. Wolfenstein, *Phys.Lett.* **B524** (2002) 319–331, [arXiv:hep-ph/0110287](#) [hep-ph].
- [194] S. Pascoli, S. Petcov, and W. Rodejohann, *Phys.Lett.* **B549** (2002) 177–193, [arXiv:hep-ph/0209059](#) [hep-ph].
- [195] V. Barger, S. Glashow, P. Langacker, and D. Marfatia, *Phys.Lett.* **B540** (2002) 247–251, [arXiv:hep-ph/0205290](#) [hep-ph].
- [196] A. de Gouvea, B. Kayser, and R. N. Mohapatra, *Phys.Rev.* **D67** (2003) 053004, [arXiv:hep-ph/0211394](#) [hep-ph].
- [197] S. Pascoli, S. Petcov, and T. Schwetz, *Nucl.Phys.* **B734** (2006) 24–49, [arXiv:hep-ph/0505226](#) [hep-ph].
- [198] A. Faessler, G. Fogli, E. Lisi, V. Rodin, A. Rotunno, *et al.*, *Phys.Rev.* **D79** (2009) 053001, [arXiv:0810.5733](#) [hep-ph].
- [199] G. Branco, R. G. Felipe, and F. Joaquim, *Rev.Mod.Phys.* **84** (2012) 515–565, [arXiv:1111.5332](#) [hep-ph].
- [200] H. Klapdor-Kleingrothaus, A. Dietz, H. Harney, and I. Krivosheina, *Mod.Phys.Lett.* **A16** (2001) 2409–2420, [arXiv:hep-ph/0201231](#) [hep-ph].
- [201] **LSND Collaboration**, A. Aguilar-Arevalo *et al.*, *Phys.Rev.* **D64** (2001) 112007, [arXiv:hep-ex/0104049](#) [hep-ex].
- [202] **MiniBooNE Collaboration**, A. Aguilar-Arevalo *et al.*, *Phys.Rev.Lett.* **98** (2007) 231801, [arXiv:0704.1500](#) [hep-ex].

- [203] **MiniBooNE Collaboration**, A. Aguilar-Arevalo *et al.*, *Phys.Rev.Lett.* **105** (2010) 181801, [arXiv:1007.1150](#) [hep-ex].
- [204] **MiniBooNE Collaboration**, A. Aguilar-Arevalo *et al.*, [arXiv:1207.4809](#) [hep-ex].
- [205] **MiniBooNE Collaboration**, A. Aguilar-Arevalo *et al.*, *Phys.Rev.Lett.* **110** (2013) 161801, [arXiv:1303.2588](#) [hep-ex].
- [206] M. A. Acero, C. Giunti, and M. Laveder, *Phys.Rev.* **D78** (2008) 073009, [arXiv:0711.4222](#) [hep-ph].
- [207] F. Kaether, W. Hampel, G. Heusser, J. Kiko, and T. Kirsten, *Phys.Lett.* **B685** (2010) 47–54, [arXiv:1001.2731](#) [hep-ex].
- [208] C. Giunti and M. Laveder, *Phys.Rev.* **D84** (2011) 073008, [arXiv:1107.1452](#) [hep-ph].
- [209] G. Mention, M. Fechner, T. Lasserre, T. Mueller, D. Lhuillier, *et al.*, *Phys.Rev.* **D83** (2011) 073006, [arXiv:1101.2755](#) [hep-ex].
- [210] C. Giunti, M. Laveder, Y. Li, Q. Liu, and H. Long, *Phys.Rev.* **D86** (2012) 113014, [arXiv:1210.5715](#) [hep-ph].
- [211] A. Y. Smirnov, in *Neutrino telescopes. Proceedings, 10th International Workshop*, M. Baldo-Ceolin, ed., pp. 23–43. Instituto Veneto Di Scienze, 2003. [arXiv:hep-ph/0305106](#) [hep-ph].
- [212] J. Schechter and J. Valle, *Phys.Rev.* **D25** (1982) 2951.
- [213] J. F. Nieves, *Phys.Lett.* **B147** (1984) 375.
- [214] E. Takasugi, *Phys.Lett.* **B149** (1984) 372.
- [215] M. Hirsch, S. Kovalenko, and I. Schmidt, *Phys.Lett.* **B642** (2006) 106–110, [arXiv:hep-ph/0608207](#) [hep-ph].
- [216] B. Schwingenheuer, *Ann. Phys. (Berlin)* **525** no. 4, (2013) 269–280, [arXiv:1210.7432](#) [hep-ex].
- [217] M. Hirsch, H. Klapdor-Kleingrothaus, and S. Kovalenko, *Phys.Rev.Lett.* **75** (1995) 17–20.
- [218] M. Hirsch, H. Klapdor-Kleingrothaus, and S. Kovalenko, *Phys.Rev.* **D57** (1998) 1947–1961, [arXiv:hep-ph/9707207](#) [hep-ph].
- [219] R. Mohapatra, *Phys.Rev.* **D34** (1986) 3457–3461.
- [220] M. Doi, T. Kotani, and E. Takasugi, *Prog.Theor.Phys.Suppl.* **83** (1985) 1.
- [221] J. Menéndez, A. Poves, E. Caurier, and F. Nowacki, *Nucl.Phys.* **A818** (2009) 139–151, [arXiv:0801.3760](#) [nucl-th].

- [222] J. Barea and F. Iachello, *Phys.Rev.* **C79** (2009) 044301.
- [223] T. R. Rodríguez and G. Martínez-Pinedo, *Phys.Rev.Lett.* **105** (2010) 252503, [arXiv:1008.5260 \[nucl-th\]](#).
- [224] P. Rath, R. Chandra, K. Chaturvedi, P. Raina, and J. Hirsch, *Phys.Rev.* **C82** (2010) 064310, [arXiv:1104.3965 \[nucl-th\]](#).
- [225] J. Suhonen and O. Civitarese, *Nucl.Phys.* **A847** (2010) 207–232.
- [226] J. Menéndez, A. Poves, E. Caurier, and F. Nowacki, *J.Phys.Conf.Ser.* **312** (2011) 072005.
- [227] F. Iachello and J. Barea, *Nucl.Phys.Proc.Suppl.* **217** (2011) 5–8.
- [228] G. Branco, R. González Felipe, F. Joaquim, and T. Yanagida, *Phys.Lett.* **B562** (2003) 265–272, [arXiv:hep-ph/0212341 \[hep-ph\]](#).
- [229] H. Klapdor-Kleingrothaus, A. Dietz, L. Baudis, G. Heusser, I. Krivosheina, *et al.*, *Eur.Phys.J.* **A12** (2001) 147–154, [arXiv:hep-ph/0103062 \[hep-ph\]](#).
- [230] **IGEX Collaboration**, C. Aalseth *et al.*, *Phys.Rev.* **D65** (2002) 092007, [arXiv:hep-ex/0202026 \[hep-ex\]](#).
- [231] E. Andreotti, C. Arnaboldi, F. Avignone, M. Balata, I. Bandac, *et al.*, *Astropart.Phys.* **34** (2011) 822–831, [arXiv:1012.3266 \[nucl-ex\]](#).
- [232] **KamLAND-Zen Collaboration**, A. Gando *et al.*, *Phys.Rev.* **C85** (2012) 045504, [arXiv:1201.4664 \[hep-ex\]](#).
- [233] **EXO Collaboration**, M. Auger *et al.*, *Phys.Rev.Lett.* **109** (2012) 032505, [arXiv:1205.5608 \[hep-ex\]](#).
- [234] **NEMO-3 Collaboration**, L. Simard, *J.Phys.Conf.Ser.* **375** (2012) 042011.
- [235] C. Kraus, B. Bornschein, L. Bornschein, J. Bonn, B. Flatt, *et al.*, *Eur.Phys.J.* **C40** (2005) 447–468, [arXiv:hep-ex/0412056 \[hep-ex\]](#).
- [236] V. Lobashev, V. Aseev, A. Belev, A. Berlev, E. Geraskin, *et al.*, *Nucl.Phys.Proc.Suppl.* **91** (2001) 280–286.
- [237] **Troitsk Collaboration**, V. Aseev *et al.*, *Phys.Rev.* **D84** (2011) 112003, [arXiv:1108.5034 \[hep-ex\]](#).
- [238] G. Drexlin, V. Hannen, S. Mertens, and C. Weinheimer, *Adv.High Energy Phys.* **2013** (2013) 293986.
- [239] J. Lesgourgues and S. Pastor, *Adv.High Energy Phys.* **2012** (2012) 608515, [arXiv:1212.6154 \[hep-ph\]](#).

- [240] **WMAP Collaboration**, E. Komatsu *et al.*, *Astrophys.J.Suppl.* **192** (2011) 18, [arXiv:1001.4538](#) [[astro-ph.CO](#)].
- [241] R. Keisler, C. Reichardt, K. Aird, B. Benson, L. Bleem, *et al.*, *Astrophys.J.* **743** (2011) 28, [arXiv:1105.3182](#) [[astro-ph.CO](#)].
- [242] C. Reichardt, L. Shaw, O. Zahn, K. Aird, B. Benson, *et al.*, *Astrophys.J.* **755** (2012) 70, [arXiv:1111.0932](#) [[astro-ph.CO](#)].
- [243] K. Story, C. Reichardt, Z. Hou, R. Keisler, K. Aird, *et al.*, [arXiv:1210.7231](#) [[astro-ph.CO](#)].
- [244] S. Das, T. Louis, M. R. Nolta, G. E. Addison, E. S. Battistelli, *et al.*, [arXiv:1301.1037](#) [[astro-ph.CO](#)].
- [245] **SDSS Collaboration**, W. J. Percival *et al.*, *Mon.Not.Roy.Astron.Soc.* **401** (2010) 2148–2168, [arXiv:0907.1660](#) [[astro-ph.CO](#)].
- [246] C. Blake, E. Kazin, F. Beutler, T. Davis, D. Parkinson, *et al.*, *Mon.Not.Roy.Astron.Soc.* **418** (2011) 1707–1724, [arXiv:1108.2635](#) [[astro-ph.CO](#)].
- [247] F. Beutler, C. Blake, M. Colless, D. H. Jones, L. Staveley-Smith, *et al.*, *Mon.Not.Roy.Astron.Soc.* **416** (2011) 3017–3032, [arXiv:1106.3366](#) [[astro-ph.CO](#)].
- [248] N. Padmanabhan, X. Xu, D. J. Eisenstein, R. Scalzo, A. J. Cuesta, *et al.*, *Mon.Not.Roy.Astron.Soc.* **427** no. 3, (2012) 2132–2145, [arXiv:1202.0090](#) [[astro-ph.CO](#)].
- [249] D. Parkinson, S. Riemer-Sørensen, C. Blake, G. B. Poole, T. M. Davis, *et al.*, *Phys.Rev.* **D86** (2012) 103518, [arXiv:1210.2130](#) [[astro-ph.CO](#)].
- [250] S. Riemer-Sørensen, D. Parkinson, and T. M. Davis, [arXiv:1306.4153](#) [[astro-ph.CO](#)].
- [251] J. Casas and A. Ibarra, *Nucl.Phys.* **B618** (2001) 171–204, [arXiv:hep-ph/0103065](#) [[hep-ph](#)].
- [252] S. Weinberg, *Phys.Rev.Lett.* **43** (1979) 1566–1570.
- [253] A. Zee, *Phys.Lett.* **B93** (1980) 389.
- [254] A. Zee, *Nucl.Phys.* **B264** (1986) 99.
- [255] K. Babu, *Phys.Lett.* **B203** (1988) 132.
- [256] G. Branco, W. Grimus, and L. Lavoura, *Nucl.Phys.* **B312** (1989) 492.
- [257] R. Barbieri, D. V. Nanopoulos, G. Morchio, and F. Strocchi, *Phys.Lett.* **B90** (1980) 91.

- [258] R. Marshak and R. N. Mohapatra, Coral Gables, Proceedings, Recent Developments In High-energy Physics. 1980.
- [259] T. Cheng and L.-F. Li, *Phys.Rev.* **D22** (1980) 2860.
- [260] M. Magg and C. Wetterich, *Phys.Lett.* **B94** (1980) 61.
- [261] G. Lazarides, Q. Shafi, and C. Wetterich, *Nucl.Phys.* **B181** (1981) 287.
- [262] J. Schechter and J. Valle, *Phys.Rev.* **D22** (1980) 2227.
- [263] R. N. Mohapatra and G. Senjanović, *Phys.Rev.* **D23** (1981) 165.
- [264] P. Minkowski, *Phys.Lett.* **B67** (1977) 421.
- [265] M. Gell-Mann, P. Ramond, and R. Slansky, in *Supergravity*, P. Van Nieuwenhuizen and D. Freedman, eds., pp. 315–321. North-Holland, 1979.
- [266] T. Yanagida, in *Workshop on the Baryon Number of the Universe and Unified Theories*, O. Sawada and A. Sugamoto, eds., p. 95. KEK, 1979.
- [267] S. Glashow, *NATO Adv.Study Inst.Ser.B Phys.* **59** (1980) 687.
- [268] R. N. Mohapatra and G. Senjanović, *Phys.Rev.Lett.* **44** (1980) 912.
- [269] R. Foot, H. Lew, X. G. He, and G. C. Joshi, *Z.Phys.* **C44** (1989) 441.
- [270] R. Mohapatra and J. Valle, *Phys.Rev.* **D34** (1986) 1642.
- [271] M. Malinský, J. C. Romão, and J. W. F. Valle, *Phys.Rev.Lett.* **95** (2005) 161801, [arXiv:hep-ph/0506296](#) [hep-ph].
- [272] A. Rossi, *Phys.Rev.* **D66** (2002) 075003, [arXiv:hep-ph/0207006](#) [hep-ph].
- [273] E. Ma, *Phys.Rev.Lett.* **81** (1998) 1171–1174, [arXiv:hep-ph/9805219](#) [hep-ph].
- [274] C. Aulakh and R. N. Mohapatra, *Phys.Lett.* **B119** (1982) 136.
- [275] G. G. Ross and J. Valle, *Phys.Lett.* **B151** (1985) 375.
- [276] J. R. Ellis, G. Gelmini, C. Jarlskog, G. G. Ross, and J. Valle, *Phys.Lett.* **B150** (1985) 142.
- [277] A. Abada, S. Davidson, and M. Losada, *Phys.Rev.* **D65** (2002) 075010, [arXiv:hep-ph/0111332](#) [hep-ph].
- [278] Y. Grossman and H. E. Haber, in *1999 Meeting of the Division of Particles and Fields of the American Physical Society*, K. Arisaka and Z. Bern, eds. University of California, 1999. [arXiv:hep-ph/9906310](#) [hep-ph].

- [279] V. Bednyakov, A. Faessler, and S. Kovalenko, *Phys.Lett.* **B442** (1998) 203–208, [arXiv:hep-ph/9808224](#) [hep-ph].
- [280] A. S. Joshipura, R. D. Vaidya, and S. K. Vempati, *Nucl.Phys.* **B639** (2002) 290–306, [arXiv:hep-ph/0203182](#) [hep-ph].
- [281] C.-H. Chang and T.-F. Feng, *Eur.Phys.J.* **C12** (2000) 137–160, [arXiv:hep-ph/9901260](#) [hep-ph].
- [282] Y. Grossman and S. Rakshit, *Phys.Rev.* **D69** (2004) 093002, [arXiv:hep-ph/0311310](#) [hep-ph].
- [283] M. Hirsch and J. Valle, *New J.Phys.* **6** (2004) 76, [arXiv:hep-ph/0405015](#) [hep-ph].
- [284] A. Vicente Montesinos, *Phenomenology of supersymmetric neutrino mass models*. PhD thesis, 2011. [arXiv:1104.0831](#) [hep-ph].
- [285] W. Porod, M. Hirsch, J. Romão, and J. Valle, *Phys.Rev.* **D63** (2001) 115004, [arXiv:hep-ph/0011248](#) [hep-ph].
- [286] L. J. Hall and M. Suzuki, *Nucl.Phys.* **B231** (1984) 419.
- [287] B. Mukhopadhyaya, S. Roy, and F. Vissani, *Phys.Lett.* **B443** (1998) 191–195, [arXiv:hep-ph/9808265](#) [hep-ph].
- [288] **R parity Working Group Collaboration**, B. Allanach *et al.*, in *Physics at Run II: Workshop on Supersymmetry / Higgs: Summary Meeting*, M. Carena and J. Lykken, eds. Fermilab, 1999. [arXiv:hep-ph/9906224](#) [hep-ph].
- [289] S. Choi, E. J. Chun, S. K. Kang, and J. S. Lee, *Phys.Rev.* **D60** (1999) 075002, [arXiv:hep-ph/9903465](#) [hep-ph].
- [290] J. Romão, M. Díaz, M. Hirsch, W. Porod, and J. Valle, *Phys.Rev.* **D61** (2000) 071703, [arXiv:hep-ph/9907499](#) [hep-ph].
- [291] A. Bartl, W. Porod, D. Restrepo, J. Romão, and J. Valle, *Nucl.Phys.* **B600** (2001) 39–61, [arXiv:hep-ph/0007157](#) [hep-ph].
- [292] D. Restrepo, W. Porod, and J. W. Valle, *Phys.Rev.* **D64** (2001) 055011, [arXiv:hep-ph/0104040](#) [hep-ph].
- [293] M. Hirsch, W. Porod, J. Romão, and J. Valle, *Phys.Rev.* **D66** (2002) 095006, [arXiv:hep-ph/0207334](#) [hep-ph].
- [294] M. Díaz, M. Hirsch, W. Porod, J. Romão, and J. Valle, *Phys.Rev.* **D68** (2003) 013009, [arXiv:hep-ph/0302021](#) [hep-ph].
- [295] A. Bartl, M. Hirsch, T. Kernreiter, W. Porod, and J. Valle, *JHEP* **0311** (2003) 005, [arXiv:hep-ph/0306071](#) [hep-ph].

- [296] M. Hirsch and W. Porod, *Phys.Rev.* **D68** (2003) 115007, [arXiv:hep-ph/0307364](#) [hep-ph].
- [297] S. Petcov, *Sov.J.Nucl.Phys.* **25** (1977) 340.
- [298] S. M. Bilenky, S. Petcov, and B. Pontecorvo, *Phys.Lett.* **B67** (1977) 309.
- [299] B. Lee, S. Pakvasa, R. Shrock, and H. Sugawara, *Phys.Rev.Lett.* **38** (1977) 937.
- [300] W. Marciano and A. Sanda, *Phys.Lett.* **B67** (1977) 303.
- [301] T. Cheng and L.-F. Li, *Phys.Rev.Lett.* **45** (1980) 1908.
- [302] A. Buras, P. Gambino, M. Gorbahn, S. Jäger, and L. Silvestrini, *Phys.Lett.* **B500** (2001) 161–167, [arXiv:hep-ph/0007085](#) [hep-ph].
- [303] M. Antonelli, D. M. Asner, D. A. Bauer, T. G. Becher, M. Beneke, *et al.*, *Phys.Rept.* **494** (2010) 197–414, [arXiv:0907.5386](#) [hep-ph].
- [304] F. Gabbiani and A. Masiero, *Nucl.Phys.* **B322** (1989) 235.
- [305] F. Gabbiani, E. Gabrielli, A. Masiero, and L. Silvestrini, *Nucl.Phys.* **B477** (1996) 321–352, [arXiv:hep-ph/9604387](#) [hep-ph].
- [306] I. Masina and C. A. Savoy, *Nucl.Phys.* **B661** (2003) 365–393, [arXiv:hep-ph/0211283](#) [hep-ph].
- [307] L. J. Hall, V. A. Kostelecky, and S. Raby, *Nucl.Phys.* **B267** (1986) 415.
- [308] P. Paradisi, *JHEP* **0510** (2005) 006, [arXiv:hep-ph/0505046](#) [hep-ph].
- [309] F. Borzumati and A. Masiero, *Phys.Rev.Lett.* **57** (1986) 961.
- [310] J. Hisano, T. Moroi, K. Tobe, and M. Yamaguchi, *Phys.Rev.* **D53** (1996) 2442–2459, [arXiv:hep-ph/9510309](#) [hep-ph].
- [311] J. Hisano, T. Moroi, K. Tobe, M. Yamaguchi, and T. Yanagida, *Phys.Lett.* **B357** (1995) 579–587, [arXiv:hep-ph/9501407](#) [hep-ph].
- [312] J. Hisano, T. Moroi, K. Tobe, and M. Yamaguchi, *Phys.Lett.* **B391** (1997) 341–350, [arXiv:hep-ph/9605296](#) [hep-ph].
- [313] J. Hisano and D. Nomura, *Phys.Rev.* **D59** (1999) 116005, [arXiv:hep-ph/9810479](#) [hep-ph].
- [314] W. Buchmüller, D. Delepine, and F. Vissani, *Phys.Lett.* **B459** (1999) 171–178, [arXiv:hep-ph/9904219](#) [hep-ph].
- [315] Y. Kuno and Y. Okada, *Rev.Mod.Phys.* **73** (2001) 151–202, [arXiv:hep-ph/9909265](#) [hep-ph].
- [316] J. R. Ellis, M. Gómez, G. Leontaris, S. Lola, and D. V. Nanopoulos, *Eur.Phys.J.* **C14** (2000) 319–334, [arXiv:hep-ph/9911459](#) [hep-ph].

- [317] S. Lavignac, I. Masina, and C. A. Savoy, *Phys.Lett.* **B520** (2001) 269–278, [arXiv:hep-ph/0106245](#) [hep-ph].
- [318] X.-J. Bi and Y.-B. Dai, *Phys.Rev.* **D66** (2002) 076006, [arXiv:hep-ph/0112077](#) [hep-ph].
- [319] J. R. Ellis, J. Hisano, M. Raidal, and Y. Shimizu, *Phys.Rev.* **D66** (2002) 115013, [arXiv:hep-ph/0206110](#) [hep-ph].
- [320] F. Deppisch, H. Päs, A. Redelbach, R. Rückl, and Y. Shimizu, *Eur.Phys.J.* **C28** (2003) 365–374, [arXiv:hep-ph/0206122](#) [hep-ph].
- [321] T. Fukuyama, T. Kikuchi, and N. Okada, *Phys.Rev.* **D68** (2003) 033012, [arXiv:hep-ph/0304190](#) [hep-ph].
- [322] A. Brignole and A. Rossi, *Nucl.Phys.* **B701** (2004) 3–53, [arXiv:hep-ph/0404211](#) [hep-ph].
- [323] A. Masiero, S. K. Vempati, and O. Vives, *New J.Phys.* **6** (2004) 202, [arXiv:hep-ph/0407325](#) [hep-ph].
- [324] T. Fukuyama, A. Ilakovac, and T. Kikuchi, *Eur.Phys.J.* **C56** (2008) 125–146, [arXiv:hep-ph/0506295](#) [hep-ph].
- [325] S. Petcov, W. Rodejohann, T. Shindou, and Y. Takanishi, *Nucl.Phys.* **B739** (2006) 208–233, [arXiv:hep-ph/0510404](#) [hep-ph].
- [326] E. Arganda and M. J. Herrero, *Phys.Rev.* **D73** (2006) 055003, [arXiv:hep-ph/0510405](#) [hep-ph].
- [327] F. Deppisch, H. Päs, A. Redelbach, and R. Rückl, *Phys.Rev.* **D73** (2006) 033004, [arXiv:hep-ph/0511062](#) [hep-ph].
- [328] C. E. Yaguna, *Int.J.Mod.Phys.* **A21** (2006) 1283–1289, [arXiv:hep-ph/0502014](#) [hep-ph].
- [329] L. Calibbi, A. Faccia, A. Masiero, and S. Vempati, *Phys.Rev.* **D74** (2006) 116002, [arXiv:hep-ph/0605139](#) [hep-ph].
- [330] S. Antusch, E. Arganda, M. Herrero, and A. Teixeira, *JHEP* **0611** (2006) 090, [arXiv:hep-ph/0607263](#) [hep-ph].
- [331] E. Arganda, M. Herrero, and A. Teixeira, *JHEP* **0710** (2007) 104, [arXiv:0707.2955](#) [hep-ph].
- [332] E. Arganda, M. Herrero, and J. Portolés, *JHEP* **0806** (2008) 079, [arXiv:0803.2039](#) [hep-ph].
- [333] J. Esteves, J. Romão, M. Hirsch, F. Staub, and W. Porod, *Phys.Rev.* **D83** (2011) 013003, [arXiv:1010.6000](#) [hep-ph].
- [334] A. J. Buras, M. Nagai, and P. Paradisi, *JHEP* **1105** (2011) 005, [arXiv:1011.4853](#) [hep-ph].

- [335] C. Biggio and L. Calibbi, *JHEP* **1010** (2010) 037, [arXiv:1007.3750](#) [[hep-ph](#)].
- [336] L. Calibbi, D. Chowdhury, A. Masiero, K. Patel, and S. Vempati, *JHEP* **1211** (2012) 040, [arXiv:1207.7227](#) [[hep-ph](#)].
- [337] D. Chowdhury and K. M. Patel, [arXiv:1304.7888](#) [[hep-ph](#)].
- [338] N. Arkani-Hamed, H.-C. Cheng, J. L. Feng, and L. J. Hall, *Phys.Rev.Lett.* **77** (1996) 1937–1940, [arXiv:hep-ph/9603431](#) [[hep-ph](#)].
- [339] N. Krasnikov, *JETP Lett.* **65** (1997) 148–153, [arXiv:hep-ph/9611282](#) [[hep-ph](#)].
- [340] S. Bitukov and N. Krasnikov, in *QUARKS'98*, F. Bezrukov, V. Matveev, V. Rubakov, A. Tavkhelidze, and S. Troitsky, eds. Inst. Nucl. Res. Acad. Sci., 1998. [arXiv:hep-ph/9806504](#) [[hep-ph](#)].
- [341] J. Hisano, M. M. Nojiri, Y. Shimizu, and M. Tanaka, *Phys.Rev.* **D60** (1999) 055008, [arXiv:hep-ph/9808410](#) [[hep-ph](#)].
- [342] K. Agashe and M. Graesser, *Phys.Rev.* **D61** (2000) 075008, [arXiv:hep-ph/9904422](#) [[hep-ph](#)].
- [343] H. Baer, C. Balázs, S. Hesselbach, J. K. Mizukoshi, and X. Tata, *Phys.Rev.* **D63** (2001) 095008, [arXiv:hep-ph/0012205](#) [[hep-ph](#)].
- [344] I. Hinchliffe and F. Paige, *Phys.Rev.* **D63** (2001) 115006, [arXiv:hep-ph/0010086](#) [[hep-ph](#)].
- [345] M. Guchait, J. Kalinowski, and P. Roy, *Eur.Phys.J.* **C21** (2001) 163–169, [arXiv:hep-ph/0103161](#) [[hep-ph](#)].
- [346] F. Deppisch, H. Päs, A. Redelbach, R. Rückl, and Y. Shimizu, *Phys.Rev.* **D69** (2004) 054014, [arXiv:hep-ph/0310053](#) [[hep-ph](#)].
- [347] F. Deppisch, J. Kalinowski, H. Päs, A. Redelbach, and R. Rückl, [arXiv:hep-ph/0401243](#) [[hep-ph](#)].
- [348] M. Cannoni, C. Carimalo, W. Da Silva, and O. Panella, *Phys.Rev.* **D72** (2005) 115004, [arXiv:hep-ph/0508256](#) [[hep-ph](#)].
- [349] D. Carvalho, J. R. Ellis, M. Gómez, S. Lola, and J. Romão, *Phys.Lett.* **B618** (2005) 162–170, [arXiv:hep-ph/0206148](#) [[hep-ph](#)].
- [350] M. R. Buckley and H. Murayama, *Phys.Rev.Lett.* **97** (2006) 231801, [arXiv:hep-ph/0606088](#) [[hep-ph](#)].
- [351] M. Cannoni and O. Panella, *Phys.Rev.* **D79** (2009) 056001, [arXiv:0812.2875](#) [[hep-ph](#)].
- [352] M. Hirsch, J. Valle, W. Porod, J. Romão, and A. Villanova del Moral, *Phys.Rev.* **D78** (2008) 013006, [arXiv:0804.4072](#) [[hep-ph](#)].

- [353] E. Carquin, J. Ellis, M. Gómez, S. Lola, and J. Rodríguez-Quintero, *JHEP* **0905** (2009) 026, [arXiv:0812.4243 \[hep-ph\]](#).
- [354] A. J. Buras, L. Calibbi, and P. Paradisi, *JHEP* **1006** (2010) 042, [arXiv:0912.1309 \[hep-ph\]](#).
- [355] M. Herrero, J. Portolés, and A. Rodríguez-Sánchez, *Phys.Rev.* **D80** (2009) 015023, [arXiv:0903.5151 \[hep-ph\]](#).
- [356] J. Esteves, J. Romão, A. Villanova del Moral, M. Hirsch, J. Valle, *et al.*, *JHEP* **0905** (2009) 003, [arXiv:0903.1408 \[hep-ph\]](#).
- [357] A. Abada, A. Figueiredo, J. Romão, and A. Teixeira, *JHEP* **1010** (2010) 104, [arXiv:1007.4833 \[hep-ph\]](#).
- [358] L. Calibbi, R. Hodgkinson, J. Jones Pérez, A. Masiero, and O. Vives, *Eur.Phys.J.* **C72** (2012) 1863, [arXiv:1111.0176 \[hep-ph\]](#).
- [359] L. Calibbi, R. Hodgkinson, J. Jones-Pérez, A. Masiero, and O. Vives, in *21st International Europhysics Conference on High Energy Physics*, vol. EPS-HEP2011, p. 160. Proceedings of Science, 2011. [arXiv:1111.6376 \[hep-ph\]](#).
- [360] I. Galon and Y. Shadmi, *Phys.Rev.* **D85** (2012) 015010, [arXiv:1108.2220 \[hep-ph\]](#).
- [361] C. Arbeláez, M. Hirsch, and L. Reichert, *JHEP* **1202** (2012) 112, [arXiv:1112.4771 \[hep-ph\]](#).
- [362] M. Hirsch, L. Reichert, and W. Porod, *JHEP* **1105** (2011) 086, [arXiv:1101.2140 \[hep-ph\]](#).
- [363] E. Carquin, J. Ellis, M. Gómez, and S. Lolab, *JHEP* **1111** (2011) 050, [arXiv:1106.4903 \[hep-ph\]](#).
- [364] A. Abada, A. Figueiredo, J. Romão, and A. Teixeira, *JHEP* **1108** (2011) 099, [arXiv:1104.3962 \[hep-ph\]](#).
- [365] A. Abada, A. Figueiredo, J. Romão, and A. Teixeira, *JHEP* **1208** (2012) 138, [arXiv:1206.2306 \[hep-ph\]](#).
- [366] M. Hirsch, W. Porod, C. Weiss, and F. Staub, *Phys.Rev.* **D87** (2013) 013010, [arXiv:1211.0289 \[hep-ph\]](#).
- [367] A. Abada, C. Biggio, F. Bonnet, M. Gavela, and T. Hambye, *JHEP* **0712** (2007) 061, [arXiv:0707.4058 \[hep-ph\]](#).
- [368] M. Raidal, A. van der Schaaf, I. Bigi, M. Mangano, Y. K. Semertzidis, *et al.*, *Eur.Phys.J.* **C57** (2008) 13–182, [arXiv:0801.1826 \[hep-ph\]](#).
- [369] K. Hagiwara, R. Liao, A. D. Martin, D. Nomura, and T. Teubner, *J.Phys.* **G38** (2011) 085003, [arXiv:1105.3149 \[hep-ph\]](#).

- [370] M. Passera, *Nucl.Phys.Proc.Suppl.* **169** (2007) 213–225, [arXiv:hep-ph/0702027](#) [HEP-PH].
- [371] P. J. Mohr, B. N. Taylor, and D. B. Newell, *Rev.Mod.Phys.* **84** (2012) 1527–1605, [arXiv:1203.5425](#) [physics.atom-ph].
- [372] **Muon G-2 Collaboration**, G. Bennett *et al.*, *Phys.Rev.* **D73** (2006) 072003, [arXiv:hep-ex/0602035](#) [hep-ex].
- [373] **DELPHI Collaboration**, J. Abdallah *et al.*, *Eur.Phys.J.* **C35** (2004) 159–170, [arXiv:hep-ex/0406010](#) [hep-ex].
- [374] T. Fukuyama, *Int.J.Mod.Phys.* **A27** (2012) 1230015, [arXiv:1201.4252](#) [hep-ph].
- [375] J. Hudson, D. Kara, I. Smallman, B. Sauer, M. Tarbutt, *et al.*, *Nature* **473** (2011) 493–496.
- [376] **Muon (g-2) Collaboration**, G. Bennett *et al.*, *Phys.Rev.* **D80** (2009) 052008, [arXiv:0811.1207](#) [hep-ex].
- [377] **Belle Collaboration**, K. Inami *et al.*, *Phys.Lett.* **B551** (2003) 16–26, [arXiv:hep-ex/0210066](#) [hep-ex].
- [378] **MEG Collaboration**, J. Adam *et al.*, *Phys.Rev.Lett.* **110** (2013) 201801, [arXiv:1303.0754](#) [hep-ex].
- [379] A. Baldini, F. Cei, C. Cerri, S. Dussoni, L. Galli, *et al.*, [arXiv:1301.7225](#) [physics.ins-det].
- [380] **BaBar Collaboration**, B. Aubert *et al.*, *Phys.Rev.Lett.* **104** (2010) 021802, [arXiv:0908.2381](#) [hep-ex].
- [381] **SuperB Collaboration**, B. O’Leary *et al.*, [arXiv:1008.1541](#) [hep-ex].
- [382] **Belle II Collaboration**, T. Abe, [arXiv:1011.0352](#) [physics.ins-det].
- [383] **SINDRUM II Collaboration**, W. H. Bertl *et al.*, *Eur.Phys.J.* **C47** (2006) 337–346.
- [384] **SINDRUM II Collaboration.**, C. Dohmen *et al.*, *Phys.Lett.* **B317** (1993) 631–636.
- [385] **COMET Collaboration**, Y. Cui *et al.*,
- [386] **Mu2e Collaboration**, D. Glenzinski, *AIP Conf.Proc.* **1222** (2010) 383–386.
- [387] R. Barlow, *Nucl.Phys.Proc.Suppl.* **218** (2011) 44–49.
- [388] **SINDRUM Collaboration**, U. Bellgardt *et al.*, *Nucl.Phys.* **B299** (1988) 1.

- [389] A. Blondel, A. Bravar, M. Pohl, S. Bachmann, N. Berger, *et al.*, [arXiv:1301.6113](#) [[physics.ins-det](#)].
- [390] K. Hayasaka, K. Inami, Y. Miyazaki, K. Arinstein, V. Aulchenko, *et al.*, *Phys.Lett.* **B687** (2010) 139–143, [arXiv:1001.3221](#) [[hep-ex](#)].
- [391] **LHCb Collaboration**, R. Aaij *et al.*, *Phys.Rev.Lett.* **110** (2013) 021801, [arXiv:1211.2674](#) [[hep-ex](#)].
- [392] **LHCb Collaboration**, M.-H. Schune, in *7th Workshop on the CKM Unitarity Triangle (CKM 2012)*. 2013. [arXiv:1301.4811](#) [[hep-ex](#)].
- [393] M. Artuso, D. Asner, P. Ball, E. Baracchini, G. Bell, *et al.*, *Eur.Phys.J.* **C57** (2008) 309–492, [arXiv:0801.1833](#) [[hep-ph](#)].
- [394] A. J. Buras, J. Girrbach, D. Guadagnoli, and G. Isidori, *Eur.Phys.J.* **C72** (2012) 2172, [arXiv:1208.0934](#) [[hep-ph](#)].
- [395] J. Laiho, E. Lunghi, and R. S. Van de Water, “Lattice Averages: End of 2011.” [www.latticeaverages.org/](#), 2011. Retrieved May 5, 2013.
- [396] J. Laiho, E. Lunghi, and R. S. Van de Water, *Phys.Rev.* **D81** (2010) 034503, [arXiv:0910.2928](#) [[hep-ph](#)].
- [397] **Fermilab Lattice Collaboration, MILC Collaboration**, A. Bazavov *et al.*, *Phys.Rev.* **D85** (2012) 114506, [arXiv:1112.3051](#) [[hep-lat](#)].
- [398] H. Na, C. J. Monahan, C. T. Davies, R. Horgan, G. P. Lepage, *et al.*, *Phys.Rev.* **D86** (2012) 034506, [arXiv:1202.4914](#) [[hep-lat](#)].
- [399] R. Cahn, *Semi-Simple Lie Algebras and Their Representations*. Dover Books on Mathematics Series. Dover, 2006.
- [400] J. Fuchs and C. Schweigert, *Symmetries, Lie Algebras and Representations: A Graduate Course for Physicists*. Cambridge Monographs on Mathematical Physics. Cambridge University Press, 2003.
- [401] R. Slansky, *Phys.Rept.* **79** (1981) 1–128.
- [402] G. B auerle and E. de Kerf, *Lie Algebras, Part 1: Finite and Infinite Dimensional Lie Algebras and Applications in Physics*. Studies in Mathematical Physics. Elsevier Science, 1997.
- [403] N. Jacobson, *Lie Algebras*. Dover books on advanced mathematics. Dover, 1979.
- [404] W. Tung, *Group theory in Physics*. World Scientific, 1985.
- [405] M. Berg, C. DeWitt-Morette, S. Gwo, and E. Kramer, *Rev.Math.Phys.* **13** (2001) 953–1034, [arXiv:math-ph/0012006](#) [[math-ph](#)].

- [406] M. Rausch de Traubenberg, in *7th International Conference on Clifford Algebras and their Applications in Mathematical Physics*. 2005.
[arXiv:hep-th/0506011](#) [hep-th].
- [407] R. Streater and A. Wightman, *PCT, spin and statistics, and all that*. W. A. Benjamin, 1964.
- [408] J. Lubański, *Physica* **9** no. 3, (1942) 310–324.
- [409] S. R. Coleman and J. Mandula, *Phys.Rev.* **159** (1967) 1251–1256.
- [410] R. Haag, J. T. Łopuszański, and M. Sohnius, *Nucl.Phys.* **B88** (1975) 257.
- [411] S. Weinberg, *The quantum theory of fields. Vol. 3: Supersymmetry*. The Quantum Theory of Fields. Cambridge University Press, 2000.
- [412] M. Sohnius, *Phys.Rept.* **128** (1985) 39–204.
- [413] J. D. Lykken, in *Theoretical Advanced Study Institute in Elementary Particle Physics (TASI'96): fields, strings and duality*, C. Efthimiou and B. Greene, eds., pp. 85–153. World Scientific, 1996.
[arXiv:hep-th/9612114](#) [hep-th].
- [414] I. Aitchison, *Supersymmetry in Particle Physics: An Elementary Introduction*. Cambridge University Press, 2007.
- [415] A. Bilal, [arXiv:hep-th/0101055](#) [hep-th].
- [416] P. Argyres, in *Non-Perturbative Aspects of Strings, Branes and Supersymmetry*, pp. 1–28. World Scientific, 1999.
- [417] J. Wess and J. Bagger, *Supersymmetry and supergravity*. Princeton Series in Physics Series. University Press, 1992.
- [418] P. C. West, *Introduction to supersymmetry and supergravity*. World Scientific, 1990.
- [419] H. P. Nilles, *Phys.Rept.* **110** (1984) 1–162.
- [420] L. O’Raifeartaigh, *Phys.Rev.* **139** (1965) B1052–B1062.
- [421] A. Galperin, L. Litov, and V. Soroka, *J.Phys.* **G9** (1983) 133.
- [422] P. Nath and R. L. Arnowitt, *Phys.Lett.* **B56** (1975) 177.
- [423] R. L. Arnowitt, P. Nath, and B. Zumino, *Phys.Lett.* **B56** (1975) 81.
- [424] D. Z. Freedman, P. van Nieuwenhuizen, and S. Ferrara, *Phys.Rev.* **D13** (1976) 3214–3218.
- [425] S. Deser and B. Zumino, *Phys.Lett.* **B62** (1976) 335.
- [426] D. Z. Freedman and P. van Nieuwenhuizen, *Phys.Rev.* **D14** (1976) 912.

- [427] E. Cremmer, B. Julia, J. Scherk, S. Ferrara, L. Girardello, *et al.*, *Nucl.Phys.* **B147** (1979) 105.
- [428] J. A. Bagger, *Nucl.Phys.* **B211** (1983) 302.
- [429] E. Cremmer, S. Ferrara, L. Girardello, and A. Van Proeyen, *Nucl.Phys.* **B212** (1983) 413.
- [430] S. P. Martin and M. T. Vaughn, *Phys.Rev.* **D50** (1994) 2282, [arXiv:hep-ph/9311340](#) [hep-ph].
- [431] U. Ellwanger, C. Hugonie, and A. M. Teixeira, *Phys.Rept.* **496** (2010) 1–77, [arXiv:0910.1785](#) [hep-ph].
- [432] Y. Yamada, *Phys.Rev.* **D50** (1994) 3537–3545, [arXiv:hep-ph/9401241](#) [hep-ph].
- [433] R. Feger and T. W. Kephart, [arXiv:1206.6379](#) [math-ph].
- [434] F. Staub, *Comput.Phys.Commun.* **181** (2010) 1077–1086, [arXiv:0909.2863](#) [hep-ph].
- [435] F. Staub, *Comput.Phys.Commun.* **182** (2011) 808–833, [arXiv:1002.0840](#) [hep-ph].
- [436] F. Staub, *Computer Physics Communications* **184** (2013) pp. 1792–1809, [arXiv:1207.0906](#) [hep-ph].
- [437] F. Staub, [arXiv:1309.7223](#) [hep-ph].
- [438] F. Lyonnet, I. Schienbein, F. Staub, and A. Wingerter, [arXiv:1309.7030](#) [hep-ph].
- [439] B. Allanach, A. Dedes, and H. K. Dreiner, *Phys.Rev.* **D60** (1999) 056002, [arXiv:hep-ph/9902251](#) [hep-ph].
- [440] F. Borzumati and T. Yamashita, *Prog.Theor.Phys.* **124** (2010) 761–868, [arXiv:0903.2793](#) [hep-ph].
- [441] R. P. Stanley, *Enumerative combinatorics. Vol 2*. Cambridge: Cambridge University Press, 1999.
- [442] M. A. A. van Leeuwen, A. M. Cohen, and B. Lisser, *LiE, A Package for Lie Group Computations*. Computer Algebra Nederland, 1992.
- [443] D. M. Snow, *ACM Trans. Math. Softw.* **19** no. 1, (1993) 95–108.
- [444] D. M. Snow, *ACM Trans. Math. Softw.* **16** no. 1, (1990) 94–108.
- [445] D. Bernstein, *J. Symb. Comput.* **37** no. 6, (2004) 727–748, [arXiv:math/0309225](#) [math].
- [446] R. P. Stanley, *Enumerative combinatorics. Vol. 1. 2nd ed.* Cambridge: Cambridge University Press, 2012.

- [447] I. Jack and D. Jones, *Phys.Lett.* **B473** (2000) 102–108, [arXiv:hep-ph/9911491](#) [hep-ph].
- [448] I. Jack and D. Jones, *Phys.Rev.* **D63** (2001) 075010, [arXiv:hep-ph/0010301](#) [hep-ph].
- [449] I. Jack, D. Jones, and S. Parsons, *Phys.Rev.* **D62** (2000) 125022, [arXiv:hep-ph/0007291](#) [hep-ph].
- [450] I. Jack and D. Jones, *Phys.Lett.* **B457** (1999) 101–108, [arXiv:hep-ph/9903365](#) [hep-ph].
- [451] I. Jack and D. Jones, *Phys.Rev.* **D61** (2000) 095002, [arXiv:hep-ph/9909570](#) [hep-ph].
- [452] M. D. Goodsell, *JHEP* **1301** (2013) 066, [arXiv:1206.6697](#) [hep-ph].
- [453] B. Holdom, *Phys. Lett.* **B166** (1986) 196.
- [454] K. S. Babu, C. F. Kolda, and J. March-Russell, *Phys. Rev.* **D57** (1998) 6788–6792, [arXiv:hep-ph/9710441](#).
- [455] M.-X. Luo and Y. Xiao, *Phys.Lett.* **B555** (2003) 279–286, [arXiv:hep-ph/0212152](#) [hep-ph].
- [456] S. Khalil and A. Masiero, *Phys. Lett.* **B665** (2008) 374–377, [arXiv:0710.3525](#) [hep-ph].
- [457] P. Fileviez Pérez and S. Spinner, *Phys. Rev.* **D83** (2011) 035004, [arXiv:1005.4930](#) [hep-ph].
- [458] V. Barger, P. Fileviez Pérez, and S. Spinner, *Phys. Rev. Lett.* **102** (2009) 181802, [arXiv:0812.3661](#) [hep-ph].
- [459] J. Pelto, I. Vilja, and H. Virtanen, *Phys. Rev.* **D83** (2011) 055001, [arXiv:1012.3288](#) [hep-ph].
- [460] K. S. Babu, Y. Meng, and Z. Tavartkiladze, *Phys. Lett.* **B681** (2009) 37–43, [arXiv:0901.1044](#) [hep-ph].
- [461] G. Golub and C. Van Loan, *Matrix Computations*. Johns Hopkins Studies in the Mathematical Sciences. Johns Hopkins University Press, 1996.
- [462] F. del Aguila, G. Coughlan, and M. Quiros, *Nucl.Phys.* **B307** (1988) 633.
- [463] I. Jack, D. R. T. Jones, S. P. Martin, M. T. Vaughn, and Y. Yamada, *Phys. Rev.* **D50** (1994) 5481–5483, [arXiv:hep-ph/9407291](#).
- [464] F. Braam and J. Reuter, *Eur.Phys.J.* **C72** (2012) 1885, [arXiv:1107.2806](#) [hep-ph].
- [465] F. del Aguila, J. A. Gonzalez, and M. Quirós, *Nucl. Phys.* **B307** (1988) 571.

- [466] P. Fileviez Perez and M. B. Wise, *Phys.Rev.* **D84** (2011) 055015, [arXiv:1105.3190 \[hep-ph\]](#).
- [467] V. De Romeri, M. Hirsch, and M. Malinský, *Phys.Rev.* **D84** (2011) 053012, [arXiv:1107.3412 \[hep-ph\]](#).
- [468] G. D. Kribs, *Nucl. Phys.* **B535** (1998) 41–82, [arXiv:hep-ph/9803259](#).
- [469] F. Staub, [arXiv:0806.0538 \[hep-ph\]](#).
- [470] **SNO Collaboration**, Q. R. Ahmad *et al.*, *Phys.Rev.Lett.* **89** (2002) 011301, [arXiv:nucl-ex/0204008 \[nucl-ex\]](#).
- [471] **KamLAND Collaboration**, K. Eguchi *et al.*, *Phys.Rev.Lett.* **90** (2003) 021802, [arXiv:hep-ex/0212021 \[hep-ex\]](#).
- [472] R. N. Mohapatra and G. Senjanović, *Phys.Rev.Lett.* **44** (1980) 912.
- [473] R. Mohapatra, *Unification and Supersymmetry: The Frontiers of Quark-Lepton Physics*. Graduate Texts in Contemporary Physics. Springer, 1986.
- [474] M. Cvetič and J. C. Pati, *Phys.Lett.* **B135** (1984) 57.
- [475] R. Kuchimanchi and R. N. Mohapatra, *Phys.Rev.* **D48** (1993) 4352–4360, [arXiv:hep-ph/9306290 \[hep-ph\]](#).
- [476] C. S. Aulakh, K. Benakli, and G. Senjanović, *Phys.Rev.Lett.* **79** (1997) 2188–2191, [arXiv:hep-ph/9703434 \[hep-ph\]](#).
- [477] C. S. Aulakh, A. Melfo, A. Rasin, and G. Senjanović, *Phys.Rev.* **D58** (1998) 115007, [arXiv:hep-ph/9712551 \[hep-ph\]](#).
- [478] S. K. Majee, M. K. Parida, A. Raychaudhuri, and U. Sarkar, *Phys.Rev.* **D75** (2007) 075003, [arXiv:hep-ph/0701109 \[hep-ph\]](#).
- [479] L. Calibbi, L. Ferretti, A. Romanino, and R. Ziegler, *Phys.Lett.* **B672** (2009) 152–157, [arXiv:0812.0342 \[hep-ph\]](#).
- [480] P. S. B. Dev and R. N. Mohapatra, *Phys.Rev.* **D81** (2010) 013001, [arXiv:0910.3924 \[hep-ph\]](#).
- [481] M. Hirsch, S. Kaneko, and W. Porod, *Phys.Rev.* **D78** (2008) 093004, [arXiv:0806.3361 \[hep-ph\]](#).
- [482] J. C. Romão *et al.*, “Supersymmetric SO(10) GUTs with sliding scales.” [porthos.ist.utl.pt/arXiv/AllSO10GUTs](#), 2013. Retrieved February 12, 2013.
- [483] E. K. Akhmedov, M. Lindner, E. Schnapka, and J. W. F. Valle, *Phys.Lett.* **B368** (1996) 270–280, [arXiv:hep-ph/9507275 \[hep-ph\]](#).

- [484] E. K. Akhmedov, M. Lindner, E. Schnapka, and J. W. F. Valle, *Phys.Rev.* **D53** (1996) 2752–2780, [arXiv:hep-ph/9509255](#) [hep-ph].
- [485] K. S. Babu, B. Dutta, and R. N. Mohapatra, *Phys.Rev.* **D60** (1999) 095004, [arXiv:hep-ph/9812421](#) [hep-ph].
- [486] S. Davidson, D. C. Bailey, and B. A. Campbell, *Z.Phys.* **C61** (1994) 613–644, [arXiv:hep-ph/9309310](#) [hep-ph].
- [487] A. V. Kuznetsov, N. V. Mikheev, and A. V. Serghienko, in *QUARKS 2012: 17th International Seminar on High Energy Physics*. 2012. [arXiv:1210.3697](#) [hep-ph].
- [488] H. Baer, V. Barger, A. Lessa, and X. Tata, *Phys.Rev.* **D86** (2012) 117701, [arXiv:1207.4846](#) [hep-ph].
- [489] **ATLAS Collaboration**, G. Aad *et al.*, *ATLAS-CONF-2012-109* (2012) .
- [490] **ATLAS Collaboration**, G. Aad *et al.*, “Higgs public results.” <https://twiki.cern.ch/twiki/bin/view/AtlasPublic/HiggsPublicResults>, 2013. Retrieved February 18, 2013.
- [491] **CMS Collaboration**, S. Chatrchyan *et al.*, “Cms higgs physics results.” <https://twiki.cern.ch/twiki/bin/view/CMSPublic/PhysicsResultsHIG>, 2013. Retrieved February 18, 2013.
- [492] O. Buchmueller, R. Cavanaugh, A. De Roeck, M. J. Dolan, J. R. Ellis, *et al.*, *Eur.Phys.J.* **C72** (2012) 2020, [arXiv:1112.3564](#) [hep-ph].
- [493] H. E. Haber and M. Sher, *Phys.Rev.* **D35** (1987) 2206.
- [494] M. Drees, *Phys.Rev.* **D35** (1987) 2910–2913.
- [495] M. Hirsch, W. Porod, L. Reichert, and F. Staub, *Phys.Rev.* **D86** (2012) 093018, [arXiv:1206.3516](#) [hep-ph].
- [496] M. Hirsch, M. Malinský, W. Porod, L. Reichert, and F. Staub, *JHEP* **1202** (2012) 084, [arXiv:1110.3037](#) [hep-ph].
- [497] V. Cirigliano and I. Rosell, *Phys.Rev.Lett.* **99** (2007) 231801, [arXiv:0707.3439](#) [hep-ph].
- [498] **NA48/2 and NA62 Collaborations**, E. Goudzovski,.
- [499] A. Masiero, P. Paradisi, and R. Petronzio, *Phys.Rev.* **D74** (2006) 011701, [arXiv:hep-ph/0511289](#) [hep-ph].
- [500] A. Masiero, P. Paradisi, and R. Petronzio, *JHEP* **0811** (2008) 042, [arXiv:0807.4721](#) [hep-ph].
- [501] J. Girrbach and U. Nierste, [arXiv:1202.4906](#) [hep-ph].

- [502] J. Ellis, S. Lola, and M. Raidal, *Nucl.Phys.* **B812** (2009) 128–143, [arXiv:0809.5211 \[hep-ph\]](#).
- [503] L. J. Hall, R. Rattazzi, and U. Sarid, *Phys.Rev.* **D50** (1994) 7048–7065, [arXiv:hep-ph/9306309 \[hep-ph\]](#).
- [504] W.-S. Hou, *Phys.Rev.* **D48** (1993) 2342–2344.
- [505] P. H. Chankowski, R. Hempfling, and S. Pokorski, *Phys.Lett.* **B333** (1994) 403–412, [arXiv:hep-ph/9405281 \[hep-ph\]](#).
- [506] K. Babu and C. F. Kolda, *Phys.Rev.Lett.* **84** (2000) 228–231, [arXiv:hep-ph/9909476 \[hep-ph\]](#).
- [507] M. S. Carena, D. Garcia, U. Nierste, and C. E. Wagner, *Nucl.Phys.* **B577** (2000) 88–120, [arXiv:hep-ph/9912516 \[hep-ph\]](#).
- [508] K. Babu and C. Kolda, *Phys.Rev.Lett.* **89** (2002) 241802, [arXiv:hep-ph/0206310 \[hep-ph\]](#).
- [509] A. Brignole and A. Rossi, *Phys.Lett.* **B566** (2003) 217–225, [arXiv:hep-ph/0304081 \[hep-ph\]](#).
- [510] E. Arganda, A. M. Curiel, M. J. Herrero, and D. Temes, *Phys.Rev.* **D71** (2005) 035011, [arXiv:hep-ph/0407302 \[hep-ph\]](#).
- [511] P. Paradisi, *JHEP* **0602** (2006) 050, [arXiv:hep-ph/0508054 \[hep-ph\]](#).
- [512] P. Paradisi, *JHEP* **0608** (2006) 047, [arXiv:hep-ph/0601100 \[hep-ph\]](#).
- [513] M. J. Ramsey-Musolf, S. Su, and S. Tulin, *Phys.Rev.* **D76** (2007) 095017, [arXiv:0705.0028 \[hep-ph\]](#).
- [514] A. Abada, D. Das, A. Teixeira, A. Vicente, and C. Weiland, *JHEP* **1302** (2013) 048, [arXiv:1211.3052 \[hep-ph\]](#).
- [515] F. Borzumati, G. R. Farrar, N. Polonsky, and S. D. Thomas, *Nucl.Phys.* **B555** (1999) 53–115, [arXiv:hep-ph/9902443 \[hep-ph\]](#).
- [516] B. Bellazzini, Y. Grossman, I. Nachshon, and P. Paradisi, *JHEP* **1106** (2011) 104, [arXiv:1012.3759 \[hep-ph\]](#).
- [517] J. Parry, *Nucl.Phys.* **B760** (2007) 38–63, [arXiv:hep-ph/0510305 \[hep-ph\]](#).
- [518] J. R. Ellis, J. S. Lee, and A. Pilaftsis, *Phys.Rev.* **D76** (2007) 115011, [arXiv:0708.2079 \[hep-ph\]](#).
- [519] **Particle Data Group**, C. Amsler *et al.*, *Phys.Lett.* **B667** (2008) 1–1340.
- [520] G. Isidori and P. Paradisi, *Phys.Lett.* **B639** (2006) 499–507, [arXiv:hep-ph/0605012 \[hep-ph\]](#).

- [521] **DAYA-BAY Collaboration**, F. An *et al.*, *Phys.Rev.Lett.* **108** (2012) 171803, [arXiv:1203.1669 \[hep-ex\]](#).
- [522] **RENO Collaboration**, J. Ahn *et al.*, *Phys.Rev.Lett.* **108** (2012) 191802, [arXiv:1204.0626 \[hep-ex\]](#).
- [523] **MINOS Collaboration**, P. Adamson *et al.*, *Phys.Rev.Lett.* **108** (2012) 191801, [arXiv:1202.2772 \[hep-ex\]](#).
- [524] W. Porod, *Comput.Phys.Commun.* **153** (2003) 275–315, [arXiv:hep-ph/0301101 \[hep-ph\]](#).
- [525] W. Porod and F. Staub, *Comput.Phys.Commun.* **183** (2012) 2458–2469, [arXiv:1104.1573 \[hep-ph\]](#).
- [526] **ATLAS Collaboration**, G. Aad *et al.*, *Phys.Rev.Lett.* **108** (2012) 241802, [arXiv:1203.5763 \[hep-ex\]](#).
- [527] **ATLAS Collaboration**, G. Aad *et al.*, *Eur.Phys.J.* **C72** (2012) 1993, [arXiv:1202.4847 \[hep-ex\]](#).
- [528] **CMS Collaboration**, S. Koay and C. Collaboration, *EPJ Web Conf.* **28** (2012) 09008, [arXiv:1202.1000 \[hep-ex\]](#).
- [529] **ATLAS Collaboration**, G. Aad *et al.*, *Phys.Lett.* **B710** (2012) 519–537, [arXiv:1111.4116 \[hep-ex\]](#).
- [530] **ATLAS Collaboration**, G. Aad *et al.*, *Phys.Lett.* **B710** (2012) 67–85, [arXiv:1109.6572 \[hep-ex\]](#).
- [531] **ATLAS Collaboration**, G. Aad *et al.*, *Eur.Phys.J.* **C71** (2011) 1744, [arXiv:1107.0561 \[hep-ex\]](#).
- [532] **ATLAS Collaboration**, G. Aad *et al.*, *Eur.Phys.J.* **C71** (2011) 1682, [arXiv:1103.6214 \[hep-ex\]](#).
- [533] **ATLAS Collaboration**, G. Aad *et al.*, *Eur.Phys.J.* **C71** (2011) 1647, [arXiv:1103.6208 \[hep-ex\]](#).
- [534] **ATLAS Collaboration**, G. Aad *et al.*, *Phys.Lett.* **B701** (2011) 398–416, [arXiv:1103.4344 \[hep-ex\]](#).
- [535] **ATLAS Collaboration**, G. Aad *et al.*, *Phys.Lett.* **B701** (2011) 1–19, [arXiv:1103.1984 \[hep-ex\]](#).
- [536] **ATLAS Collaboration**, G. Aad *et al.*, *Phys.Lett.* **B701** (2011) 186–203, [arXiv:1102.5290 \[hep-ex\]](#).
- [537] **ATLAS Collaboration**, G. Aad *et al.*, *Phys.Rev.Lett.* **106** (2011) 131802, [arXiv:1102.2357 \[hep-ex\]](#).
- [538] **CMS Collaboration**, S. Chatrchyan *et al.*, *Phys.Rev.Lett.* **107** (2011) 221804, [arXiv:1109.2352 \[hep-ex\]](#).

- [539] **CMS Collaboration**, S. Chatrchyan *et al.*, *JHEP* **1108** (2011) 156, [arXiv:1107.1870 \[hep-ex\]](#).
- [540] **CMS Collaboration**, S. Chatrchyan *et al.*, *Phys.Rev.* **D85** (2012) 012004, [arXiv:1107.1279 \[hep-ex\]](#).
- [541] **CMS Collaboration**, S. Chatrchyan *et al.*, *JHEP* **1108** (2011) 155, [arXiv:1106.4503 \[hep-ex\]](#).
- [542] **CMS Collaboration**, S. Chatrchyan *et al.*, *JHEP* **1107** (2011) 113, [arXiv:1106.3272 \[hep-ex\]](#).
- [543] **CMS Collaboration**, S. Chatrchyan *et al.*, *Phys.Lett.* **B704** (2011) 411–433, [arXiv:1106.0933 \[hep-ex\]](#).
- [544] **CMS Collaboration**, S. Chatrchyan *et al.*, *JHEP* **1106** (2011) 093, [arXiv:1105.3152 \[hep-ex\]](#).
- [545] **CMS Collaboration**, S. Chatrchyan *et al.*, *JHEP* **1106** (2011) 077, [arXiv:1104.3168 \[hep-ex\]](#).
- [546] **CMS Collaboration**, S. Chatrchyan *et al.*, *JHEP* **1106** (2011) 026, [arXiv:1103.1348 \[hep-ex\]](#).
- [547] **CMS Collaboration**, S. Chatrchyan *et al.*, *Phys.Rev.Lett.* **106** (2011) 211802, [arXiv:1103.0953 \[hep-ex\]](#).
- [548] **CMS Collaboration**, V. Khachatryan *et al.*, *Phys.Lett.* **B698** (2011) 196–218, [arXiv:1101.1628 \[hep-ex\]](#).
- [549] **CMS Collaboration**, V. Khachatryan *et al.*, *Phys.Rev.Lett.* **106** (2011) 011801, [arXiv:1011.5861 \[hep-ex\]](#).
- [550] G. Fogli, E. Lisi, A. Marrone, A. Palazzo, and A. Rotunno, *Phys.Rev.* **D84** (2011) 053007, [arXiv:1106.6028 \[hep-ph\]](#).
- [551] T. Schwetz, M. Tórtola, and J. Valle, *New J.Phys.* **13** (2011) 109401, [arXiv:1108.1376 \[hep-ph\]](#).
- [552] **MEG Collaboration**, J. Adam *et al.*, *Phys.Rev.Lett.* **107** (2011) 171801, [arXiv:1107.5547 \[hep-ex\]](#).
- [553] **LHCb Collaboration**, R. Aaij *et al.*, *Phys.Rev.Lett.* **108** (2012) 231801, [arXiv:1203.4493 \[hep-ex\]](#).
- [554] **ATLAS Collaboration**, G. Aad *et al.*, “Search for supersymmetry in all-hadronic events with α_t .” <https://twiki.cern.ch/twiki/bin/view/CMSPublic/PhysicsResultsSUS11003>, 2012. Retrieved April 16, 2013.
- [555] A. Abada, D. Das, and C. Weiland, *JHEP* **1203** (2012) 100, [arXiv:1111.5836 \[hep-ph\]](#).

- [556] J. Esteves, J. Romão, M. Hirsch, A. Vicente, W. Porod, *et al.*, *JHEP* **1012** (2010) 077, [arXiv:1011.0348 \[hep-ph\]](#).
- [557] J. Romão and J. Valle, *Neutrinos in High Energy and Astroparticle Physics*. Frontiers in physics. Wiley, Forthcoming.
- [558] T. Cheng and L. Li, *Gauge Theory of Elementary Particle Physics: Problems and Solutions*. Oxford science publications. OUP Oxford, 2000.
- [559] A. Djouadi, *Phys.Rept.* **457** (2008) 1–216, [arXiv:hep-ph/0503172 \[hep-ph\]](#).
- [560] T. M. L. Gelfand, I. M., *Dokl. Akad. Nauk SSSR* **71** (1950) 825–828.
- [561] T. M. L. Gelfand, I. M., *Dokl. Akad. Nauk SSSR* **71** (1950) 1017–1020.
- [562] M. D. Gould, *Journal of Mathematical Physics* **22** (Nov., 1981) 2376–2388.
- [563] M. D. Gould, *Journal of Mathematical Physics* **22** (Jan., 1981) 15–22.
- [564] A. I. Molev, *Communications in Mathematical Physics* **201** (1999) 591–618, [arXiv:math/9804127](#).
- [565] A. I. Molev, *Journal of Physics A Mathematical General* **33** (June, 2000) 4143–4158, [arXiv:math/9909034](#).
- [566] H. Schlosser, *Journal of Lie Theory* **1** (1991) .
- [567] I. Koh, J. Patera, and C. Rousseau, *J.Math.Phys.* **25** (1984) 2863–2872.
- [568] G. W. Anderson and T. Blažek, *J.Math.Phys.* **41** (2000) 4808–4816, [arXiv:hep-ph/9912365 \[hep-ph\]](#).
- [569] G. W. Anderson and T. Blažek, *J.Math.Phys.* **41** (2000) 8170–8189, [arXiv:hep-ph/0006017 \[hep-ph\]](#).
- [570] G. W. Anderson and T. Blažek, [arXiv:hep-ph/0101349 \[hep-ph\]](#).
- [571] C. Horst and J. Reuter, *Comput.Phys.Commun.* **182** (2011) 1543–1565, [arXiv:1011.4008 \[math-ph\]](#).
- [572] B. Gruber and L. O’Raifeartaigh, *J. Math. Phys.* **5** (1964) 1796–1804.
- [573] P. Cvitanović, *Phys.Rev.* **D14** (1976) 1536–1553.
- [574] P. Cvitanović, *Group theory: Birdtracks, Lie’s and exceptional groups*. Princeton University Press, 2008.
- [575] M. A. A. van Leeuwen, A. M. Cohen, and B. Lisser, “LiE - A Computer algebra package for Lie group computations.” <http://wwwmathlabo.univ-poitiers.fr/~maavl/LiE>, 2012. Retrieved March 17, 2013.

- [576] I. Jack and D. R. T. Jones, *Phys. Lett.* **B333** (1994) 372–379, [arXiv:hep-ph/9405233](#).
- [577] M. Sperling, D. Stöckinger, and A. Voigt, [arXiv:1305.1548 \[hep-ph\]](#).
- [578] S. Weinberg, *Phys.Lett.* **B91** (1980) 51.
- [579] L. J. Hall, *Nucl.Phys.* **B178** (1981) 75.
- [580] S. Bertolini, L. Di Luzio, and M. Malinsky, *Phys.Rev.* **D80** (2009) 015013, [arXiv:0903.4049 \[hep-ph\]](#).
- [581] J. C. Romão, “The Minimal Supersymmetric Standard Model.” <http://porthos.ist.utl.pt/~romao/homepage/publications/mssm-model/mssm-model.pdf>, 2011. Retrieved May 9, 2013.